INVESTIGATION OF CHECKPOINT ADAPTATION IN HUMAN CANCER CELLS TREATED WITH THE GENOTOXIC AGENT CISPLATIN

LUCY HANNAH SWIFT
MBiol (Hons), University of Bath (UK), 2008

A Thesis
Submitted to the School of Graduate Studies
of the University of Lethbridge
in Partial Fulfilment of the
Requirements for the Degree

DOCTOR OF PHILOSOPHY

Department of Biological Sciences
University of Lethbridge
LETHBRIDGE, ALBERTA, CANADA

© Lucy H. Swift, 2015

INVESTIGATION OF CHECKPOINT ADAPTATION IN HUMAN CANCER CELLS TREATED WITH THE GENOTOXIC AGENT CISPLATIN

LUCY HANNAH SWIFT

Date of Defence: November 3, 2015

Dr. R. Golsteyn Supervisor	Associate professor	Ph.D.
Dr. A. Russell Thesis Examination Committee Member	Assistant professor	Ph.D.
Dr. S. Wetmore Thesis Examination Committee Member	Professor	Ph.D.
Dr. N. Thakor Internal Examiner	Assistant Professor	Ph.D.
Dr. R. Johnston External Examiner University of Calgary Calgary, Alberta	Professor	Ph.D.
Dr. E. Schultz Chair, Thesis Examination Committee	Associate Professor	Ph.D.

ABSTRACT

We investigated checkpoint adaptation in HT-29 human colorectal adenocarcinoma cells treated with cisplatin. Cells that undergo checkpoint adaptation arrest at and then abrogate the G2/M checkpoint to enter mitosis with damaged DNA. We identified that cytotoxic amounts of cisplatin induce either checkpoint adaptation or apoptosis in a concentration dependent manner. We also found that some cisplatin treated cells can survive checkpoint adaptation. These survival cells may contain rearranged genomes, because they entered mitosis with damaged DNA. Additionally, cisplatin treated cells can die when they are induced to undergo checkpoint adaptation but entry into mitosis is inhibited. This might prevent cells surviving treatment with rearranged genomes and could improve the efficacy of genotoxic anti-cancer drugs. Finally, we show that the process of checkpoint adaptation is not identical in response to treatment with two different genotoxic agents; both HT-29 and M059K glioma cells treated with camptothecin spend longer in mitosis than cells treated with cisplatin.

ACKNOWLEDGEMENTS

I would like to thank my supervisor Dr. Roy Golsteyn for his guidance and support throughout my PhD. I am extremely grateful for the encouragement that I have received and the opportunities that I have been given. I am grateful to my committee members Dr. Tony Russell and Dr. Stacey Wetmore for all of the helpful advice and support that I have received. I also thank Dr. Randal Johnston and Dr. Nehal Thakor for accepting to be part of my thesis examination committee and Dr. Elizabeth Schultz for contributing to my PhD defence as the thesis examination chair.

I have enjoyed my time at the University of Lethbridge and this would not have been possible without the many friends I have made here. I have also been supported by members of the Department of Biological Sciences who were friendly in the halls and at the gym and who have gone out of their way to share equipment, knowledge and supplies, allowing me to complete my research project.

My research has also benefitted greatly from the support and advice of lab members both past and present including Dr. Sophie Kernéis-Golsteyn, Philip Kubara, Brittany Lanser, Tanzila Rahman, Cody Lewis and Alessandra Bosco.

I would also like to thank Dr. Duncan Clark and the members of GeneSys Ltd., Surrey, UK for providing me with a strong foundation in biological research. The training and advice I received during my two years at GeneSys Ltd. proved invaluable throughout my PhD.

I would not have been able to complete this PhD without encouragement from my family, including my parents Heather and Allan Swift and my Grandma Frances Davies. I

would also like to thank my brother Adam Swift for providing me with many stories to share and laugh about. Finally I would like to thank Greg Cowan for his kindness, patience and support over the last four years.

TABLE OF CONTENTS

LIST OF TABLES

LIST OF FIGURES

LIST OF ABBREVIATIONS

AA8	Chinese hamster ovarian cell line
APC/C	Anaphase promoting complex/cyclosome
ATCC	American Type Culture Collection
ATM	Ataxia telangiectasia mutated
ATP	Adenosine triphosphate
ATR	ATM and Rad3-related
ATRIP	ATR-interacting protein
A2780	Human ovarian carcinoma cell line
BSA	Bovine serum albumin
CAK	Cyclin-dependent kinase activating kinase
Caov-4	Human ovarian adenocarcinoma cell line
Cdk	Cyclin-dependent kinase
CGH	Comparative genomic hybridisation
Chk	Checkpoint kinase
CHO	Chinese hamster ovarian cell line
CIN	Chromosomal instability
CKII	Casein Kinase II
COLO320DM	Human colorectal adenocarcinoma cell line
CPT	Camptothecin
DAPI	4′, 6-diamidino-2-phenylindole
DC-3F	Chinese hamster lung fibroblastic cell line
DDR	DNA damage response
DLD1	Human colorectal adenocarcinoma cell line
DMSO	Dimethyl sulphoxide
DNA	Deoxyribonucleic acid
DNA-PKcs	DNA-dependent protein kinase catalytic subunit
DSBs	Double-strand breaks
DTT	Dithiothreitol
EDTA	Ethylenediaminetetraacetic acid
EGTA	Ethylene glycol tetraacetic acid
FBS	Fetal bovine serum
FISH	Fluorescent *in situ* hybridisation
GCT-27	Human testicular germ cell tumour cell line
GFP	Green fluorescent protein
GST	Glutathione S-transferase
G1 phase	Gap 1 phase
G2 phase	Gap 2 phase
HCC	Human hepatocellular carcinoma
HCT116	Human colorectal carcinoma cell line
HeLa	Human cervical adenocarcinoma cell line
HEPES	4-(2-hydroxyethyl)-1-piperazineethanesulfonic acid
hPNK	Human polynucleotide kinase
HR	Homologous recombination
HT-29	Human colorectal adenocarcinoma cell line
HT1080	Human fibrosarcoma cell line

HtTA-MDR1	Modified HeLa cell line
Huh-7	Human hepatocarcinoma cell line
H1299	Human non-small cell lung carcinoma cell line
H_2O_2	Hydrogen peroxide
IPEGAL	Octylphenoxypolyethoxyethanol
LA-9	Mouse fibroblastic cell line
L1210	Murine lymphocytic leukaemia cell line
MDC1	Mediator of DNA damage checkpoint protein 1
Mdm2	Mouse double minute 2 homologue
MDR1	Multidrug resistance protein 1
MEF	Mouse embryonic fibroblastic cells
MEN	Mitotic exit network
M phase	Mitotic phase
mRNA	Messenger RNA
MOLT4	Human lymphoblastic leukaemia cell line
MTT	3-((4,5)-dimethylthiazol-2-yl)-2,5-diphenyl-tetrazolium bromide
M059K	Human glioma cell line
NCI	National Cancer Institute
NER	Nucleotide excision repair
NHEJ	Non-homologous end joining
NIH 3T3	Murine embryo fibroblastic cell line
PAGE	Poly-acrylamide gel electrophoresis
PARP	Poly-ADP ribose polymerase
PBS	Phosphate buffered saline
PE	Plating efficiency
PI	Propidium iodide
Plk	Polo-like kinase
PP1	Protein phosphatase 1
PP1Cα	Protein phosphatase PP1 alpha catalytic subunit
PP2	Protein phosphatase 2
Rb	Retinoblastoma
Rfa2	Replication factor A2
RKO	Human colon carcinoma cell line
RNA	Ribonucleic acid
RNA-Seq	RNA sequencing
ROS	Reactive oxygen species
RPA	Replication protein A
RPE-1	Human retinal pigment epithelial cell line
SAC	Spindle assembly checkpoint
Sarcoma 180	Murine sarcoma cell line
SDS	Sodium dodecyl sulphate
SF	Surviving factor
SH-SY5Y	Human bone marrow neuroblastoma
siRNA	Small interfering RNA
SKOV-3	Human ovarian carcinoma cell line
SKY	Spectral karyotyping
SNU	Human hepatocellular carcinoma cell line

S phase	DNA synthesis phase
SSB	Single-strand break
ssDNA	Single stranded DNA
Susa	Human testicular germ cell tumour cell line
SW480	Human colorectal adenocarcinoma cell line
TBS	Tris-buffered saline
TCGA	The Cancer Genome Atlas
Tdp1	Tyrosyl-DNA-phosphodiesterase
TE7	Oesophageal adenocarcinoma cell line
TGCT	Testicular germ cell tumour
TNF	Tumour necrosis factor
TNFR	Tumour necrosis factor receptor
Top1	Topoisomerase I
Top 2	Topoisomerase II
TOPBP1	DNA topoisomerase binding protein 1
TPT	Topotecan
UV	Ultraviolet
UV20	Chinese hamster ovarian cell line
UV41	Chinese hamster ovarian cell line
U2OS	Human osteosarcoma cell line
V79	Chinese hamster lung fibroblastic cell line
WI-38	Human non-cancerous lung fibroblastic cell line
XP	Xeroderma pigmentosum
2008	Human ovarian carcinoma cell line
5-FU	5-Fluorouracil
883K	Human testicular germ cell tumour cell line
9-1-1	Rad9-Rad1-Hus1 complex

CHAPTER 1

General introduction

1.1 General overview of thesis

This thesis is about checkpoint adaptation in human cancer cells treated with cisplatin. Checkpoint adaptation consists of three steps: 1) arrest at a DNA damage checkpoint; 2) abrogation of the DNA damage induced checkpoint and 3) entry into mitosis with damaged DNA (Toczyski et al. 1997). Checkpoint adaptation may be a key step that lies between cell cycle arrest and cell death in human cancer cells treated with genotoxic agents but it has only been shown to occur in response to treatment with ionising radiation (Syljuåsen et al. 2006; Rezacova et al. 2011), camptothecin (CPT) and etoposide (Kubara et al. 2012). In this thesis we investigate if checkpoint adaptation occurs in response to treatment with cisplatin, because it has a different mechanism of action than that of known checkpoint adaptation inducing agents. We hypothesise that human cancer cells treated with cisplatin undergo checkpoint adaptation. If checkpoint adaptation occurs in response to treatment with cisplatin, in addition to the treatments previously described, it would support the hypothesis that checkpoint adaptation is a key cellular response by cancer cells to treatment with genotoxic agents.

Cisplatin has been widely-used to treat cancer patients since it was approved for use in ovarian and testicular cancers in 1978 (Kelland 2007). Furthermore, cisplatin has previously been shown to induce mitotic catastrophe in different cancer cell lines (Demarq et al. 1994; Chang et al. 1999; Vakifahmetoglu et al. 2008), and in some cases these cells may have been undergoing checkpoint adaptation. It is necessary to introduce

the cell cycle, cisplatin, the DNA damage response, genomic instability in cancer cells and cancer cell death pathways, to understand checkpoint adaptation and its role in cancer cell death.

1.2 Cancer and its hallmarks

The World Health Organisation has estimated that in 2012 there were 14 million new cases of cancer and 8.2 million cancer related deaths worldwide (Stewart and Wild 2014). Many anti-cancer treatments exist yet cancer remains a leading cause of death around the world. It is therefore necessary to both improve the efficacy of current anti-cancer treatments and develop new anti-cancer therapies. In this thesis we investigate the process of checkpoint adaptation in cancer cells treated with cisplatin, to investigate if this process could be targeted to improve the efficacy of current genotoxic anti-cancer drugs.

Cancer is a complex disease that was characterised by six hallmarks in 2000 (Hanahan and Weinberg 2000). These hallmarks are sustained proliferative signalling, resisting cell death, evading growth suppressors, activating invasion and metastasis, enabling replicative immortality and inducing angiogenesis. Following a decade of research, these hallmarks were revisited in 2011 and two emerging hallmarks were identified. These were deregulating cellular energetics and avoiding immune destruction (Hanahan and Weinberg 2011). Underlying these hallmarks of cancer are genomic instability and tumour promoting inflammation (Hanahan and Weinberg 2011). Genomic instability occurs in individual cells and chromosomal instability (CIN), the rate at which chromosome number changes over time due to errors in mitosis, is common in cancer

cells (Negrini et al. 2010). Most cancer cells are therefore aneuploid (have a change in chromosome number) (Thompson and Compton 2011).

Of the hallmarks of cancer, sustained proliferative signalling and resisting cell death are the most relevant to this thesis. Sustained proliferation can occur when the signals that control the production and release of growth-factors and/or the control of cell division are lost. For example, it is estimated that the majority of cancers have mutations in at least one of the genes that encode the tumour suppressors retinoblastoma (Rb), p21 or p53 (Manning et al. 2013; Rausch et al. 2012). These proteins regulate progression through the cell cycle, described in section 1.4. Mutations to the tumour suppressor genes encoding p53, pRb and p21 allow cells to divide even when conditions for division are not optimal. TP53 is one of the most commonly mutated genes found in cancers. The Cancer Genome Atlas (TCGA) analysed 3,281 tumours from 12 cancer types (breast adenocarcinoma, lung adenocarcinoma, lung squamous cell carcinoma, uterine corpus endometrial carcinoma, glioblastoma multiforme, head and neck squamous cell carcinoma, colorectal carcinoma, bladder urothelial carcinoma, kidney renal clear cell carcinoma, ovarian serous carcinoma and acute myeloid leukaemia) for point mutations and small insertions/deletions and found that TP53 was the most frequently mutated gene, mutated in 42% of samples (Kandoth et al. 2013).

The loss of p53 function also has a role in resisting cell death, because p53 can induce cell death by apoptosis in response to extensive DNA damage (Zhivotovsky and Kroemer 2004). By resisting cell death cancer cells can continue to survive and potentially divide in conditions that would kill or arrest the growth of normal cells, such as when they have damaged DNA. Because cancer cells can lose the ability to regulate

the cell cycle and to induce apoptosis, this has implications for cancer treatments. Many cancer treatments aim to inhibit cell division and induce cell death by causing irreparable amounts of DNA damage. However, because cancer cells are capable of dividing in sub-optimal conditions and are more resistant to cell death, some cells can survive treatment. This can lead to either tumour progression or cancer relapse.

1.3 The cell cycle

Cell division is a fundamental process in biology. To divide, a eukaryotic cell must pass through four phases of the cell cycle: G1 (Gap 1), when cells grow and prepare for DNA synthesis; S (DNA synthesis), when cells replicate their DNA, G2 (Gap 2), when cells continue to grow and prepare for mitosis and M, (mitosis) when cells separate copies of their DNA as chromosomes. This is followed by cytokinesis, when cells divide the cytoplasm to complete the process of cell division. G1, S and G2 collectively make up interphase, whereas mitosis and cytokinesis make up M phase. Cells in G1 phase can also enter a resting state called G0 when they do not grow or divide (Vermeulen et al. 2003). To maintain the integrity of the genome during the cell cycle several events must occur: DNA replication must be accurate; chromosomes must be distributed correctly during mitosis and cytokinesis; and damaged DNA must be detected and repaired (Jackson and Bartek 2009).

Mitosis is further divided into five processes: prophase, prometaphase, metaphase, anaphase and telophase. In prophase the chromatin begins to condense into visible chromosomes and the mitotic spindle (composed of microtubules extending from two centrosomes) begins to form. During prometaphase the nuclear envelope dissolves and the kinetochores present on sister chromatids are attached to the microtubules of the

mitotic spindle. In metaphase the centrosomes reach the opposite poles of the cell and the chromosomes are lined up along the metaphase plate. In anaphase the chromosomes are separated to opposite ends of the cell and the cell lengthens. Anaphase is followed by telophase and cytokinesis. In telophase new nuclear envelopes are formed, producing two daughter nuclei, and the chromosomes decondense.

During mitosis almost every organelle and structure in a cell is altered (Morgan 2007) and cells that are in mitosis adopt a rounded morphology, known as mitotic cell rounding (Cadart et al. 2014). Mitotic cell rounding is evolutionarily conserved and is nearly universal in metazoan and eukaryotic cells that lack a cell wall. Mitotic cell rounding is required for chromosome capture, spindle formation and spindle stability and therefore has an important role in cell division (Cadart et al. 2014). To exhibit mitotic rounding, cells must disassemble focal adhesion complexes to decrease adhesion to their substrate and reorganise the actin cytoskeleton (Heng and Koh 2010; Cadart et al. 2014).

The rounded morphology of mitotic cells can be used to visually distinguish mitotic cells from interphase cells. It can also be utilised to separate and collect mitotic cell populations from interphase cell populations during tissue culture by mechanical shake-off (Terasima and Tolmach 1963; Kubara et al. 2012). A second feature of mitotic cells is that they contain histone H3 phosphorylated on serine 10 (Hendzel et al. 1997). Phosphorylation of histone H3 at serine 10 is correlated to mitotic chromosome condensation (Hendzel et al. 1997). Dephosphorylation of histone H3 at serine 10 is initiated in anaphase and is completed before chromosomes decondense (Hendzel et al. 1997). This means that serine 10 phosphorylated histone H3 can be used to detect cells in mitosis.

1.4 Cell cycle regulation

The cell cycle is highly regulated to prevent cells from transmitting damaged DNA to daughter cells. Cyclin-dependent kinases (Cdks) are the main regulators of the cell cycle and are highly conserved catalytic subunits of a family of serine/threonine kinases (Malumbres and Barbacid 2005). To be active, these subunits must be bound to proteins called cyclins. Cdk-cyclin complexes are responsible for phosphorylating a multitude of substrates, tightly regulating progression through the cell cycle. In mammalian cells, progression through G1 phase of the cell cycle is regulated by Cdk4, Cdk6 and Cdk2 (de Cárcer et al. 2007).

Cdk4/cyclin D and Cdk6/cyclin D begin to phosphorylate and inactivate members of the Rb protein family (Malumbres 2014). The Rb proteins prevent the transcription of genes that encode proteins necessary for entry into S phase (Giacinti and Giordano 2006). Inhibition of the Rb proteins by phosphorylation allows cyclin E to be synthesised and cyclin E then binds to Cdk2 (de Cárcer et al. 2007). Active Cdk2-cyclin E further phosphorylates Rb and other transcription factors, promoting the transcription of genes whose products are needed for entry into S phase (Malumbres and Barbacid 2005). Cdk2-cyclin E also phosphorylates components of the pre-replication complex at origins of replication, inducing origin activation (Woo and Poon 2003). It is proposed that when Cdk2 is disassociated from cyclin E it interacts with newly synthesised cyclin A, phosphorylating the proteins needed to complete and exit from S phase of the cell cycle (Malumbres and Barbacid 2005).

Cyclin B is synthesised during S and G2 phases of the cell cycle, increasing the level of cyclin B in the cytoplasm (Deibler and Kirschner 2010). Cyclin B binds to Cdk1,

creating a Cdk1-cyclin B dimer, and the activity of this complex controls the transition between G2 phase and mitosis. Once Cdk1 is bound to cyclin B, Cdk1 is phosphorylated on threonine 161 by cyclin-dependent kinase activating kinase (CAK). This phosphorylation stabilises the Cdk1-cyclin B complex and induces conformational changes necessary for kinase activity (Larochelle et al. 2007; Deibler and Kirschner 2010). However, despite being bound to cyclin B, Cdk1-cyclin B is held inactive by phosphorylation on threonine 14 and tyrosine 15. Threonine 14 is phosphorylated by Myt1 kinase and tyrosine 15 is phosphorylated by Wee1 kinase (Haese et al. 1995). These phosphate groups prevent Cdk1 from binding to and hydrolysing adenosine triphosphate (ATP) (Deibler and Kirschner 2010), preventing the transfer of a phosphate group from ATP onto a Cdk1 substrate. The phosphate groups on threonine 14 and tyrosine 15 are removed by Cdc25 phosphatases, promoting entry into mitosis (Millar and Russell 1992). Once active Cdk1-cyclin B phosphorylates the Cdk1 inhibitor Wee1 and the Cdk1 activating Cdc25 phosphatases through two different feedback loops (Morgan 2007). Interestingly, overexpression of only cyclin B and Cdc25 phosphatase is necessary to cause cells in G2 phase to prematurely enter mitosis (Karlsson et al. 1999).

Once activated, the Cdk1-cyclin B complex phosphorylates over 70 proteins in mammalian cells (Malumbres and Barbacid 2005). Furthermore, a proteomic screen of the budding yeast *Saccharomyces cerevisiae* identified 360 proteins phosphorylated by Cdk1-cyclin B. Of these proteins, 181 were designated interesting because they were less abundant proteins that were highly phosphorylated (Ubersax et al. 2003). Cdk1 substrates include multiple enzymes and structural components that initiate the events of early mitosis (Morgan 2007). These substrates include; condensins, which condense

chromosomes (Abe et al. 2011); nuclear lamins, which are necessary for the structure and function of the nuclear envelope (Margalit et al. 2005) and tubulin and microtubule binding proteins, which promote the formation of the mitotic spindle (Fourest-Lieuvin et al. 2006). One specific Cdk1 substrate is protein phosphatase 1 (PP1Cα) which is inhibited by phosphorylation on threonine 320 by active Cdk1-cyclin B (Kwon 1997). It is suggested that inactivation of PP1Cα is necessary to maintain the Cdk1-cyclin B mediated phosphorylation of mitotic substrates because PP1Cα dephosphorylation is necessary for mitotic exit and occurs during anaphase, as Cdk1-cyclin B activity decreases (Kwon 1997). The decrease in Cdk1-cyclin B activity is mediated by the anaphase promoting complex/cyclosome (APC/C) degradation of cyclin B at the metaphase-anaphase transition. The APC/C is activated by Cdk1-cyclin B in a negative feedback loop (Domingo-Sananes et al. 2011). APC/C is an ubiquitin ligase that labels cyclin B for degradation by the proteasome (Sudakin et al. 1995; Domingo-Sananes et al. 2011). The degradation of cyclin B deactivates Cdk1 and APC/C activity is also inhibited (Morgan 2007).

In 2010, Deibler and Kirschner used a human cell free system to study Cdk1 activation in mammalian somatic cells by increasing the concentration of recombinant cyclin B (Deibler and Kirschner 2010). They found that the activation of Cdk1 was a three stage process where Cdk1-cyclin B substrates were phosphorylated in a sequence that was related to changes in cyclin B levels. In stage one, at low concentrations of cyclin B (approximately 100 nM), Cdk1 activity increased proportionally to the amount of cyclin B added. In stage two Cdk1 activity plateaued, with both active and inactive complexes present in the system, despite increasing the concentration of cyclin B to

approximately 400 nM. In stage three, when cyclin B concentration was above 400 nM, Cdk1 was rapidly activated and the increase in Cdk1 activity exceeded the increase in cyclin B concentration. The authors found that tyrosine 15 phosphorylation increased until this third stage, at which point the Cdc25 phosphatase feedback loop was activated (Deibler and Kirschner 2010).

The oscillating nature of cyclin B levels can be used to detect cells that are capable of entering mitosis. This is because cyclin B is synthesised through S and G2 phases of the cell cycle and then degraded at the metaphase-anaphase transition of mitosis (Pines and Hunter 1989). Cdk1 phosphorylation is also a good measure of whether cells have active Cdk1 or not; if cells have high levels of tyrosine 15 phosphorylated Cdk1 then they do not contain enough active Cdk1 to be in mitosis (Deibler and Kirschner 2010; Kubara et al. 2012). Additionally, to detect Cdk1 activity, a specific Cdk1 activity assay can be performed. In 2013, Lewis *et al*. published a protocol to detect Cdk1 activity by using western blotting to quantify the amount of phosphorylation of threonine 320 on an artificial Cdk1 substrate consisting of GST and amino acids 316-324 from the PP1-alpha catalytic subunit (PP1Cα) (Lewis et al. 2013).

1.5 Cdk1 inhibitors

Cell cycle Cdks are the potential targets of chemical inhibitors to prevent sustained proliferation, a hallmark of some cancer cells (Hanahan and Weinberg 2011). In 2013, 13 Cdk1 inhibitors were in clinical trials (Bruyère and Meijer 2013). Typically Cdk1 inhibitors are small ATP-competitive molecules (Johnson and Shapiro 2010). Roscovitine is a Cdk inhibitor that is currently undergoing phase II clinical trials for nasopharyngeal cancer and non-small cell lung cancer (Sallam et al. 2013). CR8 is a

second generation analogue of roscovitine that is at least 50-fold more potent (Bettayeb et al. 2008; Bettayeb et al. 2010). CR8 and roscovitine are both low molecular weight 2,6,9-trisubstituted purines that bind to the ATP binding site of Cdks (Bettayeb et al. 2008). Treating SH-SY5Y human neuroblastoma (Bettayeb et al. 2008) and HT-29 human colorectal adenocarcinoma cells (Kubara et al. 2012) with CR8 prevents them from entering into mitosis. CR8 can therefore be used as a Cdk1 inhibitor in the laboratory, to chemically inhibit entry into mitosis.

1.6 Cell cycle checkpoints

Cell cycle checkpoints enable a cell to ensure that important processes, such as DNA replication, are complete (Hartwell and Weinert 1989; Kastan and Bartek 2004). Cell cycle checkpoints prevent the transmission of genetic errors to daughter cells. Three major cell cycle checkpoints exist; the G1/S checkpoint, the G2/M checkpoint and the spindle assembly checkpoint (SAC). The SAC ensures that chromosome segregation occurs correctly (Holland and Cleveland 2009) and is activated at the metaphase to anaphase transition in mitosis, in response to microtubule defects (Schwartz and Shah 2005) or erroneous kinetochore attachment (Nicklas 1997). Cells also arrest at the SAC when they enter mitosis with damaged DNA (Nitta et al. 2004). Inactivation of the SAC can lead to chromosome mis-segregation and aneuploidy (a change in the number of chromosomes present in a cell) (Holland and Cleveland 2009).

The G1/S and G2/M checkpoints are initiated in response to DNA damage, to prevent the transmission of damaged or incomplete chromosomes to daughter cells. The DNA damage checkpoints provide cells with time to repair damaged DNA. If the DNA damage is irreparable cells may initiate senescence (growth arrest) or cell death. The

G1/S checkpoint prevents cells from replicating damaged DNA, whereas the G2/M checkpoint prevents cells from dividing with damaged DNA (Kastan and Bartek 2004).

1.7 Genotoxic agents as anti-cancer treatments

Genotoxic agents are a mainstay of cancer therapy (Woods and Turchi 2013) that cause high levels of DNA damage. This DNA damage induces cells to arrest at cell cycle checkpoints leading to cell cycle arrest and/or cell death (Helleday et al. 2008). There are many different genotoxic anti-cancer drugs that are grouped into different categories based on their mechanism of action. A summary of these agents is provided in Table 1.1.

The first DNA damaging drugs used to treat cancer were the nitrogen mustards and nitrosoureas (Hurley 2002; Woods and Turchi 2013). These alkylating agents were developed after studying soldiers exposed to mustard gas in World Wars I and II (Hurley 2002; Chabner and Roberts 2005). Since the discovery of nitrogen and sulphur mustards, a large number of genotoxic agents have been developed and approved for clinical use. The majority of these are chemical agents, except for ionising radiation, which is a physical agent.

It is estimated that approximately 50% of all cancer patients receive treatment with ionising radiation, either alone or in combination with chemical anti-cancer drugs (Baskar et al. 2012). Ionising radiation directly damages the DNA backbone, inducing strand breaks (Jackson and Bartek 2009). It also produces reactive oxygen species (ROS), which can form covalent bonds with DNA and induce a variety of DNA modifications (Jackson and Bartek 2009). Interestingly, ionising radiation is proposed to induce cell

death following entry into mitosis in most solid tumours (Dewey et al. 1995; Jonathan et al. 1999; Hall and Giaccia 2012).

Camptothecin (CPT) (Figure 1.1A) is a topoisomerase I (Top1) inhibitor which in this thesis is used as a positive control treatment for the cellular response of checkpoint adaptation (described in section 1.9.2). The water soluble derivatives of CPT, topotecan (TPT) and irinotecan, are widely used to treat colorectal, lung and ovarian cancers. It is relevant to this thesis that the pharmacology of CPT in humans is well understood and a peak plasma concentration of 75 nM has been reported (Raymond et al. 2002; Swift and Golsteyn 2014). Topoisomerase enzymes are essential for DNA replication because they relax DNA supercoiling by introducing transient nicks along the phosphodiester backbone of DNA (Pommier 2006). To relieve torsional stress, type 1 topoisomerases nick one strand of DNA, passing the uncleaved strand through this nick. By contrast, type 2 topoisomerases break both strands of DNA (Cheung-Ong et al. 2013). Once the DNA has been relaxed the DNA nicks are re-ligated (Froelich-Ammon and Osheroff 1995). Topoisomerases form enzyme-DNA cleavage complexes by covalently attaching to DNA. Topoisomerase inhibitors induce DNA damage by binding to the topoisomerase-DNA complexes, preventing the DNA nicks from being re-ligated (Froelich-Ammon and Osheroff 1995; Pommier 2006). This leads to the formation of DNA strand breaks.

Double strand breaks (DSBs) are directly induced by topoisomerase II (Top 2) inhibitors such as etoposide (Figure 1.1B), whereas Top1 inhibitors first induce single strand breaks (SSBs) that are then converted into DSBs when they are met by a replication fork (Hsiang et al. 1989; Froelich-Ammon and Osheroff 1995). When DNA is damaged by Top1 inhibitors, the Top1 complex covalently bound to the DNA must first

be removed, before DNA damage repair can begin. This is achieved by tyrosyl-DNA-phosphodiesterase (Tdp1) which hydrolyses the covalent bond between the Top1 complex and the DNA, generating a 3′-phosphate end (Pommier et al. 2006).

The DNA strand breaks induced by CPT and other genotoxic agents such as ionising radiation often require further processing before they can be repaired, because they have 5′-hydroxyl and 3′-phosphate ends (Meijer et al. 2002). To re-ligate DNA, the breaks must have 5′-phosphate and 3′-hydroxyl ends. This processing can occur by human polynucleotide kinase (hPNK) which has 5′-kinase and 3′-phosphatase activities and is required for non-homologous end joining (NHEJ) (Karimi-Busheri et al. 2007).

The DNA strand breaks induced by topoisomerase inhibitors can be repaired by either NHEJ or homologous recombination (HR). NHEJ is used to repair DSBs when a homologous DNA template is unavailable for HR. As such, NHEJ occurs in G1 and early-S phases and involves re-ligating the broken DNA. HR occurs when a homologous DNA template is available, such as in late S and G2. HR involves ssDNA from the site of damaged DNA invading its sister chromatid at a homologous region, forming heteroduplex DNA and Holliday junctions (Helleday et al. 2007). Holliday junctions are four-way DNA intermediates that are formed between the invading and displaced DNA strands. The invading strand is then used as a primer for extension by a DNA polymerase and the DNA nicks are repaired by ligation (Shrivastav et al. 2008). To complete HR, the Holliday junctions are cleaved by resolvases and this can lead to chromosome crossovers (Li and Heyer 2008). Because the DNA strand breaks induced by topoisomerase inhibitors are induced primarily during DNA replication by replication fork stalling and

collapse, HR is heavily involved in the repair of these breaks (Nitiss and Wang 1988; van Waardenburg et al. 2004).

A third type of DNA damage is induced by *cis*-diamminedichloroplatinum(II) (cisplatin) (Figure 1.1C). Cisplatin is a platinum based inorganic molecule (Rosenberg et al. 1969) that induces a variety of DNA adducts and crosslinks. Peak plasma concentrations of total platinum range from 12-40 μM (Vermorken et al. 1984; Oldfield et al. 1985; Charlier et al. 2004) and cisplatin is widely used to treat different cancers including ovarian, testicular, cervical, head and neck, oesophageal and non-small cell lung cancer (Jamieson and Lippard 1999). In this thesis we investigate checkpoint adaptation in human cancer cells treated with cisplatin. It is therefore necessary to introduce the history of cisplatin as an anti-cancer drug and its mechanism of action.

1.7.1 The history of cisplatin

Cisplatin was first synthesised by the Italian chemist Michele Peyrone in 1844 and was originally named Peyrone's chloride [$PtCl_2(NH_3)_2$] (Kauffman et al. 2010). In 1893 the Swiss chemist Alfred Werner published his work with cisplatin, distinguishing between the trans and cis isomer and proposing its square planar configuration (Alderden et al. 2006; Kauffman et al. 2010). This contributed to Werner winning the Nobel Prize for Chemistry in 1913 (Werner 1913). The anti-cancer properties of cisplatin were discovered in the 1960s by the American biophysicist Barnett Rosenberg (Alderden et al. 2006) and since then cisplatin has had a major impact on improving survival rates for patients with testicular and ovarian cancers (Kelland 2007).

Barnett Rosenberg was originally interested in studying the effects of electromagnetic radiation on cell division in bacterial and mammalian cells (Kelland 2007). Rosenberg used platinum electrodes (considered to be inert) to apply an electric current to *Escherichia coli* cells growing in an ammonium chloride buffer (Rosenberg et al. 1965; Kelland 2007). Strikingly, when the current was turned on, Rosenberg observed that bacterial cell division was inhibited and the cells instead grew as long filaments up to 300 times their normal length. After further testing, this effect was shown to be caused by the electrolysis products from the platinum electrodes (Rosenberg et al. 1965).

In 1968, cisplatin was administered to mice transplanted with a standard sarcoma 180 tumour and it inhibited tumour growth, with some mice showing complete tumour regression and living tumour free for a further 6 months (Rosenberg et al. 1969). Subsequently, Rosenberg left samples of cisplatin for testing at the US National Cancer Institute (NCI) where the compounds were screened using mice with L1210 leukaemia. These samples demonstrated potent anti-tumour activity (Rosenberg et al. 1969; Wiltshaw 1979) and in 1970 Rosenberg and VanCamp published that cisplatin was active in regressing large solid sarcoma 180 tumours in mice (Rosenberg and VanCamp 1970).

Cisplatin was then studied by Sir Alex Haddow at the Chester Beatty Institute in London, United Kingdom (Wiltshaw 1979; Kelland 2007) before being used for clinical trials by the NCI in 1971 (Kelland 2007). Initially cisplatin was tested in Phase I trials on cancer patients for whom no other treatments were available (Wiltshaw 1979). Surprisingly some patients showed tumour regression after these trials, especially those with either testicular or ovarian cancers (Wiltshaw 1979). However, renal toxicity was a serious limiting factor in progressing with cisplatin as an anti-cancer drug, until it was

found that this toxicity could be reduced by intravenous hydration both before and after the administration of cisplatin (Wiltshaw 1979). Phase II trials of cisplatin began in 1975, before large scale Phase III trials led to the US Food and Drug Authority approval of cisplatin as an anti-cancer drug for testicular and ovarian cancers in 1978 (Kelland 2007).

Cisplatin is now a top-selling anti-cancer drug that has revolutionised the treatment of some types of cancers. Specifically, cisplatin and combination treatments with cisplatin have increased the cure rate for testicular cancer to 90%, when tumours are diagnosed early (Bosl and Motzer 1997; Jamieson and Lippard 1999). Despite this, the efficacy of treatment with cisplatin is limited by intrinsic and acquired resistance. Intrinsic resistance is present before treatment begins whereas acquired resistance develops as treatment progresses (Giaccone and Pinedo 1996). Resistance to cisplatin is complex and multifactorial (Mayer et al. 2003). Common mechanisms of resistance include decreased drug accumulation in the cell, increased levels of thiol containing species in the cytoplasm which bind to and inactivate cisplatin, increased repair of DNA damage and resistance to cell death pathways (Woźniak and Blasiak 2002; Kelland 2007). These pathways of resistance are associated with molecular changes in the cell that are induced by genetic and epigenetic changes (Shen et al. 2012). By identifying how cancer cells acquire resistance to cisplatin, it might be possible to prevent this, improving the efficacy of this widely used genotoxic agent.

Cell lines and tumour samples that are resistant to cisplatin exhibit chromosomal abnormalities that distinguish them from cisplatin sensitive cell lines and tumour samples. The difference between cisplatin sensitive and cisplatin resistant cell lines and tumour samples has been studied using comparative genomic hybridisation (CGH). This

technique allows the detection of a change in chromosomal copy number (Weiss et al. 1999). DNA extracted from a tumour or cancer cell line of interest is labelled with a specific fluorochrome (typically green) and mixed with DNA from wild type or normal cell DNA that is labelled with a fluorochrome of a different colour (typically red). These fluorescently labelled samples of DNA are hybridised to metaphase preparations or probes from normal cells and compete for hybridisation to the metaphase preparations. The ratio of green to red is then assessed to determine loss or gain of genetic material (Weiss et al. 1999). In 1997, Wasenius *et al*. compared six ovarian carcinoma cell lines selected for resistance to cisplatin to two cisplatin sensitive parental cell lines (2008 and A2780) using CGH (Wasenius et al. 1997). They found that acquired resistance in the 2008 cells was associated with many chromosomal gains and losses by comparison to the parental cell line and the average number of chromosome aberrations per resistant cell was 15. By contrast, acquired resistance in the A2780 cell line was only associated with 5 chromosomal aberrations and all of these were losses (Wasenius et al. 1997). These data suggest that acquired resistance to cisplatin is not associated with specific genetic changes. This has also been demonstrated in testicular germ-cell tumour (TGCT) cell lines using CGH. Three cisplatin resistant TGCT cell lines (resistant GCT27, 833K and Susa) were found to contain more gains and losses of chromosomal regions by comparison to the parental cell lines (Wilson et al. 2005). However, these losses and gains were different in each of the three resistant cell lines.

The efficacy of cisplatin is also limited by clinical parameters, which include severe undesired effects such as nausea and vomiting, renal toxicity and hearing loss (Kelland 2007; Zamble and Lippard 1995). These effects limit the dose a patient can

receive, which limits the effects of platinum drugs on cancer cells (Wheate et al. 2010). To overcome some of the resistance and side effects associated with cisplatin, thousands of cisplatin analogues have been investigated (Kelland 2007). However, only 23 platinum-based drugs entered into clinical trials and only two, carboplatin and oxaliplatin (Figure 1.1D and E), are globally approved (Wheate et al. 2010). Carboplatin has fewer side effects by comparison to treatment with cisplatin, but tumours are similarly resistant to both carboplatin and cisplatin (Jamieson and Lippard 1999). Oxaliplatin is capable of overcoming the resistance associated with cisplatin, but it is still associated with severe side effects (Wheate et al. 2010). To improve the efficacy of cisplatin, research is now focused on investigating how cisplatin induces cell death (Choi et al. 2015), exploring how tumours become resistant to cisplatin (Galluzzi et al. 2012; Piskareva et al. 2015) and developing new ways to deliver platinum drugs to target cells (Zhou et al. 2014). In this thesis we investigate how cisplatin induces cell death.

1.7.2 The mechanism of action of cisplatin

Cisplatin is thought to enter cells by both passive diffusion (Gately and Howell 1993) and by the plasma membrane transporter, copper transporter-1 (Ishida et al. 2002). Once inside the cell one or both chlorine atoms are displaced by water because the cell contains a lower concentration of chlorine (4-20 mM) by comparison to the blood stream (100 mM) (Wheate et al. 2010). The water groups attached to cisplatin are then displaced by the N7 of purine bases, most commonly guanine (Baik et al. 2003). It is widely accepted that the cytotoxic effect of cisplatin is due to its interaction with nuclear DNA (Zamble and Lippard 1995; Jamieson and Lippard 1999). However, the precise mechanisms by which cisplatin induces cell death remain to be elucidated and cisplatin

also reacts with many cellular components including mitochondrial DNA, ribonucleic acid (RNA) and proteins (Jamieson and Lippard 1999). It has therefore been suggested that these interactions may also have a role in cell death when cancer cells are treated with cisplatin. For example, cisplatin can bind to phospholipids and phosphatidylserine in cellular membranes and also to intracellular proteins (Fuertes et al. 2003). In 2013, Karasawa *et al*. used agarose-cisplatin conjugates in protein pull down assays and then identified proteins that bound to cisplatin using mass-spectrometry (Karasawa et al. 2013). The authors found that cisplatin bound to a range of proteins including myosin IIA which regulates cell motility; glucose-regulated protein 94, a protein that is highly abundant in the endoplasmic reticulum; heat shock protein 90 a molecular chaperone found in the cytoplasm and ribosomal protein L5, a component of the large 60S ribosomal subunit (Karasawa et al. 2013). Furthermore, cisplatin can induce cell death by binding to mitochondrial DNA in head and neck squamous cell carcinoma cell lines (Yang et al. 2006) and cisplatin analogues designed to localise to mitochondria can induce cell death without damaging nuclear DNA (Wisnovsky et al. 2013).

When cisplatin reacts with DNA it forms monofunctional adducts as well as intra- and inter- strand crosslinks (Eastman 1987). These DNA adducts and crosslinks distort the structure of the DNA double helix. The most common types of DNA adducts in the nucleus are 1,2-intrastrand crosslinks between adjacent bases (Jamieson and Lippard 1999) with guanine-guanine1,2-intrastrand crosslinks accounting for 47-50% of DNA adducts formed by cisplatin (Fichtinger-Schepman et al. 1985). These intra-strand crosslinks are largely repaired by nucleotide excision repair (NER) in the nucleus and cancer cells that are defective in NER can be more sensitive to treatment with cisplatin

(Köberle et al. 1999). Conversely, the overexpression of NER proteins has been correlated with resistance to cisplatin (Dabholkar et al. 1994; Mendoza et al. 2013).

The DNA adducts formed by cisplatin are well characterised and the distortion of nuclear DNA induced by these adducts can block DNA and RNA polymerases, stalling DNA replication and transcription (Villani et al. 2006). Cisplatin is not considered to be cell cycle specific (Huang et al. 2004). However, it has been reported that cells treated with cisplatin do not signal damaged DNA until they pass through S phase of the cell cycle (Olive and Banàth 2009). Cisplatin is also more cytotoxic to dividing cells than it is to resting cells (Eastman 2006), suggesting that stalled replication forks have a role in the cytotoxicity of cisplatin.

1.7.3 Cisplatin induced cell death

How cisplatin damages DNA has been well studied. By contrast, the mechanism(s) by which the DNA adducts induced by cisplatin lead to cytotoxicity are poorly understood. Cisplatin has been shown to induce mitotic cell death in several different studies (Demarq et al. 1994; Chang et al. 1999; Vakifahmetoglu et al. 2008). However, these studies did not identify the pathway that cells used to enter mitosis following treatment. It is therefore possible that cells in these studies underwent checkpoint adaptation before dying.

Cells that are treated with cisplatin can arrest at the G2/M checkpoint before dying (Sorenson and Eastman 1988a; Sorenson and Eastman 1988b; Demarcq et al. 1994). Arrest at the G2/M checkpoint, followed by abrogation of this arrest, is the second step of checkpoint adaptation. In 1988, Sorenson and Eastman found that L1210 murine

leukaemia cells treated with cisplatin underwent a slowed S phase before arresting in G2 phase (Sorenson and Eastman 1988a). The authors followed this study by reporting that the Chinese hamster ovarian (CHO) cell lines AA8, UV20 and UV41 also arrested in G2 phase after treatment with cisplatin (Sorenson and Eastman 1988b). In both of these studies, the authors found that G2 arrest was transient when cells were treated with lower concentrations of cisplatin and permanent when cells were treated with higher concentrations of cisplatin (Sorenson and Eastman 1988a; Sorenson and Eastman 1988b). The authors therefore proposed that the cells treated with lower concentrations of cisplatin were able to repair their damaged DNA, prior to entering mitosis (Sorenson and Eastman 1988b). However, it is possible that these cells were actually undergoing checkpoint adaptation by entering mitosis with damaged DNA, but checkpoint adaptation had not been identified when these studies were undertaken.

Micronucleation has also been observed following treatment with cisplatin. Micronuclei are formed when lagging whole chromosomes or acentric chromosome fragments become enclosed in a separate nuclear membrane following an aberrant mitosis (Fenech et al. 2011). Micronucleation is therefore associated with entry into mitosis following treatment with genotoxic agents and is a marker for mitotic cell death (Chang et al. 1999; Vitale et al. 2011).

Following treatment with 2.2 μM cisplatin for 96 h (a dose that inhibited 85% of growth at 96 h), 47% of HT1080 3′SS6 human fibrosarcoma cells were micronucleated (Chang et al. 1999). SKOV-3 ovarian carcinoma cells treated with 33 μM cisplatin also displayed increased micronucleation following treatment (Vakifahmetoglu et al. 2008). Furthermore, treatment with either oxaliplatin or cisplatin induced micronucleation in

TE7 oesophageal cancer cells (Ngan et al. 2007). Again, these studies identified that cisplatin can induce cell death following entry into mitosis, but did not address how these cells entered mitosis or investigate if these cells were undergoing checkpoint adaptation. It is important to understand if cells treated with cisplatin undergo checkpoint adaptation or not because the final step of the process (entry into mitosis with damaged DNA) may contribute to genomic instability in cancer cells treated with cisplatin.

Treatment with cisplatin is associated with the induction of chromosomal aberrations that occur when treated cells enter mitosis. Bone marrow cells from either mice or Wistar rats treated with cisplatin contained an increased number of chromosome aberrations by comparison to not treated cells, as determined by microscopic analyses of metaphase spreads (Adler and el-Tarras 1989; Edelweiss et al. 1995). The induction of chromosomal aberrations was also observed following treatment of CHO cells with cisplatin. Krishnaswamy and Dewey (1993) found that 90.5% of CHO cells treated with 13 μM cisplatin in G1 phase entered mitosis by 28 h, as determined by trapping of mitotic cells using colcemid and multinucleation (Krishnaswamy and Dewey 1993). These authors found that as the average number of chromosome aberrations per cell increased, the fraction of cells surviving treatment decreased. They therefore suggest that entry into mitosis with chromosome aberrations in the form of chromosome/chromatid breaks and chromosome/chromatid exchanges is correlated with cisplatin induced cell death, but did not study if any cells could survive mitosis with chromosome aberrations. It is necessary to understand if cells survive mitosis with chromosome aberrations because it is possible that some cells could survive this process with rearranged genomes (discussed in section 1.10.2). This could decrease the efficacy of cisplatin by promoting the genetic changes

necessary for acquired resistance to treatment. Krishnaswamy and Dewey (1993) also suggest that cell death is enhanced when cells treated with cisplatin enter mitosis. This may mean that it is necessary for cells treated with cisplatin to enter mitosis to die, however this has not been investigated.

1.8 The DNA damage response and the G2/M checkpoint

The DNA damage response (DDR) consists of a network of DNA damage sensor, transducer and effector proteins (Zhou and Elledge 2000). These proteins initiate cell cycle checkpoints, signal for the repair of damaged DNA and are responsible for cell fate depending on whether DNA damage is repaired or not (Bartek and Lukas 2007). The DDR is an important response in eukaryotic organisms and the main proteins are conserved from yeasts to humans (Rhind and Russell 2000).

The DDR is activated by the large serine/threonine kinases, ataxia telangiectasia mutated (ATM) and ATM and Rad3-related (ATR) (Figure 1.2). These two kinases act as signal transducers and have been reported to phosphorylate as many as 700 different proteins on 900 different sites in response to 10 Gray ionising radiation (Matsuoka et al. 2007). Some of these downstream substrates included proteins involved in cell cycle checkpoint activation, DNA replication and DNA damage repair (Matsuoka et al. 2007). ATM and ATR are activated by different types of DNA damage, but the pathways that they activate are subject to large amounts of cross-talk (Kastan and Bartek 2004). ATM responds to DSBs (Kastan and Bartek 2004) while ATR responds to single-stranded DNA (ssDNA) that is generated by stalled replication forks or by DSB end-processing (Zhou and Elledge 2000).

A common substrate for ATM and ATR is the histone variant H2AX (Burma et al. 2001; Ward and Chen 2001). Histone H2AX is phosphorylated on serine 139 by ATM and ATR, becoming histone γH2AX (Rogakou et al. 1998). Histone γH2AX signals that DNA damage has occurred and is required for the assembly of DDR and DNA damage repair proteins, such as mediator of DNA damage checkpoint 1 (MDC1), at sites of damaged DNA. If damaged DNA is repaired then histone γH2AX is dephosphorylated by protein phosphatase 1 (PP1) (Nazarov et al. 2003) and protein phosphatase 2 (PP2) (Chowdhury et al. 2005). Because histone H2AX is phosphorylated when DNA damage occurs and dephosphorylated when DNA damage is repaired, it can be used to detect damaged DNA in cells (Rogakou et al. 1998; Furuta et al. 2003).

To engage the G1/S checkpoint, Cdk2 must be inhibited and this can occur by two different pathways. First, ATM and ATR activate the checkpoint kinases Chk1 and Chk2 which target the Cdc25A phosphatase for ubiquitination and proteasomal degradation (Zhao and Piwnica-Worms 2001; Sørensen et al. 2003). This prevents the dephosphorylation of Cdk2 and thus prevents the initiation of DNA replication (Lukas et al. 2004). This Chk2 mediated response is reported to induce a transient G1/S arrest that only delays entry into S phase by several hours (Mailand et al. 2000; Falck et al. 2001). The G1/S arrest is prolonged by the p53-p21 pathway. In cells without damaged DNA, p53 is bound by the ubiquitin ligase mouse double minute 2 (Mdm2), ensuring that there is a rapid turnover of p53 (Khosravi et al. 1999; Maya et al. 2001). ATM and ATR phosphorylate p53 and Mdm2 and this leads to the stabilisation and accumulation of p53 protein (Lukas et al. 2004). p53 then acts as a transcription factor, increasing the levels of the Cdk inhibitor p21 (Zhivotovsky and Kroemer 2004). p53 also has a role in the

initiation of apoptosis if damaged DNA cannot be repaired following cell cycle arrest, by acting as a transcription factor for genes that encode the pro-apoptotic BAX, BID, NOXA and PUMA proteins (Zhivotovsky and Kroemer 2004).

The G1/S checkpoint is lost when p53 or p21 are either absent or not functional (Deng et al. 1995). This checkpoint is often defective in cancer cells, because many of them have mutations in the genes that encode either p53, pRb or p21 (Schwartz and Shah 2005; Rausch et al. 2012; Manning et al. 2013). This means that the only DNA damage checkpoint available to these cancer cells is the G2/M checkpoint (Kastan and Bartek 2004; Bucher and Britten 2008; Chen et al. 2012).

Both ATM and ATR are involved in the initiation of the G2/M checkpoint, however ATR is the main effector kinase associated with G2/M arrest (Smith et al. 2010). When ssDNA is present it is bound by replication protein A (RPA) (Zou and Elledge 2003a; Flynn and Zou 2011). RPA recruits the ATR-interacting protein (ATRIP) in complex with ATR and the Rad9-Rad1-Hus1 (9-1-1) complex to the ssDNA (Delacroix et al. 2007). The 9-1-1 complex then recruits DNA topoisomerase binding protein 1 (TOPBP1), which triggers the ATR-mediated phosphorylation of Chk1 (Delacroix et al. 2007). The Rad17-replication factor C complex, the 9-1-1 complex and the adaptor protein claspin are also required for Chk1 activation (Weiss et al. 2002; Chini and Chen 2003; Zou and Elledge 2003b). The Rad17-replication factor C complex acts as a clamp loader for the 9-1-1 complex (Zou and Elledge 2003a; Flynn and Zou 2011) and claspin links ATR and Chk1, allowing for the phosphorylation of Chk1 on serine 317 and serine 345 (Liu et al. 2000; Zhao and Piwnica-Worms 2001; Kumagai et al. 2006). Of these

phosphorylation sites, serine 345 is essential for Chk1 activation while serine 317 plays a contributory role (Walker et al. 2009).

Once active, Chk1 prevents the activation of Cdk1 by phosphorylating Cdc25A and Cdc25C, targeting them for cytoplasmic sequestration by the 14-3-3 proteins (Lopez-Girona et al. 1999; Graves et al. 2001) or for ubiquitination and degradation by the proteasome (Ferguson et al. 2005; Jin et al. 2008). This prevents the removal of inhibitory phosphates on threonine 14 and tyrosine 15 of Cdk1, preventing Cdk1 activity. Active Chk1 also stabilises the Wee1 kinase, which is responsible for phosphorylating tyrosine 15 of Cdk1 (Lee et al. 2001).

It has been reported that Chk1, but not Chk2, is essential for the activation of the G2/M checkpoint. In 2000, Liu *et al*. generated an inducible Chk1 deficient line of murine embryonic stem cells (Liu et al. 2000). They found that when this cell line was irradiated and Chk1 depleted, these cells abrogated the G2/M checkpoint (Liu et al. 2000). It has also been demonstrated that H1299 human lung carcinoma cells treated with doxorubicin (a topoisomerase II inhibitor) and transfected with Chk1 small interfering RNA (siRNA) abrogated the G2/M checkpoint (Chen et al. 2003). Furthermore, when $p53^{-/-}$ HCT116 human colon carcinoma cells were treated with the genotoxic agent lidamycin, cells transfected with Chk1 siRNA abrogated the G2/M checkpoint (Pan et al. 2009). By contrast, cells transfected with Chk2 siRNA remained arrested at the G2/M checkpoint (Pan et al. 2009). Chk1 phosphorylation on serine 345 is a good measure of whether cells are arrested at the G2/M checkpoint or not. The detection of Chk1 phosphorylated on serine 345 can therefore be used to determine whether cells have activated and then abrogated the G2/M checkpoint, the second step of checkpoint

adaptation. Phosphorylation of Chk1 at serine 345 is present in interphase cells but lost in mitotic cells following the second step of checkpoint adaptation (Kubara et al. 2012). Cell cycle arrest in G2/M phases can also be detected using flow cytometry to quantify the DNA content of cells.

1.8.1 Histone γH2AX as an experimental marker for damaged DNA

DNA is packaged by coiling around nucleosomes. Each nucleosome is made up of eight proteins, two each from the H2A, H2B, H3 and H4 histone families. Histone H2AX is a histone variant of the H2A histone family that is phosphorylated on serine 139 following DNA damage, becoming histone γH2AX (Rogakou et al. 1998). The phosphorylation of histone H2AX was first characterised in response to DSBs induced by ionising radiation (Rogakou et al. 1998). Treatment with ionising radiation typically induces the formation of histone γH2AX foci and these can be detected experimentally, as a marker for DNA damage (Sharma et al. 2012). However, histone γH2AX formation can be induced by different kinases depending on how damaged DNA is induced and can also appear as either distinct foci or be pan-nuclear.

In response to DNA damage, histone H2AX can be phosphorylated by ATM, ATR or DNA-dependent protein kinase catalytic subunit (DNA-PKcs). ATM and DNA-PKcs both phosphorylate histone H2AX following ionising radiation (Stiff et al. 2004) whereas ATR phosphorylates histone H2AX following replication induced DNA DSBs (Furuta et al. 2003). Histone γH2AX staining following treatment with CPT is mediated by ATR. When cells that were either dominant negative for ATR (GM847/ATRkd) or deficient in ATM (AT fibroblasts) were treated with 1 μM CPT for 3 h, the ATR deficient cell line contained less histone γH2AX by comparison to the ATR proficient cell line and

the ATM deficient cell line (Furuta et al. 2003). Replication induced DSBs that lead to histone γH2AX formation by ATR occur when DNA lesions and SSBs are met by replication forks (Kuzminov 2001). DNA lesions and SSBs are induced by genotoxic agents such as ultra-violet (UV) irradiation, alkylating agents, topoisomerase I inhibitors and the platinum agents. In HCT116 human colorectal carcinoma cells treated with 1 μM CPT, histone γH2AX formation depends on DNA replication and can be prevented by co-treating these cells with the replication inhibitor aphidicolin (Furuta et al. 2003).

The pattern of histone γH2AX formation differs depending on which genotoxic agent cells are treated with and the amount of damaged DNA induced. Ionising radiation induces the formation of histone γH2AX foci but histone γH2AX formation can also be pan-nuclear. UV irradiation induces histone γH2AX formation without inducing direct DSBs and when detected by staining, the histone γH2AX signal is pan-nuclear (Limoli et al. 2001; Marti et al. 2006). Histone γH2AX formation in primary human fibroblasts was found to be mostly pan-nuclear following treatment with 20 J/m^2 UV irradiation (Marti et al. 2006). Marti *et al*. suggest that this γH2AX formation is related to NER. Cells that were deficient in either of the NER proteins xeroderma pigmentosum (XP) XPA or XPC had histone γH2AX levels that were only 1.2 fold higher than in mock-treated cells, by comparison to histone γH2AX levels that were 2.3 fold higher in treated normal cells (Marti et al. 2006). The results from this study might also be applicable to other genotoxic agents that do not directly induce DSBs following treatment.

Pan-nuclear histone γH2AX staining has also been observed in normal human fibroblast, U2OS human osteosarcoma, MEF mouse fibroblast, AA8 CHO and $XPA^{-/-}$ human fibroblast cell lines, following clustered DNA damage induced by localised heavy

ion irradiation with either gold or xenon ions (Meyer et al. 2013). This pan-nuclear staining was mediated by ATM and DNA-PK (Meyer et al. 2013) and this study suggests that pan-nuclear staining can occur when a localised area of DNA undergoes severe DNA damage.

Cells treated with cisplatin stain positive for histone γH2AX (Olive and Bánáth 2009). However, similar to UV irradiation, treatment with cisplatin does not induce direct DSBs (Clingen et al. 2008; Olive and Bánáth 2009). DSBs are formed when cisplatin treated cells replicate their DNA. Replicating (incubated in growth medium) *S. cerevisiae* cells treated for 1 h with 1.7 mM cisplatin contained DSBs whereas non replicating (incubated in non-growth medium) cells did not contain DSBs following treatment (Frankenberg-Schwager et al. 2005). This suggests that cells treated with cisplatin might induce histone γH2AX formation by a similar mechanism to cells treated with UV irradiation.

In 2009, Olive and Bánáth investigated the relationship between treatment with cisplatin and histone γH2AX formation (Olive and Bánáth 2009). These authors found that histone γH2AX levels peaked at 18 h, following treatment of V79 CHO cells for 2 h with either 7, 17 or 33 μM cisplatin, as determined by flow cytometry. Furthermore the levels of histone γH2AX present in these V79 cells increased as cisplatin concentration increased. Olive and Bánáth (2009) also found that histone γH2AX formation required DNA replication following treatment, unless very high doses of cisplatin were used for treatment (Olive and Bánáth 2009). This reflects the importance of considering dose or concentration in experiments. The time needed for histone γH2AX formation was shorter for cell lines with a shorter cell cycle time and flow cytometry data indicated that cells

were not positive for histone γH2AX until S phase. These authors also found that there was a correlation between how long histone γH2AX staining remained after treatment with cisplatin and cisplatin induced cell death (Olive and Bánáth 2009).

The timing of histone γH2AX formation can also differ depending on the genotoxic agent used to treat cells. Ionising radiation induces histone γH2AX formation within minutes, with levels peaking 30 min after treatment whereas histone γH2AX formation is detectable 1 h following UV irradiation, peaking at 2 h and being maintained until 8 h (Marti et al. 2006). Olive and Bánáth found that histone γH2AX levels took 18 h to peak in V79 cells treated for 2 h with 7, 17 or 33 μM cisplatin (Olive and Bánáth 2009). Furthermore, Huang *et al*. (2004) found that histone γH2AX levels in HL-60 promyelocytic leukaemia cells treated with TPT peaked 1.5 h following treatment, whereas histone γH2AX levels in cells treated with cisplatin peaked 3 h following treatment (Huang et al. 2004). These data suggest that the timing of histone γH2AX formation depends on the mechanism of action of the genotoxic agent used as a treatment.

The data from all of these studies show that histone γH2AX is a sensitive marker to detect damaged DNA in cells treated with a variety of genotoxic agents. However, these studies also highlight that it is not possible to detect the precise types of DNA damage induced by a genotoxic agent using histone γH2AX staining and detection. Although histone γH2AX staining detects DSBs it also detects other types of damaged DNA such as the DNA lesions induced by UV irradiation and cisplatin (Marti et al. 2006; Olive and Bánáth 2009; de Feraudy et al. 2010; Revet et al 2011). Thus it is possible to use histone γH2AX staining to experimentally detect and quantify damaged DNA, but it

cannot be used to confirm the presence of DSBs by comparison to other DNA lesions in cells treated with genotoxic agents that do not directly induce DSBs.

1.9 Outcomes following initiation of the G2/M checkpoint

The pathways that are involved in the initiation of DNA damage checkpoints are relatively well-understood. By contrast, the pathways associated with cell fate after the initiation of DNA damage checkpoints are less well understood. After the initiation of the G2/M checkpoint, cells can: 1) later continue with the cell cycle and enter mitosis; 2) die without entering mitosis or 3) undergo cellular senescence. The cellular response following the initiation of the G2/M checkpoint depends on many factors including: the type, quantity and location of DNA damage; whether a cell is cancerous or not; the tissue a cell originates from and the mutation status of genes that encode proteins with a key role in the DDR, such as p53 (Bunz et al. 1998; Shaltiel et al. 2015). Cells that die without entering mitosis may do so by undergoing apoptosis, necrosis or autophagy. Cells that enter mitosis following G2/M arrest do so by either checkpoint recovery or checkpoint adaptation and these have different implications for cell fate.

1.9.1 Checkpoint recovery

When damaged DNA is repaired, cells may continue with the cell cycle and enter mitosis by checkpoint recovery (Bartek and Lukas 2007; Shaltiel et al. 2015). Checkpoint recovery involves the disassembly of DNA damage foci as damaged DNA is repaired and Cdk1-cyclin B activity. Checkpoint recovery is a complex task that involves many cellular proteins acting in a highly regulated manner (Shaltiel et al. 2015). The major players in checkpoint initiation, such as histone γH2AX, ATM, ATR and Chk1 must be

deactivated by dephosphorylation. The phosphatases responsible for dephosphorylating the active checkpoint proteins must be activated in a controlled manner (Shaltiel et al. 2015). Cells that undergo checkpoint recovery completely repair their damaged DNA before entering mitosis. They can therefore divide their DNA during mitosis without an elevated risk of genomic instability.

1.9.2 A history of checkpoint adaptation

Checkpoint adaptation is the process of entering mitosis with damaged DNA and is defined by three sequential steps: 1) a cell cycle arrest induced by DNA damage; 2) overcoming this arrest and 3) resuming the cell cycle with damaged DNA (Figure 1.3) (Toczyski et al. 1997). Checkpoint adaptation was first observed in 1993 by Sandell and Zakian (Sandell and Zakian 1993). DNA damage repair deficient *S. cerevisiae* cells initiated and then overcame a G2 arrest following the loss of telomeric DNA from an extra, dispensable chromosome (Sandell and Zakian 1993).

Since the discovery that *S. cerevisiae* cells undergo checkpoint adaptation, several different research groups have explored this process in yeast cells. Because the DNA damage response is highly conserved in eukaryotes, some of this research may provide insight into how checkpoint adaptation is induced in other eukaryotic organisms such as humans. However, there are differences between G2/M checkpoint control in human and *S. cerevisiae* cells. As described in section 1.8, inhibitory phosphorylation of Cdk1 is maintained by activation of Chk1 in human cells arrested at the G2/M checkpoint. This prevents cells from entering mitosis with damaged DNA. In *S. cerevisiae*, arrest at the DNA damage checkpoint does not require inhibitory phosphorylation of Cdk1 and two distinct pathways are involved in activation of the DNA damage checkpoint (Sanchez et

al. 1999). One pathway involves Chk1 and one involves Rad53, a second checkpoint kinase that is homologous to human Chk2. These pathways have different roles in the checkpoint following DNA damage; the Chk1 pathway acts pre-anaphase to prevent chromosome segregation whereas the Rad53 pathway prevents mitotic exit (Sanchez et al. 1999). Both of these kinases are activated by Mec1, the yeast homologue of ATR (Weinert et al. 1994). Sanchez *et al*. (1999) found that Chk1 can prevent entry into anaphase by controlling both phosphorylation and levels of Pds1, preventing cleavage of cohesin. Furthermore, they suggest that Rad53 induces cell cycle arrest through inhibitory phosphorylation of its substrate Cdc5 and show that overexpression of Cdc5 overrides checkpoint arrest (Sanchez et al. 1999). Cdc5 is a polo-like kinase that induces mitotic exit by phosphorylating and inactivating proteins such as the Bfa1-Bub2 complex (Hu et al. 2001). Bfa1-Bub2 are part of the mitotic exit network (MEN) and prevent mitotic exit until mitosis is complete (Hu et al. 2001).

That Cdc5 has a role in checkpoint adaptation in *S. cerevisiae* was first observed in 1997. Toczyski *et al*. (1997) identified two *S. cerevisiae* mutants that were checkpoint adaptation deficient in response to a single dsDNA break induced using the same *S.cerevisiae* model and method as Sandell and Zakian (Toczyski et al. 1997). One of the mutants identified contained mutated CDC5 and the other mutated CKB2. Cdc5 is a member of the polo-like kinase (Plk) family of proteins. CKB2 encodes a nonessential subunit of casein kinase II (CKII), a serine-threonine kinase that is implicated in a number of pathways including the phosphorylation of the PP2 like phosphatase Ptc2 (Leroy et al. 2003).

In 2001, Galgoczy and Toczyski used the Cdc5 mutant checkpoint adaptation deficient *S. cerevisiae* strain to investigate the effects of checkpoint adaptation on cell viability and genomic instability (Galgoczy and Toczyski 2001). They found that checkpoint adaptation increased cell viability when DNA damage was induced in a nonessential chromosome. Furthermore, they demonstrated that checkpoint adaptation proficient cells irradiated with 30 Gray of X-rays contained more chromosomal losses and translocations, by comparison to checkpoint adaptation deficient cells. This indicates that checkpoint adaptation has a role in the induction of genomic instability in yeast (discussed in section 1.10.2). Pellicioli *et al*. (2001) also used *S. cerevisiae* checkpoint adaptation proficient and deficient cells to investigate checkpoint adaptation and found that the kinase activity of Rad53 was elevated for over 24 h in Cdc5 checkpoint adaptation deficient mutants, whereas Rad53 kinase phosphorylation and activity was lost in cells that underwent checkpoint adaptation (Pellicioli et al. 2001). Overexpression of Rad53 also prevented cells from undergoing checkpoint adaptation in response to the induction of a DSB. These data support the results from Sanchez *et al*. (1999) which demonstrated that Rad53 inhibited Cdc5, preventing mitotic entry (Sanchez et al. 1999).

Further studies have since confirmed that both Rad53 and Cdc5 have important roles in checkpoint adaptation in *S. cerevisiae*. Rad53 is dephosphorylated and inactivated by the PP2C like phosphatase Ptc2, promoting checkpoint adaptation (Leroy et al. 2003). When the PTC2 gene was deleted, checkpoint adaptation proficient cells were unable to undergo checkpoint adaptation and when Ptc2 was overexpressed in checkpoint adaptation deficient cells the ability to undergo checkpoint adaptation was restored (Leroy et al. 2003). To dephosphorylate Rad53, Ptc2 must be phosphorylated on

threonine 376 and the CKII kinase is responsible for this (Guilleman *et al*. 2007). This might explain why Toczyski *et al*. found that one of the checkpoint adaptation deficient mutants they discovered contained mutated CKII (Toczyski et al. 1997). In addition to Rad53 dephosphorylation, Rad53 deacetylation also has a role in checkpoint adaptation. Deletion of the histone deacetylase Rpd3 prevents checkpoint adaptation and leads to an increased level of acetylation on Rad53 (Tao et al. 2013). Checkpoint adaptation is therefore promoted by deacetylation and inhibition of Rad53.

To date the precise biochemical pathway that induces checkpoint adaptation in *S. cerevisiae* has not been identified. However, it has been demonstrated that the checkpoint kinase Rad53 and the polo-like kinase Cdc5 have central roles in this process. This reflects the important roles of Rad53 and Cdc5 in the control of the cell cycle in budding yeast. Recently, proteins involved in several cellular responses that are not directly involved in checkpoint control have been identified as having a role in the biochemical pathway(s) that induce(s) checkpoint adaptation. Many of these studies have used checkpoint adaptation deficient mutants to identify proteins that might be involved in checkpoint adaptation. However these studies are not usually capable of elucidating the precise role of these proteins in checkpoint adaptation.

In 2015 Ghospurkar *et al*. identified that phosphorylation of replication factor A2 (Rfa2), the yeast homologue of RPA, induced *S. cerevisiae* cells to undergo checkpoint adaptation (Ghospurkar et al. 2015). Cells with a phosphomimetic form of Rfa2, where all serine/threonines in the N-terminal domain (9 amino acids) were mutated to aspartic acid, underwent checkpoint adaptation. Furthermore, checkpoint adaptation deficient cells expressing these phosphomimetic proteins also underwent checkpoint adaptation. The

authors therefore propose that the induction of checkpoint adaptation occurs when the Rfa proteins (Rfa1 and Rfa2) are modified following prolonged arrest at the DNA damage checkpoint (Ghospurkar et al. 2015).

Chromatin remodelling proteins are also involved in checkpoint adaptation. This was first demonstrated by Lee *et al*. (2001) who found that checkpoint adaptation deficient *S. cerevisiae* cells contained mutated Rdh54/Tid1 (Lee *et al*. 2001). In 2006 Papamichos-Chronakis *et al*. found that the chromatin remodelling protein Ino80 was required for checkpoint adaptation in *S. cerevisiae* following the induction of a DSB (Papamichos-Chronakis et al. 2006). In 2012, Eapen *et al*. found that checkpoint deficient *S. cerevisiae* cells contained mutant Fun30, a chromatin remodelling protein involved in HR (Eapen et al. 2012). The role of these chromatin remodelling proteins in checkpoint adaptation remains to be elucidated.

These *S. cerevisiae* studies indicate that checkpoint adaptation is an important area of research, of interest to researchers worldwide. Because checkpoint adaptation increases the number *S. cerevisiae* cells that survive a DNA damaging event and also increases genomic instability (Galgoczy and Toczyski 2001), it has been suggested that checkpoint adaptation may be important in the development of tumourigenesis (Vidanes et al. 2010). Additionally, these studies indicate that a polo-like kinase and checkpoint kinases are central to checkpoint adaptation in *S. cerevisiae*. These data provide starting points for elucidating the biochemical pathway(s) that induce(s) checkpoint adaptation in higher eukaryotes. However, these studies also highlight the complexity of checkpoint adaptation and the need for more research in this area. Furthermore, although proteins involved in the DNA damage response and cell cycle regulation are largely evolutionarily

conserved across eukaryotes, from yeasts to humans, the regulation of cell cycle checkpoints in *S. cerevisiae* is not identical to the regulation of cell cycle checkpoints in humans. To understand better the process of checkpoint adaptation in humans it is therefore necessary to use human model systems such as human cancer cell lines.

Initially it was proposed that checkpoint adaptation would only occur in unicellular organisms, as a last attempt at survival if DNA damage repair was not successful (Lupardus and Cimprich 2004). This is because entry into mitosis with damaged DNA in multicellular organisms may have a detrimental effect on the survival of the organism as a whole, by increasing the risk of genomic instability. By contrast, unicellular organisms have nothing to lose by attempting cell division when DNA damage is irreparable (Lupardus and Cimprich 2004; Syljuåsen 2007). However, in 2004, Yoo *et al*. described checkpoint adaptation in *Xenopus* oocyte extracts (Yoo et al. 2004). Yoo *et al*. reported that when they blocked DNA replication with aphidicolin, the cell free extracts arrested in interphase and then entered mitosis with only partially replicated chromosomes (Yoo et al. 2004). Because *Xenopus* are multi-cellular organisms this suggested, for the first time, that checkpoint adaptation may also occur in other metazoans, such as humans (Lupardus and Cimprich 2004; Yoo et al. 2004). However, *Xenopus* oocyte extracts are different from somatic cells because they are a cell free system without intact cell membranes. They also rapidly alternate between S phase and mitosis without G1 or G2 phases of the cell cycle (Kappas et al. 2000).

Checkpoint adaptation was next identified in plant cells, in early 2006. The pathways involved in DNA damage repair and the cell cycle checkpoints are largely conserved in all eukaryotes, including plants (Carballo et al. 2006). Root cells from

Allium cepa were irradiated with 2.5 to 40 Gray X-rays and analysed for entry into mitosis with damaged DNA (Carballo et al. 2006). Cells arrested at G2/M following X-ray irradiation with either 5, 10, 20 or 40 Gray. An increase of apoptotic cells was also observed when cells were treated with 20 and 40 Gray X-rays. The number of apoptotic cells relative to the not treated control cells increased at 16 h following treatment with 20 Gray and at 4 h following treatment with 40 Gray. However, some cells treated with either of these doses of X-rays still underwent checkpoint adaptation following treatment, albeit at later times by comparison to cells treated with 5 and 10 Gray X-rays. The authors also scored the mitotic cells for aberrant mitoses. Broken chromatids and acentric chromosomal fragments (lacking a centromere) were observed in some cells that were in either metaphase, anaphase or telophase. When the percentages of aberrant mitoses were quantified following treatment with either 5, 10, 20 or 40 Gray X-rays, between 20% and 90% of mitoses were aberrant. Furthermore, the percentage of aberrant mitoses depended on the dose of X-ray irradiation and time after treatment. Cells were fixed at 0, 2 and 4 h and then at 4 h intervals to 24 h. A consistent number of mitoses were aberrant when cells were treated with 5 Gray X-rays between 2 and 24 h following treatment (between 50 and 70%). By contrast, 90% of mitoses were aberrant 24 h after treatment with either 20 or 40 Gray. Cells treated with either 20 or 40 Gray X-rays did not enter mitosis between 4 and 20 h following treatment. This suggested that they arrested at the G2/M checkpoint for a long time before entering mitosis by comparison to cells treated with 10 Gray, which entered mitosis at 16 h, and cells treated with 5 Gray, which entered mitosis at all times tested between 2 and 24 h. This study demonstrates that chromosome aberrations are present when cells undergo checkpoint adaptation, which may lead to genomic instability in cells that survive this process (discussed in section 1.10.2). Additionally, these results

suggest that cells enter mitosis at different times when they have different levels of damaged DNA; cells treated with higher doses of X-rays took longer to enter mitosis with damaged DNA (the final step of checkpoint adaptation) by comparison to cells treated with lower doses of X-rays.

1.9.3 Checkpoint adaptation in human cells

Checkpoint adaptation was first observed in human cancer cells in 2006 (Syljuåsen et al. 2006). Syljuåsen *et al*. treated U2OS cells with 6 Gray of ionising radiation and cells accumulated in G2 phase of the cell cycle. Cells were arrested at the G2/M checkpoint, as shown by flow cytometry and by Chk1 phosphorylation on serine 345 (Syljuåsen et al. 2006). The arrested cells then began to enter mitosis with damaged DNA, observed by the detection of histone γH2AX and phosphorylated serine 10 histone H3 staining using immunofluorescence microscopy. The authors found that when Chk1 was inhibited in irradiated cells by the Chk1 inhibitor UCN-01, more cells were in mitosis 18 h following treatment, by comparison to cells treated with 6 Gray ionising radiation alone (Syljuåsen et al. 2006). Furthermore, cells that inducibly over-expressed Chk1 arrested in G2 for longer than cells with wild type levels of Chk1 following treatment with 6 Gray ionising radiation. Because the polo-like kinase Cdc5 has a role in checkpoint adaptation in *S. cerevisiae* (Toczyski et al. 1997) and Plk1 was implicated in checkpoint adaptation in *Xenopus* egg extracts (Yoo et al. 2004), Syljuåsen *et al*. tested if Plk1 has a role in checkpoint adaptation in human cancer cells. Plk1 was depleted by siRNA in U2OS cells which were then treated with ionising radiation. These cells accumulated in G2/M 19 h after treatment, but did not enter mitosis, suggesting that Plk1 has a role in checkpoint adaptation in human cancer cells. However, the authors did not

determine whether checkpoint adaptation was prevented or just delayed as a result of inhibiting Plk1. Similar to the studies in *S. cerevisiae*, the results of Syljuåsen *et al*. implicated Chk1 and Plk1 in the pathway of checkpoint adaptation in human cells. However, it was unclear if this process was clinically relevant, because humans are unable to tolerate a single dose of 6 Gray of ionising radiation and are treated with fractions of ionising radiation in the clinic (Bernier et al. 2004).

The question of whether or not checkpoint adaptation occurs in cancer cells treated with fractionated doses of ionising radiation was addressed in 2011. Rezacova *et al*. (2011) reported that 26% of MOLT4 leukaemia cells treated with fractionated radiation initiated a G2/M arrest 48 h after treatment, before entering mitosis with damaged DNA (Rezacova et al. 2011). However, it was still unknown whether checkpoint adaptation occurred in response to treatments other than ionising radiation.

In 2012, checkpoint adaptation was observed in HT-29 cells treated with either CPT or etoposide and in M059K human glioma cells treated with CPT (Kubara et al. 2012). Kubara *et al*. (2012) demonstrated that HT-29 cells treated with 25 nM CPT for 48 h were arrested in G2/M phase, by analysing DNA content using flow cytometry and by the detection of serine 345 phosphorylated Chk1. These CPT treated cells then entered mitosis with damaged DNA; they contained high levels of cyclin B1, had decreased levels of Cdk1 phosphorylated on tyrosine 15 and were positive for histone γH2AX and phosphorylated serine 10 histone H3 staining (Kubara et al. 2012). Furthermore, Kubara *et al*. also demonstrated that entry into mitosis with damaged DNA could be prevented by co-treatment with the Cdk1 inhibitor CR8 (Kubara et al. 2012). Because HT-29 and

M059K cells treated with CPT undergo checkpoint adaptation, CPT can be used as a positive control for checkpoint adaptation in these cell lines.

Kubara *et al*. also investigated the roles of Chk1 and Plk1 in checkpoint adaptation. HT-29 cells treated with CPT for 24 h and then with CPT and a Plk1 inhibitor for a further 24 h were partially prevented from entering mitosis with damaged DNA. However, there was only a slight decrease in the percentage of mitotic cells present in cells co-treated with CPT and Plk1 inhibitor, by comparison to cells treated with CPT alone (Kubara et al. 2012). This suggests that proteins other than Plk1 are involved in checkpoint adaptation in human cancer cells.

The role of Plk1 in human checkpoint adaptation remains unclear. In 2014, Liang *et al*. studied how single U2OS cells from a cell population treated with 1.5 Gray ionising radiation responded to activation of the G2/M checkpoint (Liang et al. 2014). They found that different cells from the same population entered mitosis after a G2/M arrest at different times and with different levels of damaged DNA (Liang et al. 2014). This entry into mitosis was reported to be dependent on levels of Plk1 and cyclin B. However, unpublished results from the laboratory of R. H. Medema indicate that inducing expression of a constitutively active Plk1 mutant was not capable of over-riding an established DNA damage induced checkpoint (Shaltiel et al. 2015). The full molecular pathway(s) that are involved in the cellular induction of checkpoint adaptation therefore remain to be elucidated.

In their investigation of checkpoint adaptation, Kubara *et al*. (2012) used HT-29 cells because these cells display a pronounced rounded morphology when in mitosis (Kubara et al. 2012). HT-29 cells also spend a long time arrested in mitosis following

treatment. HT-29 cells treated with either nocodazole or taxol spend longer in mitosis by comparison to H1703 human non-small cell lung cancer and RKO human colon carcinoma cells treated with either nocodazole or taxol (Gascoigne and Taylor 2008). Additionally, HT-29 cells treated with the Eg5 mitotic kinesin inhibitor AZ138 spend longer in mitosis by comparison to HCT116 human colorectal adenocarcinoma, RKO, DLD-1 human colorectal adenocarcinoma and SW480 human colorectal adenocarcinoma cell lines (Gascoigne and Taylor 2008).

1.9.4 Cisplatin and checkpoint adaptation

Using HT-29 cells, Kubara *et al*. were the first to report that checkpoint adaptation occurs in response to treatment with chemical genotoxic agents (Kubara et al. 2012), as opposed to treatment with the physical agent ionising radiation. In this thesis, we build on this study by investigating if checkpoint adaptation occurs in response to treatment with cisplatin, which is a chemical genotoxic agent with a different mechanism of action to CPT and etoposide. Furthermore, we ask whether checkpoint adaptation is a major event in response to treatment with cisplatin. The fraction of cells that undergo checkpoint adaptation following treatment with genotoxic agents has not previously been quantified. If checkpoint adaptation is a major response in cells treated with different genotoxic agents, then it is likely a biologically significant event that lies between cell cycle arrest and cell death. However, it is unknown whether or not human cancer cells undergo checkpoint adaptation in response to treatment with genotoxic agents that damage DNA by a different mechanism of action to ionising radiation, CPT and etoposide.

As discussed in section 1.7.1, cisplatin has been widely used to treat cancer patients since it was approved for use in 1978, yet how cisplatin induces cell death is

poorly understood. Although cisplatin has been successful in prolonging the life of cancer patients, its long term efficacy can be limited by cells acquiring resistance to treatment (Kelland 2007). We reason that by understanding better the steps that lie between the cell cycle arrest induced by cisplatin and cell death then it might be possible to improve the efficacy of this genotoxic agent. Several studies have indicated that cells treated with cisplatin die by mitotic catastrophe (Demarq et al. 1994; Chang et al. 1999; Vakifahmetoglu 2008). Furthermore, as discussed in section 1.7.3, cells that entered mitosis with damaged DNA were positive for chromosomal aberrations (Adler and el-Tarras 1989; Krishnaswamy and Dewey 1993; Edelweiss et al. 1995) that could induce genomic instability. However, these studies did not investigate how cells were entering mitosis following treatment.

Two studies have previously suggested that cancer cells treated with cisplatin undergo checkpoint adaptation (Wang et al. 2008; Lewis 2014). However, neither of the studies were focused on the response of checkpoint adaptation itself. As such neither study fully confirmed that cells were entering mitosis with damaged DNA following a G2/M cell cycle arrest, nor investigated how many cells entered mitosis following treatment.

In 2008, Wang *et al*. found that 2-3% of HCC metastatic hepatocellular carcinoma cells were positive for serine 10 phosphorylated histone H3 following treatment with 3 μM cisplatin at 0, 12, 24 and 36 h after treatment (Wang et al. 2008). They also demonstrated that Chk1 was phosphorylated on serine 345 24 h after treatment with cisplatin. However, Chk1 was not active before this time so it may be that these cells did not arrest at the G2/M checkpoint before entering mitosis. The authors also did not

investigate if cells were entering mitosis with damaged DNA or compare the response of treated cells to not treated cells. Therefore, although the authors suggest that these cells underwent checkpoint adaptation, they did not fully test for this.

During the course of this thesis, Lewis and Golsteyn demonstrated that cisplatin induces the formation of micronuclei in M059K cells (Lewis 2014). This required a mitosis step, however, this study was focused on characterising micronuclei rather than investigating the biochemical steps leading to mitosis, which include those of checkpoint adaptation. Additionally, Lewis and Golsteyn found that WI-38 human non-cancerous lung fibroblast cells did not undergo checkpoint adaptation and that the number of micronuclei in these cells did not increase following treatment with cisplatin (Lewis 2014). These data suggest that the phenomenon of checkpoint adaptation could be limited to cancerous cells in humans.

In this thesis, we use HT-29 cells to investigate checkpoint adaptation. The pronounced cell rounding displayed by HT-29 cells in mitosis allows us to determine whether treated cells undergo checkpoint adaptation by using light and time-lapse microscopy. This pronounced cell rounding also allows the investigation of whether checkpoint adaptation is a major response to treatment or not by using time-lapse video microscopy to determine how many cells in a population display a rounded morphology (enter mitosis) following treatment. Because HT-29 cells spend a long time rounded and in mitosis following treatment, it is possible to separate mitotic cells from treated interphase cells so that the biochemical changes that occur during checkpoint adaptation can be explored. By investigating checkpoint adaptation in HT-29 cells treated with

cisplatin we are also able to compare the response of the same cell line treated with two different genotoxic agents, cisplatin and CPT.

1.10 The consequences of checkpoint adaptation

Checkpoint adaptation has several possible outcomes: 1) cells may die in mitosis; 2) cells may survive mitosis but die in subsequent phases of the cell cycle or 3) cells may survive mitosis and divide with damaged DNA (Figure 1.3) (Syljuåsen 2007; Kubara et al. 2012). It has been demonstrated that the majority of human cancer cells that undergo checkpoint adaptation will die (Syljuåsen et al. 2006; Kubara et al. 2012). This is the desired outcome of treating cancer cells with a genotoxic agent. However, checkpoint adaptation is also a mechanism by which cells can transmit damaged DNA to daughter cells. It is therefore likely that checkpoint adaptation is a source of genomic instability in human cells that undergo this process

1.10.1 The relationship between entry into mitosis with damaged DNA and genomic instability

Common causes of genomic instability are base substitutions, DNA insertions, DNA deletions, DNA translocations and a change in copy number (Stratton et al. 2009). Genomic instability can occur following DNA damage and two different events can induce this: 1) DNA damage mis-repair and 2) entry into mitosis with damaged DNA. DNA damage can be mis-repaired during interphase, inducing genomic rearrangements. Because NHEJ does not require homologous DNA sequence to repair DSBs, the ends of breaks from different chromosomes can be joined together, resulting in chromosomal translocations (Ferguson and Alt 2001).

Entry into mitosis with damaged DNA can also be a source of genomic instability. In 2006, Nakada *et al*. found that when ATM-deficient primary fibroblast cells prematurely entered mitosis after treatment with etoposide some cells survived with chromosomal translocations, including the 11q23 translocation associated with topoisomerase II inhibitor induced secondary leukaemia (Nakada et al. 2006). Entry into mitosis with damaged DNA induced by replication stress can also be a source of genomic instability. DNA damage induced by replication stress that occurred because of overexpression of the oncogene E2F1 induced chromosome bridge formation and aneuploidy (Ichijima et al. 2010). Replication stress can also occur in chromosomal instability positive (CIN^+) (aneuploid) human colorectal carcinoma cells lines and this was also found to induce structurally altered chromosomes that were subject to mis-segregation in mitosis, leading to genomic instability (Burrell et al. 2013). As described in section 1.7.3, cells treated with cisplatin can also enter mitosis with damaged DNA, leading to the induction of chromosome aberrations (Adler and el-Tarras 1989; Edelweiss et al. 1995).

Entry into mitosis with damaged DNA can lead to genomic instability by several different mechanisms. When DNA strand breaks occur, acentric fragments can be created (Jeggo and Löbrich 2006). These fragments can be lost during cell division because they lack centromeres and are unable to attach to the mitotic spindle (Hall and Giaccia 2012). These fragments can also be incorporated into micronuclei and then either lost or subjected to further genomic rearrangement (Crasta et al. 2012), discussed below. The loss of genetic material following treatment with genotoxic agents has been detected experimentally. LA-9 murine cells containing a stable chromosome with integrated green

fluorescent protein (GFP) were treated with either ionising radiation or etoposide and assessed for loss of GFP signal (Burns et al. 1999). An increase in the percentage of non-fluorescent cells was observed when cells were either irradiated (3 or 5 Gray) or treated with etoposide (0.5 and 1 μM), by comparison to the percentage of non-fluorescent cells in not treated cells (Burns et al. 1999).

DNA strand break repair is inhibited in mitosis, once sites of damaged DNA induced by irradiation have been marked by the formation of histone γH2AX and MDC1 foci (Zhang et al. 2011; Orthwein et al. 2014). Cdk1 activity is responsible for preventing DSB repair in mitosis by phosphorylating the key DSB repair protein RNF8 (a ubiquitin ligase) at threonine 198, preventing it from interacting with MDC1 (Orthwein et al. 2014). 53BP1 is also phosphorylated in mitosis, at threonine 1609 and serine 1618, preventing its recruitment to sites of damaged DNA. Because cells do not repair damaged DNA in mitosis, this means that when cells enter mitosis with damaged DNA, this damage can be transmitted to daughter cells. Instead of repairing damaged DNA in mitosis, mitotic cells progress to G1 where DNA damage repair can occur. Although repair of damaged DNA may occur in G1, it is possible that some genetic material could be lost or that micronuclei could form in cells in mitosis with damaged DNA, leading to genomic rearrangement. Furthermore, many cancer cells have a defective G1/S DNA damage checkpoint. It is therefore plausible that a cancer cell can continue through a second cell cycle with damaged DNA following entry into mitosis with DNA damage (the final step of checkpoint adaptation), contributing to genomic instability.

Aberrant mitoses are also frequently associated with the formation of micronuclei and this can induce further genomic rearrangement in cells. In 2012, Crasta *et al.*

demonstrated that micronuclei, formed by errors in chromosome segregation during mitosis, contribute to genomic instability (Crasta et al. 2012). Crasta *et al*. studied micronuclei in RPE-1 untransformed retinal pigment epithelial and U2OS cells (Crasta et al. 2012). Crasta *et al*. generated micronuclei in cells and then followed them through the cell cycle. The authors found that DNA contained in the micronuclei was damaged by DNA replication and that 7.6% of chromosome spreads prepared from cells with micronuclei contained pulverised chromosomes (Crasta et al. 2012). Additionally, Crasta *et al*. reported that micronuclei persisted for several generations and that the chromosomes contained in micronuclei could be re-incorporated into the nuclei of daughter cells (Crasta et al. 2012).

The chromosome shattering observed by Crasta *et al*. is called chromothripsis (Stephens et al. 2011). Chromothripsis describes a catastrophic event where tens to hundreds of genomic rearrangements are acquired in one or several regions of chromosomes (Stephens et al. 2011). A number of possibilities for how chromothripsis occurs have been suggested, including that chromothripsis occurs due to a high-energy ionising radiation event during mitosis, that DNA fragmentation occurs as a result of aborted apoptosis or that DSBs induced by genotoxic agents create dicentric fusions between sister chromatids that can be broken during mitosis (Forment et al. 2012). However, the model for chromosome pulverisation described by Crasta *et al*. is currently considered the most likely model for how chromothripsis arises (Forment et al. 2012). This model of chromothripsis is supported by a recent study from the same group of researchers where live cell imaging and single-cell genome sequencing were used to characterise micronucleated cells (Zhang et al. 2015). Combining these techniques

allowed the researchers to sequence cells where micronuclei were reincorporated into the main nucleus after one round of cell division. Zhang *et al*. used copy number analysis of the paired daughter cells present after the one round of cell division, to determine which chromosomes were present in the micronuclei. They found that the mis-segregated chromosomes had a large number of genomic rearrangements, by comparison to normally segregated control chromosomes, in 8 of the 9 daughter cell pairs studied (Zhang et al. 2015). To date these are the only studies that provide experimental evidence for how chromothripsis can occur, although chromothripsis has been observed in a number of different cancer types including glioma (Stephens et al. 2011; Cohen et al. 2015), melanoma (Stephens et al. 2011), multiple myeloma (Magrangeas et al. 2011), medulloblastoma, acute myeloid leukaemia (Rausch et al. 2012) and breast cancer (Przybytkowski et al. 2014). Additionally, chromothripsis has been detected in patients with congenital abnormalities (Kloosterman et al. 2011; Gamba et al. 2015; Bertelsen et al. 2015). Cells that undergo checkpoint adaptation enter mitosis with damaged DNA and it is likely that this induces aberrant mitoses that may lead to genomic rearrangement and the induction of micronuclei, which can contribute to chromothripsis.

Cells that enter mitosis with damaged DNA are at risk of genomic instability. However, the studies described above did not investigate how cells were entering mitosis following treatment or address whether these cells were undergoing checkpoint adaptation. Moreover, many of these studies did not investigate the long-term effects of entering mitosis with damaged DNA, to explore whether any of the cells in mitosis with chromosomal aberrations survive and whether any of these surviving cells contain

rearranged genomes. It is therefore necessary to explore how the process of checkpoint adaptation can contribute to the induction of genomic instability in cancer cells.

1.10.2 The relationship between checkpoint adaptation and genomic instability

As described in section 1.9.2, Galgoczy and Toczyski (2001) found that checkpoint adaptation in *S. cerevisiae* generated genomic rearrangements such as chromosome loss or chromosome rearrangement (Galgoczy and Toczyski 2001). Additionally, these authors demonstrated that checkpoint adaptation increased yeast survival following DNA damage and that adaptation deficient cells were less likely to survive a DNA damaging event (Galgoczy and Toczyski 2001). These data suggest that, in yeast, checkpoint adaptation may contribute to cell survival following a genotoxic event and that cells surviving checkpoint adaptation are more likely to contain rearranged genomes. Some plant cells that enter mitosis following treatment with 5, 10, 20 and 40 Gray X-rays also contained broken chromatids, acentric chromosomal fragments and chromosome bridges (Carballo et al. 2006). These data support the suggestion that checkpoint adaptation may induce genomic rearrangement in human cancer cells. However, these plant cells were fixed within 24 h of treatment so it is unknown if cells survived checkpoint adaptation with rearranged genomes or whether these chromosomal aberrations induced cell death.

To determine whether human cancer cells can survive checkpoint adaptation with rearranged genomes it is first necessary to collect cells undergoing checkpoint adaptation and then culture these cells to assess cell viability. HT-29 cells can be used for this type of analysis because they display a pronounced rounded morphology in mitosis and spend a long time in mitosis following treatment. This allows cells that have undergone

checkpoint adaptation and are in mitosis to be collected by mechanical shake-off. These cells can then be assessed for cell survival by the clonogenic assay (Rahman 2013). Furthermore, once survival cells have been identified these cells can be investigated to determine whether they contain rearranged genomes. Genomic rearrangement in these survival cells could be detected using cytogenetic techniques such as fluorescence *in situ* hybridisation (FISH) to observe centromeres, telomeres and chromosomal regions using fluorescent probes specific for these regions (Bishop 2010; Rahman 2013) and spectral karyotyping (SKY) which uses fluorescent probes of different colours to detect specific chromosomal regions (Imataka and Arisaka 2012). In addition to these techniques it will also be possible to sequence the genomes of individual cells surviving checkpoint adaptation, when advances are made in single cell DNA sequencing (Leung et al. 2015).

It has been reported that small numbers of HT-29 cells treated with CPT can survive entry into mitosis with damaged DNA (Kubara et al. 2012; Rahman 2013). Furthermore, preliminary data has suggested that HT-29 cells treated with CPT contain mitotic chromosomes that are shattered into different pieces (Rahman 2013). CPT treated HT-29 cells that survived checkpoint adaptation contained an average of 35 chromosomes, by comparison to not treated cells which contained an average of 65 chromosomes (Rahman 2013). It has also been reported that entry into mitosis increases the number of micronuclei present in M059K cells treated with cisplatin (Lewis 2014). Checkpoint adaptation may thus facilitate the formation of survival cells with rearranged genomes, as a consequence of these cells surviving entry into mitosis with damaged DNA.

Investigation of checkpoint adaptation can provide insight into the specific role of each step upon cell survival and genomic change. For example, cancer cells appear to need to enter mitosis following treatment with a genotoxic agent to facilitate cell death in other phases of the cell cycle (Lupardus and Cimprich 2004; Syljuåsen 2007). It is currently unknown whether cells that undergo checkpoint adaptation will still die if they are prevented from entering mitosis. If treated cancer cells can die when entry into mitosis with damaged DNA (the final step of checkpoint adaptation) is inhibited, then this could prevent cells from surviving treatment with rearranged genomes.

Current genotoxic anti-cancer treatments such as cisplatin, the agent used in this thesis, are often limited by acquired resistance to treatment, which is induced by genomic change (Wasenius et al. 1997; Wilson et al. 2005). By preventing treatment induced genomic change, it should be possible to prevent cells from acquiring resistance to treatment. These cancer cells would then be susceptible to cell killing induced by further rounds of treatment, improving the efficacy of genotoxic anti-cancer agents.

1.11 Cell death

Cell death or permanent growth arrest are the desired outcomes of cancer treatments. It is often assumed that cancer cells die by apoptosis following treatment with anti-cancer drugs and apoptosis has been extensively studied with regards to cancer development and treatment. However, other modes of cell death and growth arrest exist and understanding these may be equally or more important to understanding how cancer cells respond to current cancer treatments. Four types of cell death frequently discussed in the literature with regard to cancer therapies are apoptosis, necrosis, mitotic catastrophe

and autophagy. Senescence is also a desired outcome of cancer treatment, because senescent cells undergo permanent growth arrest.

1.11.1 Apoptosis

The term apoptosis was first used by Kerr *et al*. in 1972, following several years of research into a form of regulated cell death initially termed "shrinkage necrosis" (Kerr et al. 1972; Kerr 2008). Cell death by apoptosis was first described in 1885 by Walther Flemming, but this description of apoptosis was ignored at the time, even though Flemming was the originator of the term mitosis (Kerr 2008). In the mid-1960s, Lockshin and Williams were also studying regulated cell death and proposed the term "programmed cell death" (Lockshin and Zakeri 2008). The term programmed cell death is now synonymous with apoptosis, although it has since been shown that other types of cell death can also be programmed (Bredesen 2008). After 1990 research on apoptosis greatly increased, as genes involved in its regulation were discovered (Kerr 2008).

Apoptosis can be either extrinsically or intrinsically activated. The extrinsic pathway is activated in response to external signals and occurs through the binding of specific cytokines to cell surface receptors (Egger 2008). The intrinsic pathway is activated in response to internal factors such as excessive DNA damage or viral infection (Egger 2008). Activation of either pathway leads to the activation of caspases. Caspases are cysteine proteases which have a cysteine at their active site and cleave target polypeptides after aspartic acid residues in specific peptide sequences (Alnemri et al. 1996). Caspases degrade important cellular proteins such as those involved in cell division, DNA replication, DNA damage repair, RNA splicing and structure of the cytoskeleton (Fan et al. 2005). In mammals, specific endonucleases, endonuclease-G and

apoptosis inducing factor, are also activated (Susin et al. 1999; Li et al. 2001). This occurs in a caspase independent manner and these endonucleases are responsible for nuclear fragmentation, which is associated with apoptotic cell death (Danial and Korsmeyer 2004).

Intrinsic apoptosis involves the Bcl-2 family of proteins and the permeabilisation of the mitochondrial membrane (Zhivotovsky and Kroemer 2004). The Bcl-2 family of proteins consists of both pro- and anti- apoptotic proteins. Examples of anti-apoptotic proteins are Bcl-xL, Bcl-2 and Mcl-1 and examples of pro-apoptotic proteins are Bax, Bak, Bid and Puma. Bax and Bak begin the process of intrinsic apoptosis and exist as inactive monomers in the cell until apoptosis is initiated (Westphal et al. 2011). Bax is found in the cytosol while Bak is held inactive by binding to anti-apoptotic proteins such as Bcl-xL or Mcl-1 (Westphal et al. 2011). When active, Bax and Bak permeabilise the outer mitochondrial membrane releasing apoptosis initiating factors such as cytochrome c. Cytochrome c then binds to apoptotic protease-activating factor 1 forming the apoptosome and this recruits and activates the initiator pro-caspase 9 (Saikumar et al. 1999). Once cleaved and activated, caspase 9 cleaves the effector caspases 3 and 7 which cleave cellular proteins (Fan et al. 2005).

Extrinsic apoptosis is activated by specific tumour necrosis factor (TNF) signalling proteins (TNFα, FasL and TRAIL) and their respective TNFR receptors (Saikumar et al. 1999). When the receptors are bound by specific cytokines they initiate the activation of the initiator caspases 8 and 10 which in turn cleave and activate the effector caspases, leading to the cleavage of cellular proteins (Fan et al. 2005). Finally apoptotic cells are engulfed by phagocytes, allowing for the removal of apoptotic cells

without inducing an inflammatory response (Allen et al. 1997). The recognition of apoptotic cells by phagocytes is achieved by changes to the plasma membrane. During apoptosis a component of the inner leaflet of the plasma membrane, phosphatidylserine, is translocated to the outer leaflet of the plasma membrane and acts as a recognition signal for phagocytes (Fadok et al. 1992).

Apoptosis is well defined and the various steps of the pathway can be used to determine if dying cells are undergoing apoptosis or dying by a different mode (Figure 1.4). Apoptotic cells can be morphologically distinguished by plasma membrane blebbing, a specific pattern of chromatin condensation, nuclear fragmentation and the formation of apoptotic bodies (Krysko et al. 2008). The exposure of phosphatidylserine on the outer surface of the plasma membrane is also a recognised marker for apoptosis and is detected using annexin V conjugated to various fluorescent molecules (Krysko et al. 2008). Annexin V is a calcium dependent phospholipid binding protein and annexin V staining combined with propidium iodide (PI) staining is widely used to distinguish apoptotic cells from necrotic cells (Krysko et al. 2008). PI is unable to penetrate the membrane of live cells and cells undergoing apoptosis, but is able to stain cells that have lost membrane integrity, such as dead cells and cells undergoing necrosis (van Engeland et al. 1998).

Western blotting can also be used to detect protein changes associated with apoptosis. For example, the anti-apoptotic proteins Mcl-1 and Bcl-2 are degraded in apoptotic cells but present in cells that are not undergoing apoptosis. The presence of cleaved caspases such as the initiator caspase 9 and the effector caspase 3 indicate that cells are undergoing apoptosis (Fan et al. 2005). The presence of cleaved caspase

substrates, such as cleaved poly ADP ribose polymerase (PARP), provide further evidence that cells are apoptotic (Fan et al. 2005). Staurosporine is a non-specific kinase inhibitor that is widely used as a positive control for apoptosis in the laboratory (Zhang et al. 2004). It has been reported that HT-29 cells (the cell line used in this thesis) die by apoptosis when they are treated for 24 h with 1 μM staurosporine (Qiao et al. 1996).

Apoptosis is considered to be the major mode of cell death in cancer cells treated with genotoxic agents. This is partly because the genes for many of the proteins that regulate apoptosis are mutated in human cancers (Brown and Wouters 1999). However, there is increasing evidence that other cell death pathways have a major role in cancer cell death when solid tumours are treated with genotoxic agents. Inhibiting apoptosis is reported to have little or no effect on the clonogenic survival of cancer cells following treatment with anti-cancer drugs or ionising radiation (Roninson et al. 2001; Brown and Attardi 2005). This has been demonstrated by several studies where the anti-apoptotic protein Bcl-2 was overexpressed (Yin and Schimke 1995; Lock and Stribinskiene 1996; Kyprianou et al. 1997; Elliott et al. 1998; Elliott et al. 1999; Wouters et al. 1999; Tannock and Lee 2001). It was predicted that if Bcl-2 was overexpressed then cells would be resistant to apoptosis and would therefore be less sensitive to treatment with genotoxic agents (Brown and Attardi 2005). However in these studies, although overexpression of Bcl-2 prevented cells from undergoing apoptosis, it did not have a significant impact on clonogenic survival. This indicates that the cells died by a mode of cell death other than apoptosis (Yin and Schimke 1995; Lock and Stribinskiene 1996; Kyprianou et al. 1997; Elliott et al. 1998; Elliott et al. 1999; Wouters et al. 1999; Tannock and Lee 2001). In 1999, Wouters *et al*. also found that there was no difference in cell viability when

apoptosis proficient and apoptosis deficient HCT116 cells were treated with either 5 µg/ml etoposide or 10 Gray ionising radiation (Wouters et al. 1997). Ruth and Roninson (2000) made similar observations in cells engineered to inducibly express multidrug resistance protein 1 (MDR1), a P-glycoprotein that inhibits apoptosis (Ruth and Roninson 2000). HeLa derived HtTA-MDR1 cervical adenocarcinoma cells and NIH 3T3 murine fibroblasts were treated with 9 Gray ionising radiation and induced to express MDR1. Ruth and Roninson found that MDR1 expression prevented cells from undergoing apoptosis but did not change overall cell survival after treatment (Ruth and Roninson 2000). Instead, the treated cells either died by mitotic catastrophe or initiated a senescence-like growth arrest (Ruth and Roninson 2000).

1.11.2 Necrosis

Originally considered an uncontrolled form of cell death, necrosis (Figure 1.4) was thought to lack a true molecular signature (Ricci and Zong 2006). However, several types of regulated necrosis with molecular signatures have now been identified, of which necroptosis is the most understood (Feoktistova et al. 2014). There are therefore different types of cell death that exhibit the morphological features of uncontrolled necrosis but that are induced by specific molecular signalling pathways. The characteristics of uncontrolled necrosis are membrane damage leading to membrane permeability, depletion of cellular energy, and loss of function of ion pumps and channels that regulate cellular homeostasis (Golstein and Kroemer 2007). Uncontrolled necrosis can be morphologically characterised by cell swelling, organelle swelling and loss of membrane integrity (Feoktistova et al. 2014) which causes cells to spill their contents into the extracellular space, initiating an inflammatory response (Majno et al. 1960). Uncontrolled necrosis is

most commonly activated due to disrupted ATP production, the imbalance of intracellular calcium, the generation of ROS or the activation of non-apoptotic proteases (Ricci and Zong 2006). To detect uncontrolled necrosis cellular swelling can be observed by light microscopy and loss of membrane integrity can be detected by nuclear staining with PI and flow cytometry (Jain et al. 2013).

1.11.3 Mitotic catastrophe

Mitotic catastrophe (Figure 1.4) is a form of cell death related to mitosis; however, the exact definition of mitotic catastrophe is debated. Mitotic catastrophe has been defined as cell death resulting from inappropriate entry into mitosis (Chan et al. 1999; Vitale et al. 2011), as cell death occurring during or shortly after a failed mitosis (Kroemer et al. 2009; Vitale et al. 2011), or as cell death resulting from an aberrant mitosis characterised by premature chromosome condensation and multiple micronuclei (Rezacova et al. 2011; Vitale et al. 2011). Mitotic catastrophe has also been defined as the induction of apoptosis, necrosis or senescence following a failed mitosis (Vitale et al. 2011; Hayashi and Karlseder 2013). The induction of other cell death pathways due to a failed mitosis has three different consequences: 1) cell death during mitosis; 2) cell death once a cell has exited mitosis and 3) senescence following exit from mitosis (Vitale et al. 2011; Hayashi and Karlseder 2013). It is also debated whether mitotic catastrophe should be classified as a distinct form of cell death (Roninson et al. 2001; de Bruin and Medema 2008) or if cell death occurs by apoptosis or necrosis following aberrant mitosis (Dewey et al. 1995; Castedo et al. 2004b).

It has long been known that cells treated with ionising radiation enter mitosis. In 1961 Yamada and Puck found that following irradiation with sub-cytotoxic

concentrations of X-rays (either 0.3, 0.7 or 1.4 Gray) there was a decrease in the mitotic index of HeLa cells, followed later by an increase in the mitotic index (Yamada and Puck 1961). Because the cells delayed entry into mitosis, this suggests that they arrested at the G2/M checkpoint before entering mitosis. These cells could therefore have been undergoing checkpoint adaptation, however it is not known if they entered mitosis with damaged DNA or if they entered mitosis following the repair of damaged DNA.

By comparison to apoptosis, there are few distinguishing characteristics of mitotic catastrophe. This means it is difficult to detect mitotic catastrophe as a form of cell death (de Bruin and Medema 2008). The main characteristic associated with mitotic catastrophe is the presence of micronuclei (Vitale et al. 2011), but micronuclei only indicate that cells have undergone an aberrant mitosis. Some cells with micronuclei may not undergo mitotic catastrophe because they survive and do not die. Furthermore, cells may die directly in mitosis and micronuclei cannot be used as a marker for this type of cell death. One of the best ways to study mitotic catastrophe is therefore time-lapse video microscopy, to observe cells in real time (Rello-Varona et al. 2010).

Mitotic catastrophe can be induced by DNA damage that directly affects the integrity of chromosomes, by interference with the mitotic spindle (Vitale et al. 2011) or by deficiencies in proteins and protein complexes involved in the process of mitosis itself (Broude et al. 2008). Drugs such as the taxanes and vinca alkaloids induce mitotic catastrophe without damaged DNA, by interfering with the mitotic spindle. This induces a mitotic arrest followed by cell death. The taxanes stabilise microtubules and induce a metaphase arrest (Rowinsky 1997) whereas the vinca alkaloids induce mitotic catastrophe by disrupting the dynamics of microtubule polymerisation and depolymerisation (Jordan

et al. 1991). Nocodazole is a compound that inhibits microtubule polymerisation and is widely used as a positive control for mitotic cells in the laboratory, because it arrests cells in mitosis (Vasquez et al. 1997).

Entry into mitosis with damaged DNA induces mitotic catastrophe through the SAC. HeLa cells treated with 1.5 μM aphidicolin entered mitosis with damaged DNA and arrested at metaphase (Nitta et al. 2004). Following this metaphase arrest cells entered what the authors describe as a "precatastrophic phase" where chromosome segregation was attempted. This was followed by cell death. When either of the SAC proteins Mad2 or BubR1 were depleted by siRNA in HeLa cells treated with aphidicolin, cells did not arrest at metaphase and continued with mitosis. This increased cell viability following treatment with aphidicolin, by comparison to the viability of cells transfected with control siRNA (Nitta et al. 2004).

Mitotic catastrophe has been observed in response to treatment with a variety of genotoxic agents that have different mechanisms of action, as shown in Table 1.2. These data demonstrate that mitotic catastrophe is an important and widely observed mode of death in response to treatment with genotoxic agents. It is likely that these cells undergo checkpoint adaptation to enter mitosis with damaged DNA, but this was not addressed in the majority of these studies. Checkpoint adaptation may therefore be a common pathway that leads to cell death following treatment with genotoxic agents. It is necessary to understand whether cells undergo checkpoint adaptation or not because checkpoint adaptation may contribute to cells surviving treatment with rearranged genomes. It may be possible to target the final step of checkpoint adaptation to prevent cells from entering

mitosis with damaged DNA, preventing them from surviving treatment with rearranged genomes.

Cells that have undergone aberrant mitoses have also been observed in clinical samples. Micronuclei have been detected in clinical cervical (Widel et al. 1999; Zolzer et al. 1995) and oral carcinoma samples (Bhattathiri et al. 1998; Bhattathiri et al. 2001; Kumari et al. 2005) after patients were treated with ionising radiation. However, because mitotic catastrophe is difficult to detect, there is a lack of clinical data about mitotic catastrophe as a mode of cell death *in vivo*.

1.11.4 Dual modes of cell death

Mode of cell death can depend on different factors including the tissue origin of a cell and the amount of DNA damage that a cell contains (Yoshikawa et al. 2001; Vakifahmetoglu et al. 2008). The effect of treatment concentration on mode of cell death has been demonstrated in studies where the same cell lines treated with different concentrations of the same genotoxic agent died by different modes of cell death.

Three human colorectal adenocarcinoma cell lines, SW480, COLO320DM and HCT116 were treated with relatively low and relatively high concentrations of the antimetabolite 5-fluorouracil (5-FU) (Yoshikawa et al. 2001). SW480 and COLO320DM cells treated with 1000 ng/ml 5-FU and HCT116 cells treated with 100 ng/ml 5-FU died by apoptosis, whereas SW480 and COLO320DM cells treated with 100 ng/ml 5-FU and HCT116 cells treated with 10 ng/ml 5-FU died by mitotic catastrophe (Yoshikawa et al. 2001). The same results were observed when hepatocellular carcinoma cells were treated with doxorubicin (Eom et al. 2005). Low dose doxorubicin treatment (15-60 ng/ml

depending on the cell line) of five human hepatocellular carcinoma cell lines; Huh-7, SNU-354, -398, -449 and -475 induced entry into mitosis, followed by a senescence like phenotype (Eom et al. 2005). By contrast, Huh-7 cells treated with a high dose of doxorubicin (10 µg/ml) died by apoptosis (Eom et al. 2005). Similarly, DC-3F Chinese hamster lung fibroblast cells treated with bleomycin died by mitotic catastrophe when treated with a low concentration of bleomycin (10 nM) whereas DC-3F cells treated with a high concentration of bleomycin (10 µM) died by apoptosis (Tounekti et al. 1993). High concentrations of genotoxic agents likely induce high levels of damaged DNA. These results therefore suggest that amount of damaged DNA affects which cell death pathway is activated following treatment.

It is likely that the cells dying by mitotic catastrophe were undergoing checkpoint adaptation, but this was not tested because checkpoint adaptation had not been identified in human cell lines at the time these studies were undertaken. Checkpoint adaptation might therefore be induced in a concentration dependent manner, where relatively low cytotoxic concentrations of a genotoxic agent induce checkpoint adaptation but high concentrations induce cell death by apoptosis. The relationship between treatment dose and the induction of checkpoint adaptation has not been previously investigated and is one of the research questions studied in this thesis.

Different modes of cell death were also observed when two different ovarian carcinoma cell lines (Caov-4 and SKOV-3) were treated with 33 µM cisplatin (Vakifahmetoglu et al. 2008). Caov-4 cells died by apoptosis whereas SKOV-3 cells died by entry into mitosis followed by necrosis like lysis. However, the authors did not provide cytotoxicity data for Caov-4 and SKOV-3 cells treated with cisplatin and so it may be that

33 μM cisplatin was a high dose of cisplatin for Caov-4 cells but not for SKOV-3 cells (Vakifahmetoglu et al. 2008). Overall, these studies have identified that mode of cell death following treatment with genotoxic agents can be different and depend on either concentration of treatment or cell type. Furthermore, in all of the studies, cells underwent either cell death following entry into mitosis or cell death by apoptosis. This highlights the importance of these two cell death pathways in cells treated with genotoxic agents.

1.11.5 Autophagy

Autophagy is a regulated pathway that is evolutionarily conserved. It is initiated by cells in response to nutrient stress, as well as during development and differentiation (Ricci and Zong 2006). Autophagy is involved in the routine turnover of cellular components (Lockshin and Zakeri 2008) and is also used to maintain energy homeostasis and protein synthesis when nutrient availability is low (Wirth et al. 2013). Cellular components are enclosed by a double membrane vesicle known as the autophagosome which fuses to lysosomes and is then known as an autolysosome (Lockshin and Zakeri 2004; Wirth et al. 2013). The autolysosome degrades the cytosolic contents of the vesicle so that they can be reused by the cell (Lockshin and Zakeri 2008; Wirth et al. 2013). However, excessive autophagy can promote cell death in a process widely recognised as autophagic cell death (Ricci and Zong 2006). Autophagic cell death is characterised by the formation of autophagic vacuoles and the lack of inflammatory response. Caspases are not activated in cells undergoing autophagy (Lockshin and Zakeri 2004).

1.11.6 Senescence

Cellular senescence refers to irreversible withdrawal from the cell cycle and permanent growth arrest, as opposed to a mode of cell death (Campisi 2008). Senescence was first described in 1961 by Hayflick and Moorhead who observed that normal human cells have a limited ability to divide in cell culture, by contrast to transformed cells (Hayflick and Moorhead 1961). Senescence is relevant to understanding the response of cancer cells to treatment because when cells are senescent it means that they are no longer dividing and this can prevent further tumour growth. Features of senescence include cellular and nuclear enlargement and increased gene expression, leading to an upregulation of genes for secreted molecules (Campisi 2008). Experimentally the most widely used marker of senescent cells is β-galactosidase activity (Dimri et al. 1995).

1.12 Cancer cell lines

HT-29 and M059K cells are used in this thesis to study checkpoint adaptation following treatment with cisplatin. HT-29 cells are a good model cell line for the study of checkpoint adaptation (Kubara et al. 2012). They display a striking rounded morphology when in mitosis and arrest in mitosis for a long time following treatment (Gascoigne and Taylor 2008). HT-29 cells display chromosomal instability (CIN) (Gascoigne and Taylor 2008) and have a modal number of 71-72 chromosomes (Kawai et al. 2002). CIN is defined as an increase in the rate of gain or loss of segmental and whole chromosomes during cell division and is characterised by changes in chromosome number and structure (Pikor et al. 2013). HT-29 cells also contain mutated p53 where arginine 273 is mutated to histidine (Rodrigues et al. 1990).

M059K cells are also used in this thesis, because they have been shown to undergo checkpoint adaptation when treated with one genotoxic agent, CPT (Kubara et al.

2012). M059K cells are fibroblastic and are therefore from a different tissue of origin by comparison to HT-29 cells, which are epithelial. M059K cells have a modal number of 75 chromosomes, with a range of 65 to 79 chromosomes (ATCC data sheet 1994). Additionally, M059K cells contain mutated p53 where the glutamate 286 is mutated to a lysine (Anderson and Allalunis-Turner 2000).

1.13 Research objectives

The majority of cancer patients are treated with DNA damaging agents in the form of either ionising radiation or chemical genotoxic anti-cancer drugs. These agents induce high levels of DNA damage, initiating cell cycle arrest at cell cycle checkpoints. However, it is unclear how cancer cells die when they are treated with genotoxic agents. One process that links cell cycle arrest at the G2/M checkpoint and cell death is checkpoint adaptation. It has been proposed that checkpoint adaptation is a common response in cancer cells treated with genotoxic agents. However, checkpoint adaptation has only been shown to occur in cancer cells treated with ionising radiation (Syljuåsen et al. 2006; Rezacova et al. 2011), CPT and etoposide (Kubara et al. 2012). We therefore investigated further how cancer cells treated with genotoxic agents die, by exploring whether cells treated with cisplatin undergo checkpoint adaptation.

We hypothesised that HT-29 cells treated with cisplatin undergo checkpoint adaptation before dying. We chose to use cisplatin to investigate checkpoint adaptation because it has a different mechanism of action to CPT, etoposide and ionising radiation. In addition cisplatin is widely used both clinically and experimentally, is well characterised with regard to how it induces DNA damage and has been previously shown to induce mitotic cell death (Demarcq et al. 1994; Chang et al. 1999; Vakifahmetoglu et

al. 2008). Cells that undergo checkpoint adaptation follow three steps: 1) a DNA damage induced cell cycle arrest, 2) overcoming this cell cycle arrest and 3) resuming the cell cycle with damaged DNA (Toczyski et al. 1997). Checkpoint adaptation can therefore be investigated in cells by identifying the status of proteins involved in the signalling of damaged DNA, cell cycle progression and cell cycle arrest.

It is important to understand how cancer cells die when they are treated with genotoxic agents because these agents are not always curative (Havelka et al. 2007). We therefore asked if HT-29 cells treated with either cisplatin or CPT can survive checkpoint adaptation. Treated cells that undergo checkpoint adaptation enter mitosis with damaged DNA and checkpoint adaptation may be a source of genomic instability in cells that survive it. The potential genomic change induced in cells that survive checkpoint adaptation could be a source of cancer cells that acquire resistance to treatment. Acquired resistance limits the efficacy of genotoxic anti-cancer drugs. It might therefore be possible to prevent cells treated with genotoxic agents from entering mitosis, to prevent cells surviving treatment with rearranged genomes. However, it is unknown whether mitosis is necessary for cell death in cells that die following checkpoint adaptation. We therefore explored whether cells are able to die when entry into mitosis is inhibited.

If checkpoint adaptation is going to be targeted to improve the efficacy of current genotoxic agents, then it is important to understand this process when cells are treated with different genotoxic agents. Checkpoint adaptation has not previously been compared in the same cell line treated with different genotoxic agents. We therefore investigated whether the process of checkpoint adaptation is the same or different in human cancer cells treated with two different genotoxic agents, cisplatin and CPT.

In summary, we investigated:

1) How cancer cells treated with cisplatin die, by exploring whether HT-29 cells treated with cisplatin undergo checkpoint adaptation (Chapter 2).
2) If any HT-29 cells treated with cisplatin can survive checkpoint adaptation (Chapter 3).
3) If mitosis is necessary for cell death when HT-29 cells are treated with either cisplatin or CPT (Chapter 3).
4) If the process of checkpoint adaptation is the same or different in human cancer cells treated with either cisplatin or CPT (Chapter 4).

Table 1.1 A table of different cancer treatments that damage DNA, their mechanism of action and the main types of damage that they cause. Modified with permission from Swift and Golsteyn, 2014 (Swift and Golsteyn 2014).

Agent type	**Examples of drugs**	**Mechanism of Action**	**Type of DNA Damage**
Alkylating agents	Nitrogen mustards Nitrosoureas S23906	Base alkylation Monofunctional DNA adducts Inter, Intra and DNA-protein crosslinks	Distort the DNA double helix which can block the DNA replication and transcription and lead to DNA strand breaks
Platinum drugs	Cisplatin Carboplatin Oxaliplatin	Monofunctional DNA adducts Inter, Intra and DNA-protein crosslinks	Distort the DNA double helix which can block the DNA replication and transcription and lead to DNA strand breaks
Antimetabolites	5-Fluorouracil	Misincorporates into DNA Depletes dNTPs	Distort the DNA double helix which can block the DNA replication and transcription and lead to DNA strand breaks
Topoisomerase poisons	Camptothecin Etoposide	Inhibit topoisomerase enzymes in complex with DNA	SSBs and DSBs
Ionising radiation		Direct Indirect production of ROS	SSBs and DSBs DNA adducts, base oxidation, SSBs, DSBs, base deamination, DNA-protein crosslinks

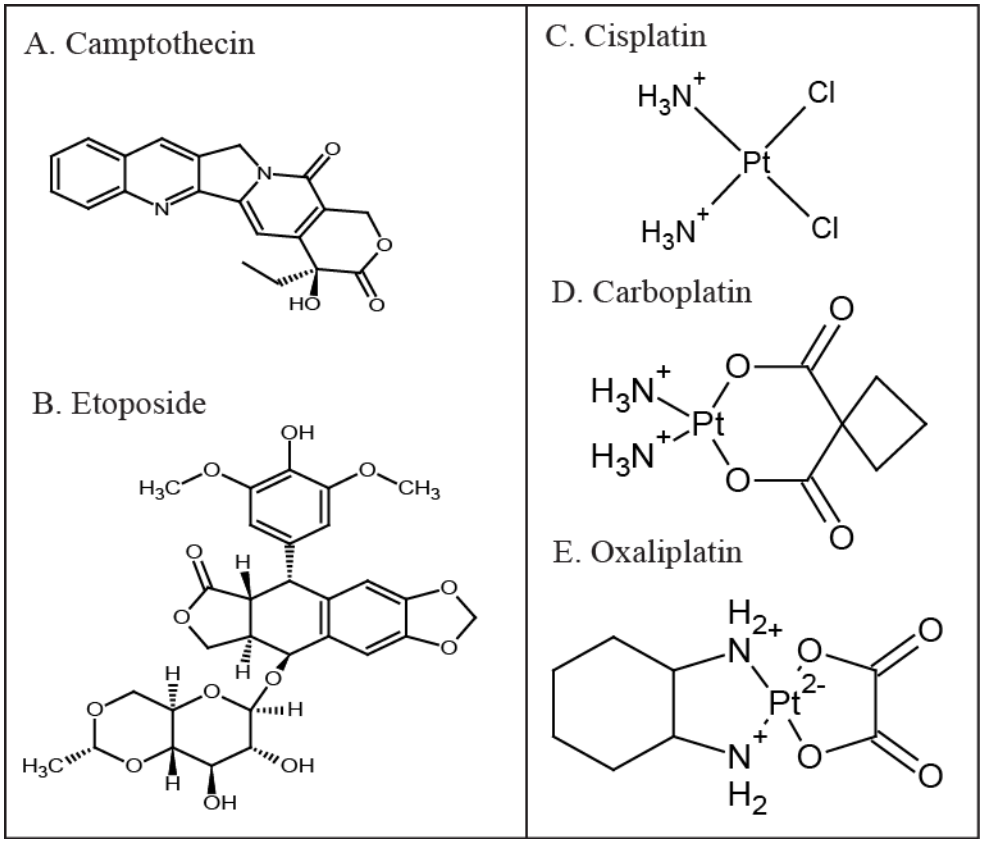

Figure 1.1 Structures of DNA damaging agents. The structures of (A) the topoisomerase I inhibitor camptothecin; (B) the topoisomerase II inhibitor etoposide; (C) the platinum drug cisplatin; (D) the platinum drug carboplatin and (E) the platinum drug oxaliplatin. Checkpoint adaptation has previously been shown to occur in cells treated with either CPT or etoposide. In this thesis we investigate checkpoint adaptation in human cancer cells treated with cisplatin.

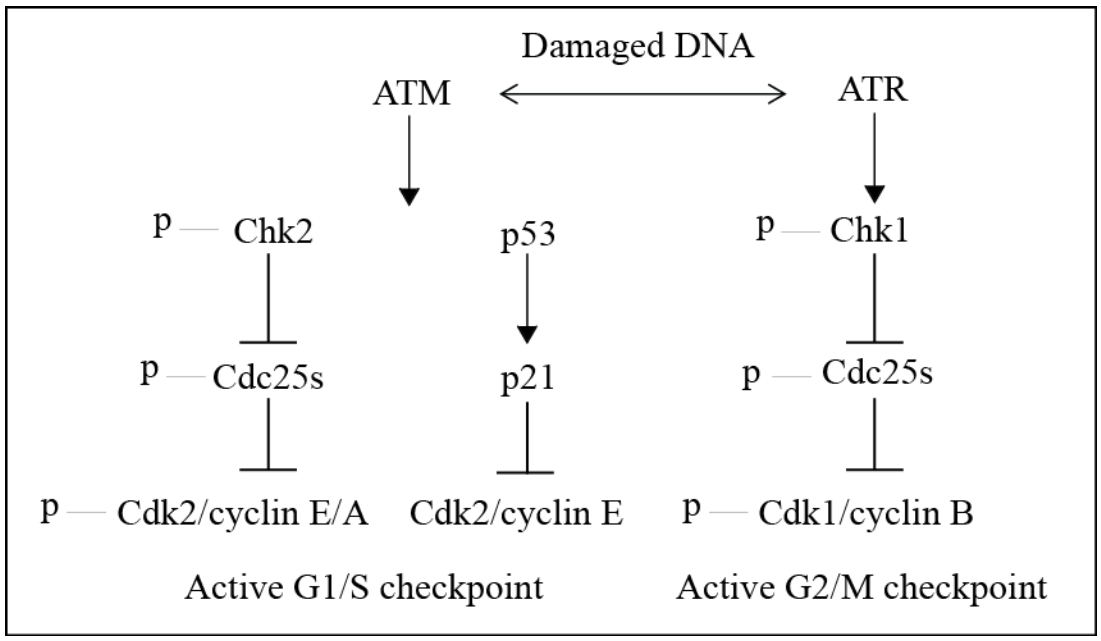

Figure 1.2 An overview of the DNA damage response (DDR). Cells with damaged DNA activate the ataxia telangiectasia mutated (ATM)/ATM and Rad3-related (ATR) kinases. These kinases phosphorylate many substrates including proteins involved in checkpoint activation, DNA replication and DNA damage repair. Checkpoint kinase 1 (Chk1) and checkpoint kinase 2 (Chk2) inactivate the Cdc25 phosphatases and this prevents the activation of the cyclin-dependent kinases (Cdks) by maintaining inhibitory phosphorylation of these enzymes. ATM also activates p53 which activates and maintains the G1/S checkpoint by promoting the transcription of the Cdk inhibitor, p21. Used with permission from Swift and Golsteyn, 2014 (Swift and Golsteyn 2014).

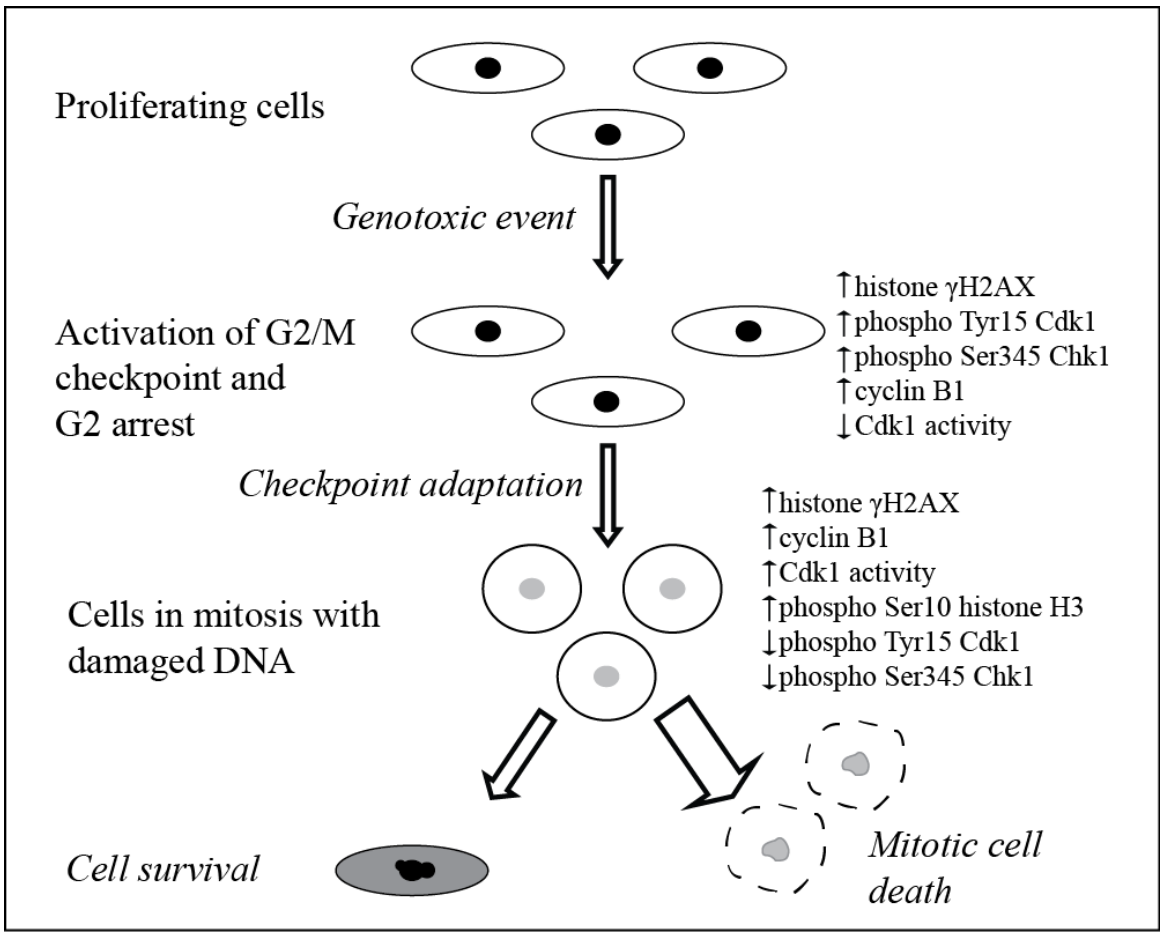

Figure 1.3 A schematic of checkpoint adaptation. Proliferating cells with damaged DNA arrest at the G2/M cell cycle checkpoint. The cells then enter mitosis with damaged DNA. The majority of cells die but some may survive, likely with changes to their genome. The grey cell with a black nucleus represents a cell surviving checkpoint adaptation with micronuclei and a rearranged genome. Modified with permission from Swift and Golsteyn, 2014 (Swift and Golsteyn 2014).

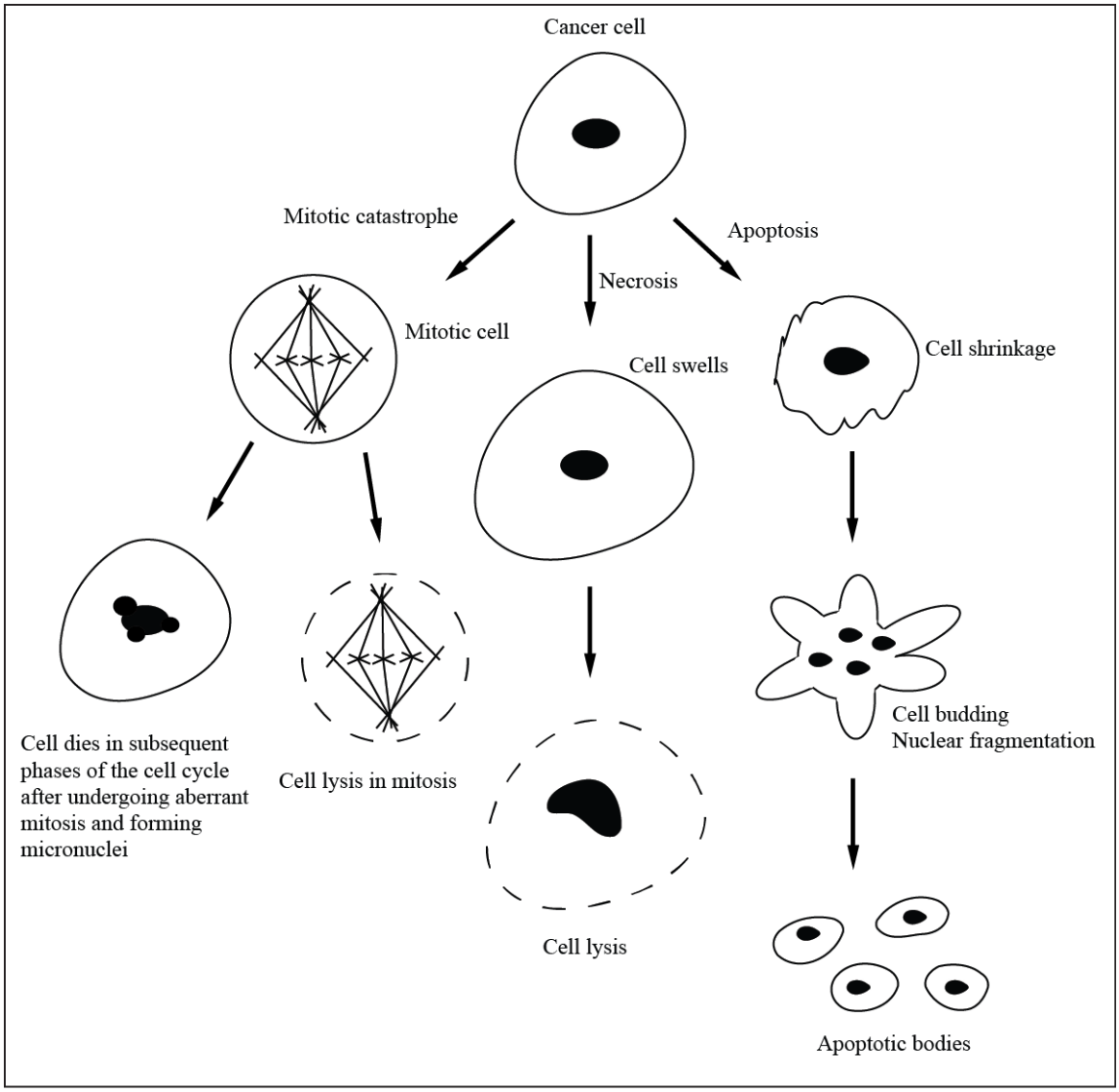

Figure 1.4 An overview of three different modes of cell death. Three of the major modes of cell death are apoptosis, necrosis and mitotic catastrophe. Apoptosis is characterised by cell shrinkage and the formation of apoptotic bodies. Necrosis is characterised by cell swelling and lysis. Mitotic catastrophe is characterised by entry into mitosis prior to cell death.

Table 1.2 A table to show treatments that induce mitotic catastrophe in different cell lines.

Treatment	Agent type	Cell Type	Features of Mitotic Catastrophe	Reference
Aphidicolin	DNA replication inhibitor	HT0180 fibrosarcoma P53$^{-/-}$ HCT116 colon carcinoma	Micronucleation Analysis of cell cycle phase, increased mitotic index	Chang et al. 1999 Nitta et al. 2004
Bleomycin	Radiomimetic, induces DSBs	DC-3F Chinese hamster lung fibroblast	Analysis of cell cycle phase, micronucleation	Tounekti et al. 1993
Cisplatin	Crosslinking agent	CHO/UV41 Chinese hamster ovary CHO HCC metastatic hepatocellular carcinoma HT0180 M059K glioma SKOV-3 ovarian carcinoma	Rounded morphology, analysis of cell cycle phase Micronucleation Ser10 phospho-H3 positive, analysis of cell cycle phase Micronucleation Micronucleation Micronucleation, high levels of cyclin B Lack of caspase activation, micronucleation	Demarq et al. 1994 Krishnaswamy and Dewey 1993 Wang et al. 2008 Chang et al. 1999 Lewis and Golsteyn 2014 Vakifahmetoglu et al. 2008
CPT	Topoisomerase I inhibitor	HT-29 human colorectal adeno carcinoma M059K	Checkpoint adaptation Checkpoint adaptation	Kubara et al. 2012
Cytarabine	Antimetabolite	HT0180	Micronucleation	Chang et al. 1999
Doxorubicin	Topoisomerase II inhibitor	HT0180 Huh-7 hepatocellular carcinoma (HCC) SNU-354 -398 -449 -475 HCC	Micronucleation Micronucleation, analysis of cell cycle phase, lack of caspase activation Micronucleation	Chang et al. 1999 Eom et al. 2005
Etoposide	Topoisomerase II inhibitor	HT-29 HT0180	Checkpoint adaptation Micronucleation	Kubara et al. 2012 Chang et al. 1999
5-FU	Antimetabolite	COLO320DM, HCT116, SW480 Colorectal adenocarcinoma	Analysis of cell cycle phase, increased levels of cyclin B	Yoshikawa et al. 2001
Ionising radiation	Physical agent that induces direct DSBs	U2OS osteosarcoma MOLT4 leukaemia HeLa cervical adenocarcinoma HT0180	Checkpoint adaptation Checkpoint adaptation Analysis of cell cycle phase, increased levels of cyclin B Micronucleation	Syljuåsen et al. 2006 Rezacova et al. 2011 Ianzini and Mackey 1998 Chang et al. 1999
Oxaliplatin	Crosslinking agent	TE7 oesophageal adenocarcinoma	Analysis of cell cycle phase, multinucleation	Ngan et al. 2008
S23906	Atypical alkylating agent	HeLa HT-29	High levels of cyclin B, increased Cdk1 activity, Ser10 phospho-H3 positive	Cahuzac et al. 2010

CHAPTER 2

Cytotoxic amounts of cisplatin induce either checkpoint adaptation or apoptosis in a concentration dependent manner in cancer cells

Lucy H. Swift and Roy M. Golsteyn

Short title: Cisplatin and checkpoint adaptation

This chapter has been submitted to Biology of the Cell for review

2.1 Abstract

Background information: Checkpoint adaptation (entry into mitosis with damaged DNA) is a key process that links arrest at the G2/M cell cycle checkpoint and cell death in cancer cells. However, it is unknown whether cells treated with the genotoxic agent cisplatin undergo checkpoint adaptation and whether checkpoint adaptation is a major pathway leading to cell death or not. We therefore investigated the relationship between treatment with cisplatin and cytotoxicity in cancer cells.

Results: We find that treatment of HT-29 human colorectal adenocarcinoma cells with cisplatin can induce cell death by one of two different mechanisms. Cells treated with 30 μM cisplatin die after undergoing checkpoint adaptation. By 72 h, almost all treated cells are positive for histone γH2AX staining and contain high levels of cyclin B1. A sub-population of 30 μM rounded cells appears at 72 h and these cells are positive for phospho-Ser10 histone H3, have low levels of phospho-Tyr15 cyclin dependent kinase 1, high levels of cyclin dependent kinase 1 activity, and checkpoint kinase 1 that is not phosphorylated on Ser345. Strikingly, by 96 h of treatment with 30 μM cisplatin, 81% of cells enter mitosis before dying. By contrast, after treatment with 100 μM cisplatin, nearly all cells die but only 7% of cells enter mitosis. Instead these cells die by apoptosis; they are positive for annexin V staining, contain cleaved caspase 3, cleaved caspase 9 and cleaved PARP and do not contain Mcl-1.

*Conclusions***:** Our data demonstrate that cancer cells treated with cisplatin undergo dual modes of cell death in a concentration dependent manner. These findings suggest that checkpoint adaptation is likely a primary pathway in genotoxic cell death at

pharmacological concentrations of cisplatin and that it may be possible to target specific cell death pathways to improve the efficacy of genotoxic anti-cancer drugs.

2.2 Introduction

Cisplatin is a genotoxic agent that is widely used to treat a range of cancers, including testicular and ovarian carcinomas (Wheate et al. 2010) and glioblastoma (Brandes et al. 2004). Cisplatin forms monofunctional DNA adducts and intra- and inter-strand crosslinks (Eastman 1987) that damage DNA and cause cell death (Eastman 2006). Cells that are treated with cisplatin initiate a DNA damage response checkpoint before dying (Sorenson and Eastman 1988a, 1988b; Demarcq et al. 1994); however, the steps that lie between the DNA damage response and cell death following treatment with cisplatin are not well understood.

Cells that undergo checkpoint adaptation follow three steps: 1) a DNA damage induced cell cycle arrest, 2) overcoming this cell cycle arrest and 3) resuming the cell cycle with damaged DNA (Toczyski et al. 1997). Checkpoint adaptation may be a process that links the G2/M cell cycle arrest and cell death and has been observed in experiments in which cancer cell lines were treated with either ionising radiation (Syljuåsen et al. 2006; Rezacova et al. 2011), camptothecin (CPT) or etoposide (Kubara et al. 2012). It is not known whether cisplatin treated cells can undergo checkpoint adaptation and, importantly, if it is a major pathway leading to cell death.

When cells detect damaged DNA they phosphorylate histone H2AX on Ser139, which is known as γH2AX (Rogakou et al. 1998). Damaged DNA can be readily detected in cells by the identification of histone γH2AX using microscopy or western

blotting (Mah et al. 2010; Löbrich et al. 2010). In a parallel pathway, cells initiate the G2/M checkpoint by phosphorylating checkpoint kinase 1 (Chk1) on Ser345 and Ser317 (Liu et al. 2000; Zhao and Piwnica-Worms 2001), which prevents cells from entering mitosis. Active Chk1 targets the Cdc25 phosphatases for sequestration and degradation (Ferguson et al. 2005; Jin et al., 2008), which in turn prevents the removal of inhibitory phosphates on Thr14 and Tyr15 of cyclin-dependent kinase 1 (Cdk1). To activate Cdk1 and enter mitosis, cells must have low levels of Cdk1 phosphorylated at Tyr15 and high levels of cyclin B. When cells are in mitosis they display cell rounding, have condensed chromosomes and contain phosphorylated Ser10 histone H3 which can be used to confirm that treated cells are in mitosis (Hendzel et al. 1997). By identifying the status of proteins that signal damaged DNA and cell cycle progression, it is possible to detect checkpoint adaptation in cells treated with genotoxic agents.

We report that HT-29 cells undergo checkpoint adaptation when treated with cytotoxic amounts of cisplatin. Treated cells signal damaged DNA and arrest in the cell cycle. These cells then escape cell cycle arrest and enter mitosis with damaged DNA. Strikingly, at concentrations of cisplatin that are above those required for cell death and which induce higher levels of histone γH2AX signals, cells no longer undergo checkpoint adaptation but die by apoptosis. Finally, we show that M059K glioma cells also exhibit dual modes of cell death when treated with different concentrations of cisplatin.

2.3 Materials and Methods

2.3.1 Cell culture

The human cell lines HT-29 (ATCC HTB-38) and M059K (ATCC CRL-2365) were obtained from the American Type Culture Collection (ATCC). HT-29 cells were maintained in RPMI 1640 medium (Gibco; 21870-092) supplemented with 10% (v/v) heat inactivated fetal bovine serum (FBS) (Gibco; 12484028) and 1.6 mM GlutaMAX (Gibco; 35050-061). M059K cells were maintained in Dulbecco's Modified Eagle Medium/F-12 (Gibco; 11320-082) supplemented with 10% (v/v) heat inactivated FBS (Gibco; 12484028), 2 mM Modified Eagle Medium non-essential amino acids (Gibco; 11140050) and 15 mM HEPES (4-(2-hydroxyethyl)-1-piperazineethanesulfonic acid), pH 7.4. Cells were grown at 37°C in 5% CO_2 and the media were changed every 3-4 d. HT-29 cells were plated at a density of 3.0 x 10^5 cells/25 cm^2 flask and cultured for 72 h prior to treatment. M059K cells were plated at a density of 7.5 x 10^5/75 cm^2 flask and cultured for 24 h prior to treatment. The compound cisplatin (Sigma; 479306-1G) was dissolved in dimethyl sulphoxide (DMSO) (Sigma-Aldrich; D2438) to a concentration of 100 mM and stocks were freshly made every two weeks. CPT (Sigma; 7689-03-4) and nocodazole (Sigma; M1404-10MG) were dissolved in DMSO to a concentration of 10 mM and 200 μg/ml respectively. Staurosporine (Cayman Chemicals; 81590-250) and H_2O_2 (VWR; BDH7742-1) were diluted in DMSO prior to use. H_2O_2 was stored at 4°C and all other compounds were stored at -20°C until use. Not treated cells were treated with the solvent only (0.1% (v/v) DMSO).

2.3.2 Cytotoxicity assay

The cytotoxicity of cisplatin was measured by the MTT (3-((4,5)-dimethylthiazol-2-yl)-2,5-diphenyl-tetrazolium) assay (Sigma-Aldrich; M2128-1G). HT-29 cells were plated at 3.8 x 10^5 cells/96 well culture plate and cultured at 37°C for 72 h prior to treatment. M059K cells were plated at 2.5 x 10^5 cells/96 well culture plate and cultured at

37°C for 24 h prior to treatment. All treatments were run in triplicate at 24, 48, 72 and 96 h and experiments were performed three times. After the specified treatment time, 20 µl MTT solution (5 mg/ml MTT in phosphate buffered saline (PBS) (137 mM NaCl, 3 mM KCl, 100 mM Na_2HPO_4, 18 mM KH_2PO_4) was added to the media in each well and the plates were incubated at 37°C for 3.5 h. The media were then aspirated and 100 µl MTT solvent (4 mM HCl, 0.1% (v/v) octylphenoxypolyethoxyethanol, in isopropanol) was added to each well. Plates were placed on a shaker for 30 min in the dark, and absorbance was measured at 590 nm using a BioTek microplate spectrophotometer powered by Eon software. Results were expressed as IC_{50} concentrations; the concentration of the compound that reduced the absorbance of MTT by 50%, by comparison to 0.1% (v/v) DMSO treated cells. The normalised percent absorbance was calculated as shown:

Normalised percent absorbance = (absorbance/DMSO absorbance) x 100

The log concentrations of the compound were plotted against the normalised percent absorbance using Microsoft Excel software. Analysis was performed with GraphPad Prism 5 software, using non-linear regression (log(inhibitor) versus normalised response), to estimate the IC_{50} concentrations. Standard curves were plotted using the equation:

$$Y = \text{maximum} + (\text{maximum} - \text{minimum})/(1+10^{(x-\text{LogIC50})})$$

where maximum is the percentage of viable cells after treatment with 0.1% DMSO, minimum is the percentage of viable cells after treatment with the highest concentration of the genotoxic molecule and x is the log10 value of the treatment concentration.

2.3.3 Light microscopy

HT-29 cells were seeded at 1.0 x 10^5/well in a 6 well culture plate and incubated at 37°C for 72 h prior to treatment. Images were captured at room temperature with an Infinity 1 camera powered by Infinity Capture imaging software (Lumenera Corporation) on an Olympus CKX41 inverted microscope using an Olympus LUCPlanFLN 20x objective with 0.45 numerical aperture. Images were processed using Adobe Photoshop (CC 2014.1.0). Rounded cells were counted using Image J software (IJ 1.46r).

2.3.4 Flow cytometry

HT-29 cells were plated at 1 x 10^6 cells/75 cm^2 flask and incubated at 37°C for 72 h prior to treatment. Total cell cultures were collected by trypsinisation while rounded mitotic cells were collected by mechanical shake-off. Cells were washed with 1% (w/v) bovine serum albumin (BSA) in PBS and fixed in ice cold 90% ethanol for at least 24 h. Fixed samples were stored at -20°C until use. For analysis, samples were centrifuged at 750 x g for 5 min at 4°C and washed with ice cold PBS. Cells were then washed twice with ice cold wash buffer (1% (w/v) BSA in PBS) before being incubated with labelling buffer (1% (w/v) BSA, 20 μg/ml propidium iodide (PI) (Life technologies; P1304MP) and 200 μg/ml RNAse A (Sigma; R6513-250MG) in PBS) for 30 min. Samples were analysed by a FACSCanto II flow cytometer (BD Biosciences) using BD FACSDiva software (BD Biosciences). Gating was set using a not treated sample and experiments were performed three times.

2.3.5 Immunofluorescence microscopy

HT-29 cells were plated on glass coverslips at 1.0 x 10^5/well in a 6 well culture plate and incubated at 37°C for 72 h prior to treatment. After treatment, cells were fixed

at room temperature for 20 min in 3% (v/v) formaldehyde (Ted Pella Inc; 18505), diluted in PBS. Fixation was quenched with 50 mM NH_4Cl in PBS and cells were permeabilised for 5 min using 0.2% (v/v) Triton X-100 in PBS and blocked for 1 h with 3% (w/v) BSA in PBS-T (0.1% (v/v) Tween-20 diluted in PBS). Cells were then incubated with primary antibodies as described: anti-histone γH2AX (Millipore; 05-636; 1:400) for 1 h at room temperature; anti-cyclin B1 (Santa Cruz Biotechnology; SC-752; 1:100) for 2 h at room temperature or anti-phospho-Ser10 histone H3 (Millipore; 06-570(CH); 1:1000) for 18 h at 4°C. After washing with PBS-T, cells were incubated with secondary antibodies for 2 h at room temperature as follows: Alexa Fluor 488-conjugated anti-mouse (Life Technologies; A11059; 1:400) for anti-histone γH2AX and Texas Red-conjugated anti-rabbit (Jackson ImmunoResearch; 111-075-003; 1:400) for anti-phospho-Ser10 histone H3 and anti-cyclin B1. Nuclei were stained with 300 nM DAPI (4′,6-diamidino-2-phenylindole) in PBS for 15 min and coverslips were mounted onto microscope slides using ProLong Gold Antifade reagent (Molecular probes; P36934). Cells were observed at room temperature on an Olympus BX41 microscope using either an Olympus UPlanFL N 20x objective with 0.50 numerical aperture or an Olympus UPlanFL N 60x objective with 1.25 numerical aperture. Images were captured using an Infinity 3 camera operated by Infinity Capture imaging software (Lumenera Corporation). Images were prepared using Adobe Photoshop (CC 2014.1.0) software. Cells positive for histone γH2AX, phospho-Ser10 histone H3 and cyclin B1 were counted using Image J (IJ 1.46r) software. To prevent the detection of background histone γH2AX staining, the signal from not treated cells was set to zero using exposure settings on the microscope camera (Borgne et al. 2006). At least 500 cells were counted for each treatment, unless otherwise stated, and experiments were performed three times.

2.3.6 Mechanical shake-off

HT-29 cells were plated at 1 x 10^6 cells/75 cm^2 flask and incubated at 37°C for 72 h prior to treatment. After treatment, medium was aspirated and cells were gently washed with PBS. Fresh medium was added at 1 ml/25 cm^2 and the flask was tapped with medium force on all edges to extract rounded cells from flattened cells.

2.3.7 Extract preparation

HT-29 cells were plated at 1 x 10^6 cells/75 cm^2 flask and incubated at 37°C for 72 h prior to treatment. After treatment, cells were either trypsinised or collected by mechanical shake-off and washed with ice cold PBS. Cells were re-suspended in ice cold lysis buffer (50 mM HEPES, pH 7.4, 50 mM NaF, 10 mM EGTA (ethylene glycol tetraacetic acid), 50 mM β-glycerophosphate, 1 mM ATP, 1 mM DTT (dithiothreitol), 1% Triton X-100 (v/v), 10 µg/ml RNase A (Sigma-Aldrich; R6513-250MG), 0.4 U/ml DNase I (Invitrogen; I354Ba) and protease inhibitor cocktail (Roche; 11836170001)) at a concentration of 20,000 cells/µl, passed through a 26-gauge needle five times and incubated on ice for 30 min. The suspension was centrifuged at 10,000 x g for 10 min at 4°C, aliquoted into 1.5 ml microfuge tubes and stored at -80°C. Extracts were either used for electrophoresis after being boiled for 5 min in the presence of 2x SDS (sodium dodecyl sulphate) sample buffer (20% (v/v) glycerol, 10% (v/v) DTT, 6% (w/v) SDS, 500 mM Tris, pH 6.8) or used for the detection of Cdk1 activity. The concentration of proteins in each extract was quantified using the Agilent 2100 Bioanalyzer and samples were prepared using the Agilent Protein 230 kit: 4 µl of protein sample and 2 µl denaturing solution were mixed in a 0.5 ml microfuge tube and incubated at 95°C for 5 min. The samples were then briefly centrifuged and 84 µl deionised water was added. Samples

were mixed by vortexing and loaded onto the Agilent Protein 230 chip which was loaded into the Agilent 2100 Bioanalyzer. Samples were analysed using Agilent Expert 2100 software to quantify the amount of protein present.

2.3.8 Electrophoresis and western blotting

Cell extracts were separated on 10% (v/v) SDS-PAGE (poly-acrylamide gel electrophoresis) gels with 4% (v/v) stacking gels. Precision Plus Dual Colour marker (BioRad; 161-0394) was used to determine molecular weight in kilodaltons (kDa). Proteins were transferred onto nitrocellulose membranes by wet transfer (BioRad) for 16.5 h at 30 volts. Transfer was confirmed using Ponceau S stain (0.1% (w/v) in 5% acetic acid) and membranes were blocked with either 5% (w/v) low fat milk or 2% (w/v) BSA in Tris buffered saline with Tween-20 (TBS-T) (50 mM Tris base, 150 mM NaCl and 0.1% (v/v) Tween-20, pH 7.6) for 2 h. Membranes were then incubated with the following primary antibodies at 4°C overnight: anti-Cdk1/Cdc2 (Signalway Antibodies; 21236-2; 1:500); anti-phospho-Tyr15 Cdk1/Cdc2 (Signalway Antibodies; 11244-2; 1:500); anti-Chk1 (Santa Cruz Biotechnology; sc-8408; 1:200); anti-phospho-Ser345 Chk1 (Cell Signaling Technology; 2348S; 1:1000); anti-cyclin B1 (Santa Cruz Biotechnology; sc-245; 1:200); anti-actin (Santa Cruz Biotechnology; sc-58673; 1:200); anti-cleaved PARP (Asp214) (Cell Signaling Technology; 5625; 1:100); anti-cleaved caspase 9 (Asp330) (Cell Signaling Technology; 9501S; 1:100); anti-Mcl-1 (Santa Cruz Biotechnology; sc-819; 1:100); anti-caspase 3 p17 (Santa Cruz Biotechnology; sc-271028; 1:100) and anti-histone γH2AX (Millipore; 05-636; 1:200). The membranes were then washed with TBS-T and incubated with the following secondary antibodies for 1 h at room temperature: alkaline phosphatase coupled anti-mouse IgG (Promega;

PRS3721; 1:2500) or alkaline phosphatase coupled anti-rabbit IgG (Promega; PRS3731; 1:2500). The membranes were washed with TBS-T and developed using an alkaline phosphatase conjugate substrate kit (BioRad; 172-1063). Development was stopped with Tris-EDTA (ethylenediaminetetraacetic acid) buffer (10 mM Tris base, 1 mM EDTA, pH 8.0). Western blot analyses were performed three times. In some analyses, the signals were quantified for each treatment using Image J software; the signal from each treatment was normalised to the corresponding actin signal, to control for differences in protein loading. The signal from each treatment was then normalised to the not treated signal, which was set to represent one arbitrary unit.

2.3.9 Cdk1 Kinase Assay

Cdk1 phosphorylation reactions (20 µl total volume) were prepared as follows: 10 µl 2x Cdk1 phosphorylation buffer (50 mM β-glycerophosphate pH 7.4, 10 mM $MgCl_2$, 10 mM NaF, 1 mM DTT) with 200 µM ATP and 5 µl of either 80 ng/µl glutathione S-transferase (GST) or GST-PP1C-S artificial substrates (Lewis et al. 2013). Reactions were initiated by adding 5 µl of whole cell extracts diluted in cold lysis buffer (50 mM HEPES, pH 7.4, 50 mM NaF, 10 mM EGTA, 50 mM β-glycerophosphate, 1 mM ATP, 1 mM DTT, 1% Triton X-100 (v/v), 10 µg/ml RNase A (Sigma-Aldrich; R6513-250MG), 0.4 U/ml DNase I (Invitrogen; I354Ba) and protease inhibitor cocktail (Roche; 11836170001)) to 100 lysed cells/µl. Reactions were incubated for 5 min at 30°C and were stopped by adding an equal volume of 2x SDS sample buffer and heating at 95°C for 5 min. Reaction mixtures were separated on 12% (v/v) SDS-PAGE gels. Proteins were transferred to nitrocellulose membranes with a semi-dry electroblotter system (BioRad) for 40 min at 25 volts. The membranes were blocked with either 5% (w/v) low

fat milk or 5% (w/v) BSA in TBS-T and incubated overnight at room temperature with either anti-phospho-Thr320 PP1Cα (Abcam; Ab62334; 1:300,000) or anti-GST (Sigma-Aldrich; G7781; 1:20,000) primary antibodies. After washing with TBS-T, the membranes were incubated with alkaline phosphatase coupled anti-rabbit IgG (Promega; PRS3731; 1:2500). The membranes were washed with TBS-T and developed using an alkaline phosphatase conjugate substrate kit (BioRad; 172-1063). Development was stopped using Tris-EDTA buffer. The membranes were then analysed using Image J (IJ 1.46r) software to calculate the relative signal intensity of the bands. The signal from each phospho-Thr320 PP1Cα band was normalised to the signal from the corresponding band of GST, to control for differences in protein loading. The signal from each treatment was then normalised to the not treated signal, which was set to represent one arbitrary unit. Cdk1 assays were performed three times.

2.3.10 Time-lapse video microscopy

HT-29 cells were plated at 3.0 x 10^5/25 cm^2 flask and incubated at 37°C for 72 h prior to treatment. M059K cells were plated at 2.0 x 10^5/25 cm^2 and incubated at 37°C for 24 h prior to treatment. Time-lapse video microscopy images were collected from the start of treatment, using a Lumascope 500 microscope (etaluma) powered by LumaView software (etaluma; V.13.4.25.99). Images were captured at 37°C every 10 min for 96 h using a Meiji Techno Japan UPlan 20x objective with 0.40 numerical aperture. Cells were manually scored for a rounded morphology, indicative of mitosis, or not between 0 and 96 h. Cells that left the field of view before rounding were not counted. At least 250 HT-29 cells and 50 M059K cells were counted for each treatment. Experiments were performed three times.

2.3.11 Annexin V and propidium iodide staining

HT-29 cells were plated at 0.3 x 10^6 cells/25 cm^2 flask and incubated at 37°C for 72 h prior to treatment. Cells were processed using the RAPID Annexin V Binding protocol provided with the Annexin V-Biotin Apoptosis Detection Kit (EMD Millipore; PF036). For the detection of annexin V positive cells, cells were collected by trypsinisation 24, 48, 72, 96 and 120 h after treatment. Cells were re-suspended in media to a final concentration of 1 x 10^6 cells/ml and 0.5 ml was transferred to a microfuge tube. Ten µl media binding reagent and 1.25 µl Annexin V-Biotin were added and samples were incubated in the dark at room temperature for 15 min. Samples were then centrifuged at 1000 x g for 5 min at room temperature and the media were aspirated. The cells were re-suspended in 0.5 ml cold 1x binding buffer and 15 µl streptavidin Alexa Fluor 488 conjugate (Life technologies; S-11223) at 15 µg/ml in 1x binding buffer was added. For the detection of PI positive cells, cells were collected by trypsinisation 24, 48, 72, 96 and 120 h after treatment. Cells were re-suspended at 1 x 10^6/ml in cold 1x binding buffer, 0.5 ml was transferred to a microfuge tube and 10 µl 30 mg/ml PI diluted in PBS was added. All samples were immediately analysed using an Olympus BX41 microscope and images were captured using an Infinity 3 camera operated by Infinity Capture imaging software (Lumenera Corporation). Experiments were performed three times.

2.3.12 Statistical analysis

Data were analysed using Microsoft Excel 2010 software. Data were plotted as means from three separate experiments ± standard errors of the means. Statistical significance was calculated using the student's t-test for two paired sample means and values were considered significantly different when $p < 0.05$.

2.4 Results

2.4.1 Identification of cytotoxic effects of cisplatin upon HT-29 cells

We identified concentrations of cisplatin that were cytotoxic to HT-29 cells, to investigate if cisplatin induces checkpoint adaptation. HT-29 cells were treated with different concentrations of cisplatin (0.3-300 μM) for 24, 48, 72 and 96 h and cell viability was measured using the MTT assay (Figure 2.1). The results from each treatment were normalised to treatment with 0.1% (v/v) DMSO. The IC_{50} values ranged from 120 μM at 24 h to 5 μM at 96 h (Table 2.1), revealing that the cells were sensitive to cisplatin in time and concentration dependent manners. We identified two concentrations of cisplatin that were cytotoxic to HT-29 cells, 30 and 100 μM. Cells treated with 30 μM cisplatin were 83 ± 3% viable at 24 h but only 17 ± 3% viable at 96 h indicating that cells viable at 24 h were destined to die by 96 h, and providing a window of time for the study of cisplatin induced cell death. Cells treated with 100 μM cisplatin were 49 ± 3% viable at 24 h, 10 ± 2% viable at 72 h and 5 ± 1% viable at 96 h.

2.4.2 HT-29 cell populations treated with either 30 or 100 μM cisplatin contain different amounts of damaged DNA

Knowing that cisplatin is a genotoxic agent and that cells treated with 30 and 100 μM die at different times, we compared the timing and levels of DNA damage signals. HT-29 cells were treated with either 30 or 100 μM cisplatin and analysed for histone γH2AX staining at 24, 48 and 72 h by immunofluorescence microscopy (Figure 2.2A). Not treated and 50 nM CPT treated cells were used as control treatments. The percentages of cells positive for histone γH2AX staining were determined using Image J software (Figure 2.2B). Cells were considered positive for histone γH2AX staining when they

exhibited a staining intensity greater than background levels, as determined by Image J software. At 24 h, 56 ± 4% of the 30 μM cisplatin treated cells were positive for histone γH2AX staining, whereas 93 ± 3% of 100 μM treated cells contained histone γH2AX. By 48 h, however, 30 and 100 μM treated populations had similar numbers of cells that stained positive for histone γH2AX (96 ± 1% and 94 ± 2%, respectively). By 72 h, the 30 μM cisplatin treated cells remained positive for histone γH2AX staining (93 ± 4%), whereas the majority of 100 μM treated cells were dead and showed variable staining. As expected, not treated cells rarely displayed histone γH2AX staining (2 ± 1% at 24 h) and CPT treated cells were positive for histone γH2AX at all times tested. These data confirm that treatment with cisplatin damages DNA at the cytotoxic concentrations of 30 and 100 μM cisplatin, although the histone γH2AX staining appeared earlier following treatment with 100 μM cisplatin.

We compared the relative levels of histone γH2AX by western blotting in not treated, 30 μM and 100 μM cisplatin treated cells at different times (Figure 2.3) (Lopez et al. 2012). Actin was used as a loading control (Figure 2.3A). Cells treated for 72 h with 30 μM cisplatin had a histone γH2AX signal intensity of 7 ± 1 arbitrary units. By contrast, cells treated with 100 μM cisplatin for 24 and 48 h had histone γH2AX signal intensities of 11 ± 2 and 12 ± 2 arbitrary units respectively. These data indicate that 100 μM cisplatin treated cells have almost double the amount of damaged DNA prior to dying by comparison to cells treated with 30 μM cisplatin.

2.4.3 HT-29 cells treated with either 30 or 100 μM cisplatin arrest at different phases of the cell cycle

We then compared the effects of the two cytotoxic concentrations of cisplatin upon the cell cycle by flow cytometric analysis of DNA amounts. HT-29 cells were treated for 72 h with 30 μM cisplatin and for 24 and 48 h with 100 μM cisplatin (Figure 2.4). Not treated, mitotic (200 ng/ml nocodazole treated) and 50 nM CPT treated cells were used as controls. In the not treated sample 69 ± 3% of cells were in the G1 phase and 13 ± 3% of cells were in G2/M phases, whereas 96 ± 3% nocodazole treated cells and 63 ± 12% of CPT treated cells were in G2/M phases. In the 30 μM cisplatin treated sample only 14 ± 5% of cells were in G1 phase and 48 ± 8% were in G2/M phases (Table 2.2). By contrast, 77 ± 5% of 24 h 100 μM cisplatin treated cells and 76 ± 5% of 48 h 100 μM cisplatin treated cells were in G1 phase of the cell cycle. These data show that cells treated with 30 μM cisplatin arrest predominantly in the G2/M-phases prior to dying whereas 100 μM cisplatin treated cells do not progress in the cell cycle before dying.

2.4.4 HT-29 cells treated with 30 μM cisplatin acquire a rounded morphology whereas 100 μM cisplatin treated cells do not

During the course of our experiments with different cytotoxic amounts of cisplatin, we observed that some treated cells displayed a rounded morphology prior to dying. We investigated the timing and number of rounded cells present in populations either not treated, treated with a range of concentrations of cisplatin or treated with CPT (Figure 2.5). The total number of cells present in the not treated cell population increased between 24 and 96 h and rounded cells were present at all times. Rounded cells were present 48 h after treatment with CPT (10 ± 2%), as previously reported (Kubara et al. 2012). In the 10 and 30 μM cisplatin treated cell populations many rounded cells were present by 72 h (12 ± 2% and 7 ± 1% respectively). Cell number decreased between 72

and 96 h in the 30 μM cisplatin treated cell population. This confirmed that 30 μM cisplatin was cytotoxic to HT-29 cells at 96 h. By contrast, cells treated with 100 μM cisplatin did not display a rounded morphology after treatment (1 ± 0.4% at 24 h, 1 ± 0.2% at 48 h and 0.1 ± 0.01 at 72 h). Few 100 μM cisplatin treated cells were present 96 h after treatment, consistent with the toxicity of 100 μM cisplatin to HT-29 cells. As cells died they detached from the culture plates and were lost during media changes. Cell rounding is a morphology change associated with cells in mitosis (Kubara et al. 2012; Cadart et al. 2014). These data therefore provided a first indication that cells treated with 30 μM cisplatin might enter mitosis before dying, whereas 100 μM cisplatin treated cells did not enter mitosis before dying.

2.4.5 HT-29 cells treated with 30 μM cisplatin have high levels of cyclin B1

The cytotoxicity, DNA damage signalling, and morphology data suggested that cells treated with 30 μM cisplatin were undergoing checkpoint adaptation before dying, whereas 100 μM cisplatin treated cells were not undergoing checkpoint adaptation. If cells treated with 30 μM cisplatin were undergoing checkpoint adaptation we predicted that they would contain proteins and protein modifications required for mitosis. HT-29 cells were treated with either 30 or 100 μM cisplatin and analysed for cyclin B1 staining at 24, 48 and 72 h by immunofluorescence microscopy (Figure 2.6A). Not treated and 50 nM CPT treated cells were used as control treatments. The percentages of cells staining positive for cyclin B1 were determined using Image J software (Figure 2.6B).

A small number of not treated cells were positive for cyclin B1 staining at 24 h (11 ± 0.7%), 48 h (14 ± 2%) and 72 h (11 ± 1%). As expected, most of the CPT treated cells were positive for cyclin B1 at 48 h (95 ± 1%) and this was maintained at 72 h (93 ±

1%). The number of 30 μM cisplatin treated HT-29 cells staining positive for cyclin B1 increased from 24 ± 3% at 24 h to 95 ± 1% at 48 and 72 h. By contrast only a small number of 100 μM cisplatin treated cells stained positive for cyclin B1 (14 ± 1% at 24 h, 17 ± 5% at 48 h and 7 ± 1% at 72 h).

2.4.6 HT-29 cells treated with 30 μM cisplatin can enter mitosis

We reasoned that because cells treated with 30 μM cisplatin had high levels of cyclin B1 and displayed a rounded morphology, then cells might be entering mitosis. HT-29 cells were treated with either 30 or 100 μM cisplatin and analysed for phospho-Ser10 histone H3 staining at 24, 48 and 72 h by immunofluorescence microscopy (Figure 2.7A). Histone H3 phosphorylated at Ser10 is present in cells in mitosis (Hendzel et al. 1997) and in cells undergoing checkpoint adaptation (Kubara et al. 2012). Not treated and 50 nM CPT treated cells were used as control treatments (Figure 2.7B). The percentages of not treated cells staining positive for phospho-Ser10 histone H3 were 6 ± 1% at 24 h, 5 ± 1% at 48 h and 2 ± 0.5% at 72 h. As expected, at 48 and 72 h, 8 ± 0.5% and 9 ± 1% of CPT treated cells were positive for phospho-Ser10 histone H3. The number of 30 μM cisplatin treated HT-29 cells staining positive for phospho-Ser10 histone H3 increased from 0.2 ± 0.07% at 24 h and 1 ± 0.3% at 48 h to 7 ± 1% at 72 h. By contrast, only a small number of 100 μM cisplatin treated cells stained positive for phospho-Ser10 histone H3 after treatment (0 ± 0.05% at 24 h, 2 ± 0.2% at 48 h and 0.4 ± 0.3% at 72 h)

2.4.7 Cdk1 is dephosphorylated on Tyr15 in rounded 30 μM cisplatin treated HT-29 cells

In addition to having cyclin B1, cells that are in mitosis have low levels of Cdk1 phosphorylated on Tyr15. To investigate if the rounded cells present 72 h after treatment

with 30 μM cisplatin were mitotic, we used mechanical shake-off to separate the 30 μM cisplatin treated culture into a rounded cell population and an adherent cell population and prepared cell extracts. It was not possible to do this with the 100 μM treated population because no rounded cells were present. We then used western blotting to compare levels of Cdk1, phospho-Tyr15 Cdk1, cyclin B1 and actin, which was used as a loading control (Figure 2.8A). Not treated and 200 ng/ml nocodazole treated (mitotic) cell extracts were used as controls.

As expected, not treated cells contained Cdk1 that was phosphorylated on Tyr15 and were not positive for cyclin B1. The nocodazole treated cells contained Cdk1, which was not phosphorylated on Tyr15, and were positive for cyclin B1, also as expected. The 30 μM cisplatin treated total and interphase cells contained Cdk1 that was phosphorylated on Tyr15 and were positive for cyclin B1. By contrast, the 30 μM cisplatin treated rounded cells contained Cdk1 with decreased levels of Tyr15 phosphorylation and were positive for cyclin B1.

2.4.8 Chk1 is dephosphorylated on Ser345 in rounded 30 μM cisplatin treated HT-29 cells

Chk1 is activated by phosphorylation on Ser345 in response to damaged DNA and is responsible for the initiation and maintenance of the G2/M checkpoint (Liu et al. 2000). To test if 30 μM cisplatin treated cells arrested at and then abrogated the G2/M checkpoint, we used western blotting to detect levels of Chk1 and phospho-Ser345 Chk1 (Figure 2.8B). Extracts were prepared as in Figure 2.8A. Actin was used as a loading control. Both the not treated and nocodazole treated mitotic cells contained Chk1, which was not phosphorylated on Ser345. The 30 μM cisplatin treated total and interphase cells

contained Chk1 that was phosphorylated on Ser345. Strikingly, Chk1 was dephosphorylated on Ser345 in the 30 μM cisplatin treated mitotic cells. These results are consistent with the observation that the rounded cells present following treatment with 30 μM cisplatin are in mitosis.

2.4.9 Cdk1 is active in rounded 30 μM cisplatin treated HT-29 cells

To confirm that the rounded cells were in mitosis we measured activity of the Cdk1-cyclin B complex in 72 h 30 μM cisplatin treated total, interphase and mitotic cell extracts. The cell extracts were incubated with glutathione S-transferase-PP1Cα (GST-PP1Cα), an artificial Cdk1 substrate containing a Thr320 PP1Cα site that is phosphorylated by active Cdk1 (Lewis et al. 2013). The cell extracts were also incubated with GST alone, a negative control substrate that lacked the Thr320 PP1Cα phosphorylation site. Not treated cell extracts, nocodazole treated (mitotic) cell extracts and extraction buffer were used as controls. The levels of phospho-Thr320 PP1Cα were analysed by western blotting (Figure 2.9A). Levels of GST were also detected, as a loading control (Figure 2.9B).

The phospho-Thr320 PP1Cα signal for the extraction buffer was 0.9 ± 0.3 arbitrary units, whereas the phospho-Thr320 PP1Cα signal for the nocodazole treated cell extracts was 23 ± 6 arbitrary units. The phospho-Thr320 PP1Cα signals for the 30 μM cisplatin treated total and interphasic cell extracts were similar at 5 ± 0.7 and 4 ± 1.7 arbitrary units, respectively. Noticeably, the phospho-Thr320 PP1Cα signal for the 30 μM cisplatin treated mitotic cell extracts was high at 20 ± 5 arbitrary units, a value similar to that of the nocodazole extract. The high phospho-Thr320 PP1Cα signal detected for 30 μM cisplatin treated mitotic cell extracts indicated that these cells contained active Cdk1.

2.4.10 HT-29 cells treated with 30 μM cisplatin have condensed chromosomes that are positive for damaged DNA

We were able to detect that cells treated with a cytotoxic concentration of cisplatin (30 μM) have damaged DNA, arrest in the cell cycle and then enter mitosis. These are events found in cells that undergo checkpoint adaptation. However, it remained to be determined whether the mitotic cells contained damaged DNA or not. We therefore investigated if mitotic 30 μM cisplatin treated cells were positive for histone γH2AX staining. First, to verify that cells with condensed chromosomes were mitotic, we used immunofluorescence microscopy to detect phospho-Ser10 histone H3 staining (Figure 2.10A). HT-29 cells were either not treated, treated with 50 nM CPT for 48 h or treated with 30 μM cisplatin for 72 h. Cells with condensed chromosomes from the not treated, CPT treated and 30 μM cisplatin treated cell populations were positive for phospho-Ser10 histone H3 staining. This confirmed that cells with condensed chromosomes were mitotic.

We then stained 30 μM cisplatin treated cells with DAPI and with histone γH2AX antibodies and observed them by immunofluorescence microscopy to detect condensed, damaged chromosomes (Figure 2.10B). Cells with condensed chromosomes from not treated and 50 nM CPT treated cell populations were used as controls (Figure 2.10C). All of the CPT treated cells with condensed chromosomes were positive for histone γH2AX staining (100 ± 0%). Nearly all of the 72 h 30 μM cisplatin treated cells with condensed chromosomes were positive for histone γH2AX staining (97 ± 2%). These data confirm that 30 μM cisplatin treated cells are in mitosis with damaged DNA, the final step of checkpoint adaptation.

2.4.11 The majority of HT-29 cells treated with 30 μM cisplatin enter mitosis while the majority of 100 μM cisplatin treated cells do not

Having demonstrated that treatment with 30 μM cisplatin induces cells to undergo checkpoint adaptation, we asked what fraction of a treated population undergoes checkpoint adaptation. To answer this question we used time-lapse video microscopy to observe cell rounding in 30 μM cisplatin treated cells. Images were captured every 10 min for 96 h and individual cells were manually observed to detect the presence or absence of cell rounding. The percentages of cells that entered mitosis post-treatment were then determined. Not treated cells were used as a control (Figure 2.11). The percentages of cell death were calculated from the MTT cytotoxicity data presented in Figure 2.1. As previously described, the cytotoxicity data were normalised so that not treated cells represented 0% cell death. Nearly all of the not treated cells (99 ± 0.06%) entered mitosis over the 96 h observation period. Strikingly, the majority of 30 μM cisplatin treated cells were dead at 96 h (83 ± 3%) and 81 ± 3% of 30 μM cisplatin treated cells entered mitosis after treatment. We also observed that the majority of the 30 μM cisplatin treated cells that entered mitosis died in mitosis. By contrast, only 7 ± 0.04% of the 100 μM treated sample entered mitosis. This suggested that 30 μM cisplatin treated cells died by a different mode of cell death by comparison to 100 μM treated cells.

2.4.12 HT-29 cells treated with 100 μM cisplatin are positive for annexin V staining

We reasoned that if 100 μM cisplatin treated cells were not entering mitosis before dying, then they could be dying by either apoptosis or necrosis. We observed cell morphology by light microscopy and combined this with immunofluorescence microscopy to detect annexin V and PI staining (Figure 2.12). Not treated cells were used

as a negative control, 1 μM staurosporine treated cells were used as a positive control for apoptosis (Qiao et al. 1996) and 5 mM hydrogen peroxide (H_2O_2) treated cells were used as a positive control for necrosis (McKeague et al. 2003). Cells were treated for 24, 48, 72, 96 and 120 h, collected and stained for annexin V. Cells were then analysed by light and immunofluorescence microscopy and representative images of cells 48 h after treatment are shown (Figure 2.12). This procedure was then repeated except that cells were stained with PI instead of for annexin V.

At 24 h, some staurosporine treated cells were positive for annexin V staining, no cells were positive for PI staining and some cells treated with 100 μM cisplatin and staurosporine displayed cell blebbing (unpublished data). At 48 h, not treated cells did not display cell blebbing and were negative for both annexin V and PI staining. Some staurosporine treated cells displayed cell blebbing and these cells were positive for annexin V staining and negative for PI staining. Cells treated with H_2O_2 were morphologically distinct from the staurosporine treated cells that displayed cell blebbing and were negative for annexin V staining. However, some H_2O_2 treated cells were positive for PI staining. Cells treated with 30 μM cisplatin did not demonstrate cell blebbing and were negative for both annexin V and PI staining. By contrast some 100 μM cisplatin treated cells displayed cell blebbing and these cells were positive for annexin V staining and negative for PI staining. The same results were observed at 72 h (unpublished data). Observation of cells at 96 and 120 h demonstrated that 30 μM cisplatin treated cells did not stain positive for annexin V or PI at either of these times (unpublished data). These data suggested that 100 μM cisplatin treated cells were dying by apoptosis whereas 30 μM cisplatin treated cells were not dying by apoptosis.

2.4.13 HT-29 cells treated with 100 μM cisplatin die by apoptosis

To explore further whether 100 μM cisplatin treated cells were undergoing apoptosis while 30 μM cisplatin treated cells were not, we used western blotting to detect levels of proteins associated with apoptosis (Figure 2.13). Total 72 h 30 μM cisplatin, 24 h 100 μM cisplatin and 48 h 100 μM cisplatin treated cell extracts were prepared. Not treated and 24 h 1 μM staurosporine treated cell extracts were used as controls. Cell extracts were analysed by western blotting to detect levels of cleaved poly-ADP ribose polymerase (PARP), pro-caspase 3, cleaved caspase 3, cleaved caspase 9, Mcl-1 and actin. Actin was used as a loading control.

Not treated cells were negative for cleaved PARP, cleaved caspase 3 and cleaved caspase 9 but were positive for pro-caspase 3 and Mcl-1. Staurosporine treated cells were positive for cleaved PARP, cleaved caspase 3 and cleaved caspase 9, had slightly decreased levels of pro-caspase 3 and were negative for Mcl-1. Cells treated for 72 h with 30 μM cisplatin and for 24 h with 100 μM cisplatin were negative for cleaved PARP, cleaved caspase 3 and cleaved caspase 9 and were positive for pro-caspase 3 and Mcl-1. Noticeably, cells treated for 48 h with 100 μM cisplatin were positive for cleaved PARP, cleaved caspase 3 and cleaved caspase 9, had slightly decreased levels of pro-caspase 3 and were negative for Mcl-1. These data indicate that cells treated for 48 h with 100 μM cisplatin undergo apoptosis whereas cells treated for 72 h with 30 μM cisplatin do not.

2.4.14 Cisplatin is cytotoxic to M059K cells

We then investigated if our observations about checkpoint adaptation using HT-29 cells extended to a second unrelated cell line, M059K. We first treated M059K cells with

different concentrations of cisplatin (0.3-300 μM) for 24, 48, 72 and 96 h and measured cell viability by the MTT assay (Figure 2.14). M059K cell viability decreased in a time dependent manner as concentration of cisplatin increased. The IC_{50} values range from 30 μM at 24 h to 1 μM at 96 h (Table 2.3), indicating that M059K cells were more sensitive to treatment with cisplatin by comparison to HT-29 cells.

2.4.15 M059K cells undergo dual modes of cell death when treated with either relatively low or relatively high concentrations of cisplatin

We then replicated the conditions of the MTT assay and observed the cells by time-lapse video microscopy (Figure 2.15). M059K cells were treated with 3, 10, 30 and 100 μM cisplatin and the percentage of cells that entered mitosis post-treatment was determined for each cell population. Not treated and 50 nM CPT treated cells were used as controls. Almost all not treated (99 ± 0.7%) and 75 ± 8% of CPT treated cells entered mitosis after treatment. Of the cisplatin treated cells, 96 ± 0.6% of the 3 μM and 75 ± 5% of the 10 μM cisplatin treated cells entered mitosis after treatment. Strikingly however, only 18 ± 3% of 30 μM and 8 ± 1% of 100 μM cisplatin treated cells entered mitosis after treatment. These data indicate that, like HT-29 cells, M059K cells undergo checkpoint adaptation at cytotoxic concentrations of cisplatin. At higher concentrations of cisplatin, M059K cells die without undergoing checkpoint adaptation.

2.5 Discussion

Cisplatin is a widely used genotoxic anti-cancer drug and yet how cells die when they are treated with it remains poorly understood. Cells treated with cisplatin initiate a DNA damage checkpoint before dying (Sorenson and Eastman 1988a, 1988b; Demarcq et

al. 1994); however, the steps that lie between this cell cycle arrest and cell death following treatment are not well characterised. Checkpoint adaptation (entry into mitosis with damaged DNA) has been identified as a key pathway linking cell cycle arrest and cell death in response to treatment with either ionising radiation (Syljuåsen et al. 2006; Rezacova et al. 2011), CPT or etoposide (Kubara et al. 2012). In this paper, we report that cisplatin can induce checkpoint adaptation, but only when used at certain concentrations.

We used HT-29 cells to study checkpoint adaptation by virtue of their change in morphology when entering mitosis and prolonged mitotic arrest (Gascoigne and Taylor 2008; Kubara et al. 2012). We first identified concentrations of cisplatin that were cytotoxic to HT-29 cells and chose two concentrations with which to investigate checkpoint adaptation, 30 and 100 μM. The 30 μM concentration is similar to that present in the serum of treated cancer patients whereas the 100 μM concentration is suprapharmacological (Vermorken et al. 1984; Swift and Golsteyn 2014). We then compared the timing and levels of DNA damage signalling in cells treated with these different concentrations of cisplatin by the detection of histone γH2AX. This analysis confirmed that cisplatin was genotoxic to HT-29 cells (Olive and Banàth 2009) and indicated that DNA damage signals were present earlier and were higher in 100 μM treated cells by comparison to 30 μM treated cells. Knowing that there were differences in DNA damage signalling in cells treated with either 30 or 100 μM cisplatin, we next used flow cytometry to compare how these different concentrations affected the cell cycle. We found that cells treated with 30 μM cisplatin arrested predominantly at G2/M phases whereas 100 μM cisplatin treated cells did not progress through the cell cycle and

as such were predominantly in G1. We therefore first explored if cells treated with 30 μM cisplatin were entering mitosis following treatment.

Cells treated with 30 μM cisplatin displayed a rounded cell morphology (typical of cell in mitosis) (Kubara et al. 2012; Cadart et al. 2014) and most 30 μM cisplatin treated cells accumulated cyclin B1. Additionally a sub-population of 30 μM cisplatin treated cells was positive for phospho-Ser10 histone H3. These data suggested that 30 μM cisplatin treated cells were entering mitosis before dying. Entry into mitosis was confirmed by studying rounded 30 μM cisplatin treated cells which contained low levels of Cdk1 phosphorylated on Tyr15, high levels of cyclin B1 and high levels of Cdk1 activity.

Having confirmed that cells treated with 30 μM cisplatin were entering mitosis, we asked if they were undergoing checkpoint adaptation. To undergo checkpoint adaptation treated cells must 1) induce a DNA damage arrest, 2) overcome this cell cycle arrest and 3) resume the cell cycle with damaged DNA (Toczyski et al. 1997). We found that cells treated with 30 μM cisplatin were undergoing checkpoint adaptation because mitotic 30 μM cisplatin treated cells contained Chk1 dephosphorylated on Ser345, whereas the total and interphasic cell populations contained active Chk1 phosphorylated on Ser345 (Liu et al. 2000). This indicated that cells treated with 30 μM cisplatin arrested at and then abrogated the G2/M cell cycle checkpoint. To confirm that these cells were undergoing all three steps of checkpoint adaptation we determined that nearly all 30 μM cisplatin treated cells contained damaged DNA. We also observed that 30 μM cisplatin treated cells in mitosis were positive for histone γH2AX staining and thus demonstrated that cells treated with 30 μM cisplatin undergo checkpoint adaptation.

Previous studies have shown that checkpoint adaptation occurs in cells treated with either ionising radiation (Syljuåsen et al. 2006; Rezacova et al. 2011), CPT or etoposide (Kubara et al. 2012). However, these studies did not investigate what fraction of the treated population was undergoing checkpoint adaptation and so did not address whether this was a major response to treatment or not. We used time-lapse video microscopy to observe mitotic cells and determined that most 30 μM cisplatin treated cells entered mitosis before dying. These data demonstrate that checkpoint adaptation is a major response to treatment with 30 μM cisplatin. Because cisplatin has a different mechanism of action to the genotoxic agents previously reported to induce checkpoint adaptation, our data support the suggestion that checkpoint adaptation and mitotic cell death play a major role in the cytotoxicity of genotoxic agents (Chang et al. 1999; Roninson et al. 2001; Brown and Attardi 2005; Broude et al. 2008; Kubara et al. 2012; Swift and Golsteyn 2014).

We found that by contrast to cells treated with 30 μM cisplatin, cells treated with 100 μM cisplatin did not display a rounded morphology, did not accumulate cyclin B1 and were not positive for phospho-Ser10 histone H3. We therefore reasoned that these cells could be dying by apoptosis. Results from light and immunofluorescence microscopy revealed that these cells were positive for annexin V staining and negative for PI staining. This was confirmed by western blotting which demonstrated that 100 μM cisplatin treated cells were positive for cleaved PARP, cleaved caspase 3 and cleaved caspase 9 and negative for Mcl-1. Strikingly, M059K cells treated with low concentrations of cisplatin also died following entry into mitosis whereas cells treated with high concentrations of cisplatin died without entering mitosis. These data provide

one explanation for why inhibiting apoptosis in cancer cells does not affect clonogenic survival (Lock and Stribinskiene 1996; Elliott et al. 1999; Wouters et al. 1999; Ruth and Roninson 2000), because we show that when cells are treated with lower concentrations of cisplatin they die by mitotic cell death instead of by apoptosis.

It has been suggested that mitotic cell death is a special type of apoptosis that involves activation of the caspases (Castedo et al. 2004a, 2004b). Our results suggest that this is not the case and that mitotic cell death and apoptosis are two different mechanisms of cell death in HT-29 cells treated with cisplatin. By contrast to 100 μM cisplatin treated cells, 30 μM cisplatin treated cells were not positive for annexin V, cleaved-PARP, cleaved caspase 3 and cleaved caspase 9 and were positive for Mcl-1.

The induction of different modes of cell death in response to high and low concentrations of different genotoxic agents in different cell lines has been previously reported, suggesting that this phenomenon may be a common response to treatment with genotoxic agents. DC3-F Chinese hamster lung fibroblasts treated with a low concentration of bleomycin arrested in G2/M phases of the cell cycle and were micronucleated, whereas cells treated with a high concentration of bleomycin died by apoptosis (Tounekti et al. 1993). High and low concentrations of 5-fluorouracil also induced cell death by either apoptosis or following entry into mitosis in three human colorectal adenocarcinoma cell lines (SW480, COLO320DM and HCT-116) (Yoshikawa et al. 2001). Similarly, low dose doxorubicin induced entry into mitosis followed by induction of a senescence like phenotype, characterised by increased β-galactosidase activity, in human hepatoma cell lines. Mitotic catastrophe was identified by the observation of micronuclei, abnormal spindle formation and lack of an apoptotic

response. By contrast, cells treated with a high dose of doxorubicin died by apoptosis (Eom et al. 2005). It has also been previously reported that cells treated with either cisplatin or oxaliplatin die by mitotic catastrophe (Demarcq et al. 1994; Chang et al. 1999; Ngan et al. 2008; Vakifahmetoglu et al. 2008). We have now expanded upon these studies by using mechanical shake-off to collect treated rounded cells which allowed us to identify that cells treated with 30 μM cisplatin enter mitosis by checkpoint adaptation.

Our data suggest that cancer cells treated with cisplatin are more likely to undergo checkpoint adaptation than they are to undergo apoptosis, because the concentration of cisplatin needed to induce apoptosis is above the concentration of cisplatin needed to induce cell death. Using this information it may be possible to target the process of checkpoint adaptation to improve the efficacy of genotoxic anti-cancer drugs. The aim of using genotoxic agents to treat cancer patients is that they induce cancer cell death to prevent further growth of a tumour. However, it has been observed that a small number of cells can survive checkpoint adaptation following treatment with CPT and cisplatin (Kubara et al. 2012, chapter 3) and it has been proposed that these survival cells may contain rearranged genomes (Syljuåsen et al. 2006; de Bruin and Medema 2008; Kubara et al. 2012). Cells that survive treatment with rearranged genomes could be detrimental to the success of genotoxic anti-cancer drugs because they may acquire the genetic changes necessary for resistance to treatment or be the source of some secondary tumours (Nakada et al. 2006).

We have identified that cancer cells treated with cisplatin switch between undergoing checkpoint adaptation when they are treated with a pharmacological concentration of cisplatin to undergoing apoptosis when they are treated with a

suprapharmacological concentration of cisplatin. Our data suggest that this switch occurs in response to different levels of damaged DNA. By investigating further the biochemical switch that treated cells use to undergo either checkpoint adaptation or apoptosis, it might be possible to target components of this switch to inhibit checkpoint adaptation and induce cell death by apoptosis, without increasing the concentration of cisplatin that cells are treated with. This would prevent cells from surviving checkpoint adaptation with rearranged genomes and might increase the efficacy of genotoxic anti-cancer drugs. To understand better the clinical relevance of our findings, it will be necessary to investigate the relationship between checkpoint adaptation and cell death in tumour models.

In conclusion we have found that checkpoint adaptation is a key response that links cell cycle arrest and cell death in cancer cells treated with cisplatin. Furthermore, we demonstrate that treatment of cells with different concentrations of cisplatin induces different modes of cell death. We predict that checkpoint adaptation is a major pathway that leads to cell death in cancer cells treated with genotoxic agents. It may therefore be possible to target this pathway to improve the efficacy of current genotoxic anti-cancer drugs.

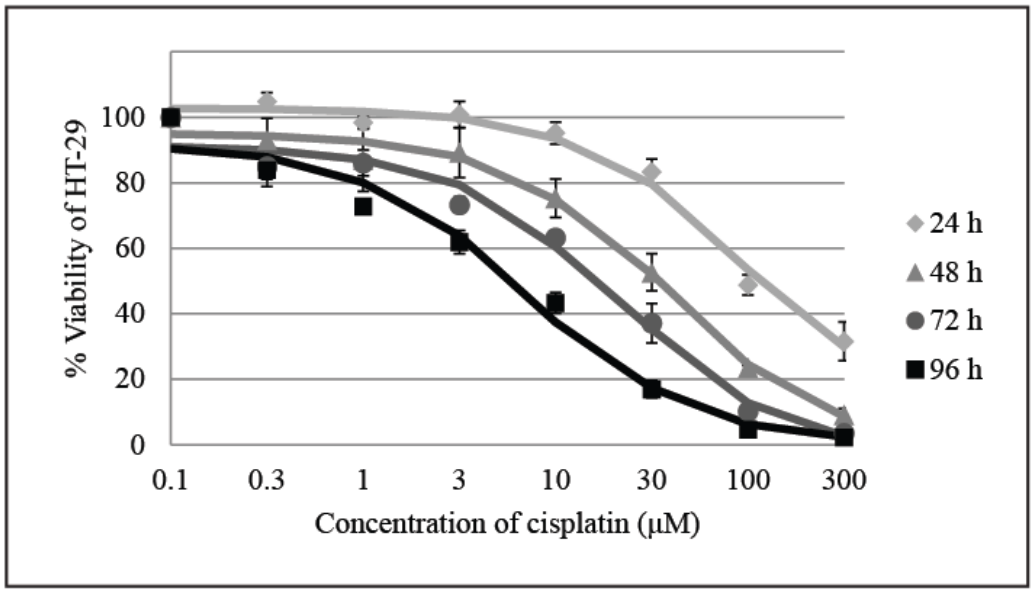

Figure 2.1 Both 30 and 100 µM cisplatin are cytotoxic to HT-29 cells. HT-29 cells were treated with different concentrations of cisplatin for 24 h (diamonds), 48 h (triangles), 72 h (circles) and 96 h (squares). The MTT assay was used to measure cell viability. Each treatment was run in triplicate and the results from each treatment condition were normalised to treatment with 0.1% (v/v) DMSO. Mean percentages of viability were calculated from three separate experiments and standard errors of the means are shown.

Table 2.1 Mean IC_{50} concentrations of cisplatin used to treat HT-29 cells for 24, 48, 72 and 96 h.

	Time (h)			
Genotoxic agent	24	48	72	96
Cisplatin (μM)	120	31	14	5

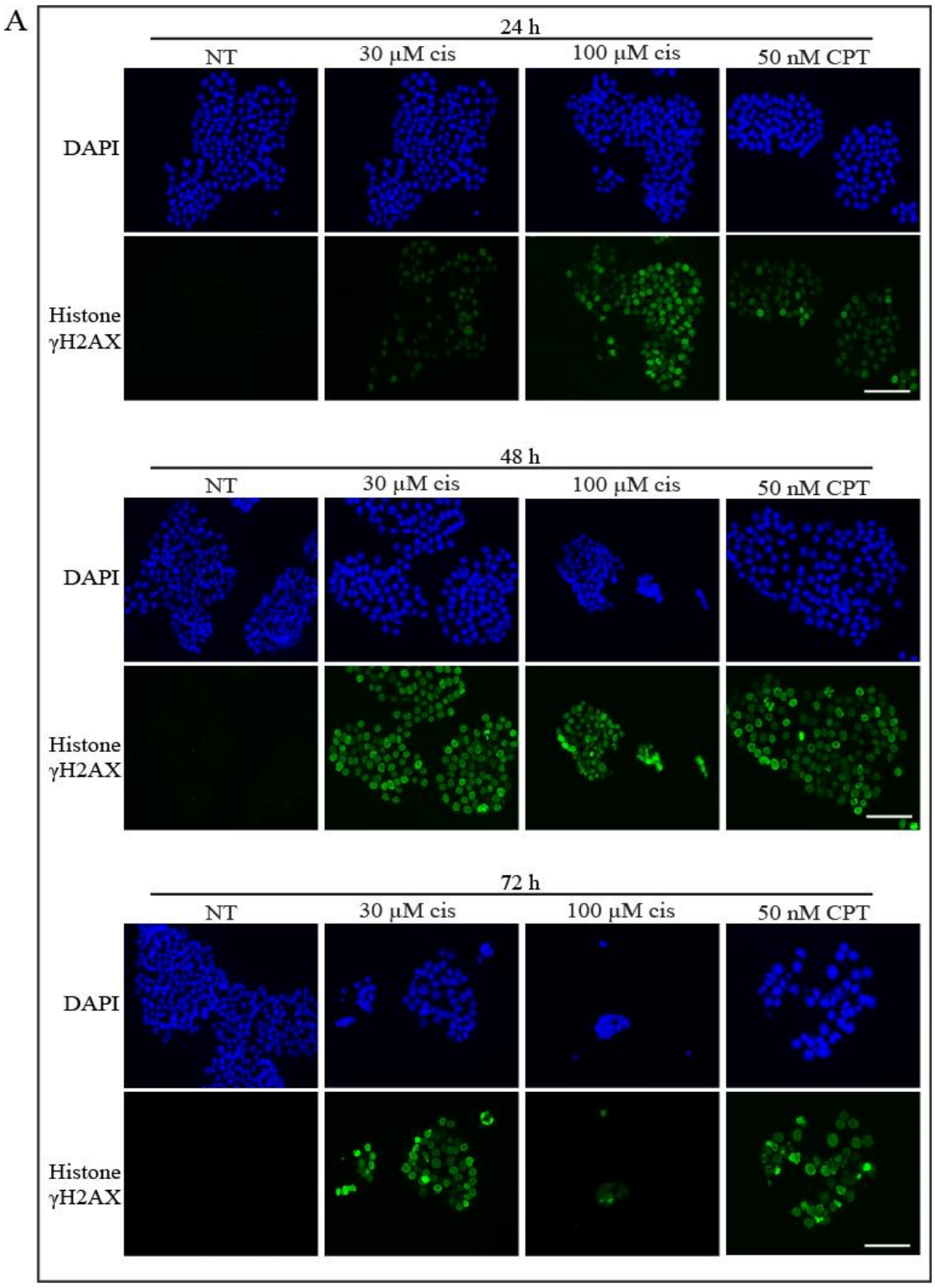
A
24 h
NT
30 μM cis
100 μM cis
50 nM CPT
DAPI
Histone γH2AX
48 h
NT
30 μM cis
100 μM cis
50 nM CPT
DAPI
Histone γH2AX
72 h
NT
30 μM cis
100 μM cis
50 nM CPT
DAPI
Histone γH2AX

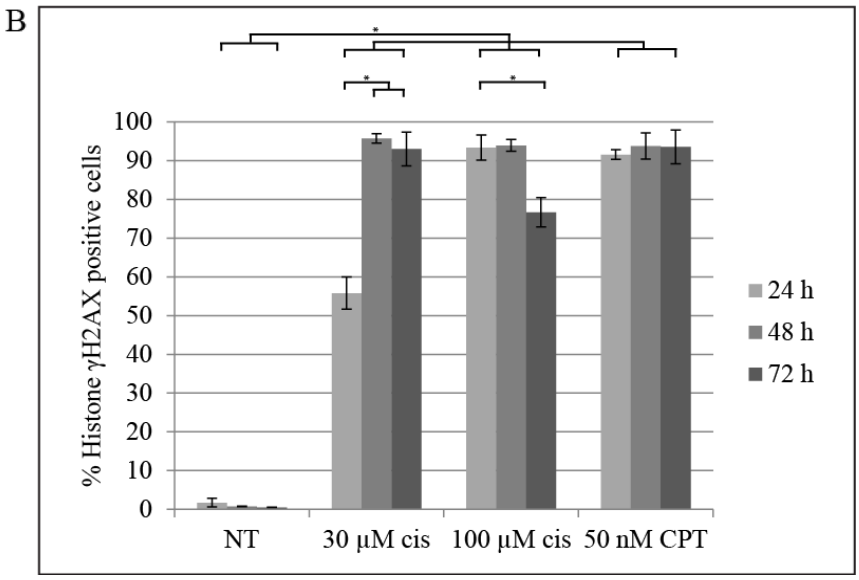

Figure 2.2 Cisplatin is genotoxic to HT-29 cells. A. HT-29 cells were either not treated (NT), treated with either 30 or 100 µM cisplatin or treated with 50 nM CPT and stained with DAPI (blue) to detect DNA and with anti-histone γH2AX antibodies (green). Cells were analysed at 24, 48 and 72 h by immunofluorescence microscopy and representative images are shown. Scale bar equals 100 µm. B. The percentages of cells staining positive for histone γH2AX 24, 48 and 72 h after treatment were determined using Image J software. At least 500 cells were counted for each treatment per experiment. Mean percentages of cells staining positive for histone γH2AX, calculated from three separate experiments, and standard errors of the means are shown. Asterisks show significant differences, paired student's t-test, 2 degrees of freedom, $p < 0.05$.

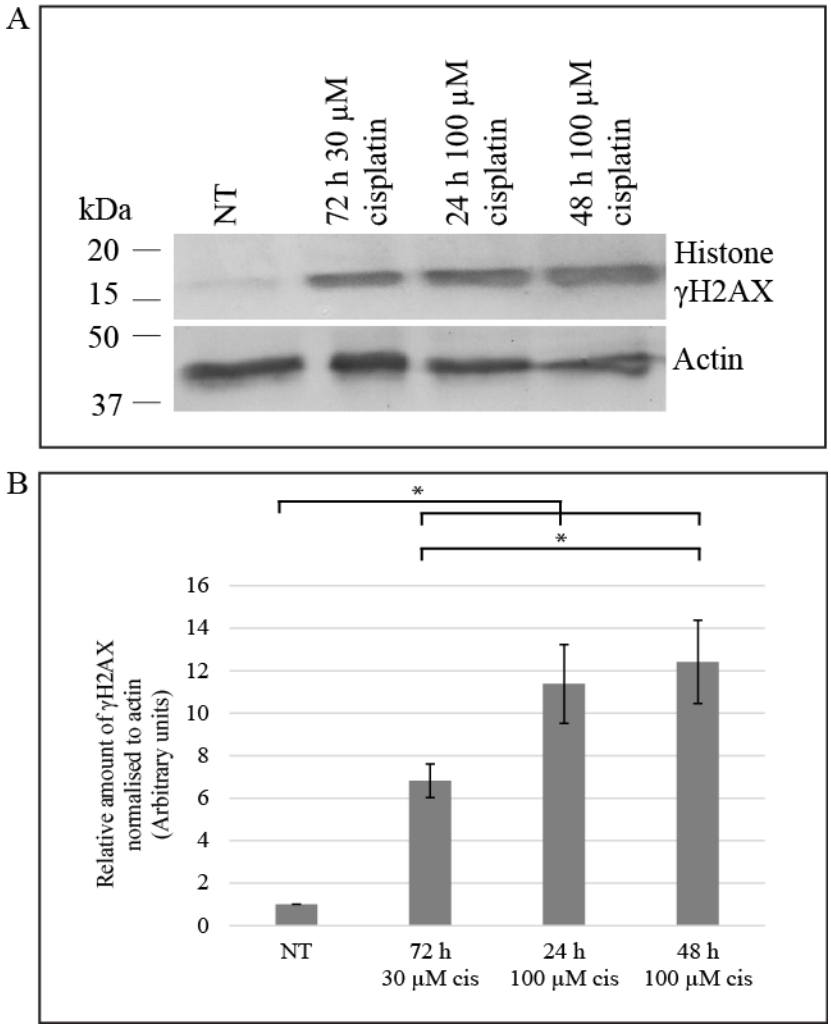

Figure 2.3 HT-29 cell populations treated with either 30 or 100 µM cisplatin contain different amounts of damaged DNA. A. HT-29 cells were either not treated (NT), treated for 72 h with 30 µM cisplatin or treated for 24 and 48 h with 100 µM cisplatin. Cell extracts were prepared and analysed by western blotting with anti-histone γH2AX and anti-actin antibodies. B. The relative amount of histone γH2AX signal was quantified for each treatment using Image J software. Means of arbitrary units of histone γH2AX signal normalised to actin and relative to not treated cells were calculated from three separate experiments. Standard errors of the means are shown. Asterisks show significant differences, paired student's t-test, 2 degrees of freedom, $p < 0.05$.

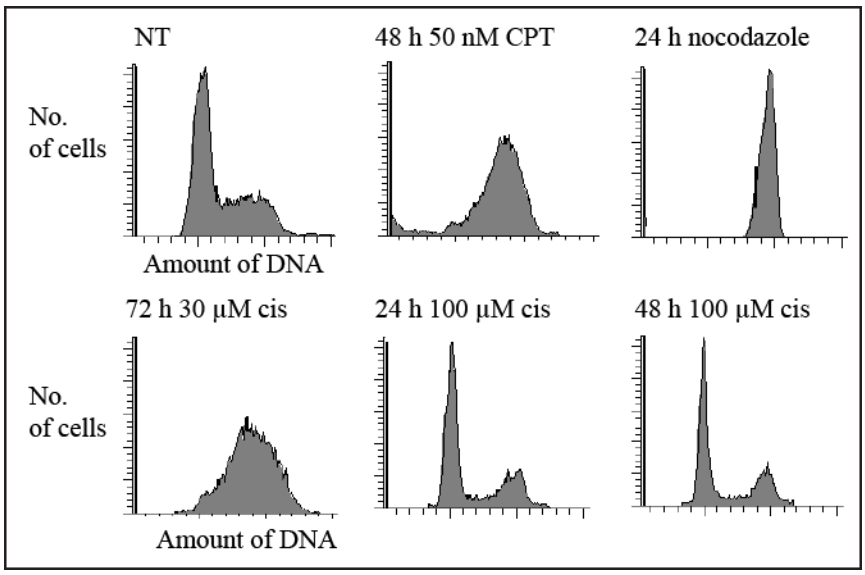

Figure 2.4 HT-29 cells treated with 30 µM cisplatin arrest predominantly in G2/M phase whereas 100 µM cisplatin treated cells do not progress in the cell cycle. HT-29 cells were treated for 72 h with 30 µM cisplatin and for 24 and 48 h with 100 µM cisplatin and analysed by flow cytometry. Not treated, 48 h 50 nM CPT treated and 24 h nocodazole treated (mitotic) cells were used as controls. DNA content was analysed by propidium iodide staining.

Table 2.2 The percentages of cells in either G1, S or G2/M phases of the cell cycle, as determined by analysis of DNA content using flow cytometry. Mean percentages from three separate experiments and standard errors of the means are shown.

Treatment	**G1 (Mean % ± SEM)**	**S (Mean % ± SEM)**	**G2/M (Mean % ± SEM)**
NT	69 ± 3	18 ± 3	13 ± 3
72 h 30 µM cisplatin	14 ± 5	38 ± 5	48 ± 5
24 h 100 µM cisplatin	77 ± 5	13 ± 1	10 ± 5
48 h 100 µM cisplatin	76 ± 5	13 ± 1	11 ± 4
50 nM CPT	9 ± 2	28 ± 10	63 ± 12
Nocodazole	1 ± 1	3 ± 3	96 ± 3

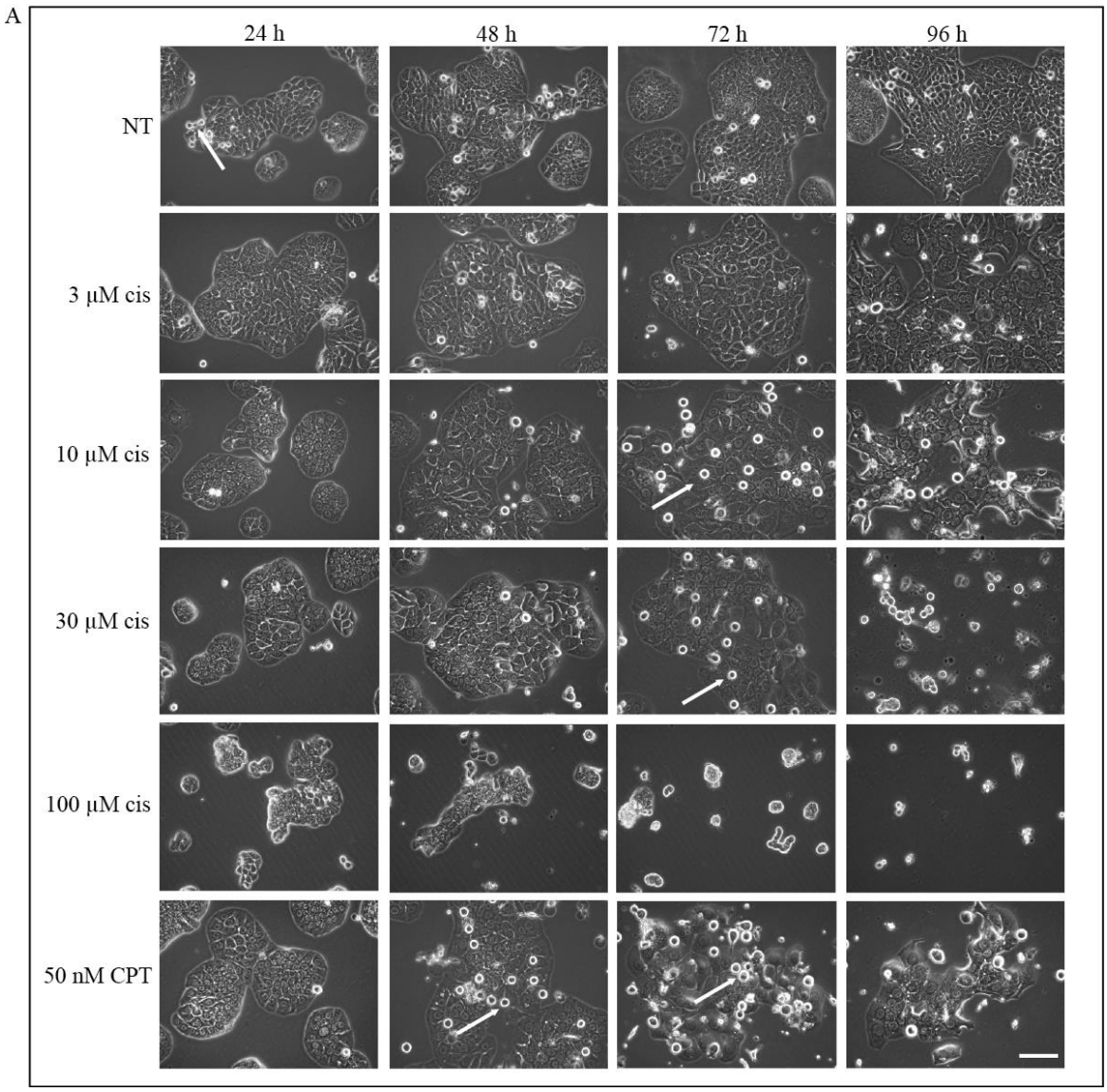
A
24 h
48 h
72 h
96 h
NT
3 μM cis
10 μM cis
30 μM cis
100 μM cis
50 nM CPT

B

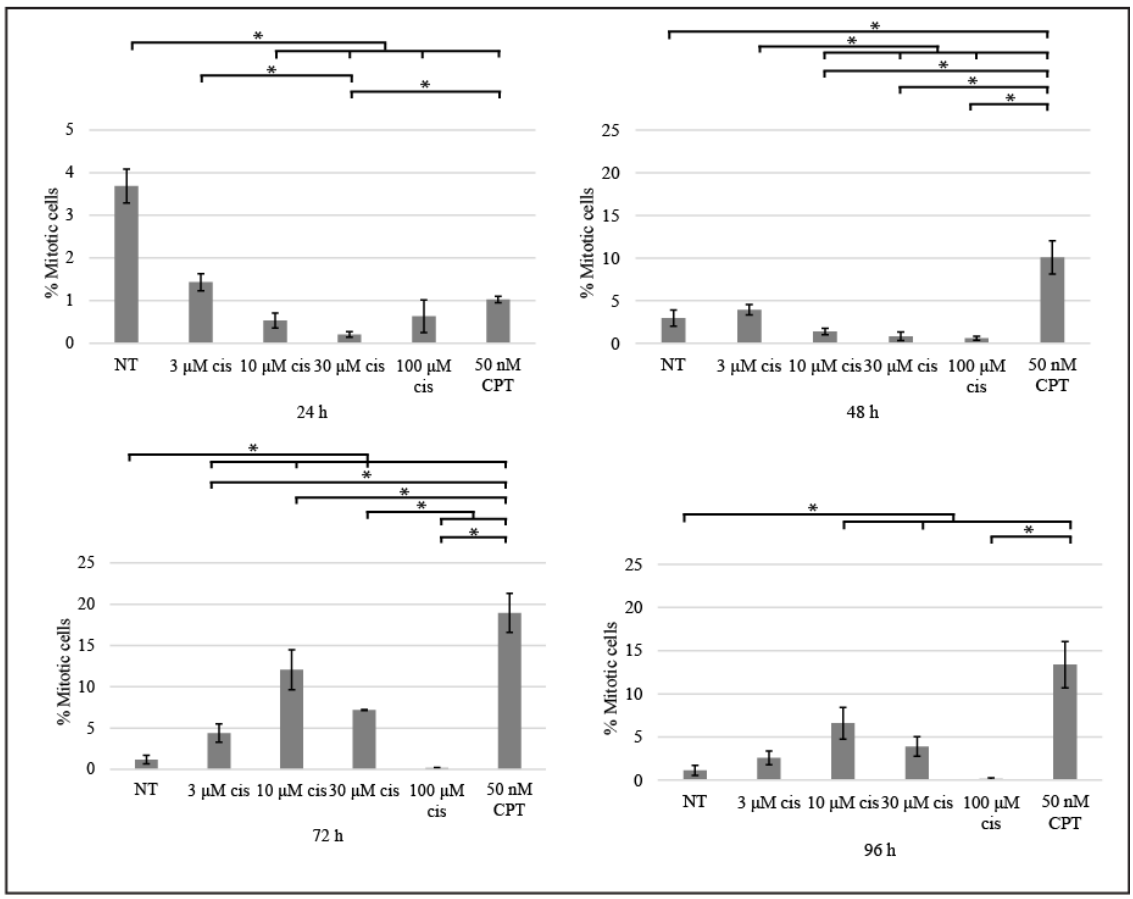

Figure 2.5 HT-29 cells treated with 30 µM cisplatin acquire a rounded morphology whereas 100 µM cisplatin treated cells do not. A. HT-29 cells were treated with 3, 10, 30 or 100 µM cisplatin. Not treated and 50 nM CPT treated cells were used as controls. Cells were observed by phase-contrast light microscopy at 24, 48, 72 and 96 h. Representative images are shown and arrows indicate mitotic cells. Scale bar equals 100 µm. B. HT-29 cells were treated with 3, 10, 30 or 100 µM cisplatin. Not treated and 50 nM CPT treated cells were used as controls. Cells were observed by phase-contrast light microscopy and percentages of rounded cells were manually determined using Image J software at 0, 24, 48, 72 and 96 h. At least 500 cells were counted for each treatment per experiment. Mean percentages from three separate experiments and standard errors of the means are shown. Asterisks show significant differences, paired student's t-test, 2 degrees of freedom, $p < 0.05$.

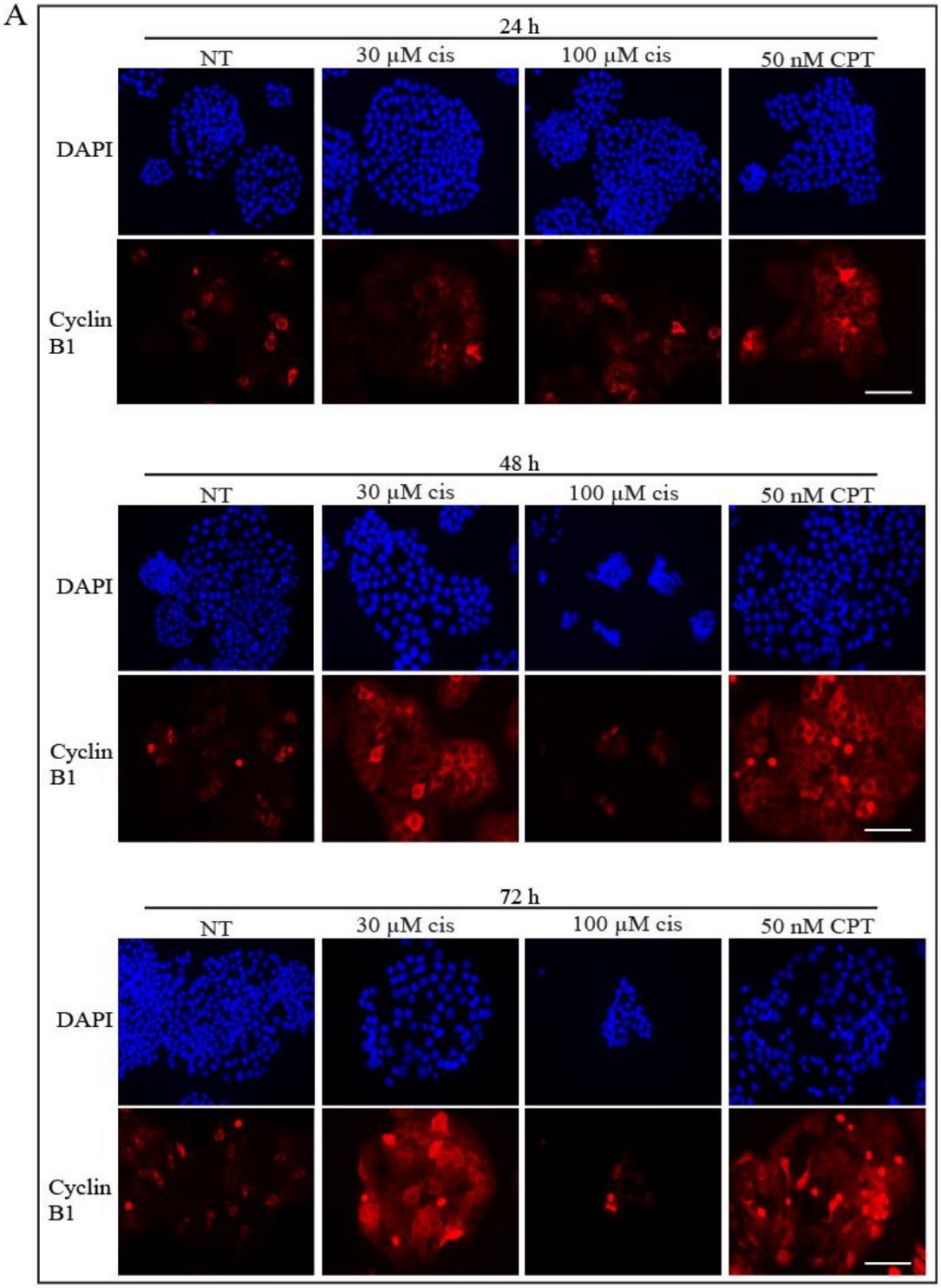
A
24 h
NT
30 μM cis
100 μM cis
50 nM CPT
DAPI
Cyclin B1
48 h
NT
30 μM cis
100 μM cis
50 nM CPT
DAPI
Cyclin B1
72 h
NT
30 μM cis
100 μM cis
50 nM CPT
DAPI
Cyclin B1

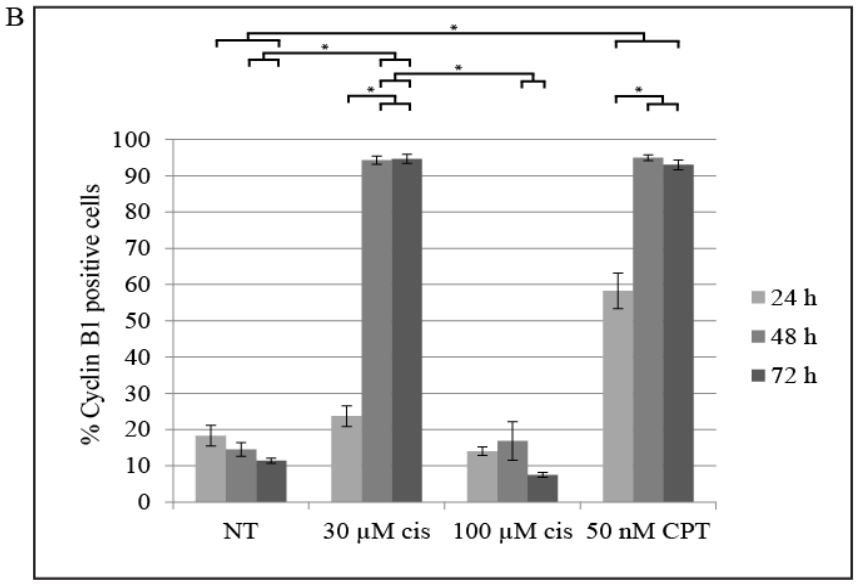

Figure 2.6 HT-29 cells treated with 30 µM cisplatin accumulate cyclin B1 whereas 100 µM cisplatin treated cells do not. A. HT-29 cells were not treated (NT), treated with either 30 or 100 µM cisplatin or treated with 50 nM CPT and stained with DAPI to detect DNA and with anti-cyclin B1 antibodies (red). Cells were analysed at 24, 48 and 72 h by immunofluorescence microscopy and representative images are shown. Scale bar equals 100 µm. B. The percentages of cells staining positive for cyclin B1 24, 48 and 72 h after treatment were determined using Image J software. At least 500 cells were counted for each treatment per experiment. Mean percentages of cells staining positive for cyclin B1, calculated from three separate experiments, and standard errors of the means are shown. Asterisks show significant differences, paired student's t-test, 2 degrees of freedom, $p < 0.05$.

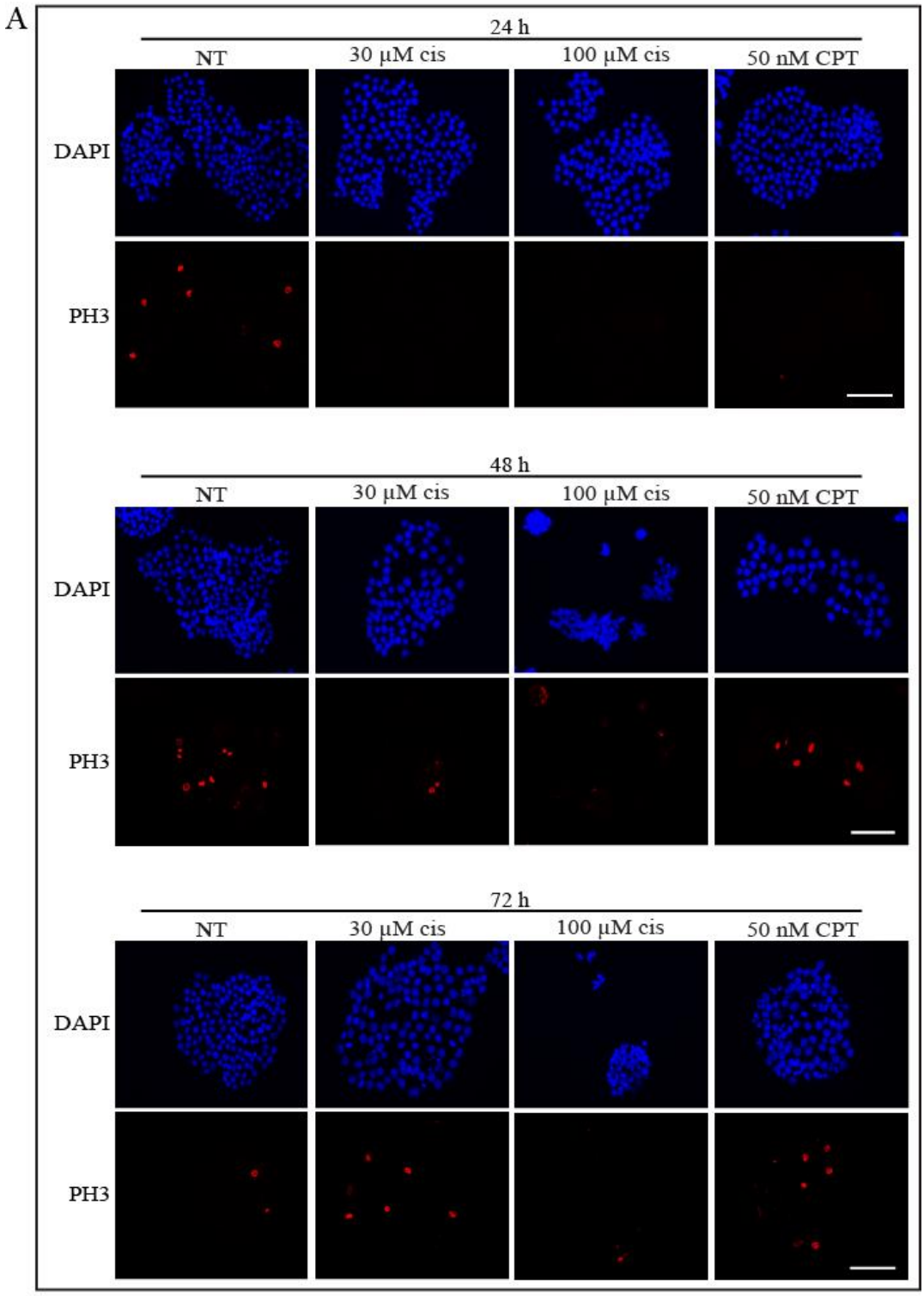
A
24 h
NT
30 μM cis
100 μM cis
50 nM CPT
DAPI
PH3
48 h
NT
30 μM cis
100 μM cis
50 nM CPT
DAPI
PH3
72 h
NT
30 μM cis
100 μM cis
50 nM CPT
DAPI
PH3

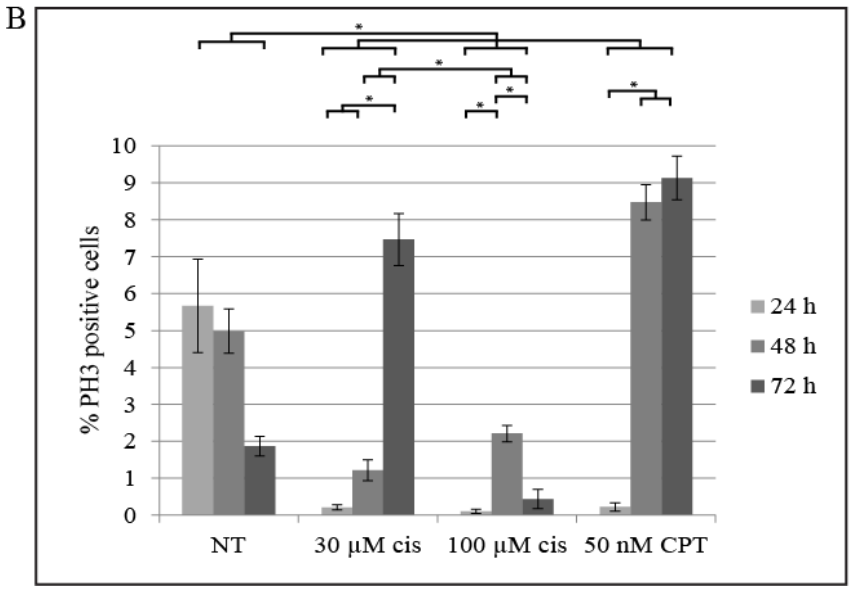

Figure 2.7 A sub-population of HT-29 cells treated with 30 µM cisplatin enter mitosis, whereas 100 µM cisplatin treated cells do not. A. HT-29 cells were not treated (NT), treated with either 30 or 100 µM cisplatin or treated with 50 nM CPT and stained with DAPI (blue) to detect DNA and with anti-phospho-Ser10 histone H3 antibodies (PH3) (red). Cells were analysed at 24, 48 and 72 h by immunofluorescence microscopy and representative images are shown. Scale bar equals 100 µm. B. The percentages of cells staining positive for phospho-Ser10 histone H3 (PH3) 24, 48 and 72 h after treatment were determined using Image J software. At least 500 cells were counted for each treatment per experiment. Mean percentages of cells staining positive for PH3, calculated from three separate experiments, and standard errors of the means are shown. Asterisks show significant differences, paired student's t-test, 2 degrees of freedom, $p < 0.05$.

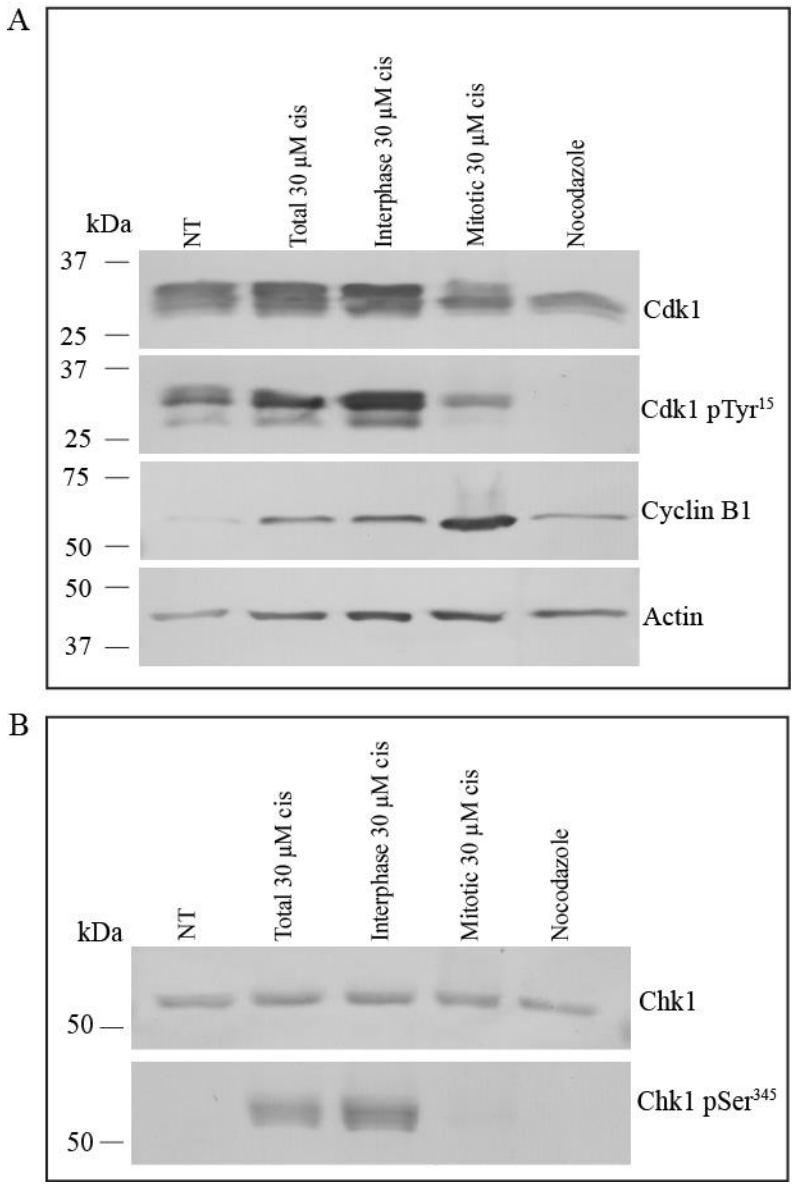

Figure 2.8 Rounded 30 µM cisplatin treated cells contain cyclin B1, dephosphorylated Cdk1 and dephosphorylated Chk1. A. HT-29 cells were either not treated (NT), treated for 72 h with 30 µM cisplatin or treated for 24 h with 200 ng/ml nocodazole. Mechanical shake-off was used to separate treated rounded (mitotic) cells from flattened interphasic cells and not treated, cisplatin treated total, interphasic and mitotic and nocodazole treated mitotic cell extracts were prepared. Cell extracts were analysed by western blotting using anti-Cdk1, anti-phospho Tyr15 Cdk1, anti-cyclin B1 and anti-actin antibodies. Molecular masses are indicated in kDa. B. Cell extracts were prepared as in (A) and analysed by western blotting using anti-Chk1 and anti-phospho Ser345 Chk1 antibodies. The actin loading control is presented in (A). Molecular masses are indicated in kDa.

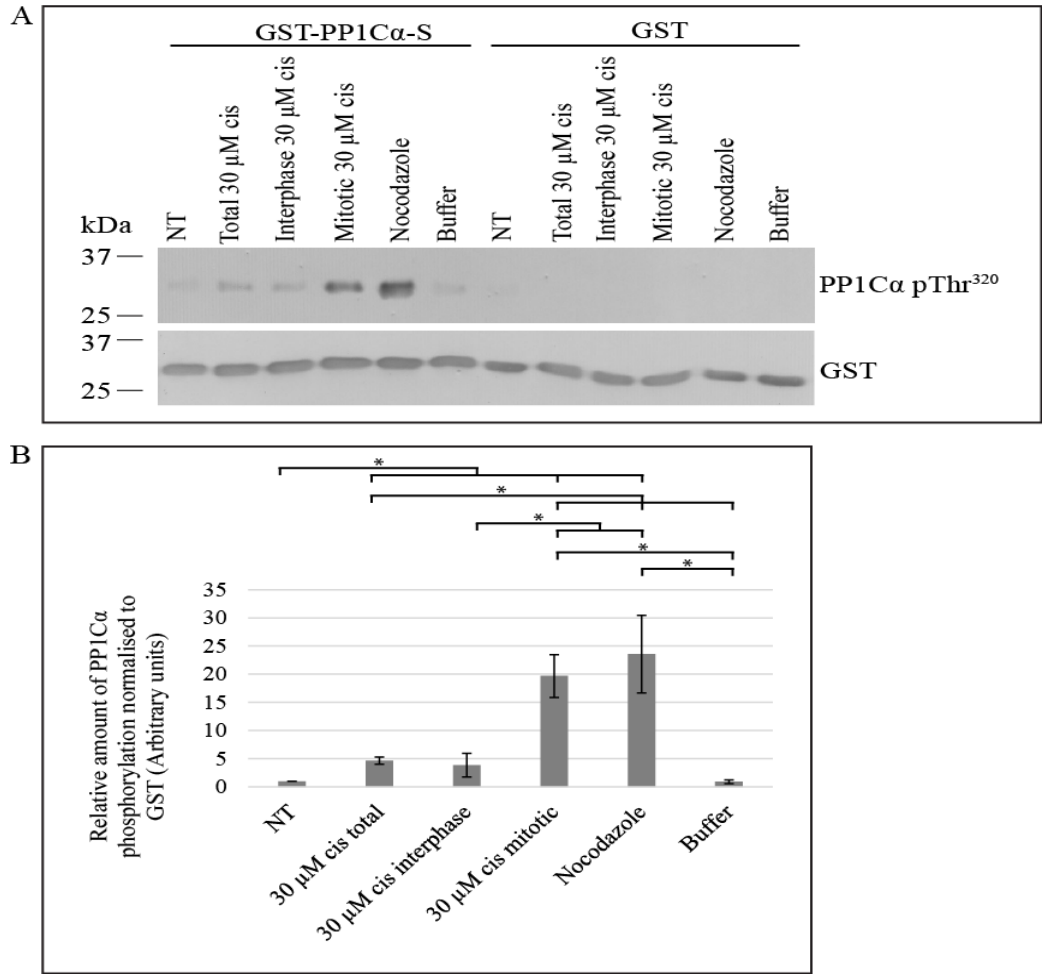

Figure 2.9 Rounded HT-29 cells treated with 30 µM cisplatin have active Cdk1. A. HT-29 cells were either not treated (NT), treated for 72 h with 30 µM cisplatin or treated for 24 h with 200 ng/ml nocodazole. Mechanical shake-off was used to separate treated rounded (mitotic) cells from flattened interphasic cells and not treated, cisplatin treated total, interphasic and mitotic and nocodazole treated mitotic cell extracts were prepared. Cell extracts were incubated with an artificial GST-Thr320-PP1Cα substrate (lanes 1-6) or a GST control substrate (lanes 7-12). Extraction buffer was used as a negative control. Samples were analysed by western blotting using anti-phospho Thr320 PP1Cα (top panel) and anti-GST (lower panel) antibodies. Molecular masses are indicated in kDa. B. The relative amount of phospho-Thr320 PP1Cα signal was quantified for each treatment using Image J software. Means of arbitrary units of phospho-Thr320 PP1Cα signal normalised to GST and relative to not treated cells were calculated from three separate experiments and standard errors of the means are shown. Asterisks show significant differences, paired student's t-test, 2 degrees of freedom, $p < 0.05$.

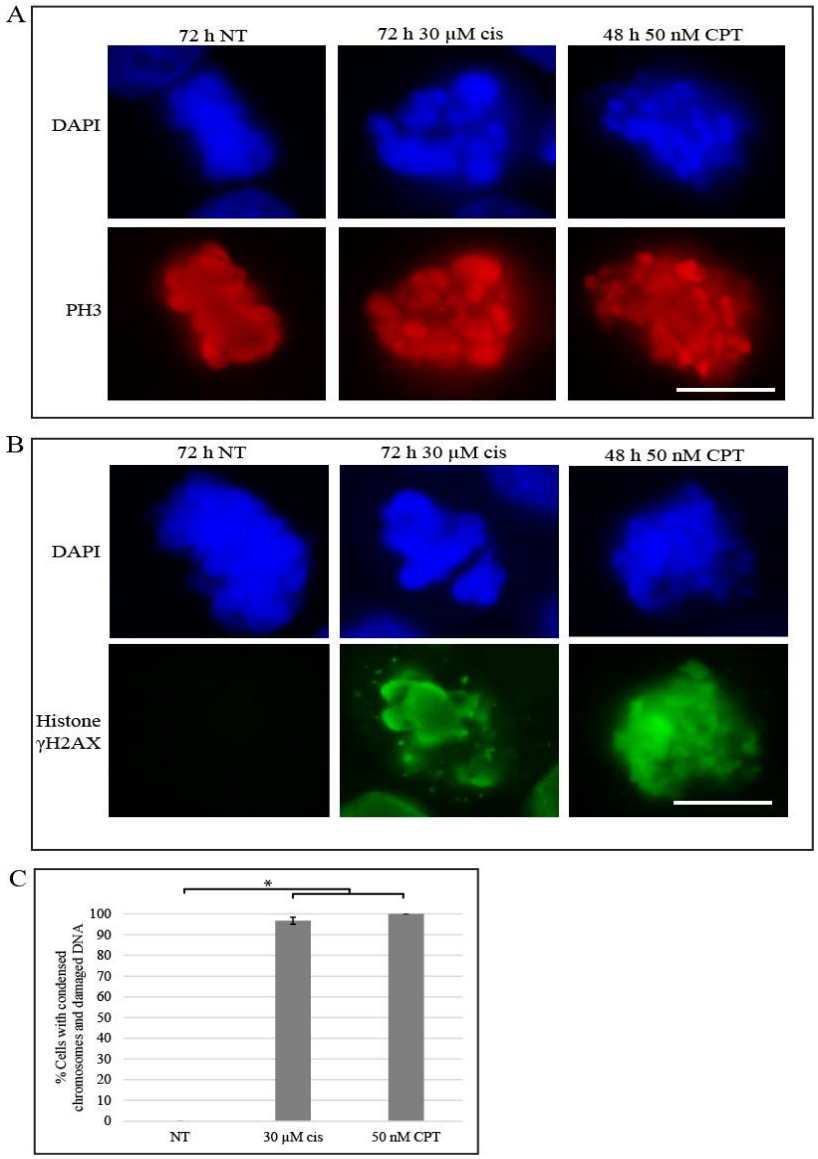

Figure 2.10 HT-29 cells treated with 30 µM cisplatin are in mitosis with damaged DNA. A. HT-29 cells were either not treated (NT), treated for 72 h with 30 µM cisplatin or treated for 48 h with 50 nM CPT. Cells were stained with DAPI to detect condensed chromosomes (blue) and with anti-phospho Ser10 histone H3 (PH3) antibodies (red). Scale bar equals 10 µm. B. HT-29 cells were either not treated (NT), treated for 72 h with 30 µM cisplatin or treated for 48 h with 50 nM CPT. Cells were stained with DAPI to detect condensed chromosomes (blue) and with anti-histone γH2AX antibodies (green). Scale bar equals 10 µm. C. HT-29 cells were either treated for 72 h with 30 µM cisplatin or for 48 h with 50 nM CPT. Mean percentages of cells with condensed chromosomes staining positive for histone γH2AX were calculated from three separate experiments and standard errors of the means are shown Twenty cells were counted for each treatment per experiment. Asterisks show significant differences, paired student's t-test, 2 degrees of freedom, $p < 0.05$.

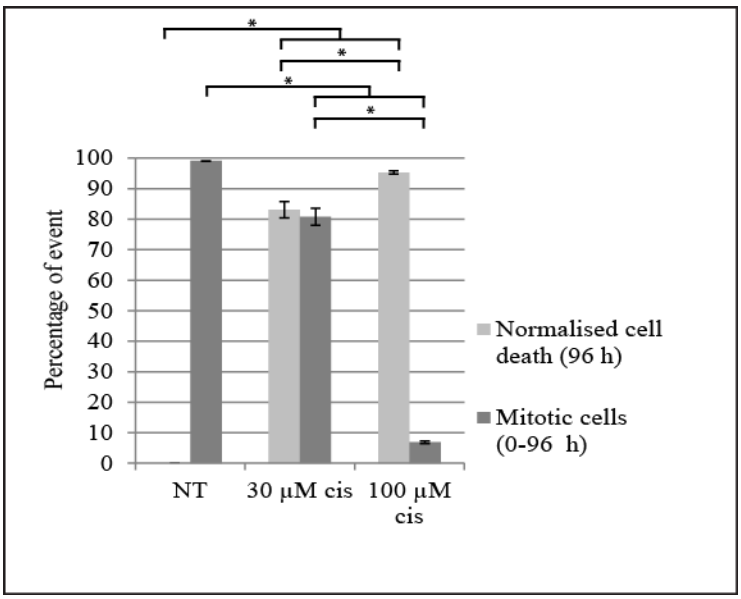

Figure 2.11 Most HT-29 cells treated with 30 µM cisplatin enter mitosis before dying, whereas most 100 µM cisplatin treated cells do not. HT-29 cells were not treated (NT) or treated with either 30 or 100 µM cisplatin and observed by time-lapse video microscopy. Images were captured every 10 min for 96 h and individual cells were manually observed to detect the presence or absence of cell rounding. The percentages of cells that entered mitosis post-treatment were then determined for each treated cell population. The percentage of normalised cell death is also presented for each treatment, as determined by the MTT assay (Figure 2.1). Mean percentages of event from three separate experiments and standard errors of the means are shown. Asterisks show significant differences, paired student's t-test, 2 degrees of freedom, $p < 0.05$.

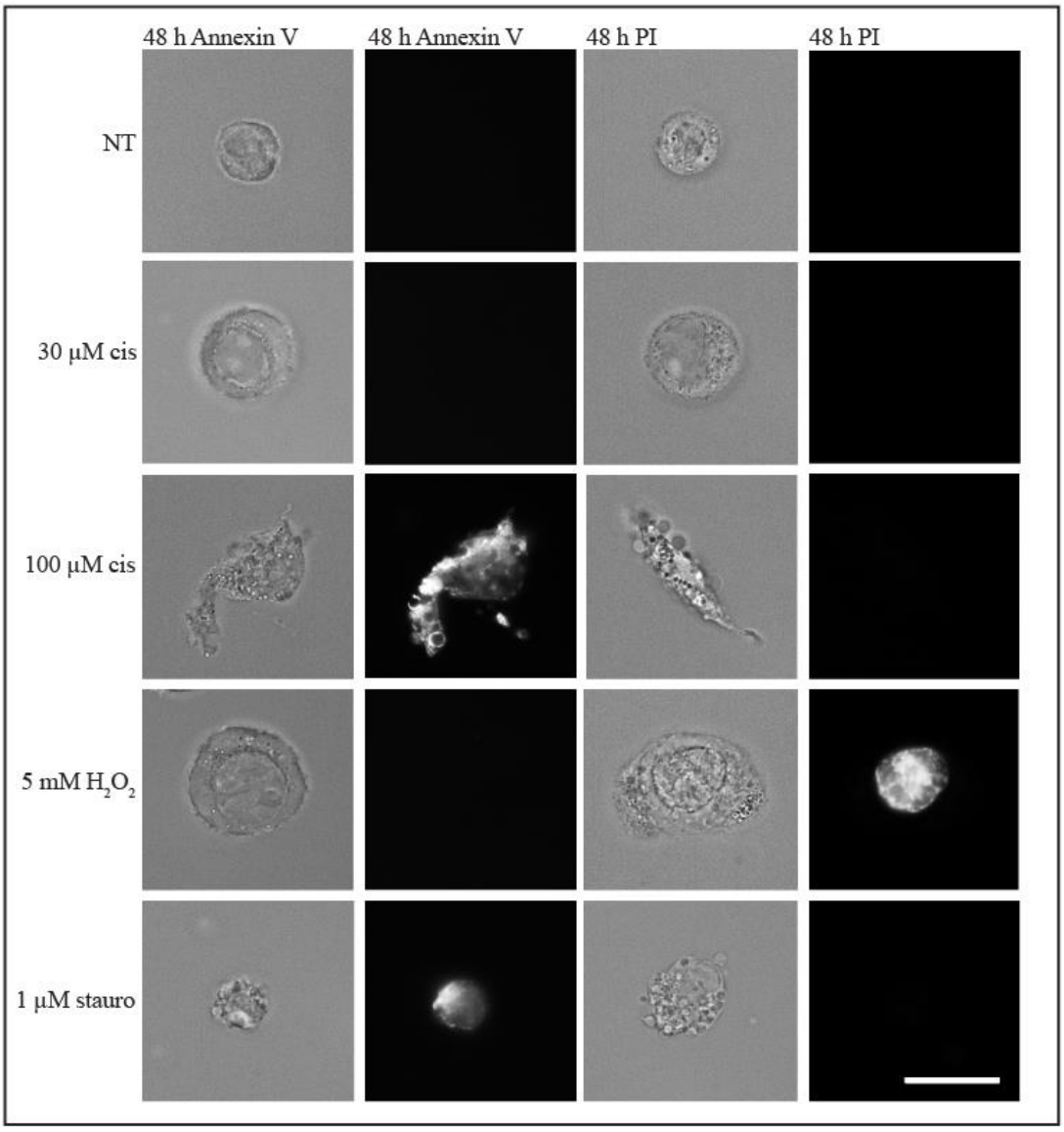

Figure 2.12 HT-29 cells treated with 100 µM cisplatin are positive for annexin V staining. HT-29 cells were treated with either 30 or 100 µM cisplatin for 24, 48, 72, 96 and 120 h. Cells were then collected by trypsinisation and stained for annexin V or treated for 24, 48, 72, 96 and 120 h, collected by trypsinisation and stained with propidium iodide (PI). Not treated cells were used as a negative control, 1 µM staurosporine treated cells were used as a positive control for apoptosis and 5 mM hydrogen peroxide (H_2O_2) treated cells were used as a positive control for necrosis. Cells were then analysed by light and immunofluorescence microscopy. Representative images of cells 48 h after treatment are shown. Scale bar equals 10 µm.

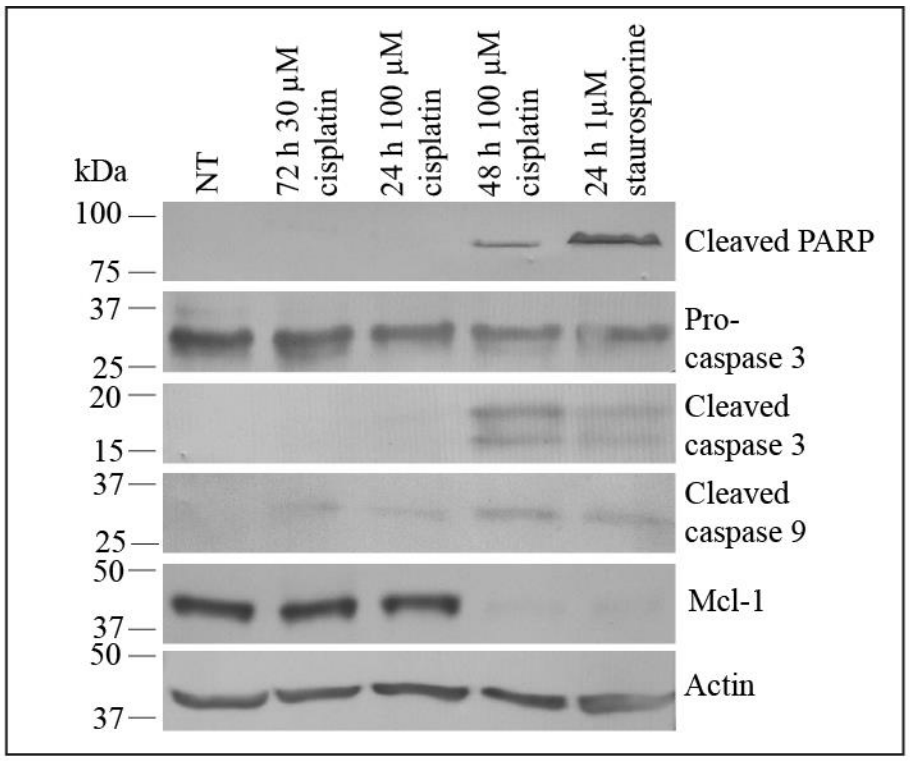

Figure 2.13 HT-29 cells treated with 100 µM cisplatin undergo apoptosis. HT-29 cells were either treated for 72 h with 30 µM cisplatin or treated for 24 and 48 h with 100 µM cisplatin. Not treated and 24 h 1 µM staurosporine treated cells were used as controls. Total cell extracts were prepared and analysed by western blotting with anti-cleaved PARP, anti-pro-caspase 3, anti-cleaved caspase 3, anti-cleaved caspase 9, anti-Mcl1 and anti-actin antibodies. Molecular masses are indicated in kDa.

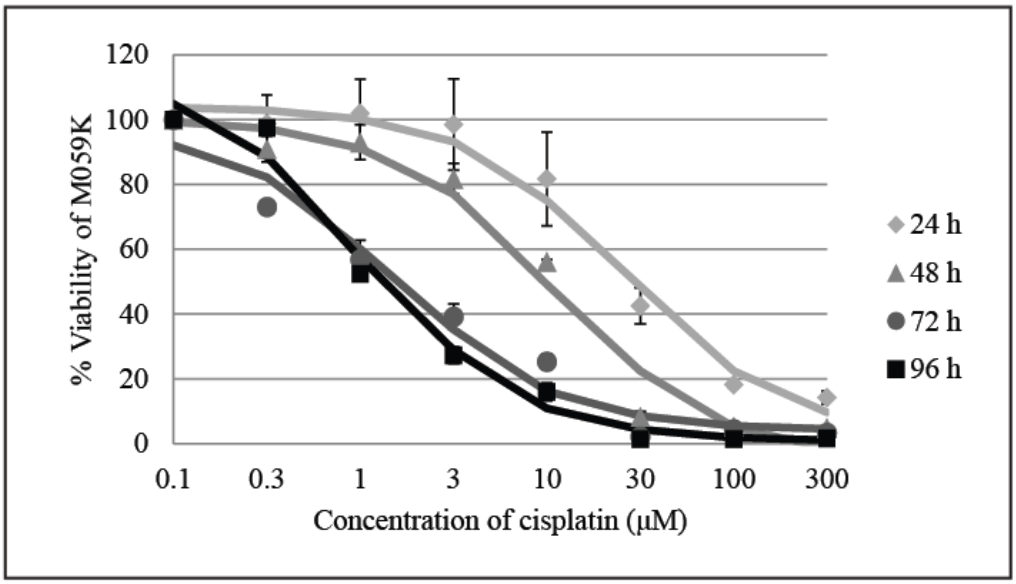

Figure 2.14 Cisplatin is cytotoxic to M059K cells. M059K cells were treated with different concentrations of cisplatin for 24 h (diamonds), 48 h (triangles), 72 h (circles) and 96 h (squares). The MTT assay was used to measure cell viability. Each treatment was run in triplicate and the results from each treatment condition were normalised to treatment with 0.1% (v/v) DMSO. Mean percentages of viability were calculated from three separate experiments and standard errors of the means are shown.

Table 2.3 Mean IC_{50} concentrations of cisplatin used to treat M059K cells for 24, 48, 72 and 96 h

	Time (h)			
Genotoxic agent	24	48	72	96
Cisplatin (μM)	30	9	2	1

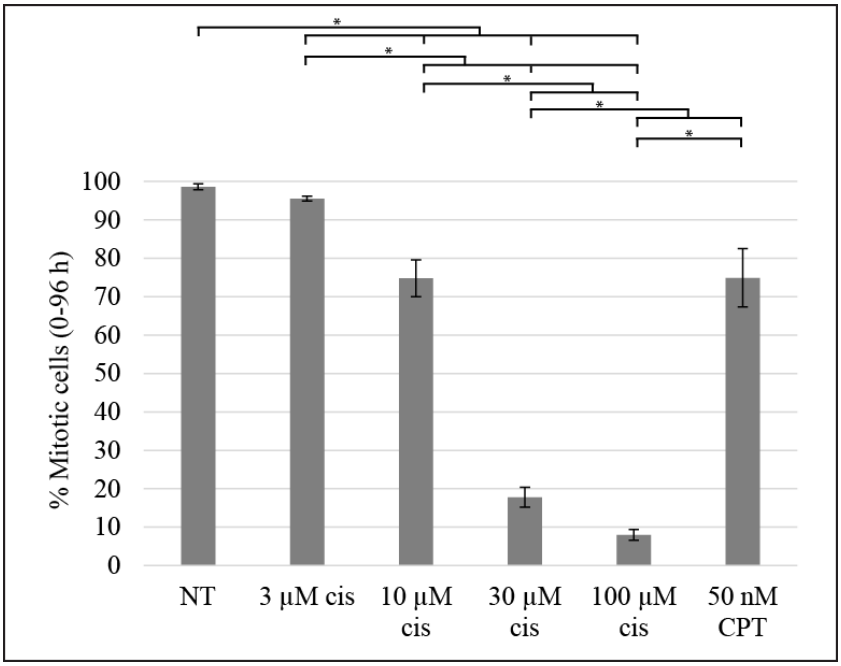

Figure 2.15 M059K cells undergo dual modes of cell death when treated with either relatively low or relatively high concentrations of cisplatin. M059K cells were either not treated (NT), treated with 3, 10, 30 or 100 µM cisplatin or treated with 50 nM CPT and observed by time-lapse video microscopy. Images were captured every 10 min for 96 h and individual cells were manually observed to detect the presence or absence of cell rounding. The percentages of cells that entered mitosis were manually determined for each treated cell population. Mean percentages of mitotic cells from three separate experiments and standard errors of the means are shown. Asterisks show significant differences, paired student's t-test, 2 degrees of freedom, $p < 0.05$.

CHAPTER 3

Mitosis is not required for cell death in human colorectal adenocarcinoma cells that undergo checkpoint adaptation

3.1 Abstract

Checkpoint adaptation may provide cells with an opportunity to survive treatment with rearranged genomes, by transmitting damaged DNA to daughter cells. HT-29 human colorectal adenocarcinoma cells undergo checkpoint adaptation when they are treated with a relatively low, yet cytotoxic concentration of cisplatin. We investigated the role of mitosis in cell death following treatment with cisplatin and found that a small, but biologically significant number of cisplatin treated cells survive checkpoint adaptation. To assess if cells treated with cisplatin can die without entering mitosis, we co-treated cells with CR8, an inhibitor of Cdk1. We show that mitosis is not required for cell death in HT-29 cells treated with cisplatin. We expanded these observations by investigating checkpoint adaptation induced by a second genotoxic agent, camptothecin (CPT), which has a different mechanism of action to that of cisplatin. We found that a small number of CPT treated cells also survive checkpoint adaptation. Furthermore, we demonstrate that mitosis is not required for cell death in HT-29 cells treated with CPT. The inhibition of mitosis in cells treated with genotoxic agents that usually induce checkpoint adaptation is therefore an attractive option to investigate further, with the aim of preventing cells from acquiring genomic change following treatment, which may increase the efficacy of current genotoxic anti-cancer drugs.

3.2 Introduction

HT-29 human colorectal adenocarcinoma cells undergo checkpoint adaptation (entry into mitosis with damaged DNA) when they are treated with camptothecin (CPT) (Kubara et al. 2012). The majority of these CPT treated cells die following entry into mitosis with damaged DNA, but it has been observed that a small number of CPT treated cells can survive checkpoint adaptation (Kubara et al. 2012; Rahman 2013). In chapter 2 we demonstrated that HT-29 cells treated with a cytotoxic concentration of cisplatin (30 µM) undergo checkpoint adaptation. The discovery that treated cancer cells undergo checkpoint adaptation before dying permitted us to ask new questions about the role of mitosis in cell death and to determine the number of cells that can survive checkpoint adaptation.

Resisting cell death is one hallmark of cancer (Hanahan and Weinberg 2011). To understand how cancer cells resist cell death, we first explored the pathways by which they die when treated with genotoxic agents such as cisplatin. In chapter 2, we demonstrated that HT-29 cells are capable of dying without entering mitosis, when they are treated with 100 µM cisplatin. However, 100 µM cisplatin is above the peak plasma concentrations of cisplatin reported from human patients (Vermorken et al. 1984; Oldfield et al. 1985; Charlier et al. 2004). Peak plasma concentrations of platinum in patients treated with cisplatin have reached 40 µM (Vermorken et al. 1984) and typically range from 3-17 µM (Charlier et al. 2004). Cisplatin treatment is associated with severe side effects and treatment with concentrations of cisplatin above those tolerated in the patient can cause patient death with symptoms including blindness, ototoxicity, septicaemia and kidney failure (Charlier et al. 2004).

By contrast to cells treated with 100 μM cisplatin, at a lower concentration of cisplatin (30 μM), HT-29 cells first entered mitosis before dying. By using HT-29 cells, which spend a prolonged time in mitosis (Gascoigne and Taylor 2008), we were able to collect cells that undergo checkpoint adaptation and investigate whether any of these cells could survive. It is important to understand whether cells can survive checkpoint adaptation because checkpoint adaptation may promote genomic change in treated cancer cells (Syljuåsen et al. 2006; Kubara et al. 2012).

Checkpoint adaptation can cause genomic change in the yeast *Saccharomyces cerevisiae* when exposed to X-ray irradiation (Galgoczy and Toczyski 2001). Checkpoint adaptation proficient and checkpoint adaptation deficient *S. cerevisiae* cells were irradiated with 30 Gray of X-rays and checkpoint adaptation proficient cells contained more chromosomal losses and translocations, by comparison to checkpoint adaptation deficient cells (Galgoczy and Toczyski 2001). Checkpoint adaptation has also been shown to induce the formation of acentric chromosome fragments and chromosomal bridges in irradiated *Allium cepa* plant cells (Carballo et al. 2006). Preliminary data obtained by investigating HT-29 cells has also suggested that human cancer cells surviving checkpoint adaptation following treatment with CPT contain rearranged genomes (Rahman 2013). These survival cells contained an average of 35 chromosomes. By comparison, not treated cells contained an average of 65 chromosomes. Because cells that survive checkpoint adaptation are transmitting damaged DNA to daughter cells then this may induce acquired resistance to treatment, reducing the efficacy of genotoxic anti-cancer drugs.

Clinically, the long-term efficacy of cisplatin is severely limited by acquired resistance to treatment (Oliver et al. 2010). Treatment with cisplatin has also been associated with the induction of chromosomal aberrations in cell lines and animal models (Adler and El-Tarras 1989; Krishnaswaky and Dewey 1993; Edelweiss et al. 1995) and it is likely that checkpoint adaptation contributes to this genomic change. Genomic change underlies acquired resistance in cancer cells treated with cisplatin (Shen et al. 2012), thus cells that survive checkpoint adaptation might acquire resistance to treatment.

To prevent treated cancer cells from acquiring resistance to genotoxic anti-cancer agents, it may be beneficial to maintain the cytotoxicity of cisplatin and prevent treated cells from entering mitosis with damaged DNA (the final step of checkpoint adaptation). However, it is not known whether cytotoxicity is maintained when mitosis is inhibited in cells that die following checkpoint adaptation. By understanding the process of checkpoint adaptation it is possible to target the proteins involved in this pathway (Figure 1.3), to test if cells can die when mitosis is inhibited. For example, cyclin dependent kinase 1 (Cdk1) (the enzyme responsible for entry into mitosis) (Lee and Nurse 1987) can be inhibited to prevent cells from entering mitosis.

We investigated if HT-29 cells with cisplatin induced DNA damage could die when they were prevented from entering mitosis. We found that it is possible to direct cisplatin treated cells towards the pathway of checkpoint adaptation but prevent them from entering mitosis by co-treatment with the Cdk1 inhibitor, CR8 (Bettayeb et al. 2008). Importantly, cell death can be maintained when cisplatin treated cells are prevented from entering mitosis. Furthermore, we identified that cells treated with a

different genotoxic agent, CPT, can also survive checkpoint adaptation and that cell death can be maintained when CPT treated cells are prevented from entering mitosis.

3.3 Materials and methods

3.3.1 Cell culture

The human cell line HT-29 (ATCC HTB-38) was obtained from the American Type Culture Collection (ATCC). HT-29 cells were maintained in RPMI 1640 medium (Gibco; 21870-092) supplemented with 10% (v/v) heat inactivated fetal bovine serum (FBS) (Gibco; 12484028) and 1.6 mM GlutaMAX (Gibco; 35050-061). Cells were grown at 37°C in 5% CO_2 and the medium was changed every 3-4 d. HT-29 cells were plated at a density of 3.0 x 10^5 cells/25 cm^2 flask and cultured for 72 h prior to treatment. Cells were counted using a Luna automated cell counter (Logos Biosystems). The compound cisplatin (Sigma; 479306-1G) was dissolved in dimethyl sulphoxide (DMSO) (Sigma-Aldrich; D2438) to a concentration of 100 mM and stocks were freshly made every two weeks. Camptothecin (Sigma; 7689-03-4) was dissolved in DMSO to a concentration of 10 mM. The compounds were stored at -20°C until use. Not treated cells were treated with the solvent only (0.1% (v/v) DMSO).

3.3.2 Mechanical shake-off to investigate cell survival by light microscopy

HT-29 cells were plated at 1 x 10^6 cells/75 cm^2 flask and incubated at 37°C for 72 h prior to treatment. After treatment, medium was aspirated and cells were gently washed with phosphate buffered saline (PBS) (137 mM NaCl, 3 mM KCl, 100 mM Na_2HPO_4, 18 mM KH_2PO_4). Fresh medium was added at 1 ml/25 cm^2 and the flask was tapped with

medium force on all edges to isolate mitotic cells from flattened cells. The rounded cells were then cultured in the wells of a 6 well culture plate and incubated at 37°C. Cell medium was changed every 3-4 d. Images were captured with an Infinity 1.5 camera powered by Infinity Capture imaging software (Lumenera Corporation) on an Olympus IX41 inverted microscope. Images were processed using Adobe Photoshop (CC 2014.1.0) software. Experiments were performed three times.

3.3.3 Clonogenic assay

HT-29 cells were plated at 1 x 10^6 cells/75 cm^2 flask and incubated at 37°C for 72 h prior to treatment. Following treatment, rounded cells were collected by mechanical shake-off and counted using a Luna automated cell counter (Logos Biosystems). The cells were then re-seeded. It was necessary to seed treated cells at a higher density by comparison to the not treated cells, to account for the cell death induced by the genotoxic agents. The 6 well plates were incubated at 37°C for 14 d and media were changed every 3-4 d. The cells were then fixed and stained with 6% (v/v) glutaraldehyde (Ted Pella Inc; 18426) and 0.5% (w/v) crystal violet (Electron Microscopy Services; 12785) diluted in deionised water at room temperature for 30 min. The wells were rinsed with deionised water and left to dry at room temperature. The number of colonies were counted using Image J software. Only colonies containing 50 or more cells were considered viable. This was verified by light microscopy. Not treated cells were then analysed to determine plating efficiency (PE) using the formula:

PE = number of colonies formed/number of cells seeded x 100

The surviving fraction (SF) for the surviving cells was then calculated using the formula:

SF = number of colonies formed after treatment/(number of cells seeded x PE).

Experiments were performed three times.

3.3.4 Time-lapse video microscopy

HT-29 cells were plated at 3.0 x 10^5/25 cm^2 flask and incubated at 37°C for 72 h prior to treatment. Time-lapse video microscopy images were collected from the start of treatment, using a Lumascope 500 microscope (etaluma) powered by LumaView software (etaluma; V.13.4.25.99). Images were captured every 10 min for 96 h. Cells were manually scored for mitotic entry by observing whether they displayed a rounded morphology, indicative of mitosis, or not between 0 and 96 h. Cells that left the field of view before rounding were not counted. At least 250 HT-29 cells were counted for each treatment. Experiments were performed three times.

3.3.5 Trypan blue assay to detect cell survival

HT-29 cells were seeded at precisely 1.0 x 10^5/well of a 6 well plate and incubated at 37°C for 72 h prior to treatment. Following treatment cells were washed with PBS and collected by trypsinisation. An equal amount of medium was added and a 50 µl aliquot was removed. Cells were then mixed with trypan blue solution at a ratio of 1:1. Cells were counted twice using a Luna automated cell counter (Logos Biosystems) to determine the number of live cells present in each treated cell population. An average of the two values was calculated and used to determine the relative viability of cells from each treated cell population, normalised to cells treated with 0.1% (v/v) DMSO. The normalised percent viability was calculated as shown:

Normalised percent viability = (number of live treated cells/number of live DMSO treated cells) x 100

3.3.6 Statistical analysis

Graphs were produced using Microsoft Excel 2010 software. Data were collected and plotted as means ± standard error of the means from three separate experiments. Statistical significance was calculated using the student's t-test for two paired sample means and values were considered significantly different when $p < 0.05$.

3.4 Results

3.4.1 A small number of HT-29 cells can survive entry into mitosis after treatment with 30 µM cisplatin

We first investigated if any of the cells that entered mitosis 72 h after treatment with 30 µM cisplatin were able to survive. HT-29 cells were treated for 72 h with 30 µM cisplatin and the rounded mitotic cells were collected by mechanical shake-off. Mitotic cells were then re-cultured without further treatment for over 30 d and observed by light microscopy. Images were captured 96 h, 10 d, 21 d and 31 d after mechanical shake-off (Figure 3.1). Not treated cells were collected as controls.

Multiple colonies were present in the not treated cell culture 96 h after shake-off and these expanded over time. By 10 d the not treated cell culture had reached confluence. The mitotic cells collected after treatment with cisplatin colonised the culture dish after mechanical shake-off (Figure 3.1A). Small colonies were observed 96 h after mechanical shake-off and these continued to expand for over 30 d. Fewer cells were

present in the cisplatin treated colonies at 10 d by comparison to the number of cells present in not treated colonies.

Having identified that cisplatin treated cells could survive checkpoint adaptation we used treatment with a second genotoxic agent, CPT, to confirm that cells can survive checkpoint adaptation following treatment with a genotoxic agent that has a different mechanism of action by comparison to cisplatin. The CPT treated mitotic cells also colonised the culture dish (Figure 3.1B) and fewer cells were present in the CPT treated colonies at 10 d by comparison to the number of cells present in not treated colonies.

We next used the clonogenic assay to quantify the number of cells that survived checkpoint adaptation following treatment with cisplatin (Figure 3.2). HT-29 cells were treated for 72 h with 30 μM cisplatin and mitotic cells were collected by mechanical shake-off, counted and then cultivated without further treatment for 14 d. Mitotic cells from not treated cell populations were also collected, as controls. Five hundred and 1,000 not treated cells were cultivated. It was necessary to plate more treated cells than not treated cells to account for the cell death induced by treatment with cisplatin. Numerous colonies were formed when the mitotic not treated cells were cultured. The percentage of colonies formed was used to determine the plating efficiency of mitotic HT-29 cells (17.4%). The clonogenic survival of mitotic cells collected from cells treated with cisplatin was 0.01 ± 0.005%.

We also quantified the number of cells that survive checkpoint adaptation following treatment with a second genotoxic agent, CPT (Figure 3.2). When mitotic cells were collected after treatment with 50 nM CPT, 0.09 ± 0.03% survived. These data

demonstrate that a small percentage of cells that undergo checkpoint adaptation following treatment with either cisplatin or CPT can survive.

3.4.2 Entry into mitosis can be prevented in HT-29 cells co-treated with 30 µM cisplatin and 10 µM CR8

We previously confirmed that 30 µM cisplatin is cytotoxic to HT-29 cells, and demonstrated that cells treated with 30 µM cisplatin undergo checkpoint adaptation prior to cell death (Chapter 2). We also found that a small number of mitotic cells collected by mechanical shake-off were able to survive checkpoint adaptation. To test if mitosis was required for cell death in the 99% of cisplatin treated cells that died, we first confirmed that we could prevent entry into mitosis in cisplatin treated cells that were destined to undergo checkpoint adaptation (Figure 1.3). To prevent entry into mitosis in cisplatin treated cells we chose to use CR8, a small molecule inhibitor of Cdk1 (Bettayeb et al. 2008) because it has been well described in the literature and has been previously shown to prevent cells from entering mitosis in our laboratory (Kubara et al. 2012). HT-29 cells were co-treated with 30 µM cisplatin and 10 µM CR8 and observed by time-lapse video microscopy. Images were captured every 10 min for 96 h (Figure 3.3A-C) and individual cells were manually observed to detect the presence or absence of cell rounding. The percentages of cells that entered mitosis post-treatment were then determined (Figure 3.3D). Not treated and 30 µM cisplatin treated cells were used as controls and data from these treatments have been previously presented in Figure 2.6. Nearly all not treated (99 ± 0.06%) and most cisplatin treated (81 ± 3%) cells entered mitosis after treatment. Only 5 ± 1% of cells co-treated with cisplatin and CR8 entered mitosis. This confirmed that CR8 could block mitosis in this experimental model.

3.4.3 The cytotoxicity of either 30 µM cisplatin or 50 nM CPT is maintained when HT-29 cells are prevented from entering mitosis

We then used HT-29 cells co-treated with cisplatin and CR8 to determine whether it was necessary for cells treated with cisplatin to enter mitosis to die. Cells were either treated with 30 µM cisplatin for 96 h or co-treated with 30 µM cisplatin for 96 h and 10 µM CR8 for 72 h. In the co-treated cell population cells were treated with 30 µM cisplatin for 24 h prior to the addition of CR8, to ensure that a DNA damaging event had occurred prior to inhibiting mitosis. This method of co-treatment was identical to conditions previously used to prevent entry into mitosis by co-treating HT-29 cells with CPT and CR8 (Kubara et al. 2012). Not treated and 10 µM CR8 treated cells were used as controls. The treated cells were observed by light microscopy at 24, 48, 72 and 96 h after treatment with cisplatin. Representative images of cells at 96 h are shown (Figure 3.4A). Fewer cells were present in the cisplatin treated and the cisplatin and CR8 co-treated cell populations, by comparison to the control cell populations which were either not treated or treated with CR8.

Having observed the treated cells by light microscopy, we used trypan blue staining to quantify the number of live cells present after treatment. HT-29 cells were either treated with 30 µM cisplatin for 96 h or co-treated with 30 µM cisplatin for 96 h and 10 µM CR8 for 72 h. Not treated cells were used as controls. The values from each treatment condition were normalised to treatment with 0.1% (v/v) DMSO. Relative viability was calculated as percentage of control (Figure 3.4B). There was no significant difference in relative cell viability between cells treated with cisplatin (1.2 ± 0.2%) and cells co-treated with cisplatin and CR8 (1.2 ± 0.2%).

We then determined if mitosis was required for cell death using a different source of genotoxicity, CPT. Although it had been shown previously that co-treating cells with CPT and CR8 prevented cells from entering mitosis (Kubara et al. 2012), it has not been reported whether cells treated with CPT need to enter mitosis to die. HT-29 cells were either treated with 50 nM CPT for 96 h or co-treated with 50 nM CPT for 96 h and 10 μM CR8 for 72 h and then observed by light microscopy (Figure 3.4A). In parallel, cells were either not treated or treated with 10 μM CR8 alone. By contrast to the not treated and CR8 treated cell populations, fewer cells were present in CPT treated or CPT and CR8 co-treated cell populations. We also quantified the number of live cells present after treatment (Figure 3.4B). HT-29 cells were either treated with 50 nM CPT for 96 h or co-treated with 50 nM CPT for 96 h and 10 μM CR8 for 72 h. Not treated cells were used as controls. Trypan blue staining was performed and cell viability calculated. There was little difference in the percentage of viable cells when cells were either treated with CPT (0.7 ± 0.2%) or co-treated with CPT and CR8 (0.9 ± 0.2%). These data suggest that mitosis is not required for cell death when cells are cultivated under conditions that induce checkpoint adaptation following treatment with two different genotoxic agents.

3.5 Discussion

Checkpoint adaptation is defined by three steps: 1) a cell cycle arrest induced by DNA damage; 2) overcoming this arrest and 3) resuming the cell cycle with damaged DNA (Toczyski et al. 1997). Checkpoint adaptation occurs in irradiated U2OS osteosarcoma (Syljuåsen et al. 2006) and MOLT4 leukaemia cells (Rezacova et al. 2011), in HT-29 cells treated with either CPT or etoposide and in M059K glioma cells treated

with CPT (Kubara et al. 2012). Furthermore, as described in chapter 2, we found that the majority of HT-29 cells treated with a low but cytotoxic concentration of cisplatin also undergo checkpoint adaptation.

Mitotic cell death has been observed in different cell lines treated with different genotoxic agents such as ionising radiation (Ianzini and Mackey 1997), bleomycin (Tounekti et al. 1993), cisplatin (Vakifahmetoglu et al. 2008), 5-fluorouracil (Yoshikawa et al. 2001), doxorubicin (Chang et al. 1999; Eom et al. 2005) and the atypical DNA binding compound S23906 (Cahuzac et al. 2010). The range of genotoxic treatments with different mechanisms of action that induce mitotic cell death suggests that this response is biologically important. Investigating the role of mitosis in cell death may therefore be central to improving the efficacy of genotoxic anti-cancer drugs. Although genotoxic agents are a mainstay of anti-cancer therapy, the majority of these drugs are not always curative in a clinical setting and are limited by factors such as acquired resistance, tumour metastasis and the formation of secondary tumours (Khanna 2015) which can lead to either tumour recurrence or progression.

Genomic instability can be caused by single base mutations, DNA deletions, DNA insertions, DNA translocations and a change in copy number (Stratton 2009) affecting key cellular processes such as cell division, cell growth, cell function and cell death (Shen 2011). Cells that are treated with cisplatin have an increased number of chromosomal aberrations by comparison to not treated cells. Chinese hamster ovarian (CHO) cells treated with a range of concentrations of cisplatin (3-40 μM) and analysed by metaphase spreads in either the first or second mitosis following treatment displayed an increased number of chromosome aberrations, in the form of chromosome/chromatid breaks and

chromosome/chromatid exchanges, by comparison to not treated cells (Krishnaswaky and Dewey 1993). Cisplatin also induces chromosome aberrations in bone marrow cells collected from Wistar rats (Edelweiss et al. 1995) and mice (Adler and El-Tarras 1989). In Wistar rats the majority of chromosome aberrations were observed 6-24 h after treatment and consisted of chromosome breaks. The percentage of cells with chromosome aberrations ranged from 17.7% at 6 h to 5% at 96 h (Edelweiss et al. 1995). In mice, the number of cells with chromosome aberrations also increased with cisplatin dose and these chromosome aberrations also consisted of breaks (Adler and El-Tarras 1989). These data indicate that treatment with cisplatin is capable of inducing genomic change in both cell lines and animal models. However, because these cells were fixed in the first and second mitoses after treatment these studies did not address if cells subsequently survived cisplatin treatment with rearranged genomes.

Entry into mitosis with damaged DNA can also induce genomic change when DNA is damaged by either treatment with etoposide or by replication stress. In 2006, Nakada *et al*. demonstrated that when ATM-deficient fibroblast cells entered mitosis following treatment with etoposide some cells survived with chromosomal translocations and formed stable clones (Nakada et al. 2006). It has also been demonstrated that entry into mitosis with damaged DNA acquired by replication stress in U2OS cells overexpressing the oncogene E2F1 resulted in chromosome bridge formation and aneuploidy (Ichijima et al. 2010). Additionally, Ichijima *et al*. (2010) found that entry into mitosis with replication stress induced DNA damage in MEF mouse embryonic fibroblast cells induced tetraploidy followed by cell immortalisation. Furthermore, induction of replication stress in chromosomal instability positive (CIN^+) (aneuploid)

human colorectal carcinoma cell lines resulted in an increase in the percentage of cells with DNA damage in prometaphase, which was associated with structurally abnormal chromosomes that mis-segregated in mitosis (Burrell et al. 2013).

When cells enter mitosis with damaged DNA it can cause the production of acentric (lacking a centromere) chromosome fragments (Jeggo and Löbrich 2006). Because these fragments do not contain a centromere they will not be attached to the mitotic spindle and may be lost during cell division (Hall and Giaccia 2012). Irradiation or etoposide treatment of LA-9 murine cells containing a stable chromosome with an integrated green fluorescent protein (GFP) gene increased chromosome loss, as detected by an increase in the percentage of non-fluorescent cells (Burns et al. 1999). These data, which indicate that treatment with a genotoxic agent can induce loss of genetic material, are supported by preliminary data which indicates that cells surviving checkpoint adaptation following treatment with CPT contain fewer chromosomes than not treated cells (Rahman 2013).

It has also been suggested that chromosomes with regions of damaged DNA might mis-segregate during mitosis because sister chromatids are connected by DNA-DNA or DNA-protein crosslinks (Lengauer et al. 1998). This would induce aneuploidy, a change in the number of chromosomes contained in a cell. Moreover, it has been proposed that DNA damage interferes with the correct attachment of microtubules to kinetochores in mitosis (Rieder 2004) and this might also result in the loss of genetic material or aneuploidy.

One outcome of aberrant mitosis is the formation of micronuclei. Micronuclei can be formed when lagging acentric chromosomes or chromosome fragments do not

segregate correctly at anaphase, as a result of either misrepaired or unrepaired DNA strand breaks, and are subsequently enclosed in a separate nuclear membrane (Fenech et al. 2011). The formation of micronuclei requires either a mitotic or meiotic division (Kirsch-Volders et al. 2011) and has been observed in several cell lines treated with different genotoxic agents such as bleomycin (Tounekti et al. 1993), cisplatin (Vakifahmetoglu et al. 2008), ionising radiation (Ianzini and Mackey 1997; Chang et al. 1999; Balajee et al. 2014), doxorubicin, aphidicolin, cytarabine or etoposide (Chang et al. 1999). An increased number of cells with micronuclei have also been detected in clinical samples of oral (Bhattathiri et al. 1998; Bhattathiri 2001; Kumari et al. 2005) and cervical (Zolzer et al. 1995; Widel et al. 1999) carcinomas following treatment with ionising radiation.

The formation of micronuclei can induce genomic instability in two ways. First, the DNA present in the micronucleus can be permanently lost from the main nucleus (Ford et al. 1988), although the frequency of chromosome loss induced by micronucleation is debated (Huang et al. 2012). Second, the formation of micronuclei can induce chromosome shattering which can be followed by reincorporation of the damaged chromosome into the main nucleus (Crasta et al. 2012; Zhang et al. 2015). In 2012, Crasta *et al*. found that micronuclei can further induce genomic rearrangement through chromosome pulverisation (Crasta et al. 2012). They generated and then followed micronuclei as cells progressed through the cell cycle and observed that premature chromosome compaction led to chromosome pulverisation when micronucleated cells entered mitosis before DNA replication was complete. Strikingly, Crasta *et al*. found that chromosomes reincorporate from micronuclei into daughter nuclei at a frequency of 38%.

Thus entry into mitosis with damaged DNA may lead to genomic instability by inducing the formation of micronuclei, which can subsequently lead to the reincorporation of damaged chromosomes into the main nuclei (Crasta et al. 2012). A follow-up study from the same research group used live cell imaging and single-cell genome sequencing to characterise the relationship between micronuclei and chromosome shattering (Zhang et al. 2015). They found that mis-segregated chromosomes contained a large number of genomic rearrangements when compared to chromosomes that segregated correctly.

The chromosome shattering observed by Crasta *et al*. is called chromothripsis, a phenomenon that was discovered using next generation sequencing of both tumour samples from cancer patients and cancer cell lines (Stephens et al. 2011). In chromothripsis, tens to hundreds of genomic rearrangements are acquired in an event involving localised genomic regions, such as regions of one or several chromosomes (Stephens et al. 2011). Because checkpoint adaptation provides a mechanism by which cells can enter mitosis with damaged DNA, it may be a source of genomic instability by loss of genetic material, chromosomal translocation or chromothripsis induced by the formation of micronuclei.

Checkpoint adaptation is a mechanism by which damaged DNA is transmitted to daughter cells. This process likely induces genomic instability in human cells, although to date genomic instability induced by checkpoint adaptation has only been directly observed in *S. cerevisiae* (Galgoczy and Toczyski 2001) and *A. cepa* root meristemic cells (Carballo et al. 2006). Galgoczy and Toczyski (2001) found that checkpoint adaptation proficient *S. cerevisiae* cells experienced increased chromosome loss and translocation by comparison to checkpoint adaptation deficient cells (Galgoczy and

Toczyski 2001). Carballo *et al*. (2006) observed that *A. cepa* cells irradiated with 5, 10, 20 and 40 Gray X-rays entered mitosis following treatment and that broken chromatids, acentric chromosomal fragments and chromosome bridges were present in some of these mitotic cells (Carballo 2006). These studies, from two different eukaryotic organisms, suggest that checkpoint adaptation might also induce genomic instability in human cancer cells. The transmission of damaged DNA to daughter cells during cell division may also be enhanced because cells do not repair damaged DNA in mitosis (Orthwein et al. 2014). This means that if cells do not die in mitosis following treatment, then it is likely that they will exit mitosis and enter G1 with damaged DNA. Many cancer cells also have a defective G1/S DNA damage checkpoint owing to mutations in genes encoding proteins that are essential for the initiation and maintenance of this checkpoint such as p53, p21 and pRb (Schwartz and Shah 2005; Rausch et al. 2012; Manning et al. 2013). This allows the cell to once again progress through the cell cycle with damaged DNA. Furthermore, once a cell has completed mitosis with damaged DNA, even if the damage is subsequently repaired in a different phase of the cell cycle, it is likely that the cell will contain a rearranged genome as a result of segregating damaged DNA prior to DNA damage repair.

It is only possible for checkpoint adaptation to be a source of genomic change if cells can survive this process. We therefore first investigated whether cells treated with cisplatin can survive checkpoint adaptation. Although the number of survival cells was very small (0.01%), the number of cells in a tumour make even small percentages biologically significant. It is reported that 1 cm^3 of an epithelial tumour contains 1 x 10^8 cells (Del Monte 2009). This means that for every 1cm^3 of tumour up to 10,000 cells

could survive checkpoint adaptation following treatment with cisplatin. We also found that 0.09% of cells survive checkpoint adaptation following treatment with CPT. CPT is a topoisomerase I inhibitor that induces the formation of DNA strand breaks (Pommier 2006), whereas cisplatin is a crosslinking agent that forms intra- and inter- strand DNA crosslinks (Eastman 1987). These results indicate that a cell's ability to survive checkpoint adaptation is likely independent of type of DNA damage.

Clinically the efficacy of cisplatin is limited by resistance (Oliver et al. 2010). Resistance can be either intrinsic, where resistance is already present at the time of diagnosis or acquired, where cells develop resistance following treatment (Giaccone and Pinedo 1996). Acquired resistance to cisplatin is complex and multifactorial (Mayer et al. 2003). Common mechanisms of cisplatin resistance are decreased drug accumulation in the cell, increased levels of thiol containing species in the cytoplasm, increased repair of DNA damage and resistance to cell death pathways (Woźniak and Błasiak 2002; Kelland 2007). The pathways of resistance are associated with numerous molecular changes in the cell and these are often the consequence of genetic and epigenetic changes (Shen et al. 2012). One of the most common changes found in cisplatin resistant cells is the overexpression of proteins, including those that contain thiols that bind to platinum, leading to detoxification (Kelland 2007) and those involved in DNA damage repair by nucleotide excision repair (NER) (Florea and Büsselberg 2011).

The acquisition of cisplatin resistance is associated with changes at the genetic level. Cisplatin resistant cell lines and tumour samples exhibit chromosomal abnormalities, such as loss of chromosomal regions, which are not present in cisplatin sensitive cell lines and tumour samples; however, a specific genotype associated with

resistance has yet to be identified (Wasenius et al. 1997; Rao et al. 1998; Leyland-Jones et al. 1999; Nessling et al. 1999; Wilson et al. 2005; Noel et al. 2008; Österberg et al. 2009; Oliver et al. 2010). This might be because there are many pathways that can lead to resistance. Additionally, the majority of studies that have investigated genomic change in samples resistant to cisplatin used cytogenetic techniques such as comparative genomic hybridisation either alone or in combination with microarrays to detect changes in gene expression (Wilson et al. 2005) or single nucleotide polymorphism analysis (Noel et al. 2008). Whereas these techniques have been successful in detecting genomic change such as chromosome loss in resistant cancer cells, it will be interesting to compare cisplatin resistant cell lines and tumour samples to cisplatin sensitive cell lines and tumour samples using next generation sequencing techniques which provide enhanced sensitivity for the detection of genomic instability including loss of genetic material, chromosomal translocations and chromosomal shattering (Stephens et al. 2011). It is plausible that some cells that survive checkpoint adaptation may develop acquired resistance following treatment with cisplatin. By preventing cells from entering mitosis with damaged DNA (the final step of checkpoint adaptation) it might be possible to prevent cells from surviving treatment with rearranged genomes and therefore prevent some cells from acquiring resistance to treatment.

To determine the relationship between checkpoint adaptation and genomic change it is necessary to characterise the extent of genomic rearrangement in cells that survive this process. This can be investigated using cytogenetic techniques such as fluorescence *in situ* hybridisation (FISH) to observe centromeres, telomeres and highly specific chromosomal regions (Bishop 2010; Rahman 2013) and spectral karyotyping (SKY)

which uses different coloured fluorescent probes to detect different chromosomal regions (Imataka and Arisaka 2012). As single cell sequencing techniques advance it will also be possible to sequence the genomes of individual cells that survive checkpoint adaptation (Leung et al. 2015).

Entry into mitosis with damaged DNA can be prevented by inhibiting Cdk1 (Kubara et al. 2012). However, it was not known whether mitosis was necessary for cell death in cells that die following checkpoint adaptation, and it has been suggested that cells may undergo checkpoint adaptation so that they can induce cell death in other phases of the cell cycle (Lupardus and Cimprich 2004; Syljuåsen 2007). We explored whether entry into mitosis is required for cell death in cells treated with either cisplatin or CPT by co-treating cells with a small molecule inhibitor of Cdk1, CR8 (Bettayeb et al. 2008). We found that percentage of cell death is not significantly changed when cells treated with either cisplatin or CPT are co-treated with CR8. Because CPT and cisplatin are genotoxic agents with different mechanisms of action, these data suggest that the strategy of preventing checkpoint adaptation to prevent genomic rearrangement could be successful in cancer cells treated with different genotoxic agents.

Cdk1 inhibitors have already been tested in combination with cisplatin in animal models and cell lines (Coley et al. 2007; Chen et al. 2015). In 2013, 13 Cdk1 inhibitors were being tested in clinical trials (Bruyère and Meijer 2013). The rationale behind using Cdk inhibitors as cancer treatments is that Cdk activity is necessary for cell division to occur. By inhibiting Cdk activity, cell division should also be inhibited (Johnson and Shapiro 2010). However, the therapeutic efficacy of Cdk inhibitors in clinical trials has been modest to date (Siemeister et al. 2012). Our results indicate that although percentage

of cell death is similar when cells are either treated with cisplatin alone or co-treated with cisplatin and CR8, co-treatment with a Cdk1 inhibitor might prevent cancer cells from surviving treatment with rearranged genomes. These results provide a rationale for the use of Cdk1 inhibitors in the clinic and warrant the investigation of the effects of co-treatment with genotoxic agents and a Cdk1 inhibitor in an animal model.

Our results provide a rationale for inhibiting entry into mitosis with damaged DNA (the final step of checkpoint adaptation) in cells treated with genotoxic agents. We show that cell death is maintained when cells are prevented from entering mitosis while undergoing checkpoint adaptation. It is likely that inhibiting entry into mitosis with damaged DNA will prevent some cells from acquiring additional rearrangement to their genomes. However, treatment with a genotoxic agent can also induce genomic instability if DNA strand breaks are mis-repaired in interphase prior to entry into mitosis. For example, non-homologous end-joining re-joins DNA strand breaks without using homologous sequence as a template. This can induce chromosomal rearrangements when more than two DNA strand breaks are present, because breaks on different chromosomes can be joined together (Mani and Chinnaiyan 2010). It is therefore likely that both checkpoint adaptation and entry into mitosis with mis-repaired DNA damage contribute to genomic instability following treatment with genotoxic agents.

Genotoxic agents are not always curative and tumours often progress or recur. In an animal model we predict that co-treatment with cisplatin and a Cdk1 inhibitor would prevent some cells from surviving treatment with rearranged genomes. This could be investigated by determining the relationship between treatment and genomic rearrangement in animals either treated with cisplatin alone or treated with cisplatin and a

Cdk1 inhibitor. We hypothesise that cancer cells of animals treated with cisplatin alone would contain more genomic change by comparison to the cancer cells of animals co-treated with cisplatin and a Cdk1 inhibitor. If our predictions are correct it is likely that the cancer cells of animals co-treated with cisplatin and a Cdk1 inhibitor would be prevented from acquiring resistance to treatment and would be susceptible to further rounds of treatment. This could mean that a recurring tumour would either take longer to return or not return at all.

In summary, our findings indicate that cells treated with either cisplatin or CPT can survive checkpoint adaptation. We also show that cell death is maintained when cells treated with either cisplatin or CPT are prevented from entering mitosis with damaged DNA. As such, preventing cells from entering mitosis following treatment with genotoxic agents warrants further investigation, because this may prevent cells from surviving treatment with genotoxic agents and prevent treatment induced genomic instability.

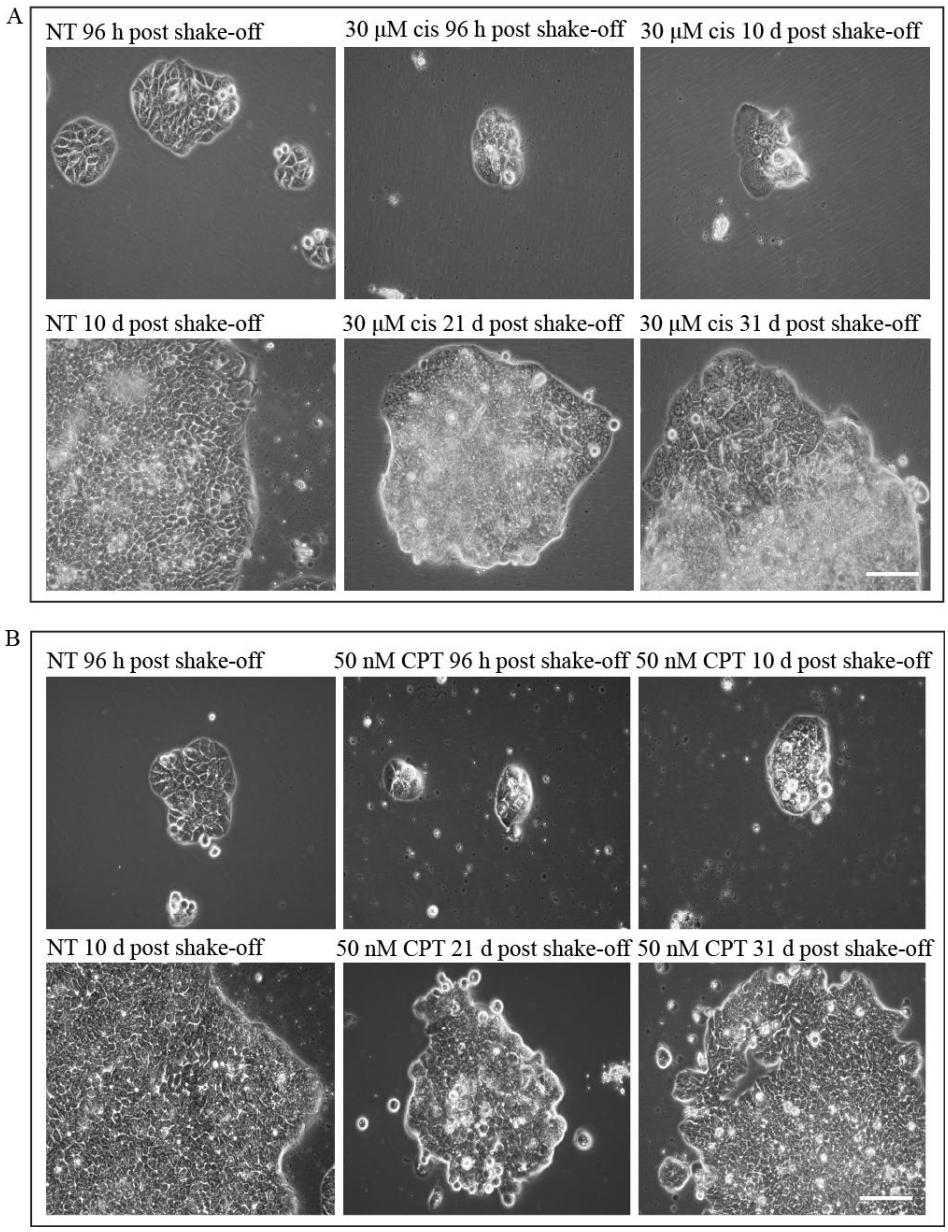

Figure 3.1 Some HT-29 cells can survive checkpoint adaptation following treatment with 30 µM cisplatin. A. HT-29 cells were either not treated (NT) or treated with 30 µM cisplatin for 72 h. Rounded cells were collected by mechanical shake-off and cultured without further treatment. Cells were observed by phase-contrast light microscopy at 96 h, 10 d, 21 d and 31 d. Representative images are shown. Scale bar equals 100 µm. B. HT-29 cells were either not treated (NT) or treated with 50 nM CPT for 48 h. Cells were collected and observed as described in (A).

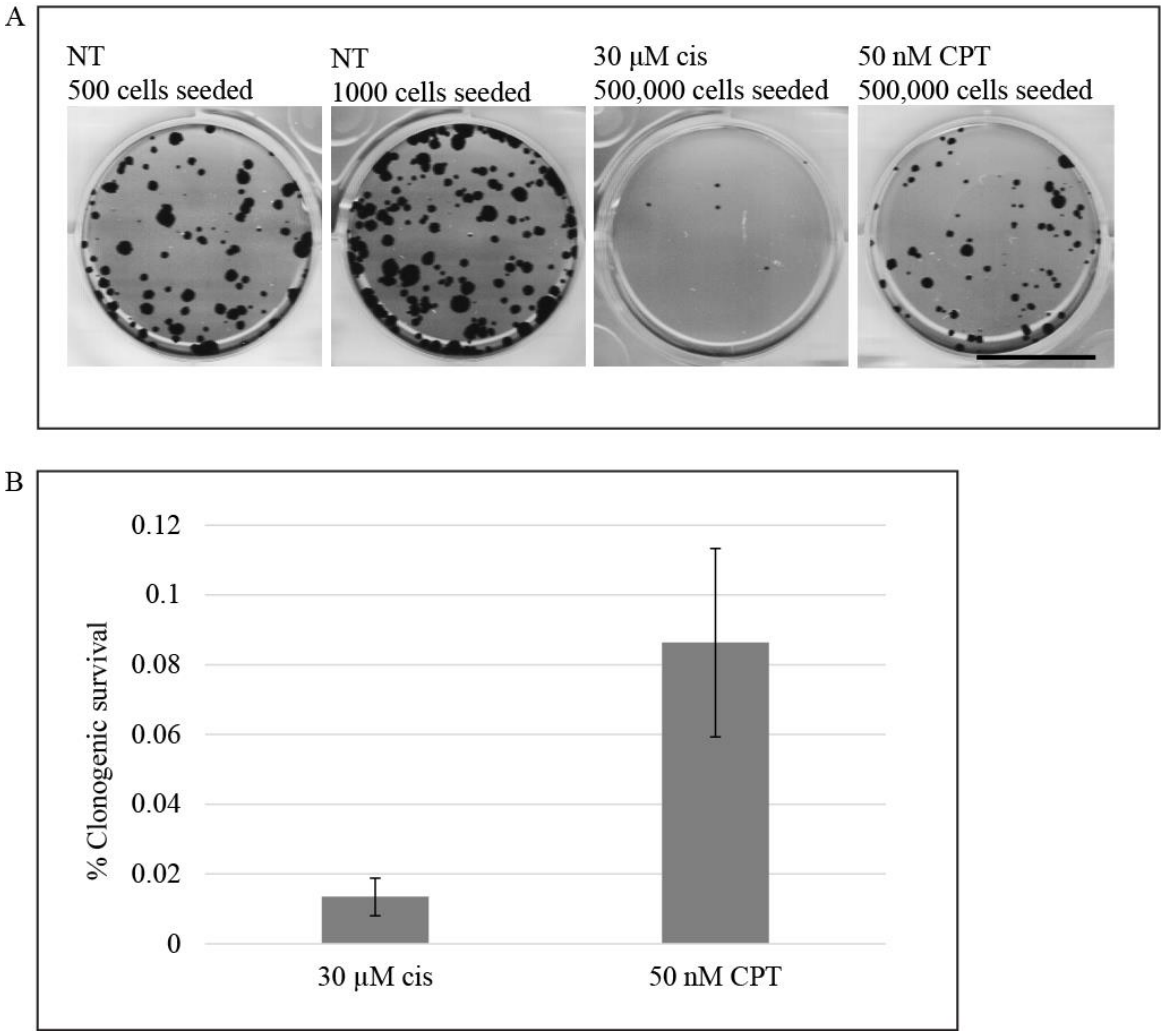

Figure 3.2 A small percentage of HT-29 cells can survive checkpoint adaptation following treatment with 30 µM cisplatin. A. HT-29 cells were either not treated (NT), treated with 30 µM cisplatin for 72 h or treated with 50 nM CPT for 48 h. Rounded cells were collected by mechanical shake-off and cultured without further treatment for 14 d. Colonies were then analysed by the clonogenic assay. Representative images of colonies are shown. Scale bar equals 17.5 mm. B. HT-29 cells were treated and collected as in (A). Mean percentages of clonogenic survival were calculated from three separate experiments and standard errors of the means are shown.

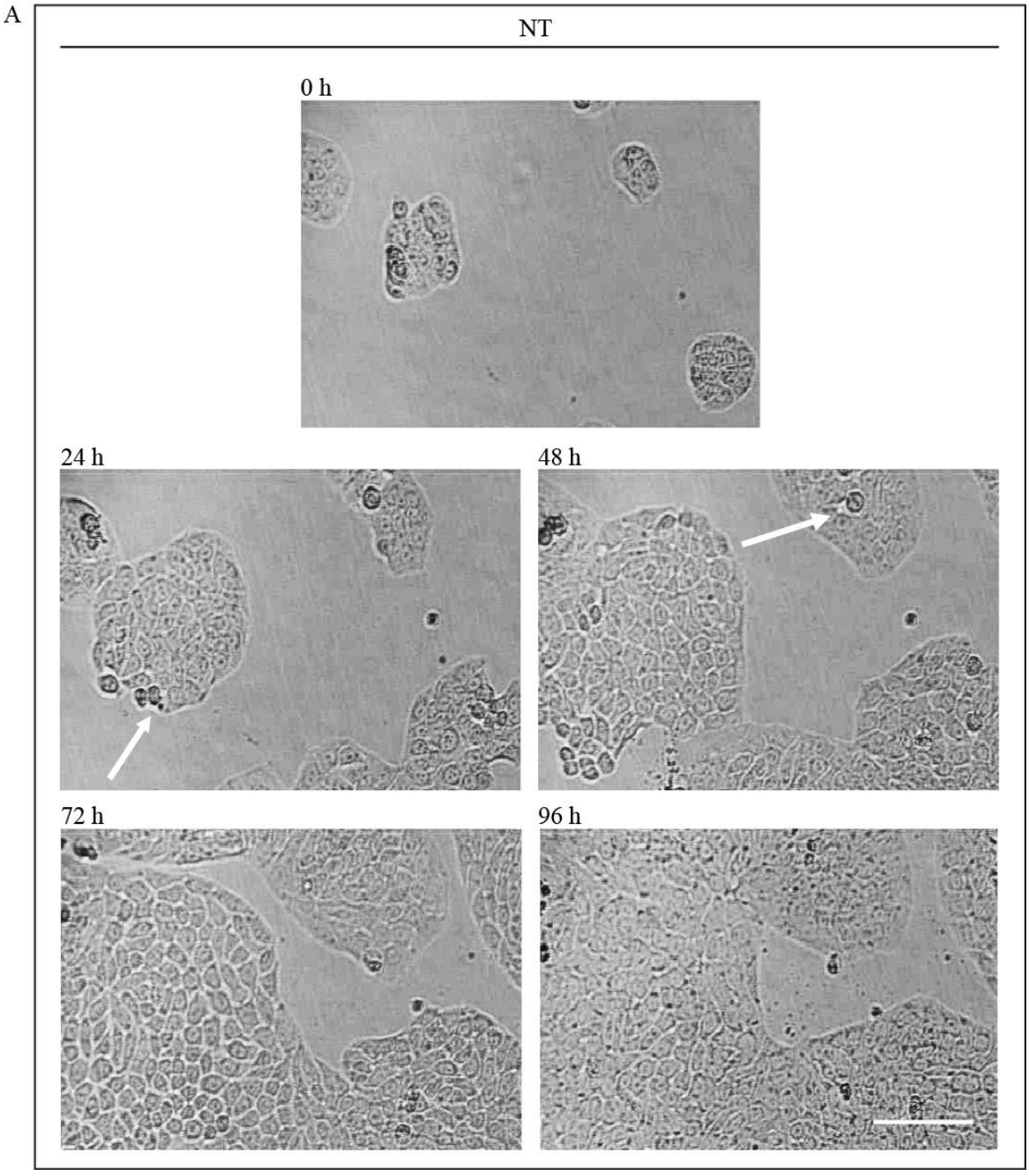
A
NT
0 h
24 h
48 h
72 h
96 h

B

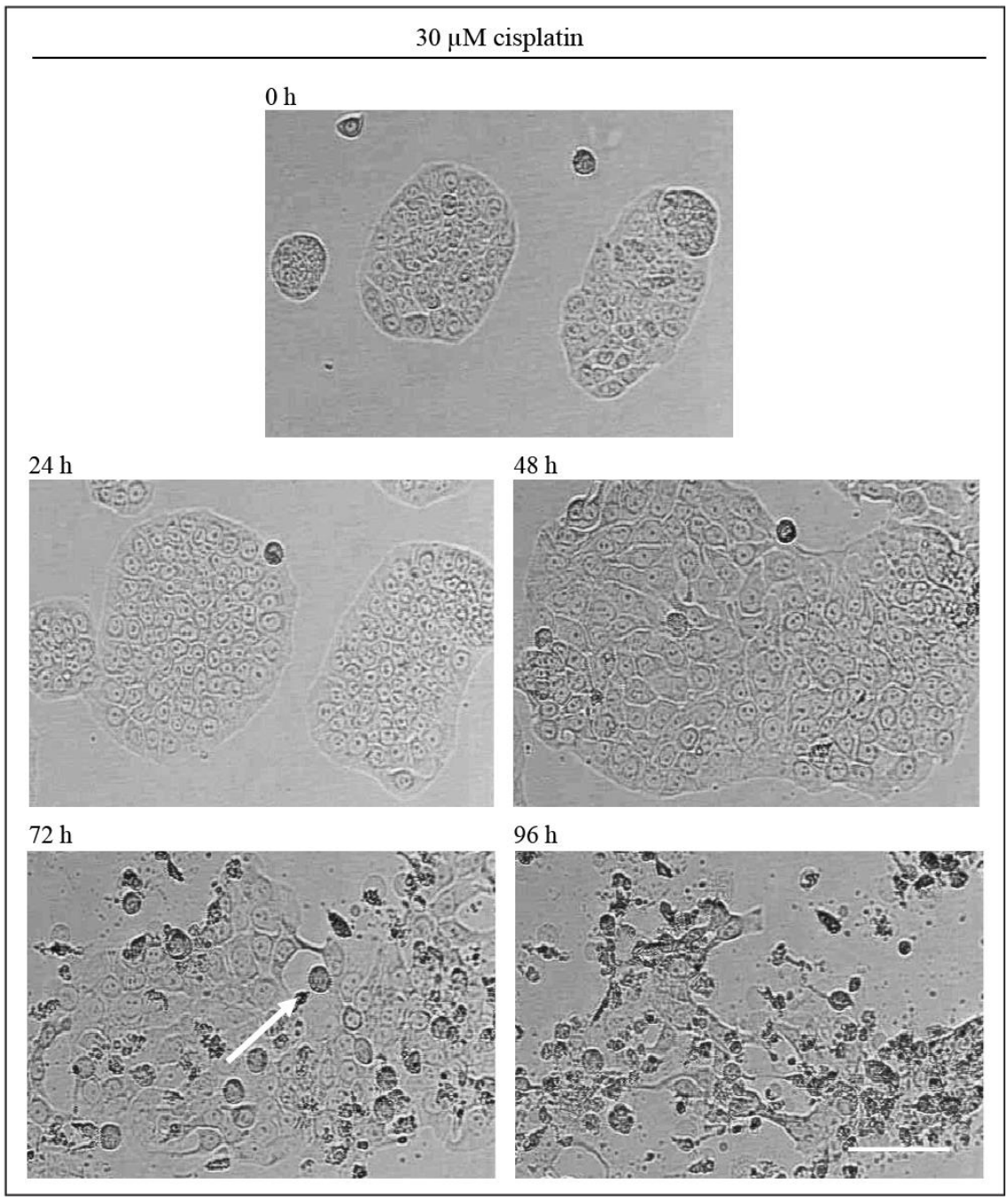

C

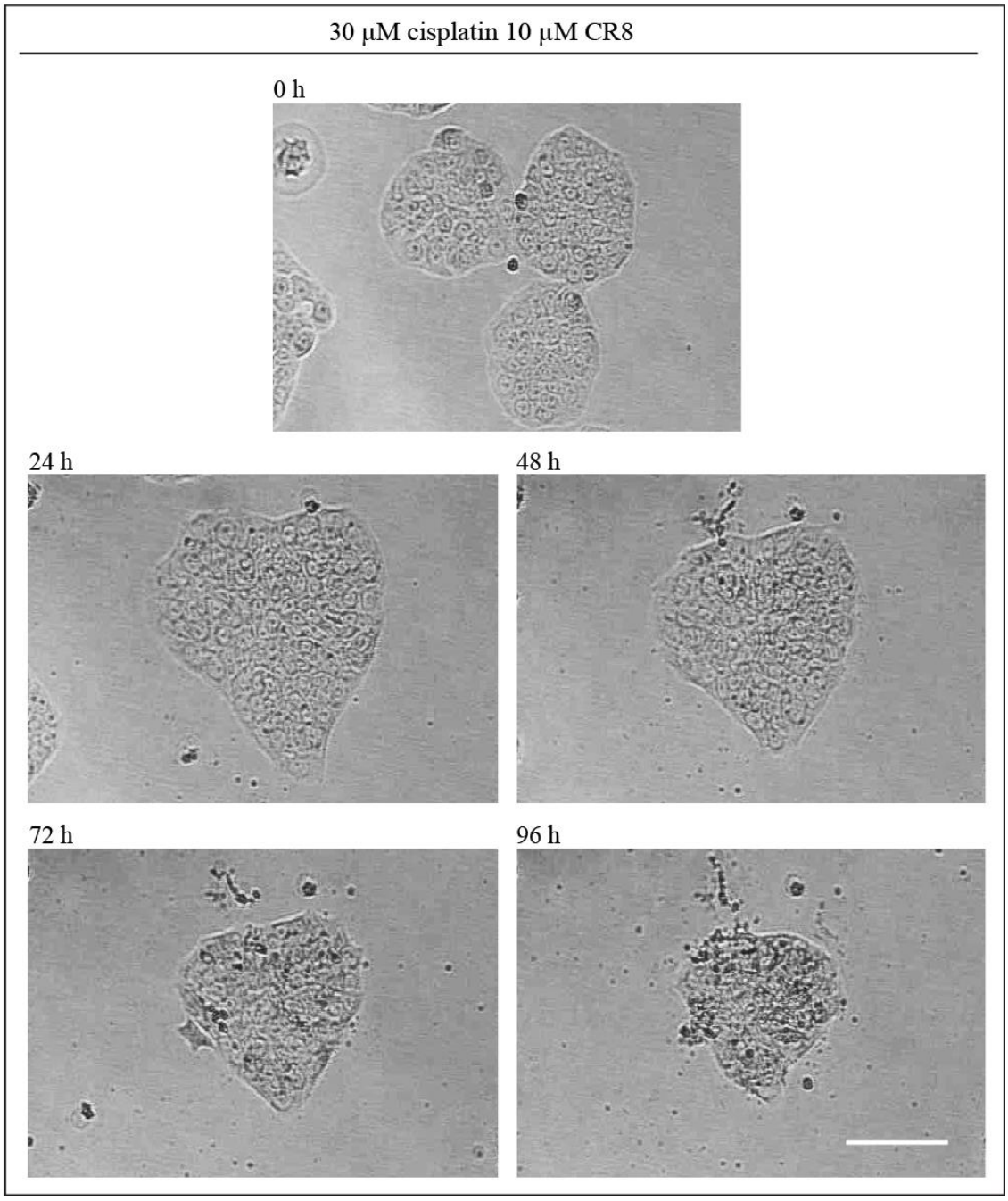

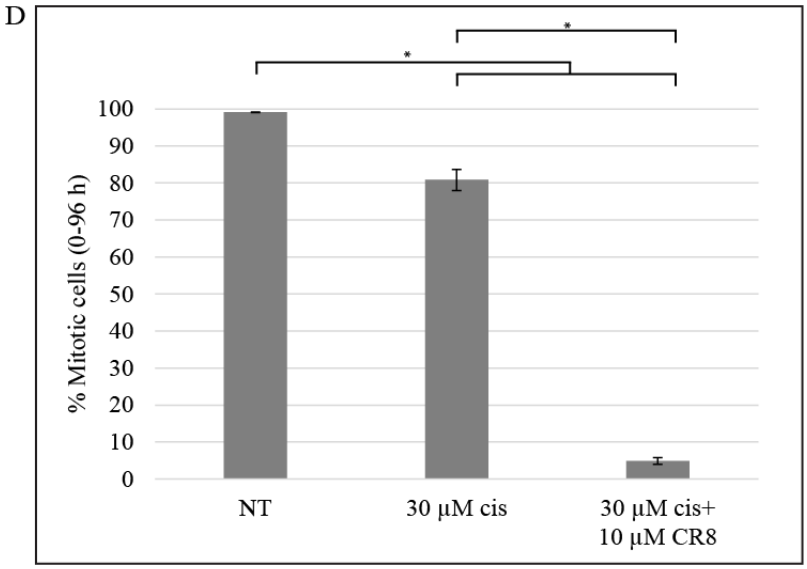

Figure 3.3 Entry into mitosis can be chemically inhibited in HT-29 cells treated with 30 µM cisplatin. A. HT-29 cells were not treated (NT) and observed by time-lapse video microscopy. Images were captured every 10 min for 96 h and representative images captured every 24 h from 0-96 h are shown. Arrows indicate mitotic cells. Scale bar equals 100 µm. B. HT-29 cells were treated with 30 µM cisplatin and observed as in (A). C. HT-29 cells were co-treated with 30 µM cisplatin and 10 µM CR8 and observed as in (A). D. The mean percentages of cells that enter mitosis between 0 and 96 h post-treatment were calculated from three separate experiments. Standard errors of the means are shown. Asterisks show significant differences, paired student's *t*-test, 2 degrees of freedom, $p < 0.05$.

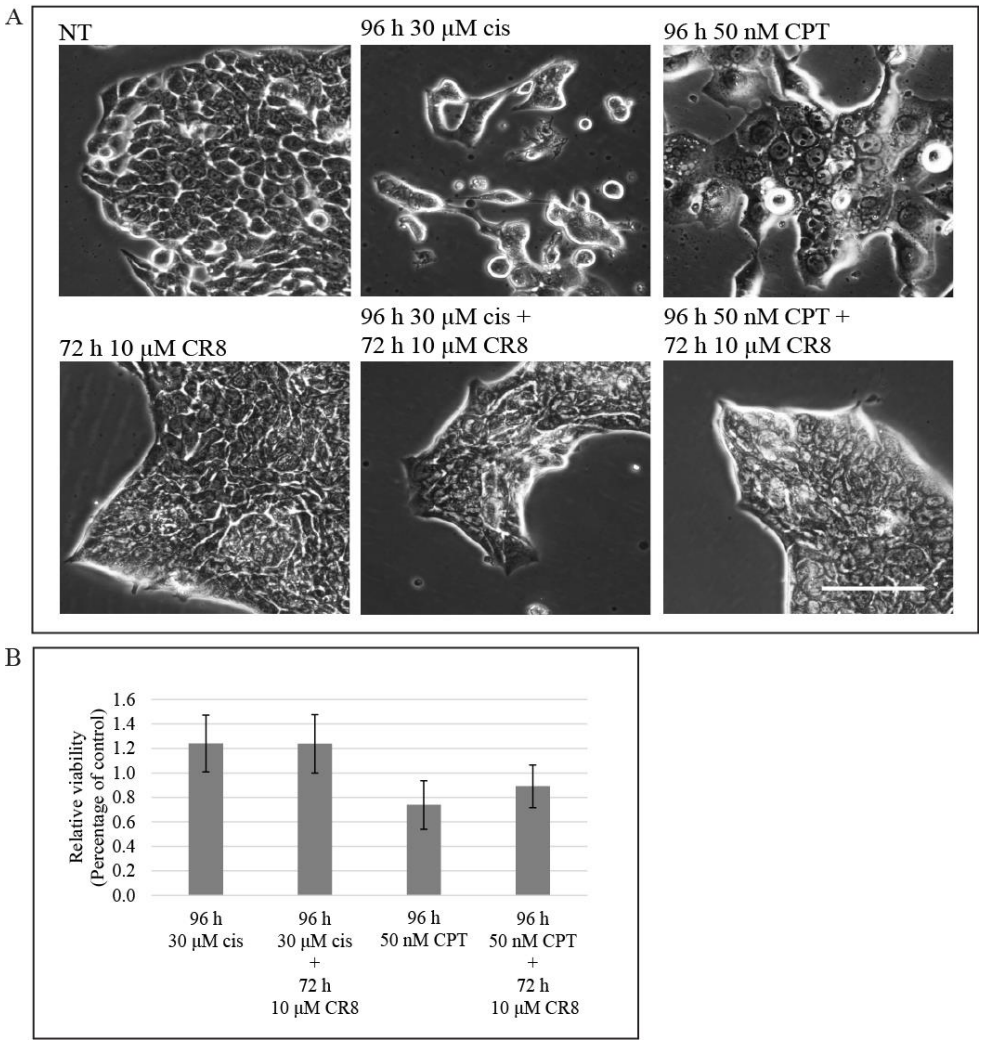

Figure 3.4 Cytotoxicity is maintained when cells treated with either 30 µM cisplatin or 50 nM CPT are prevented from entering mitosis. A. HT-29 cells were either not treated (NT), treated for 72 h with 10 µM CR8, treated for 96 h with 30 µM cisplatin, treated with 30 µM cisplatin for 24 h and then co-treated with 30 µM cisplatin and 10 µM CR8 for 72 h, treated for 96 h with 50 nM CPT or treated with 50 nM CPT for 24 h and the co-treated with 50 nM CPT and 10 µM CR8 for 72 h. Cells were observed by phase-contrast light microscopy 96 h after treatment with either cisplatin or CPT. Representative images are shown. Scale bar equals 100 µm. B. HT-29 cells were either not treated, treated for 96 h with 30 µM cisplatin, treated with 30 µM cisplatin for 24 h and then co-treated with 30 µM cisplatin and 10 µM CR8 for 72 h, treated for 96 h with 50 nM CPT or treated with 50 nM CPT for 24 h and then co-treated with 50 nM CPT and 10 µM CR8 for 72 h. Trypan blue staining was then used to measure cell viability. The results from each treatment were normalised to treatment with 0.1% (v/v) DMSO. Mean percentages of relative viability were calculated from three individual experiments. Standard errors of the means are shown.

CHAPTER 4

Investigation of the process of checkpoint adaptation in human cancer cells treated with either cisplatin or camptothecin

4.1 Abstract

Checkpoint adaptation is a major response to treatment with either cisplatin or CPT in HT-29 human colorectal adenocarcinoma cells. This process might be a source of genomic instability in some human cancer cells and could lead to acquired resistance to treatment. It may therefore be possible to improve the efficacy of current genotoxic anti-cancer drugs by preventing treated cancer cells from entering mitosis with damaged DNA (the final step of checkpoint adaptation), so that these cancer cells do not survive treatment with rearranged genomes. We reasoned that if checkpoint adaptation is to be targeted therapeutically then it is necessary to understand whether the process is the same or different in response to treatment with different genotoxic agents. We therefore compared checkpoint adaptation in human cancer cells treated with either cisplatin or CPT. We report that CPT treated HT-29 cells enter mitosis with damaged DNA 24 h earlier than cisplatin treated cells. At 24 h 58% of CPT treated HT-29 cells are positive for cyclin B1, whereas only 24% of cisplatin treated cells are positive for cyclin B1. At 48 h, 10% of CPT treated cells are rounded and 9% of cells are positive for phospho-Ser10 histone H3 staining. By contrast, mitotic cells do not accumulate following treatment with cisplatin until 72 h when 7% of cells are rounded and 7% of cells are positive for phospho-Ser10 histone H3 staining. Additionally, at 24 h, 92% of CPT treated cells are positive for histone γH2AX staining, by comparison to 56% of cisplatin treated cells. CPT treated cells also spend an average of 440 min in mitosis whereas cisplatin treated

cells spend an average of 280 min in mitosis. These data demonstrate that the steps of checkpoint adaptation are similar in HT-29 cells treated with either cisplatin or CPT, but that the timing of checkpoint adaptation is different. We also found that the timing of entry into mitosis is similar in M059K glioma cells treated with either cisplatin or CPT; however, the duration of mitosis is longer in M059K cells treated with CPT by comparison to cells treated with cisplatin. These data indicate that length of time spent in mitosis is different when two human cancer cell lines are treated with either cisplatin or CPT and undergo checkpoint adaptation.

4.2 Introduction

Checkpoint adaptation consists of three steps 1) initiation of a DNA damage induced cell cycle arrest; 2) overcoming this arrest and 3) continuing the cell cycle with damaged DNA. HT-29 human colorectal adenocarcinoma cells treated with either camptothecin (CPT) (Kubara et al. 2012) or cisplatin (Chapter 2) undergo checkpoint adaptation. These genotoxic agents damage DNA by different mechanisms of action; CPT is a topoisomerase I inhibitor (Hsiang et al. 1985) and induces DNA strand breaks (Pommier 2006) whereas cisplatin is a crosslinking agent that induces monofunctional DNA adducts and intra- and inter- strand DNA crosslinks (Eastman 1987). Checkpoint adaptation has also been observed in different human cancer cell lines treated with either ionising radiation (Syljuåsen et al. 2006; Rezacova et al. 2011) or etoposide (Kubara et al. 2012). Furthermore mitotic catastrophe, which under some conditions is an outcome of checkpoint adaptation, has been detected in HT-29 cells treated with a representative

range of genotoxic agents, but the precise steps and timing of checkpoint adaptation have not been investigated (Cahuzac et al. 2010).

In chapter 2 we demonstrated that biochemical processes guide cells to undergo checkpoint adaptation because cells treated with two different cytotoxic concentrations of cisplatin died by either undergoing checkpoint adaptation or by apoptosis. In chapter 3 we demonstrated that HT-29 cells treated with either cisplatin or CPT will die when they are prevented from entering mitosis, the final step of checkpoint adaptation. These results suggest that treated cells make a biochemical "decision" to undergo checkpoint adaptation. Cells are capable of inducing cell death without undergoing checkpoint adaptation and will die by apoptosis when treated with a higher concentration of cisplatin, which induces a higher level of damaged DNA. However, the biochemical events that underlie whether cells undergo checkpoint adaptation or apoptosis are not well understood.

Genotoxic agents are widely used to treat cancer patients but are not always curative. Many of these agents, such as cisplatin, are limited by the development of resistance to treatments (Cheung-Ong et al. 2013) and genomic change can be responsible for this acquisition of resistance to treatment (Shen et al. 2012). Checkpoint adaptation may be a source of genomic change in treated cancer cells because some cells can survive this process, which involves entry into mitosis with damaged DNA (Kubara et al. 2012; Rahman 2013; Chapter 3). Cells that survive checkpoint adaptation might therefore be the source of some cells that acquire resistance to treatment. In chapter 3 we demonstrated that it is possible to induce cell death when entry into mitosis with damaged DNA (the final step of checkpoint adaptation) is prevented in HT-29 cells treated with either

cisplatin or CPT. If checkpoint adaptation is to be targeted to prevent cells surviving with rearranged genomes, then it is necessary to understand if the process is the same or different in response to treatment with different genotoxic agents. Furthermore, identification of differences in the engagement of checkpoint adaptation may provide insights into the biochemical pathways that induce it. Checkpoint adaptation has not previously been compared in the same cancer cell line treated with two different genotoxic agents. We therefore compared the cellular response of checkpoint adaptation in HT-29 cells treated with either cisplatin or CPT.

We report that HT-29 cells treated with either cisplatin or CPT demonstrate differences in their initiation of checkpoint adaptation following treatment. HT-29 cells treated with CPT signal damaged DNA 24 h earlier by comparison to cisplatin treated cells. CPT treated HT-29 cells also enter mitosis 24 h earlier than cells treated with cisplatin. Furthermore, these CPT treated cells spend a longer time in mitosis by comparison to cells treated with cisplatin. We also find that in a second unrelated cell line, M059K, cells treated with CPT spend longer in mitosis by comparison to cells treated with cisplatin.

4.3 Materials and methods

4.3.1 Cell culture

The human cell lines HT-29 (ATCC HTB-38) and M059K (ATCC CRL-2365) were obtained from the American Type Culture Collection (ATCC). HT-29 cells were maintained in RPMI 1640 medium (Gibco; 21870-092) supplemented with 10% (v/v) heat inactivated fetal bovine serum (FBS) (Gibco; 12484028) and 1.6 mM GlutaMAX

(Gibco; 35050-061). M059K cells were maintained in Dulbecco's Modified Eagle Medium/F-12 (Gibco; 11320-082) supplemented with 10% (v/v) heat inactivated FBS (Gibco; 12484028), 2 mM Modified Eagle Medium non-essential amino acids (Gibco; 11140050) and 15 mM HEPES, pH 7.4. Cells were grown at 37°C in 5% CO_2 and media were changed every 3-4 d. HT-29 cells were plated at a density of 3.0 x 10^5 cells/25 cm^2 flask and cultured for 72 h prior to treatment. M059K cells were plated at a density of 7.5 x 10^5/75 cm^2 flask and cultured for 24 h prior to treatment. The compound cisplatin (Sigma; 479306-1G) was dissolved in dimethyl sulphoxide (DMSO) (Sigma-Aldrich; D2438) to a concentration of 100 mM and stocks were freshly made every two weeks. CPT (Sigma; 7689-03-4) was dissolved in DMSO to a concentration of 10 mM. The compounds were stored at -20°C until use. Not treated cells were treated with the solvent only (0.1% (v/v) DMSO).

4.3.2 Cytotoxicity assay

The cytotoxicity of either cisplatin or CPT was measured by the MTT (3-(4,5)-dimethylthiazol-2-yl)-2,5-diphenyl-tetrazolium bromide) assay (Sigma-Aldrich; M2128-1G)). HT-29 cells were plated at 3.8 x 10^5 cells/96 well culture plate and cultured at 37°C for 72 h prior to treatment. M059K cells were plated at 2.5 x 10^5 cells/96 well culture plate and cultured at 37°C for 24 h prior to treatment. All treatments were run in triplicate at 24, 48, 72 and 96 h and experiments were performed three times. After the specified treatment time, 20 µl MTT solution (5 mg/ml MTT in phosphate buffered saline (PBS) (137 mM NaCl, 3 mM KCl, 100 mM Na_2HPO_4, 18 mM KH_2PO_4) was added to the media in each well and the plates were incubated at 37°C for 3.5 h. The media were then aspirated and 100 µl MTT solvent (4 mM HCl, 0.1% (v/v)

octylphenoxypolyethoxyethanol, in isopropanol) was added to each well. Plates were placed on a shaker for 30 min in the dark, and absorbance was measured at 590 nm using a BioTek microplate spectrophotometer powered by Eon software. Results were expressed as IC_{50} concentrations; the concentration of the compound that reduced the absorbance of MTT by 50%, by comparison to 0.1% (v/v) DMSO treated cells. The normalised percent absorbance was calculated as shown:

Normalised percent absorbance = (absorbance/DMSO absorbance) x 100

The log concentrations of the compound were plotted against the normalised percent absorbance using Microsoft Excel software. Analysis was performed with GraphPad Prism 5 software, using non-linear regression (log(inhibitor) versus normalised response), to estimate the IC_{50} concentrations. Standard curves were plotted using the equation:

$Y = \text{maximum} + (\text{maximum} - \text{minimum})/(1+10^{(x-\text{LogIC50})})$

Where maximum is the percentage of viable cells after treatment with 0.1% DMSO, minimum is the percentage of viable cells after treatment with the highest concentration of the genotoxic molecule and x is the log10 value of the treatment concentration.

4.3.3 Light microscopy

HT-29 cells were seeded at 1.0 x 10^5/well in a 6 well culture plate and incubated at 37°C for 72 h prior to treatment. Images were captured at room temperature with an Infinity 1 camera powered by Infinity Capture imaging software (Lumenera Corporation) on an Olympus CKX41 inverted microscope. Images were processed using Adobe Photoshop (CC 2014.1.0) and Image J (IJ 1.46r) software. At least 500 cells were counted for each treatment and experiments were performed three times.

4.3.4 Immunofluorescence microscopy

HT-29 cells were plated on glass coverslips at 1.0 x 10^5/well in a 6 well culture plate and incubated at 37°C for 72 h prior to treatment. After treatment, cells were fixed at room temperature for 20 min in 3% (v/v) formaldehyde (Ted Pella Inc; 18505), diluted in PBS. Fixation was quenched with 50 mM NH_4Cl in PBS, and cells were permeabilised for 5 min using 0.2% (v/v) Triton X-100 in PBS and blocked for 1 h with 3% (w/v) bovine serum albumin (BSA) in PBS-T (0.1% (v/v) Tween-20 diluted in PBS). Cells were then incubated with primary antibodies as described: anti-histone γH2AX (Millipore; 05-636; 1:400) for 1 h at room temperature; anti-cyclin B1 (Santa Cruz Biotechnology; SC-752; 1:100) for 2 h at room temperature or anti-phospho-Ser10 histone H3 (Millipore; 06-570(CH); 1:1000) for 18 h at 4°C. After washing with PBS-T, cells were incubated with secondary antibodies for 2 h at room temperature as follows: Alexa Fluor 488-conjugated anti-mouse (Life Technologies; A11059; 1:400) for anti-histone γH2AX and Texas Red-conjugated anti-rabbit (Jackson ImmunoResearch; 111-075-003; 1:400) for anti-phospho-Ser10 histone H3 and anti-cyclin B1. Nuclei were stained with 300 nM 4′,6-diamidino-2-phenylindole (DAPI) in PBS for 15 min and coverslips were mounted onto microscope slides using ProLong Gold Antifade reagent (Molecular probes; P36934). Cells were observed on an Olympus BX41 microscope and images were captured using an Infinity 3 camera operated by Infinity Capture imaging software (Lumenera Corporation). Images were prepared using Adobe Photoshop (CC 2014.1.0) software. Cells positive for histone γH2AX, phospho-Ser10 histone H3 and cyclin B1 were counted using Image J (IJ 1.46r) software. At least 500 cells were counted for each treatment and experiments were performed three times.

4.3.5 Time-lapse video microscopy

HT-29 cells were plated at 3.0 x 10^5/25 cm^2 flask and incubated at 37°C for 72 h prior to treatment. M059K cells were plated at 2.0 x 10^5/25 cm^2 and incubated at 37°C for 24 h prior to treatment. Time-lapse video microscopy images were collected from the start of treatment at 37°C, using a Lumascope 500 microscope (etaluma) powered by LumaView software (etaluma; V.13.4.25.99). Images were captured every 10 min for 96 h. Cells were manually scored for mitotic entry by observing whether they displayed a rounded morphology, indicative of mitosis, or not between 0 and 96 h. Cells that left the field of view before rounding were not counted. At least 250 HT-29 cells and 50 M059K cells were counted for each treatment. Time-lapse video microscopy images were also analysed to determine how long cells spent in mitosis. Thirty individual HT-29 cells and 20 individual M059K cells were analysed for each of the treated cell populations between 48 and 96 h, to determine how long cells displayed a rounded morphology for, to the nearest 10 minutes. Experiments were performed three times.

4.3.6 Statistical analysis

Graphs were produced using Microsoft Excel 2010 software. Data were collected and plotted as means from three separate experiments ± standard errors of the means. Statistical significance was calculated using the student's t-test for two paired sample means and values were considered significantly different when $p < 0.05$.

4.4 Results

4.4.1 Both 30 µM cisplatin and 50 nM CPT are cytotoxic to HT-29 cells

To compare the response of checkpoint adaptation it is necessary to draw from data previously presented in this thesis. For convenience these data are presented for a second time in this chapter. By using these previously presented data and combining them with new data we are able to answer new questions about checkpoint adaptation because checkpoint adaptation has not previously been compared in the same cell line treated with two different genotoxic agents. We first compared the cytotoxicity of 30 μM cisplatin or 50 nM CPT on HT-29 cells. HT-29 cells were treated with different concentrations of either cisplatin or CPT for 24, 48, 72 and 96 h and cell viability was measured using the MTT assay (Figure 4.1). The results from each treatment condition were normalised to treatment with 0.1% (v/v) DMSO.

HT-29 cell viability decreased in a time dependent manner, as the concentration of either cisplatin or CPT increased. The IC_{50} values for cisplatin ranged from 120 μM at 24 h to 5 μM at 96 h (Table 4.1). The IC_{50} values for CPT ranged from 517 nM at 24 h to 16 nM at 96 h (Table 4.1). As described in previous chapters, we selected 30 μM cisplatin and 50 nM CPT as cytotoxic concentrations, because they were higher than the respective IC_{50} values at 96 h and yet below suprapharmacological concentrations (Swift and Golsteyn 2014).

4.4.2 Cisplatin treated cells take longer to signal damaged DNA by comparison to CPT treated cells

We next investigated if cells treated with either cisplatin or CPT signalled damaged DNA at different times by using immunofluorescence microscopy to detect histone γH2AX staining. HT-29 cells were treated with either 30 μM cisplatin or 50 nM CPT and analysed for histone γH2AX staining at 24, 48 and 72 h (Figure 4.2). Not treated

cells were used as controls. At 24 h, a higher percentage of CPT treated cells were positive for histone γH2AX staining (92 ± 1%) by comparison to cisplatin (56 ± 4%). However, at 48 and 72 h similar percentages of cisplatin and CPT treated cells were positive for histone γH2AX staining. At 48 h, 96 ± 1% of 30 μM cisplatin treated cells and 94 ± 3% of CPT treated cells were positive for histone γH2AX. At 72 h, 93 ± 4% of cisplatin treated cells and 94 ± 4% of CPT treated cells were positive for histone γH2AX staining. These results indicate that CPT damages DNA earlier by comparison to cisplatin.

4.4.3 Cisplatin treated cells take longer to accumulate cyclin B1 by comparison to CPT treated cells

To explore if there were differences between the numbers of cells expressing cyclin B1, which is required for cells to undergo the final step of checkpoint adaptation, we examined HT-29 cells treated with either 30 μM cisplatin or 50 nM CPT by immunofluorescence microscopy at 24, 48 and 72 h to detect cyclin B1 staining (Figure 4.3). Not treated cells were used as a control. The percentages of cyclin B1 positive cells present in the not treated cell population were 6 ± 1% at 24 h, 5 ± 1% at 48 h and 2 ± 0.3% at 72 h.

At 24 h, 58 ± 5% of CPT treated cells were positive for cyclin B1, by comparison to 24 ± 3% of cisplatin treated cells. However, at 48 and 72 h, similar percentages of cisplatin and CPT treated cells were positive for cyclin B1 staining. At 48 h, 94 ± 1% of cisplatin treated cells and 95 ± 1% of CPT treated cells were positive for cyclin B1. At 72 h, 95 ± 1% of cisplatin treated cells and 93 ± 1% of CPT treated cells were positive for

cyclin B1. These results indicate that cells treated with CPT accumulate cyclin B1 earlier than cisplatin treated cells.

4.4.4 Mitotic cells are present 24 h earlier in HT-29 cells treated with CPT by comparison to cells treated with cisplatin

In chapter 2, light microscopy images (Figure 4.4A) suggested that rounded cells were present 24 h earlier in cells treated with CPT, by comparison to cells treated with cisplatin. We determined the percentage of mitotic HT-29 cells present at 24, 48, 72 and 96 h after treatment with either 30 μM cisplatin or 50 nM CPT (Figure 4.4B). Not treated cells were used as controls. Mitotic cells were present as part of a normal proliferating culture but did not accumulate in the not treated cell population. The percentage of mitotic cells also decreased in a time dependent manner, consistent with a slowing of the cell cycle when cells reached confluence. Mitotic cells were first present 48 h after treatment with CPT (10 ± 2%) and remained at 72 h (19 ± 2%) and 96 h (13 ± 3%). By contrast, few mitotic cells were present in the cisplatin treated cell population until 72 h after treatment (7 ± 0.04%).

After finding that cells treated with CPT were entering mitosis at 48 h and that cells treated with cisplatin entered mitosis at 72 h, we used time-lapse video microscopy to determine the percentages of cells in mitosis at 12 h intervals between 0 and 72 h after treatment with either 30 μM cisplatin or 50 nM CPT (Figure 4.5). Not treated cells were used as controls and mitotic cells were present as part of a normal proliferating cell culture. At 12 and 24 h few cells treated with either cisplatin or CPT entered mitosis. At 36 h the percentage of cisplatin treated cells in mitosis remained low (1 ± 0.5%) whereas the percentage of CPT treated cells in mitosis increased (8 ± 1%). A similar result was

observed at 48 h, 2 ± 0.5% of cisplatin treated cells and 21 ± 2% of CPT treated cells were in mitosis. At 60 h, cisplatin treated cells were beginning to enter mitosis (5 ± 1%) and the percentage of CPT treated cells in mitosis remained high (27 ± 2%). At 72 h, 10 ± 1% of cisplatin treated cells and 18 ± 1% of CPT treated cells were in mitosis.

Finally, we used phospho-histone H3 staining to confirm that the rounded cells observed by light and time-lapse video microscopy were in mitosis. HT-29 cells were treated with either 30 μM cisplatin or 50 nM CPT for 24, 48 and 72 h and observed by immunofluorescence microscopy to detect phospho-Ser10 histone H3 staining (Figure 4.6). Not treated cells were used as a control. Phospho-histone H3 positive cells were present in the not treated cell population at 24 h (6 ± 1%), 48 h (5 ± 1%) and 72 h (2 ± 0.3%) and values were similar to those determined by light microscopy.

At 24 h, the percentages of phospho-Ser10 histone H3 positive cells were low in cells treated with either cisplatin (0.2 ± 0.07%) or CPT (0.2 ± 0.1%). By contrast, the percentage of phospho-Ser10 histone H3 positive cells was significantly higher in CPT treated cells at 48 h (9 ± 0.05%) by comparison to cells treated with cisplatin (1 ± 0.3%) (p <0.05). At 72 h, the percentages of cells staining positive for phospho-Ser10 histone H3 were similar in cell populations treated with either cisplatin (7 ± 1%) or CPT (9 ± 1%). These results indicate that cells treated with CPT enter mitosis 24 h before cells treated with cisplatin.

4.4.5 Most HT-29 cells treated with either cisplatin or CPT enter mitosis following treatment

It has been reported that the majority of cells treated with either cisplatin (Chapter 2) or CPT (Kubara et al. 2012) enter mitosis following treatment. However, the fraction of cells entering mitosis following treatment with either cisplatin or CPT has not been previously compared. We used time-lapse video microscopy to observe cells treated with either 30 μM cisplatin or 50 nM CPT. Not treated cells were used as a control. Images were captured every 10 min for 96 h (Figure 4.5) and individual cells were manually observed to detect the presence or absence of cell rounding. The percentages of cells that entered mitosis post-treatment were then determined (Figure 4.7). Nearly all not treated cells (99 ± 0.06%) entered mitosis. The majority of cells treated with either cisplatin (81 ± 3%) or CPT (94 ± 1%) entered mitosis after treatment.

4.4.6 CPT treated HT-29 cells spend a longer time in mitosis by comparison to cisplatin treated cells

The majority of not treated, cisplatin treated and CPT treated cells entered mitosis when observed by time-lapse video microscopy. We noted that entry into mitosis per se was not sufficient as a criterion to distinguish not treated cells from those treated with either cisplatin or CPT because under each condition cells would enter mitosis, albeit at different times. However, during the course of our experiments we observed that cells remained in mitosis for different lengths of time, we therefore decided to measure this precisely using time-lapse video microscopy. Images were captured every 10 min for 96 h, as such results are presented to the nearest 10 min (Figure 4.8). Not treated cells spent an average of 50 ± 0 min in mitosis. By contrast to the not treated cells, cells treated with either cisplatin (280 ± 30 min) or CPT (440 ± 20 min) spent a longer time in mitosis.

Cells treated with CPT also spent a significantly longer time in mitosis (160 min) by comparison to cells treated with cisplatin ($p < 0.05$).

4.4.7 Both 10 µM cisplatin and 50 nM CPT are cytotoxic to M059K cells

Having identified that CPT treated HT-29 cells undergo checkpoint adaptation 24 h before cisplatin treated cells, we used a second cell line to investigate whether these cells exhibited a similar response to treatment with two different genotoxic agents. It was first necessary to investigate the cytotoxicity of either cisplatin or CPT on M059K cells. M059K cells were treated with different concentrations of either cisplatin or CPT for 24, 48, 72 and 96 h and cell viability was measured by the MTT assay (Figure 4.9). The results from each treatment condition were normalised to treatment with 0.1% (v/v) DMSO.

M059K cell viability decreased in a time and concentration dependent manner following treatment with either cisplatin or CPT. The IC_{50} values for cisplatin ranged from 30 µM at 24 h to 1 µM at 96 h (Table 4.2). The IC_{50} values for CPT ranged from 567 nM at 24 h to 6 nM at 96 h (Table 4.2). We selected 10 µM cisplatin and 50 nM CPT for further study because they were higher than the respective IC_{50} values at 96 h, below the suprapharmacological concentrations for these drugs (Swift and Golsteyn 2014), and were equitoxic. It has also been reported that M059K cells treated with a similar concentration of CPT undergo checkpoint adaptation (Kubara et al. 2012) and 50 nM CPT was used as a positive control treatment for checkpoint adaptation in M059K cells in chapter 2.

4.4.8 Similar percentages of M059K cells enter mitosis following treatment with either cisplatin or CPT

To understand better the relationship between M059K cells treated with either 10 μM cisplatin or 50 nM CPT we compared the fraction of cells entering mitosis following treatment using time-lapse video microscopy. Not treated cells were used as a control. Images were captured every 10 min for 96 h (Figure 4.10A-C) and individual cells were manually observed to detect the presence or absence of cell rounding. The percentages of cells that entered mitosis were then determined (Figure 4.10D). Nearly all not treated (99 ± 0.7%) cells entered mitosis. Similar percentages of cells treated with either cisplatin (75 ± 5%) or CPT (75 ± 8%) entered mitosis following treatment.

4.4.9 M059K cells treated with either cisplatin or CPT undergo checkpoint adaptation at similar times

Having identified that 10 μM cisplatin and 50 nM CPT were equitoxic concentrations of genotoxic agents that induced similar numbers of cells to enter mitosis following treatment, we investigated if M059K cells treated with either cisplatin or CPT entered mitosis at different times. M059K cells were treated with either 10 μM cisplatin or 50 nM CPT and observed by time-lapse video microscopy to determine the percentage of cells in mitosis at 12 h intervals between 0 and 72 h after treatment (Figure 4.11). Images were captured every 10 min. Not treated cells were used as controls and mitotic cells were present as part of the normal proliferating culture. The percentages of mitotic cells in the cisplatin treated cell population remained relatively constant and ranged from 2 ± 1% at 12 h to 4 ± 1% at 48, 60 and 72 h. By contrast, the percentages of mitotic cells in the CPT treated cell population increased from 2 ± 1% at 12 h to 7 ± 2% at 48 h and 60

h and 7 ± 0.3% at 72 h. These data indicate that M059K cells treated with either cisplatin or CPT do not undergo checkpoint adaptation at different times.

4.4.10 CPT treated M059K cells spend a longer time in mitosis by comparison to cisplatin treated cells

Although we did not see a difference in the timing of checkpoint adaptation in M059K cells treated with either cisplatin or CPT, we reasoned that these cells might still spend different periods of time in mitosis by comparison to not treated cells and each other. M059K cells were treated with either 10 μM cisplatin or 50 nM CPT and observed by time-lapse video microscopy. Images were captured every 10 min for 96 h and results are presented to the nearest 10 min (Figure 4.12). Not treated cells spent an average of 50 ± 0 min in mitosis. By contrast, cells treated with either cisplatin (170 ± 10 min) or CPT (240 ± 10 min) spent a longer time in mitosis. Cells treated with CPT also spent a significantly longer time in mitosis (70 min) by comparison to cells treated with cisplatin ($p < 0.05$).

4.5 Discussion

Checkpoint adaptation occurs when cells arrest at and then abrogate the G2/M checkpoint to enter mitosis with damaged DNA. HT-29 cells undergo checkpoint adaptation when they are treated with either cisplatin (chapter 2) or CPT (Kubara et al. 2012). Checkpoint adaptation also occurs in human cancer cell lines treated with either ionising radiation (Syljuåsen et al. 2006; Rezacova et al. 2011) or etoposide (Kubara et al.

2012). It has therefore been proposed that checkpoint adaptation is a key cellular response to treatment with different genotoxic agents in human cancer cells.

In chapter 3 we found that some HT-29 cells treated with cisplatin can survive checkpoint adaptation. Because these cells enter mitosis with damaged DNA we predict that some of these survival cells will contain rearranged genomes which could induce acquired resistance to treatment. We also found that cell death can be maintained when entry into mitosis is inhibited in HT-29 cells treated with either cisplatin or CPT. We therefore suggest that preventing entry into mitosis with damaged DNA (the final step of checkpoint adaptation) might increase the efficacy of genotoxic anti-cancer drugs by preventing cancer cells from surviving treatment with rearranged genomes.

If checkpoint adaptation is to be targeted to improve the efficacy of current genotoxic anti-cancer treatments, then it is necessary to understand if this process is the same or different in cancer cells treated with genotoxic agents that damage DNA by different mechanisms of action. Additionally, the biochemical processes that underlie the engagement of checkpoint adaptation are not well understood. Investigation of differences in the induction of checkpoint adaptation may provide new information about the biochemical steps that precede and induce this event. We therefore compared the cellular response of checkpoint adaptation in HT-29 cells treated with either cisplatin or CPT.

To compare checkpoint adaptation in HT-29 cells treated with either cisplatin or CPT, we first identified that 30 μM cisplatin and 50 nM CPT were equitoxic to HT-29 cells by the MTT assay. Most cells treated with either 30 μM cisplatin or 50 nM CPT died by 96 h and both of these concentrations were above the IC_{50} concentrations of the

compounds at 96 h. When we compared the response of HT-29 cells treated with cisplatin to cells treated with CPT we identified that cells treated with either cisplatin or CPT undergo similar biochemical events during checkpoint adaptation. Cell populations treated with either cisplatin or CPT signal damaged DNA, accumulate cyclin B1 and enter mitosis, as determined by phospho-Ser10 histone H3 staining and cell rounding observed by both light and time-lapse video microscopy. These data support the suggestion that checkpoint adaptation occurs in response to treatment with different genotoxic agents. Moreover, because these cells underwent the same biochemical events to enter mitosis with damaged DNA, these data support our observations from chapter 3 that cancer cells treated with genotoxic agents can be co-treated with Cdk1 inhibitors, to prevent them from entering mitosis with damaged DNA.

However, although biochemical events were the same in cells that underwent checkpoint adaptation following treatment with either cisplatin or CPT, we found the biochemical events that induce checkpoint adaptation occur at different times in HT-29 cells treated with either cisplatin or CPT. Cells treated with CPT display cell rounding at 36 h and are positive for phospho-Ser10 histone H3 staining at 48 h, whereas cells treated with cisplatin display cell rounding at 60 h and are positive for phospho-Ser10 histone H3 staining at 72 h. Twice as many CPT treated cells are also positive for cyclin B1 at 24 h, by comparison to cisplatin treated cells. Additionally, most CPT treated cells are positive for damaged DNA at 24 h by comparison to only half of cisplatin treated cells, indicating that CPT treated cells signal damaged DNA earlier than cisplatin treated cells.

Peak histone γH2AX staining in HL-60 promyelocytic leukemic cells treated with 150 nM topotecan (TPT), a water soluble analogue of CPT, occurred 1.5 h following

treatment. By contrast, histone γH2AX staining did not peak in cisplatin treated cells until 3 h following treatment (Huang et al. 2004). At 3 h 38% of cells were positive for histone γH2AX staining, as determined by flow cytometry, when cells were treated with 1 μM cisplatin (Huang et al. 2004). These data suggest that a difference in the timing of histone γH2AX induction is a common phenomenon when cells are treated with either cisplatin or a CPT related topoisomerase I inhibitor. The authors suggest that these differences in timing can be explained if the repair of the DNA lesions induced by cisplatin, as opposed to the DNA lesions themselves, induced histone γH2AX formation (Huang et al. 2004). However, this is debated by Olive and Banáth (2009) who found that DNA replication is the source of histone γH2AX formation in cisplatin treated cells (Olive and Banáth 2009).

Our results indicate that the response of checkpoint adaptation is distinguishable when DNA is damaged by two different genotoxic agents with different mechanisms of action. We suggest that the timing of checkpoint adaptation could be linked to the time when cells signal damaged DNA, because almost all CPT treated cells signal damaged DNA at 24 h by comparison to half of cisplatin treated cells. However, one might expect that the cisplatin treated cells with damaged DNA at 24 h would enter mitosis at similar times to the CPT treated cells. It might be that the CPT treated cells that enter mitosis earlier by comparison to cisplatin treated cells signal damaged DNA earlier than any of the cisplatin treated cells. If there is a link between the timing of DNA damage signalling and time of entry into mitosis, then this could be investigated at the single cell level by time-lapse video microscopy of cells expressing fluorescent mediator of DNA damage checkpoint 1 (MDC1) (Liang et al. 2014). MDC1 is a DNA damage response protein that

binds to histone γH2AX foci at sites of damaged DNA. This allows quantification of damaged DNA in single cells.

By time-lapse video microscopy, we also identified that cells treated with either cisplatin or CPT spend a longer time in mitosis by comparison to not treated cells. Cells that have damaged DNA in mitosis are unable to satisfy the spindle assembly checkpoint (SAC) and spend a prolonged time in mitosis. Irradiated HeLa cells co-treated with the Chk1 inhibitor UCN-01 spent a prolonged time arrested at the metaphase-anaphase transition of mitosis by comparison to not treated cells and time spent in mitosis was associated with treatment dose (On et al. 2011). Cells treated with 15 Gray ionising radiation spent less time in mitosis by comparison to cells treated with 40 Gray ionising radiation. Furthermore, when the SAC was inhibited by depleting or inhibiting the SAC protein Mad2 then mitosis was shorter (On et al. 2011). The SAC also delayed HeLa cells in mitosis when they were irradiated with laser pulses and this was also attributed to Mad2 which was present at kinetochores in these cells (Mikhailov et al. 2002). HeLa cells treated with aphidicolin also spent a prolonged time in mitosis by comparison to not treated cells (Nitta et al. 2004). Our data therefore provide further indication that HT-29 cells treated with either cisplatin or CPT enter mitosis with damaged DNA. If treated cells entered mitosis with fully repaired DNA damage, then one would expect them to respond similarly to not treated cells. Additionally, cells treated with CPT spent 1.6 times longer in mitosis by comparison to cisplatin treated cells.

Having identified that HT-29 cells treated with CPT undergo checkpoint adaptation 24 h before cells treated with cisplatin and that CPT treated cells spend longer in mitosis by comparison to cisplatin treated cells, we investigated if these differences

were also observed in a second unrelated cell line, M059K. We first identified, by the MTT assay, that 10 μM cisplatin and 50 nM CPT were equitoxic to M059K cells. We also demonstrated that a similar percentage of M059K cells (75%) entered mitosis following treatment with either 10 μM cisplatin or 50 nM CPT. We then used time-lapse video microscopy to observe cell rounding and found that M059K cells treated with cisplatin entered mitosis in similar numbers between 0 and 72 h, whereas the number of mitotic cells in the CPT treated cell population increased between 24 and 48 h. This could be because, by contrast to HT-29 cells, M059K cells signal damaged DNA at similar times when treated with either cisplatin or CPT.

M059K cells do not enter mitosis at different times in response to treatment with either cisplatin or CPT. However, these cells do exhibit differences in the length of time spent in mitosis. Cells treated with either cisplatin or CPT spend a longer time in mitosis by comparison to not treated cells. CPT treated cells also spend 1.4 times longer in mitosis by comparison to cisplatin treated cells. The differences between the amount of time that cells treated with either cisplatin or CPT spend in mitosis mirrors that observed in HT-29 cells, but is less pronounced. It has been shown that HT-29 cells treated with either nocodazole or taxol spend a longer time arrested in mitosis by comparison to RKO human colon carcinoma and H1703 human non-small cell lung cancer cells (Gascoigne and Taylor 2008). HT-29 cells treated with 1 μM AZ138 (an Eg5 mitotic kinesin inhibitor) also spend longer in mitosis by comparison to the DLD-1 human colorectal adenocarcinoma, HCT-116 human colorectal adenocarcinoma, RKO human colon carcinoma and SW480 human colorectal adenocarcinoma cell lines (Gascoigne and Taylor 2008). Thus one explanation for our observations is that HT-29 cells arrest in

mitosis for a longer time by comparison to M059K cells and so differences between cells treated with either cisplatin or CPT are more pronounced in HT-29 cells by comparison to in M059K cells.

HT-29 cells treated with either taxol or nocodazole arrest in mitosis for similar times (Gascoigne and Taylor 2008). These drugs both arrest cells at the SAC by interfering with the mitotic spindle, but have different mechansims of action. Taxol stabilises microtubules whereas nocodazole inhibits microtubule assembly (Gascoigne and Taylor 2008). We found that cells treated with CPT spend longer in mitosis by comparison to cells treated with cisplatin. This suggests that CPT and cisplatin do not induce mitotic arrest for different times by acting on the mitotic spindle because if this were the case then we would expect length of time in mitosis to be similar, as for HT-29 cells treated with either taxol or nocodazole. It is therefore likely that the genotoxic agents cisplatin and CPT induce cells to arrest in mitosis for different times by an action that is not related to formation of the mitotic spindle. However, it also possible that length of time spent in mitosis is a concentration dependent effect. If length of time spent in mitosis is concentration dependent, then we would expect cells treated with lower concentrations of CPT to spend less time in mitosis by comparison to cells treated with higher concentrations of CPT. Thus HT-29 cells treated with a concentration of CPT lower than 50 nM might spend a similar amount of time in mitosis by comparison to HT-29 cells treated with 30 μM cisplatin.

Our data suggest that the biochemical events occurring during checkpoint adaptation (accumulation of cyclin B1 and entry into mitosis with damaged DNA) are similar when HT-29 cells are treated with either cisplatin or CPT. We also show that once

DNA has been damaged these events occur at different times in HT-29 cells. The difference in timing of the induction of checkpoint adaptation in HT-29 cells treated with either cisplatin or CPT could be used to elucidate the biochemical steps that underlie this process. Identification of these steps might provide further information about how best to target checkpoint adaptation to improve the efficacy of genotoxic anti-cancer drugs.

We also found that both HT-29 and M059K cells treated with CPT spend a longer time in mitosis by comparison to cisplatin treated cells. These data indicate that following checkpoint adaptation the length of mitotic arrest in response to treatment with two different genotoxic agents, either cisplatin or CPT, is different. The cellular response of checkpoint adaptation is therefore not identical in human cancer cells treated with two different genotoxic agents.

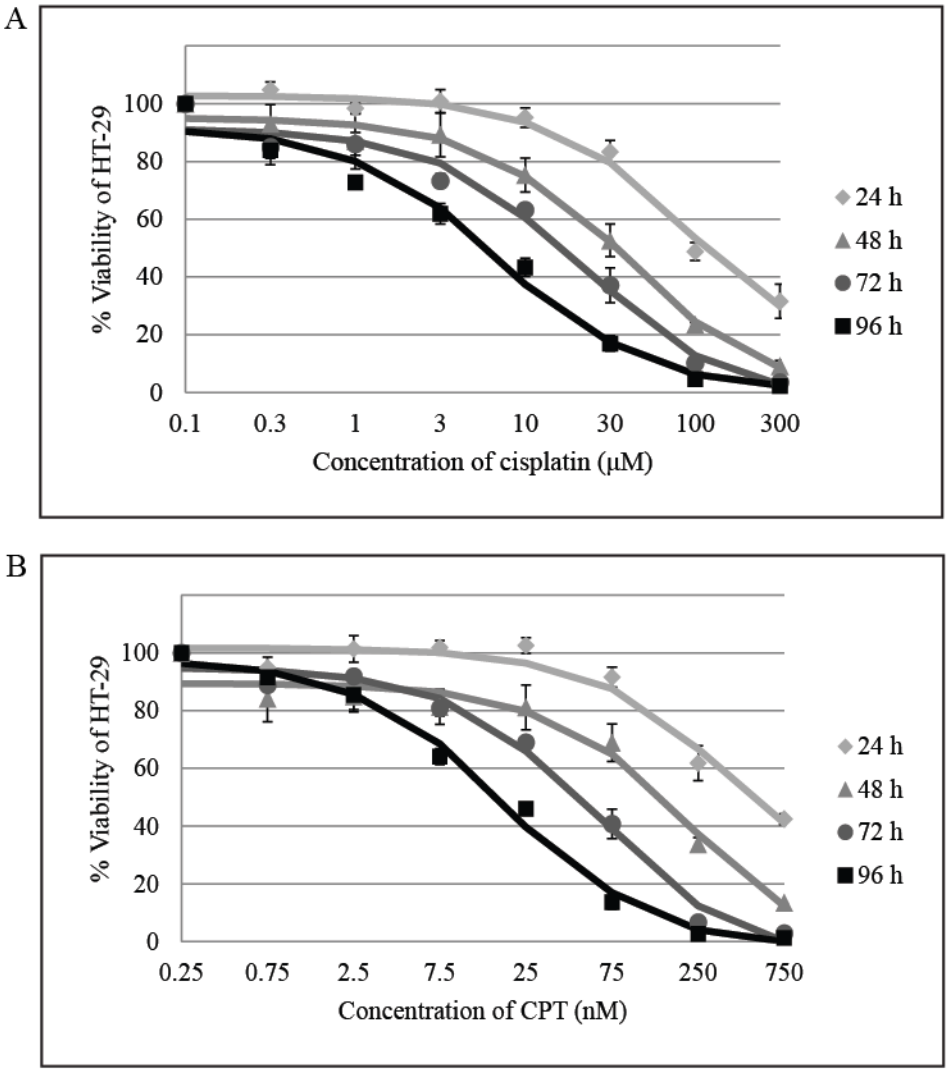

Figure 4.1 Both 30 μM cisplatin and 50 nM CPT are cytotoxic to HT-29 cells. A. HT-29 cells were treated with different concentrations of cisplatin for 24 h (diamonds), 48 h (triangles), 72 h (circles) and 96 h (squares). The MTT assay was used to measure cell viability. Each treatment was run in triplicate and the results from each treatment condition were normalised to treatment with 0.1% (v/v) DMSO. Mean percentages of viability were calculated from three separate experiments and standard errors of the means are shown. B. HT-29 cells were treated with different concentrations of CPT for 24 h (diamonds), 48 h (triangles), 72 h (circles) and 96 h (squares). The MTT assay was used to measure cell viability as described in (A).

Table 4.1 Mean IC50 concentrations of either cisplatin or CPT used to treat HT-29 cells for 24, 48, 72 and 96 h.

	Time (h)			
Genotoxic agent	24	48	72	96
Cisplatin (μM)	120	31	14	5
CPT (nM)	517.2	126.4	44.1	15.7

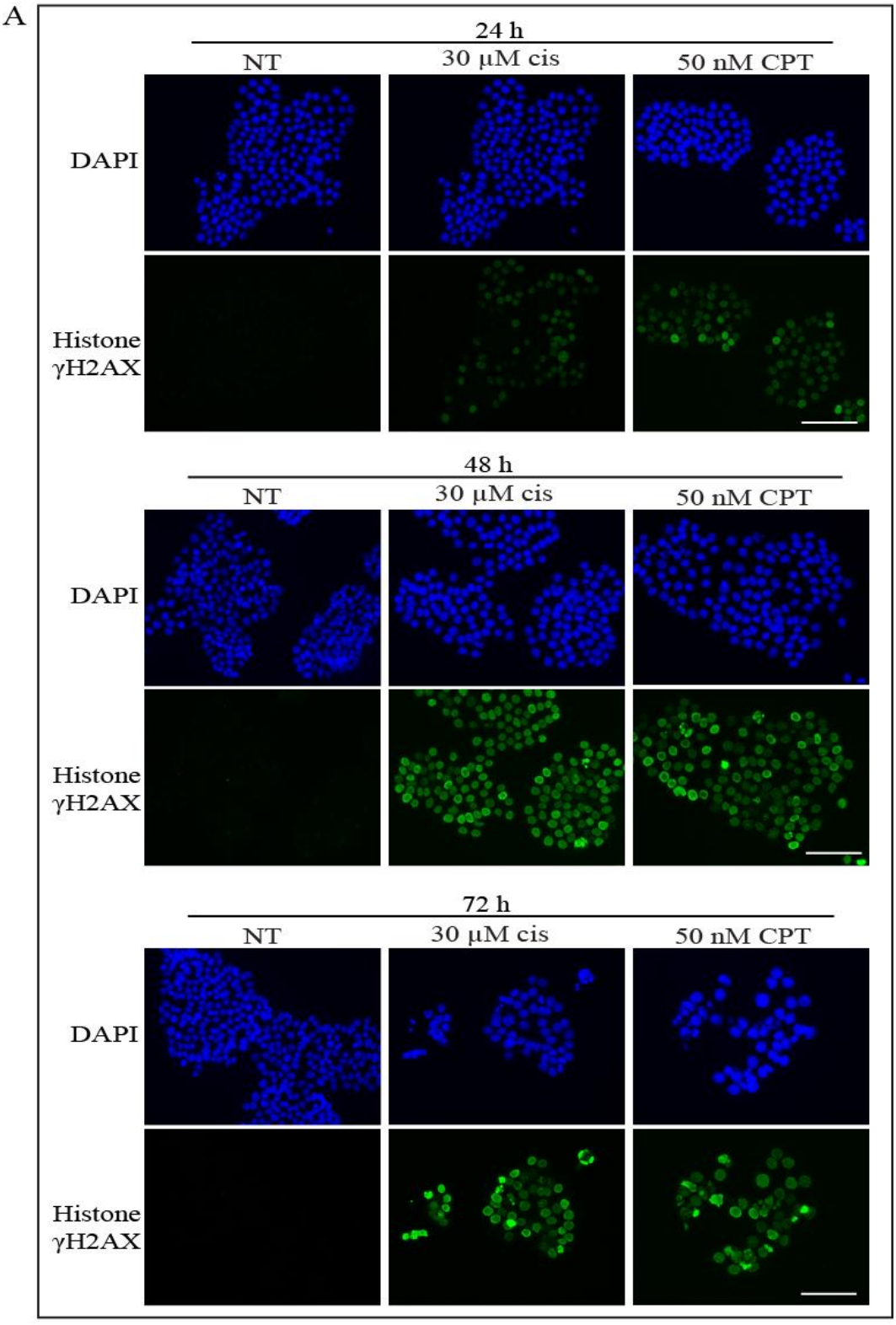
A
24 h
NT
30 μM cis
50 nM CPT
DAPI
Histone γH2AX
48 h
NT
30 μM cis
50 nM CPT
DAPI
Histone γH2AX
72 h
NT
30 μM cis
50 nM CPT
DAPI
Histone γH2AX

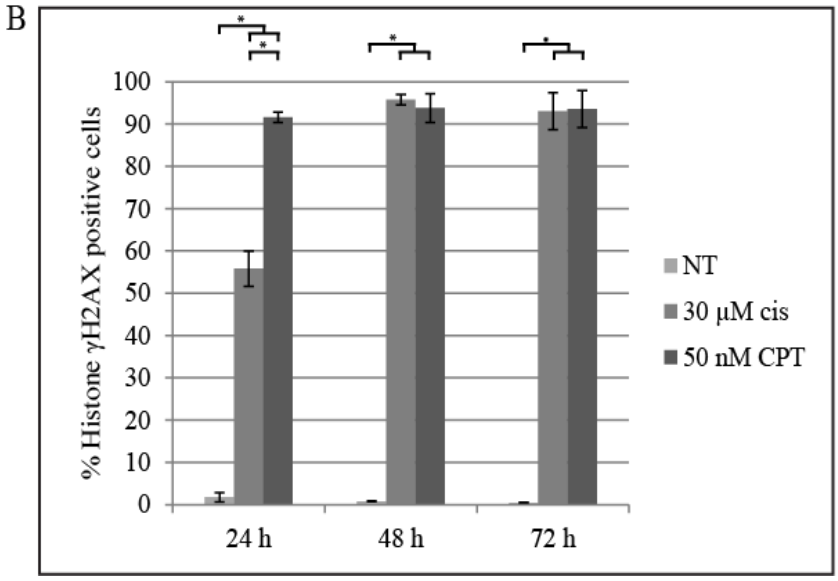

Figure 4.2 More HT-29 cells treated with CPT are positive for histone γH2AX staining at 24 h, by comparison to cells treated with cisplatin. A. HT-29 cells were either not treated (NT), treated with 30 μM cisplatin or treated with 50 nM CPT for 24, 48 or 72 h. Cells were stained with DAPI to detect DNA (blue) and with anti-histone γH2AX antibodies (green) and analysed by immunofluorescence microscopy. Representative images are shown. Scale bar equals 100 μm. B. The percentages of cells staining positive for histone γH2AX 24, 48 and 72 h after treatment were determined using Image J software. At least 500 cells were counted for each treatment per experiment. Mean percentages of cells staining positive for γH2AX, calculated from three separate experiments, and standard errors of the means are shown. Asterisks show significant differences, paired student's t-test, 2 degrees of freedom, $p < 0.05$.

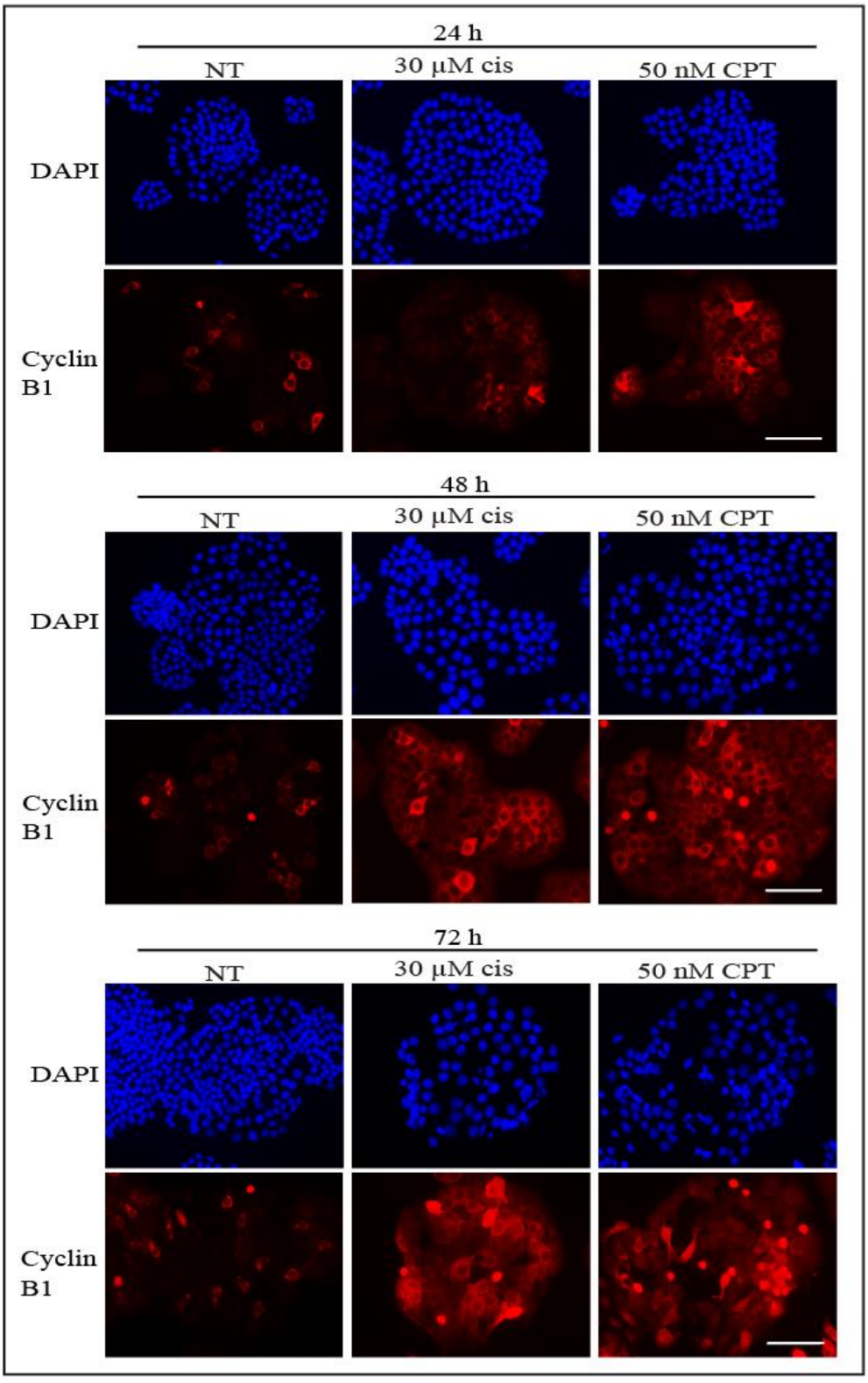
24 h
NT
30 μM cis
50 nM CPT
DAPI
Cyclin B1
48 h
NT
30 μM cis
50 nM CPT
DAPI
Cyclin B1
72 h
NT
30 μM cis
50 nM CPT
DAPI
Cyclin B1

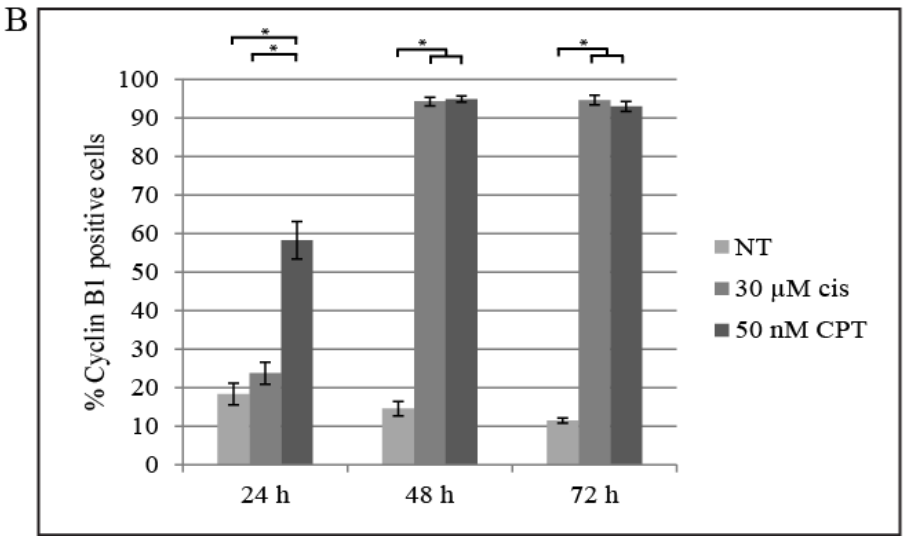

Figure 4.3 More HT-29 cells treated with CPT are positive for cyclin B1 staining at 24 h, by comparison to cells treated with cisplatin. A. HT-29 cells were either not treated (NT), treated with 30 µM cisplatin or treated with 50 nM CPT for 24, 48 or 72 h. Cells were stained with DAPI to detect DNA (blue) and with anti-cyclin B1antibodies (red) and analysed by immunofluorescence microscopy. Representative images are shown. Scale bar equals 100 µm. B. The percentages of cells staining positive for cyclin B1 24, 48 and 72 h after treatment were determined using Image J software. At least 500 cells were counted for each treatment per experiment. Mean percentages of cells staining positive for cyclin B1, calculated from three separate experiments, and standard errors of the means are shown. Asterisks show significant differences, paired student's t-test, 2 degrees of freedom, $p < 0.05$.

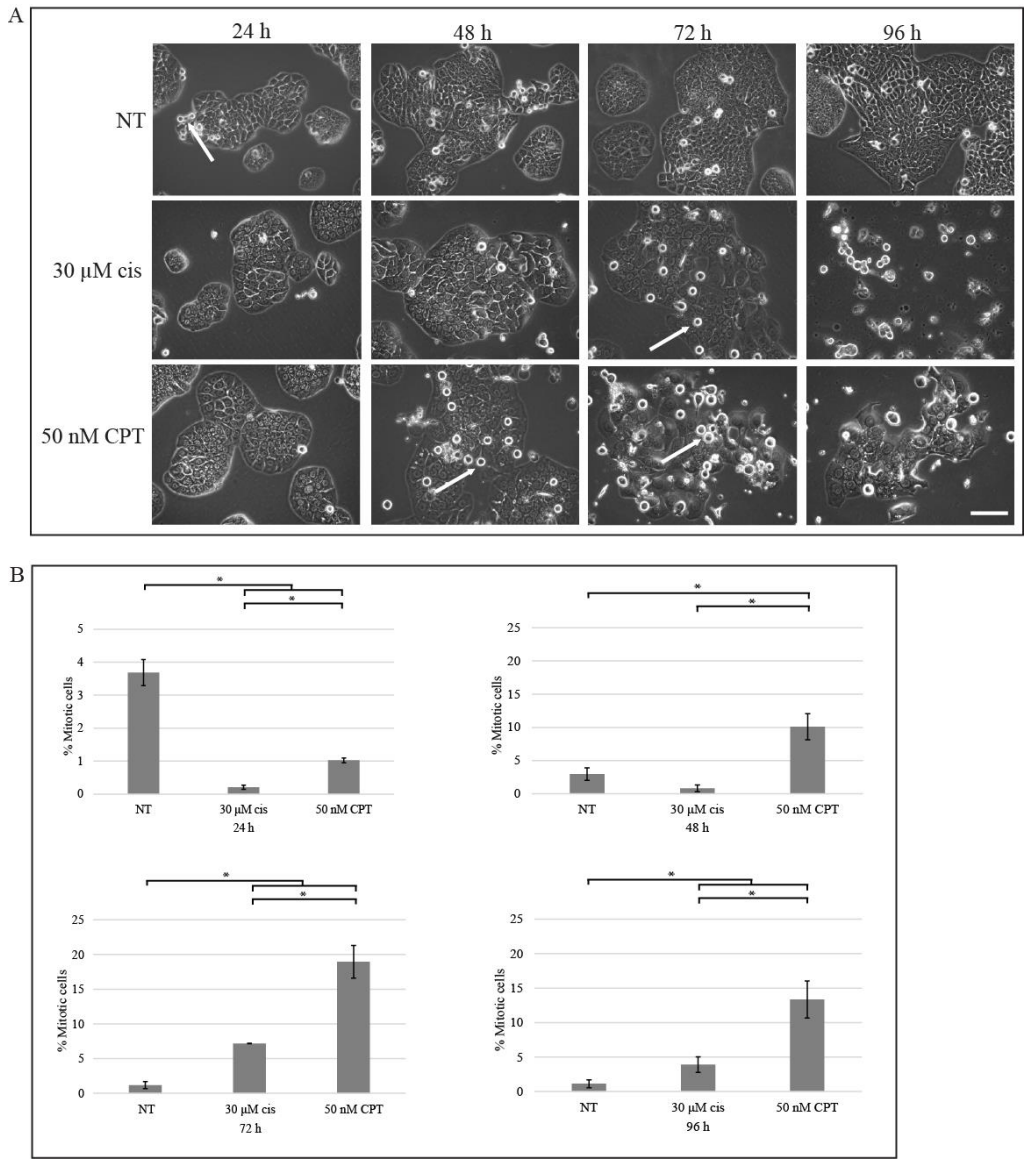

Figure 4.4 Mitotic cells are present earlier in HT-29 cell populations treated with CPT, by comparison to cell populations treated with cisplatin. A. HT-29 cells were either not treated (NT), treated with 30 µM cisplatin or treated with 50 nM CPT and observed by phase-contrast light microscopy. Representative images are shown. Scale bar equals 100 µm. B. HT-29 cells were either not treated (NT), treated with 30 µM cisplatin or treated with 50 nM CPT. The mean percentages of rounded mitotic cells were manually determined using Image J software at 24, 48, 72 and 96 h. At least 500 cells were counted for each treatment per experiment and experiments were performed three times. Standard error of means are shown. Asterisks show significant differences, paired student's t-test, 2 degrees of freedom, $p < 0.05$.

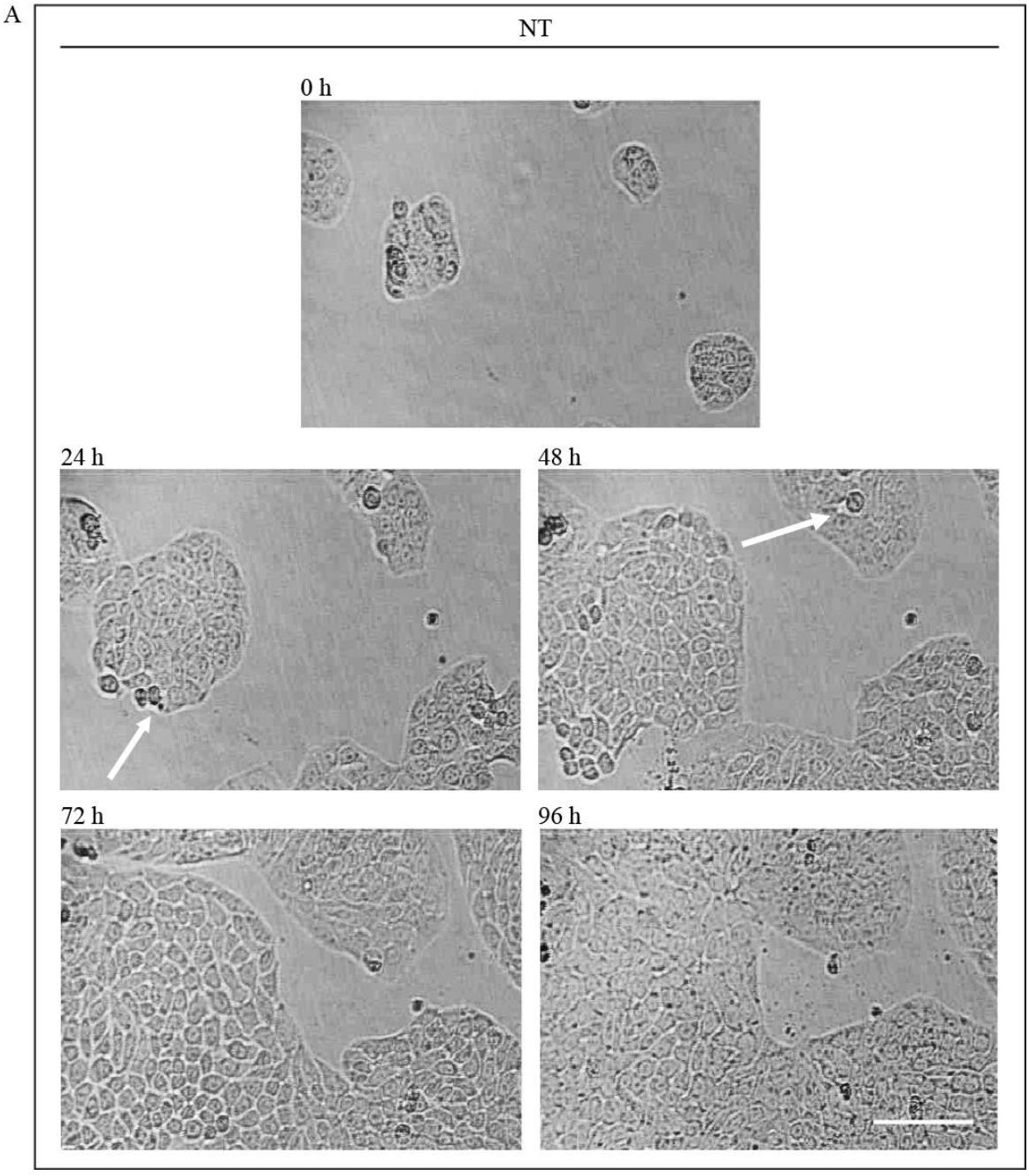
A
NT
0 h
24 h
48 h
72 h
96 h

B

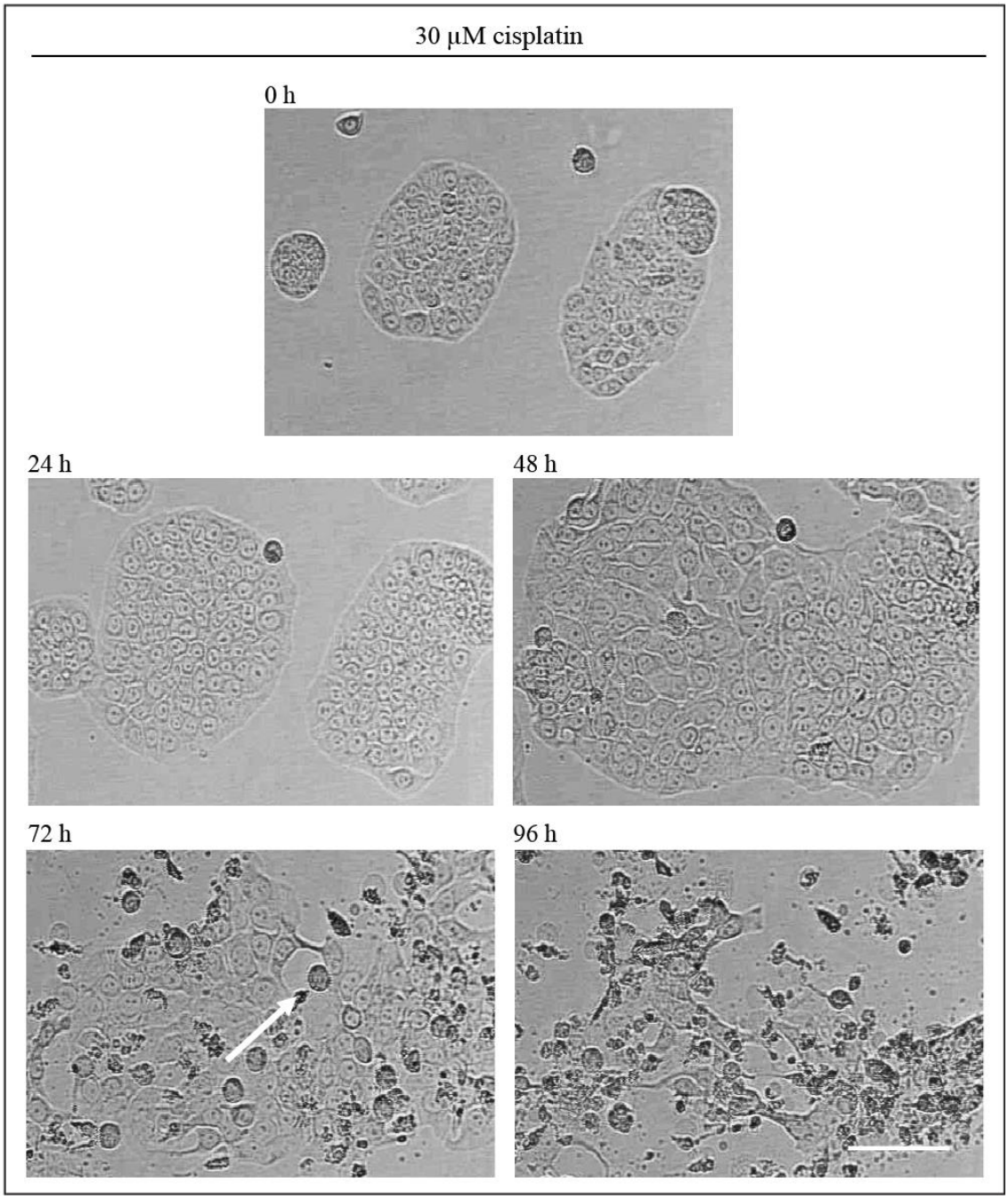

C

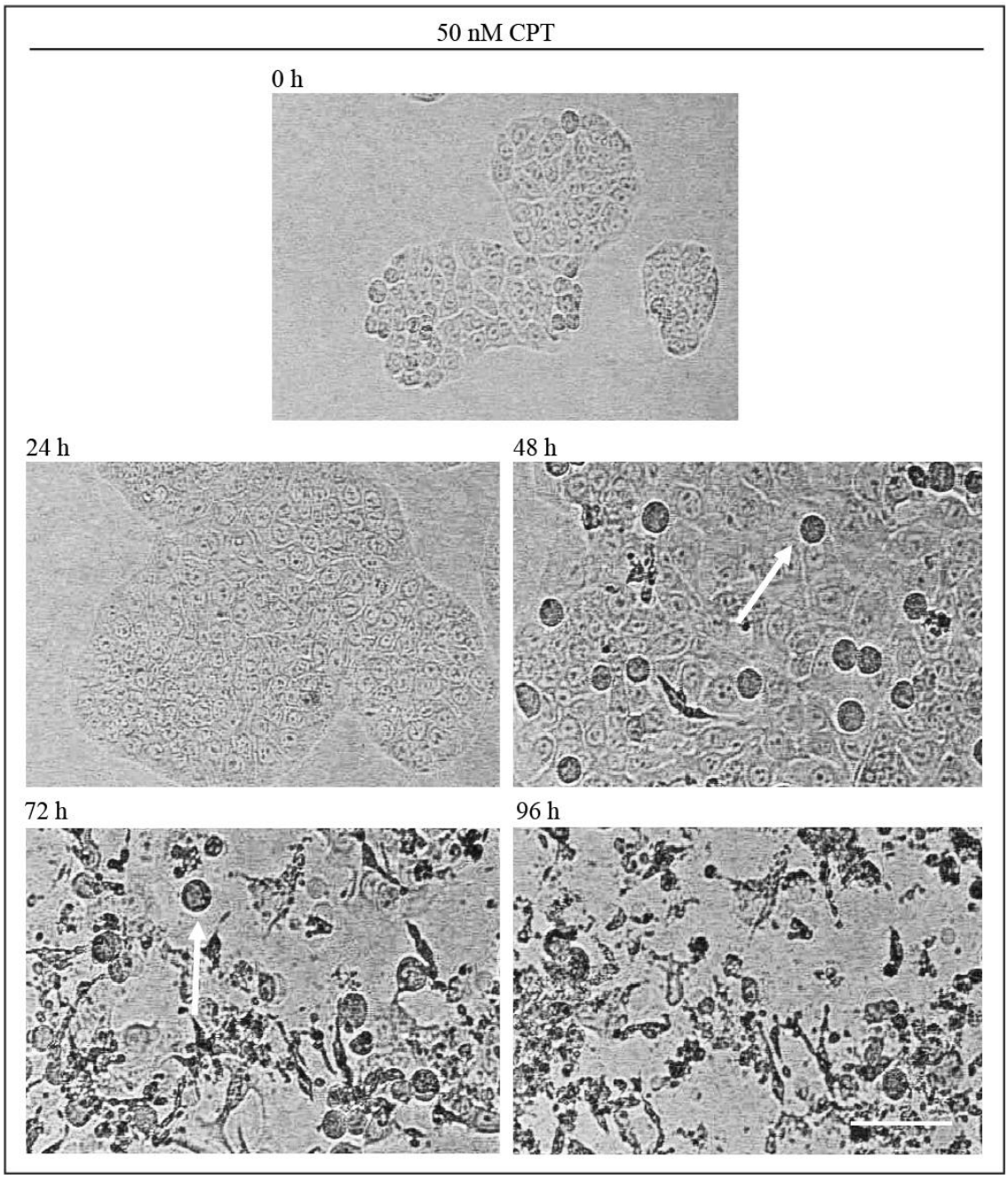

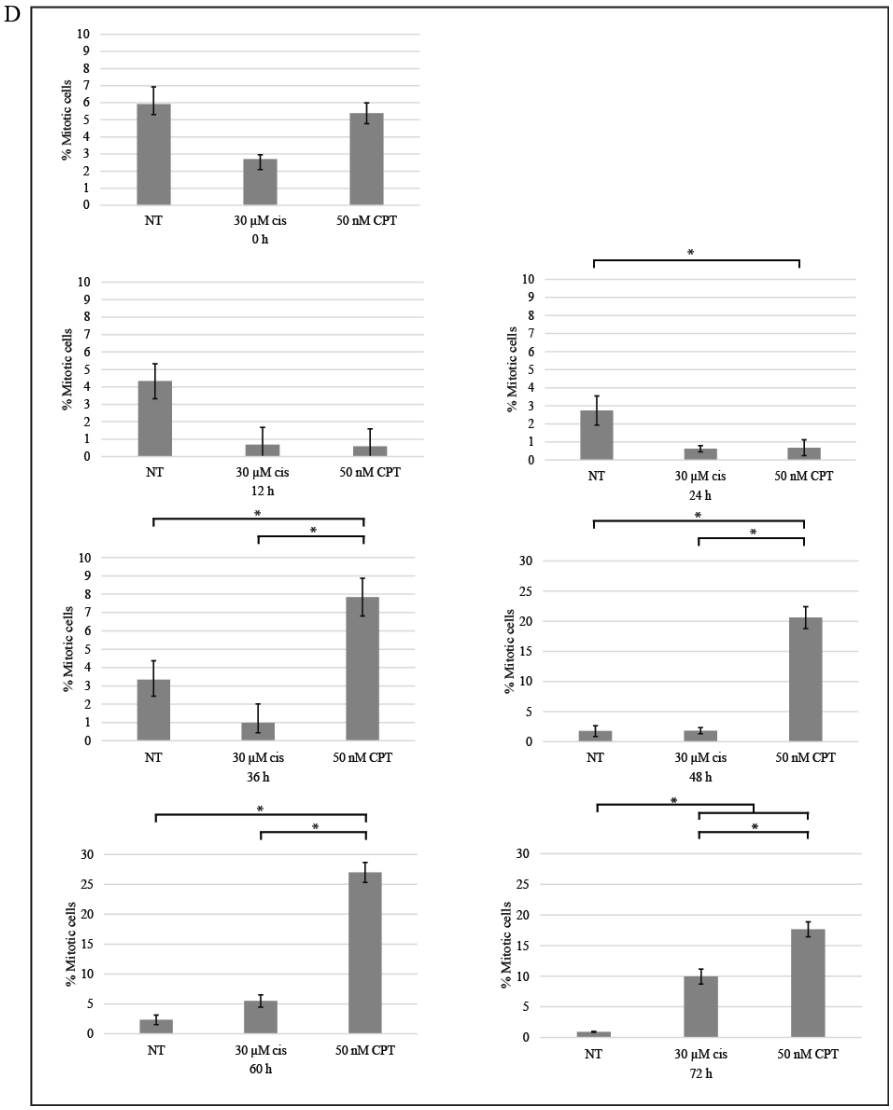

Figure 4.5 Mitotic cells are present earlier in HT-29 cell populations treated with CPT, by comparison to in cell populations treated with cisplatin. A. HT-29 cells were not treated (NT) and observed by time-lapse video microscopy. Images were captured every 10 min for 96 h and representative images from 0, 24, 48, 72 and 96 h are shown. Arrows indicate mitotic cells. Scale bar equals 100 µm. B. HT-29 cells were treated with 30 µM cisplatin and observed by time-lapse video microscopy, as described in (A). C. HT-29 cells were treated with 50 nM CPT and observed by time-lapse video microscopy, as described in (A). D. HT-29 cells were either not treated (NT), treated with 30 µM cisplatin or treated with 50 nM CPT and observed by time-lapse video microscopy, as described in (A). The mean percentages of rounded mitotic cells from three separate experiments were calculated at 12 h intervals from 0-72 h. At least 250 cells were counted per experiment. Standard errors of the means are shown. Asterisks show significant differences, paired student's t-test, 2 degrees of freedom, $p < 0.05$.

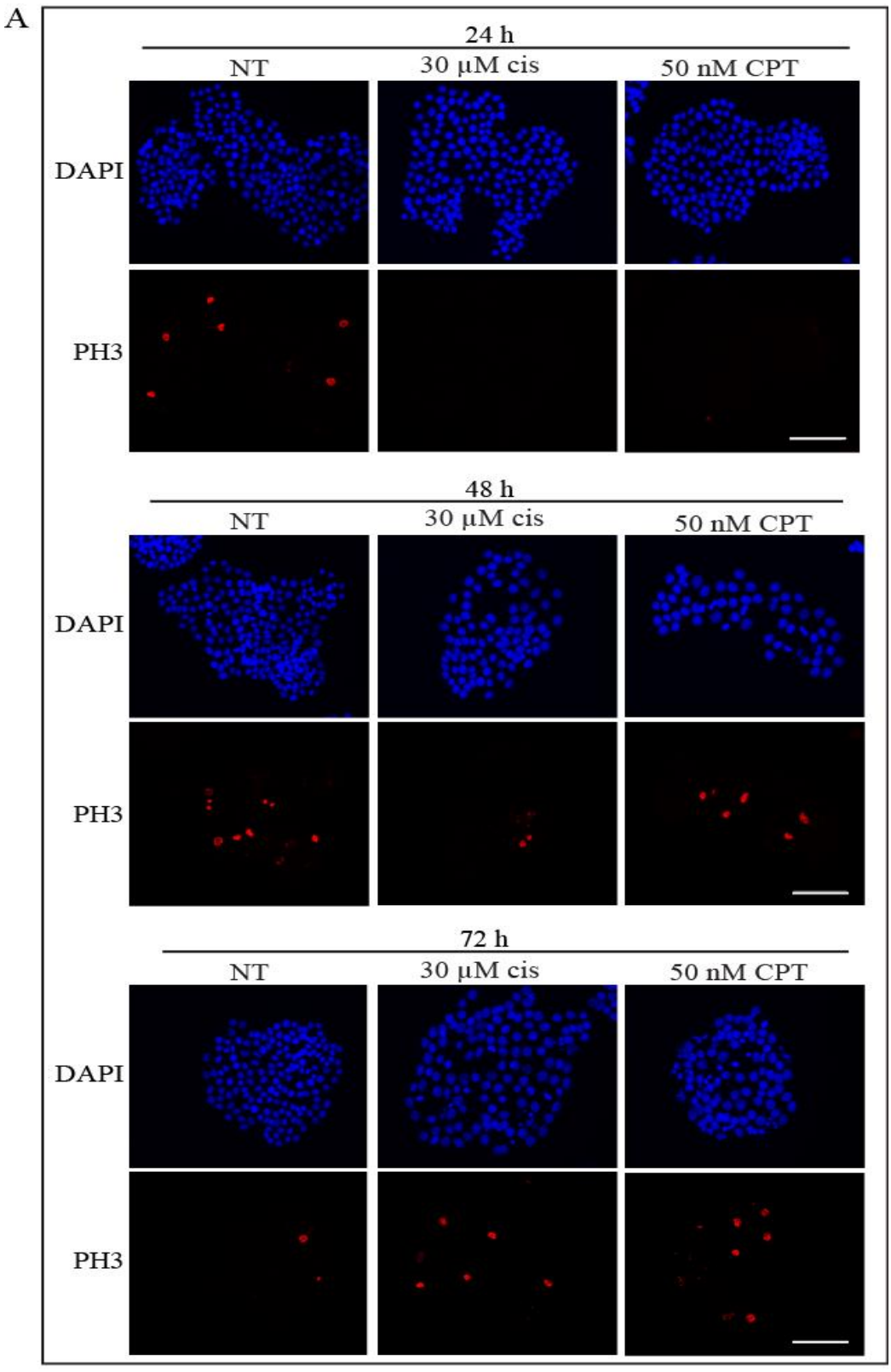
A
24 h
NT
30 μM cis
50 nM CPT
DAPI
PH3
48 h
NT
30 μM cis
50 nM CPT
DAPI
PH3
72 h
NT
30 μM cis
50 nM CPT
DAPI
PH3

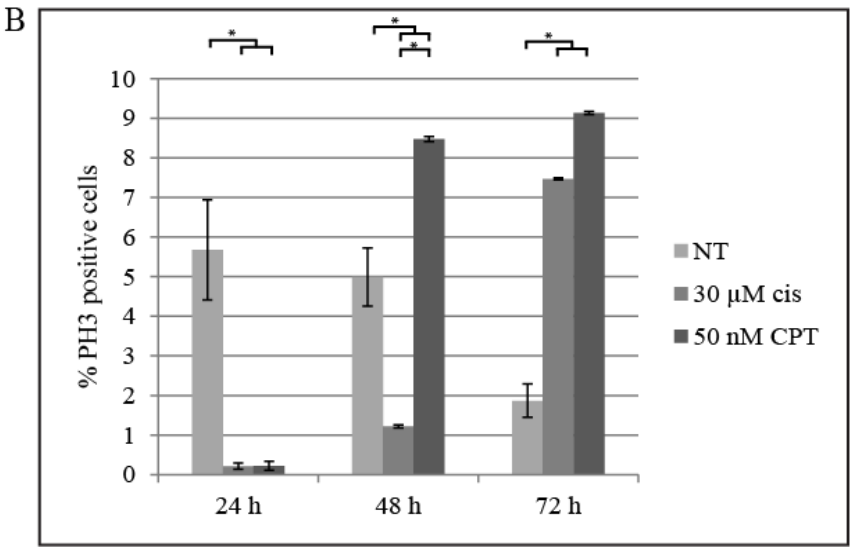

Figure 4.6 Mitotic cells are present 24 h earlier in HT-29 cell populations treated with CPT, by comparison to cell populations treated with cisplatin. A. HT-29 cells were either not treated (NT), treated with 30 µM cisplatin or treated with 50 nM CPT for 24, 48 or 72 h. Cells were stained with DAPI to detect DNA (blue) and with anti-phospho Ser10 histone H3 antibodies (PH3) (red) and analysed by immunofluorescence microscopy. Representative images are shown. Scale bar equals 100 µm. B. The percentages of cells staining positive for phospho Ser10 histone H3 (PH3) 24, 48 and 72 h after treatment were determined using Image J software. At least 500 cells were counted for each treatment per experiment. Mean percentages of cells staining positive for PH3, calculated from three separate experiments, and standard errors of the means are shown. Asterisks show significant differences, paired student's t-test, 2 degrees of freedom, $p < 0.05$.

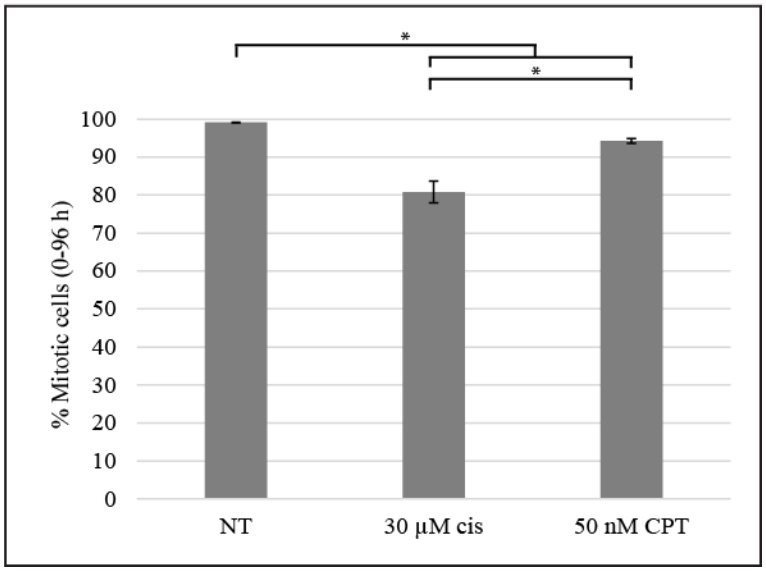

Figure 4.7 Most HT-29 cells treated with either cisplatin or CPT enter mitosis. HT-29 cells were either not treated (NT), treated with 30 µM cisplatin or treated with 50 nM CPT and observed by time-lapse video microscopy as described in Figure 4.5. Images were manually analysed to determine the mean percentages of cells that entered mitosis between 0 and 96 h post-treatment from three separate experiments. At least 250 cells were counted per experiment. Standard errors of the means are shown. Asterisks show significant differences, paired student's t-test, 2 degrees of freedom, $p < 0.05$.

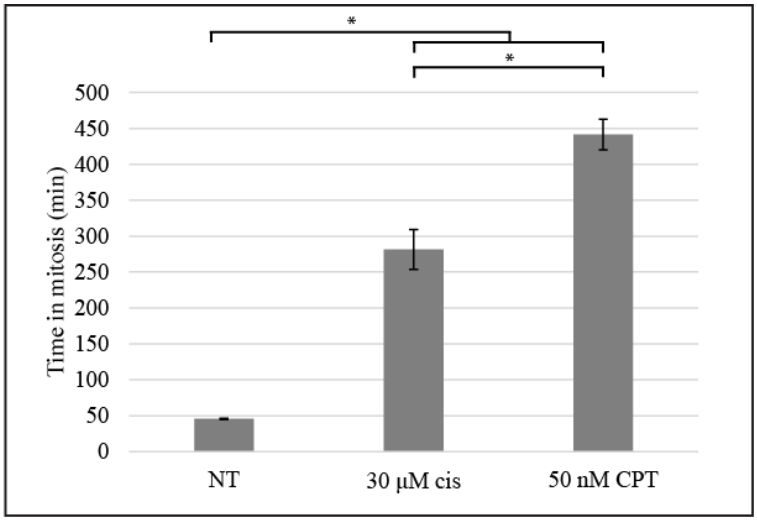

Figure 4.8 HT-29 cells treated with CPT spend a longer time in mitosis by comparison to cisplatin treated cells. HT-29 cells were either not treated (NT), treated with 30 µM cisplatin or treated with 50 nM CPT and observed by time-lapse video microscopy as described in Figure 4.5. Images were manually analysed to determine how long individual cells spent in mitosis, to the nearest 10 min. Thirty cells were analysed for each treatment. Mean times in mitosis from three separate experiments were calculated and standard errors of the means are shown. Asterisks show significant differences, paired student's t-test, 2 degrees of freedom, $p < 0.05$.

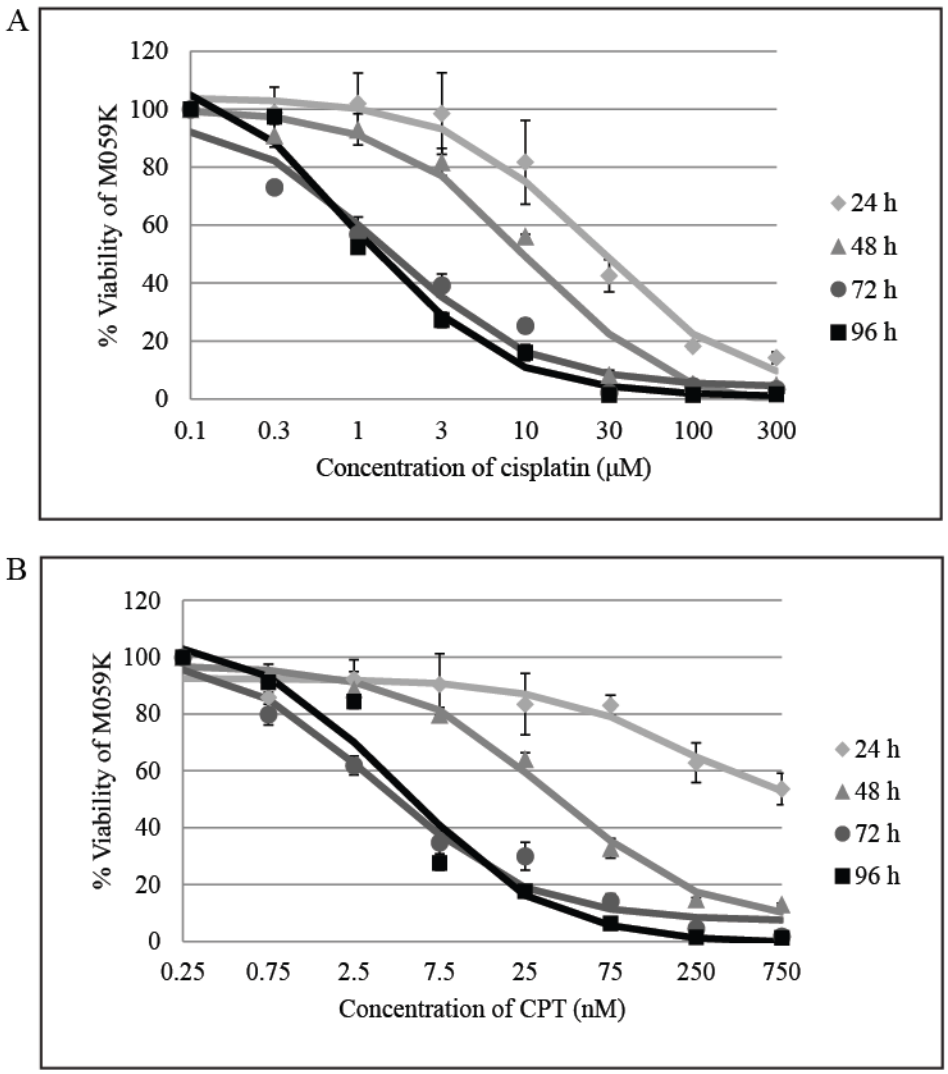

Figure 4.9 Both 10 μM cisplatin and 50 nM CPT are cytotoxic to M059K cells. A. M059K cells were treated with different concentrations of cisplatin for 24 h (diamonds), 48 h (triangles), 72 h (circles) and 96 h (squares). The MTT assay was used to measure cell viability. Each treatment was run in triplicate and the results from each treatment condition were normalised to treatment with 0.1% (v/v) DMSO. Mean percentages of viability were calculated from three separate experiments and standard errors of the means are shown. B. M059K cells were treated with different concentrations of CPT for 24 h (diamonds), 48 h (triangles), 72 h (circles) and 96 h (squares). The MTT assay was used to measure cell viability, as described in (A).

Table 4.2 Mean IC_{50} concentrations of either cisplatin or CPT used to treat M059K cells for 24, 48, 72 and 96 h.

	Time (h)			
Genotoxic agent	24	48	72	96
Cisplatin (μM)	29.5	9.4	1.6	1.4
CPT (nM)	567.2	39.1	4.8	5.6

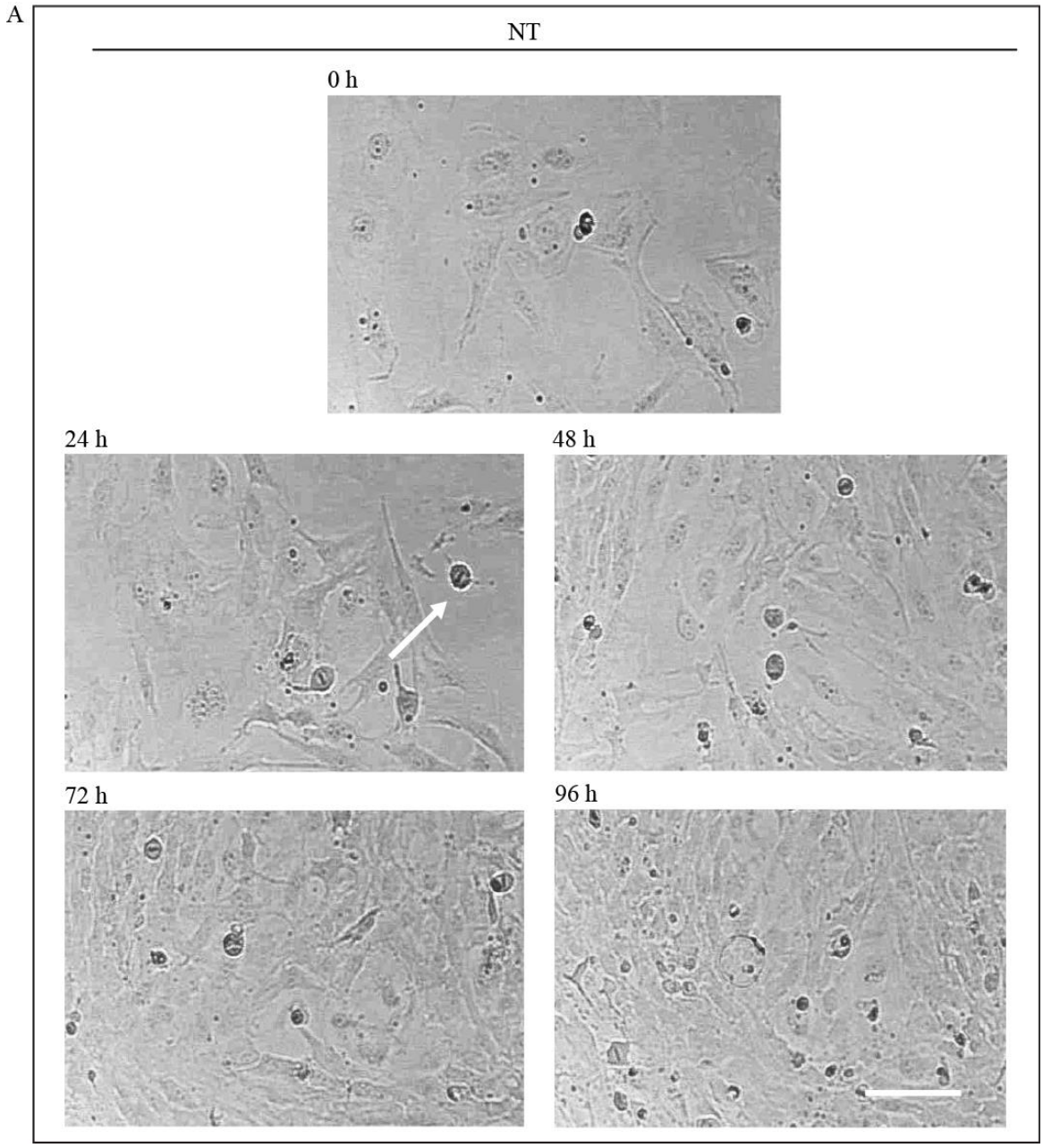
A
NT
0 h
24 h
48 h
72 h
96 h

B

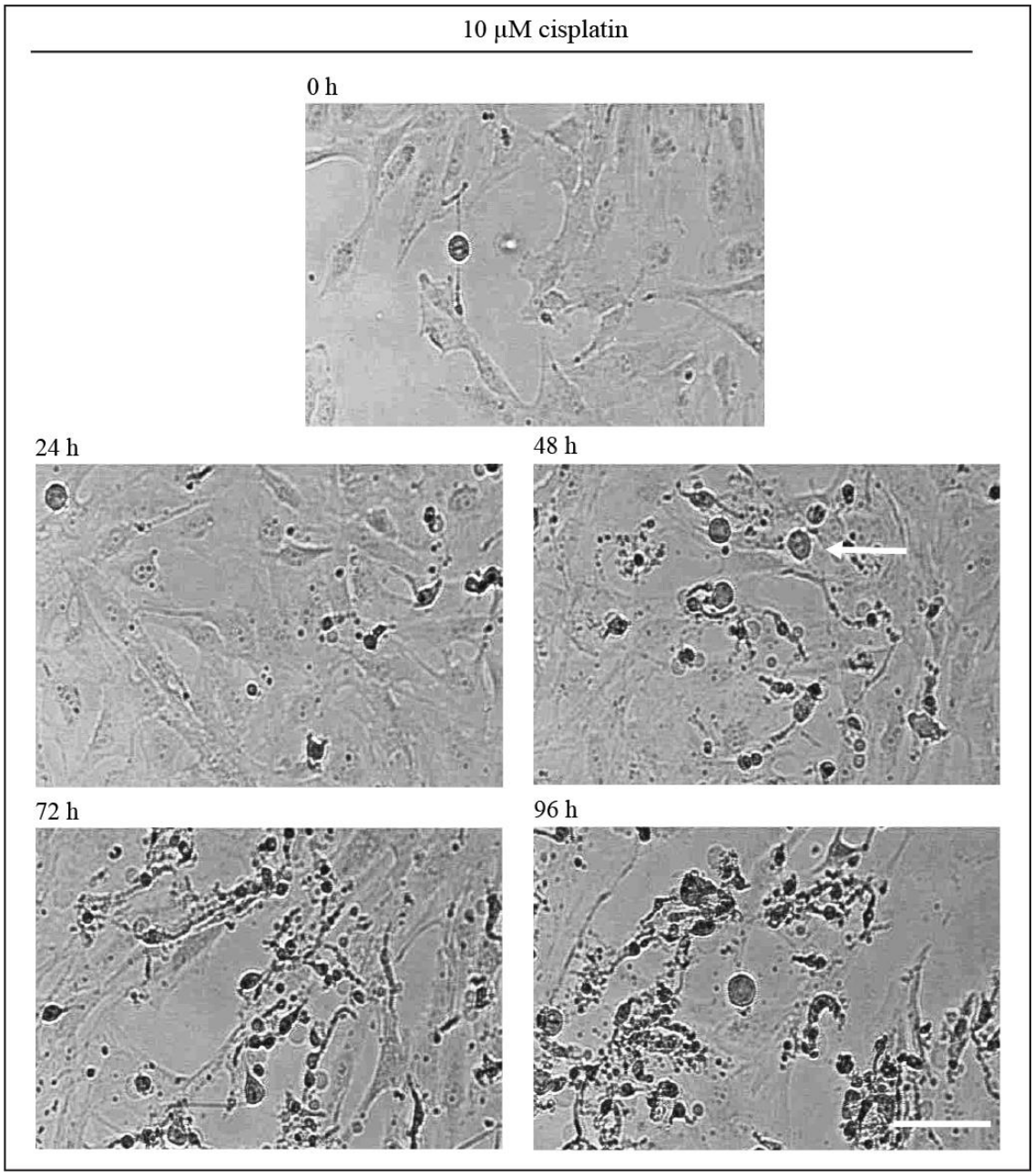

C

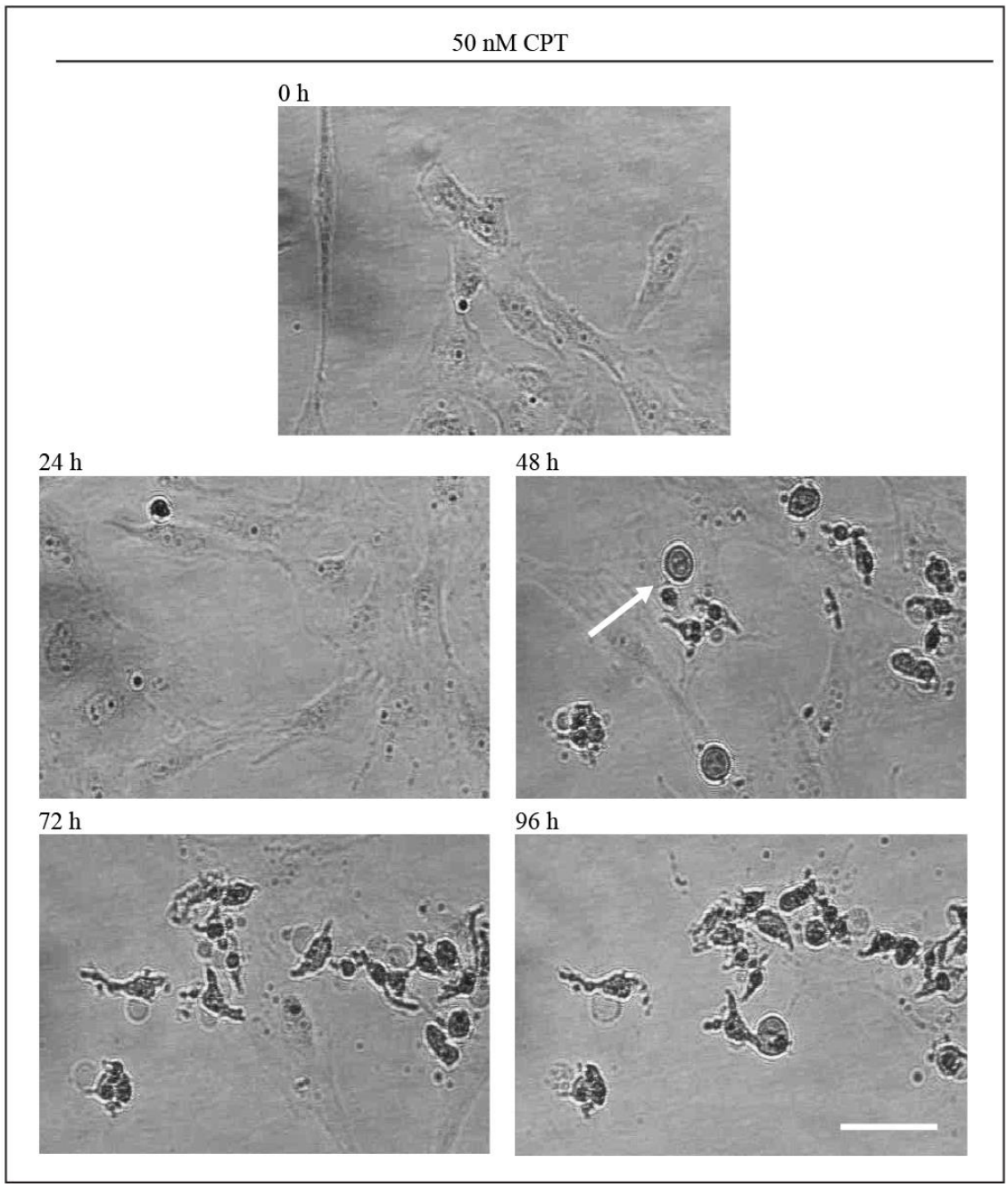

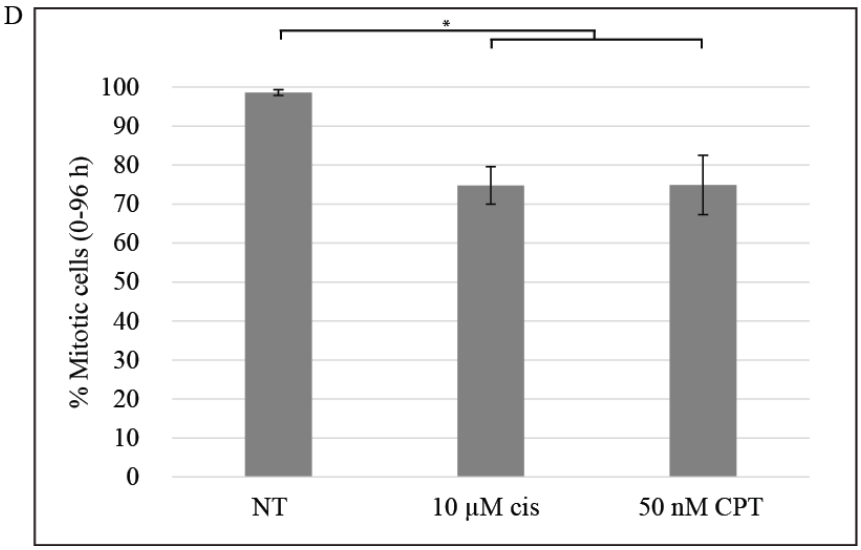

Figure 4.10 Similar percentages of M059K cells enter mitosis following treatment with either cisplatin or CPT. A. M059K cells were not treated (NT) and observed by time-lapse video microscopy. Images were captured every 10 min for 96 h and representative images captured every 24 h from 0-96 h are shown. Arrows indicate mitotic cells. Scale bar equals 100 µm. B. M059K cells were treated with 10 µM cisplatin and observed using time-lapse video microscopy, as described in (A). C. M059K cells were treated with 50 nM CPT and observed using time-lapse video microscopy, as described in (A). D. M059K cells were either not treated (NT), treated with 10 µM cisplatin or treated with 50 nM CPT and observed by time-lapse video microscopy as described in (A). Images were manually analysed to determine the mean percentages of cells that entered mitosis between 0 and 96 h post-treatment from three separate experiments. At least 50 cells were counted per experiment. Standard errors of the means are shown. Asterisks show significant differences, paired student's t-test, 2 degrees of freedom, $p < 0.05$.

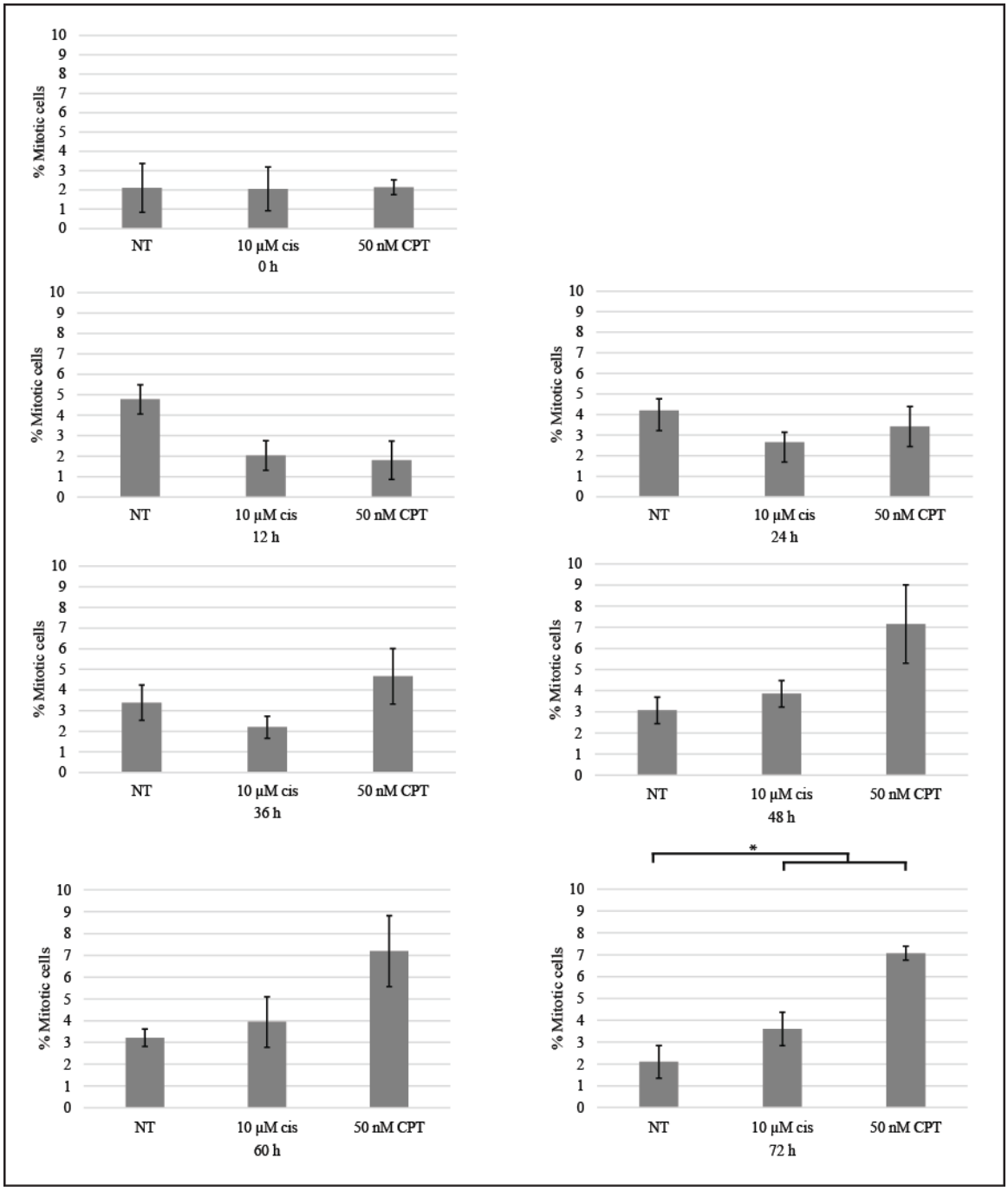

Figure 4.11 M059K cells treated with either cisplatin or CPT enter mitosis at similar times following treatment. M059K cells were either not treated (NT), treated with 10 µM cisplatin or treated with 50 nM CPT and observed by time-lapse video microscopy, as described in Figure 4.10. The mean percentages of rounded mitotic cells from three separate experiments were calculated at 12 h intervals from 0-72 h. At least 50 cells were counted per experiment. Standard errors of the means are shown. Asterisks show significant differences, paired student's *t*-test, 2 degrees of freedom, $p < 0.05$.

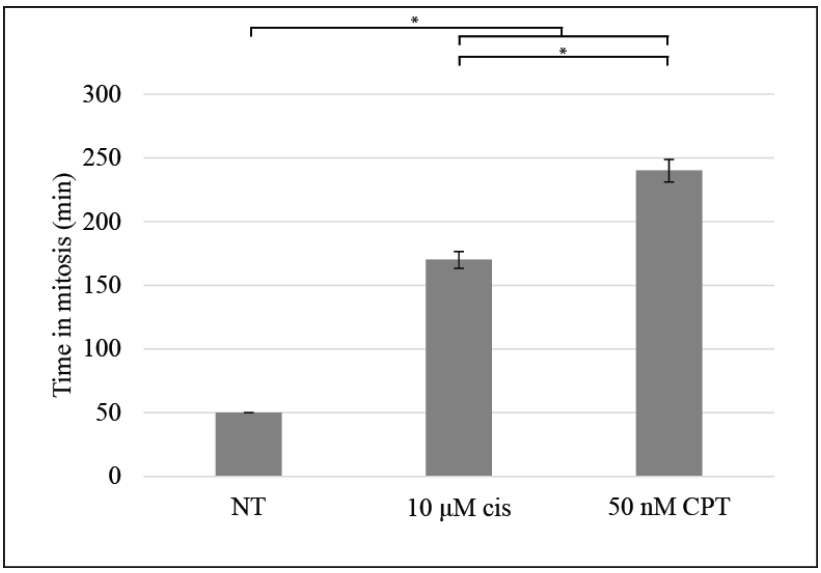

Figure 4.12 M059K cells treated with CPT spend a longer time in mitosis by comparison to cisplatin treated cells. M059K cells were either not treated (NT), treated with 10 µM cisplatin or treated with 50 nM CPT and observed by time-lapse video microscopy as described in Figure 4.10. Images were manually analysed to determine how long individual cells spent in mitosis, to the nearest 10 min. Twenty cells were analysed for each treatment. Mean times in mitosis from three separate experiments were calculated and standard errors of the means are shown. Asterisks show significant differences, paired student's t-test, 2 degrees of freedom, $p < 0.05$.

CHAPTER 5

General discussion

In this thesis we investigated checkpoint adaptation in human cancer cells treated with cisplatin. When cells undergo checkpoint adaptation following a genotoxic event they arrest at and then abrogate the G2/M checkpoint and enter mitosis with damaged DNA (Toczyski et al. 1997). We hypothesised that cancer cells treated with cisplatin undergo checkpoint adaptation because cisplatin can induce cell death by mitotic catastrophe (Demarq et al. 1994; Chang et al. 1999; Vakifahmetoglu et al. 2008). Our results show that the majority of HT-29 human colorectal adenocarcinoma cells treated with a relatively low but cytotoxic concentration of cisplatin undergo checkpoint adaptation before dying. By contrast, cells treated with a suprapharmacological concentration of cisplatin die by apoptosis. We also found that M059K glioma cells treated with different concentrations of cisplatin undergo dual modes of cell death.

A concentration dependent induction of dual modes of cell death has been observed in human colorectal adenocarcinoma cell lines treated with 5-fluorouracil (Yoshikawa et al. 2001), hepatocarcinoma cell lines treated with doxorubicin (Eom et al. 2005) and Chinese hamster lung fibroblasts treated with bleomycin (Tounekti et al. 1993). These studies and our data suggest that the induction of dual modes of cell death is a common response to treatment with different concentrations of a genotoxic agent, because the agents used in these studies damage DNA by different mechanisms of action. It is therefore important to explore the relationship between concentration or dose of treatment and cytotoxicity in experiments where cell death is being investigated because

concentrations of treatments that induce apoptosis may be above those required to induce cell death.

Checkpoint adaptation is a mechanism that might transmit damaged DNA to daughter cells. Checkpoint adaptation has been shown to induce genomic instability in *Saccharomyces cerevisiae* (Galgoczy and Toczyski 2001) and *Allium cepa* root meristemic cells (Carballo et al. 2006). It is therefore likely that checkpoint adaptation can induce genomic instability in human cells. If the biochemical pathway that induces cells to switch between checkpoint adaptation and apoptosis were identified, then it might be possible to prevent cells from undergoing checkpoint adaptation and induce cell death by apoptosis. This should prevent cells from surviving treatment with rearranged genomes. Our data indicate that cells treated with a lower concentration of cisplatin contain less damaged DNA, by comparison to cells treated with a higher concentration of cisplatin. We therefore predict that the switch between checkpoint adaptation and apoptosis is regulated by levels of damaged DNA.

To quantify further the levels of damaged DNA in cells treated with different concentrations of cisplatin, cells could be transfected with fluorescent mediator of DNA damage checkpoint protein 1 (MDC1), a protein that binds to histone γH2AX at sites of damaged DNA (Stewart et al. 2003). These transfected cells could then be observed by time-lapse video microscopy (Liang et al. 2014) and the amount of fluorescent signal could be quantified and compared. By quantifying the amount of damaged DNA in cells treated with a range of concentrations of cisplatin it should be possible to identify the amount of damaged DNA that is necessary to induce cells to die by apoptosis instead of by undergoing checkpoint adaptation. If the switch between the induction of checkpoint

adaptation or apoptosis is linked to a specific amount of damaged DNA then this would provide a measure for the induction of checkpoint adaptation that does not rely on treatment concentration and that might be applicable to different genotoxic agents.

Having identified that checkpoint adaptation is a key cellular response in HT-29 cells treated with a low but cytotoxic concentration of cisplatin, we asked if any cells could survive this process. Checkpoint adaptation can only be a source of genomic instability if cells can survive it. We found that a small but biologically significant number of cells can survive checkpoint adaptation following treatment with cisplatin. To understand better the consequences of checkpoint adaptation in cancer cells treated with genotoxic agents it will be necessary to characterise the extent of genomic rearrangement in these survival cells.

Cells that survive checkpoint adaptation could be studied using fluorescence *in situ* hybridisation (FISH), using fluorescent probes specific for telomeres and centromeres (Bishop 2010; Rahman 2013). If genomic rearrangement was occurring in cells surviving checkpoint adaptation, then telomeres and centromeres might be over represented on certain chromosomes and under represented on others (Rahman 2013). A special type of FISH, spectral karyotyping (SKY), could also be used to paint all of the chromosomes in a cell. This would allow the observation of chromosomal translocations and large insertion and deletion events (Imataka and Arisaka 2012) in survival cells. The occurrence of micronuclei could also be quantified to assess levels of genomic instability in cells that survive checkpoint adaptation (Lewis 2014). Furthermore, cells could be transfected with fluorescent histone H2B (Kanda et al. 1998) and observed by high resolution time-lapse video microscopy (Rello-Varona et al. 2010) to identify DNA strand

breaks and follow the movement of chromosomes in cells undergoing checkpoint adaptation. This would allow the observation of genome rearrangement in real-time and would provide information about how common and extensive genomic rearrangement is following checkpoint adaptation. Finally, as single cell sequencing techniques advance, it will also be possible to sequence the genomes of individual cells that survive checkpoint adaptation (Leung et al. 2015). We would expect that every genome would be different in these cells, because DNA is not damaged identically in all cells treated with genotoxic agents such as cisplatin.

If, as suggested, checkpoint adaptation is a source of genomic instability in treated cancer cells then it may be a mechanism by which some cancer cells acquire genomic change that leads to resistance to further treatment. Acquired resistance to cisplatin is known to be induced by genetic change. Cancer cell lines and tumour samples that are resistant to cisplatin exhibit chromosomal abnormalities such as loss of chromosomal regions which are not present in cisplatin sensitive cancer cell lines and tumour samples (Wasenius et al. 1997; Rao et al. 1998; Leyland-Jones et al. 1999; Nessling et al. 1999; Wilson et al. 2005; Noel et al. 2008; Österberg et al. 2009; Oliver 2010). When cells acquire resistance to treatment, this can lead to tumour progression or cancer relapse.

Preventing cells from entering mitosis with damaged DNA (the final step of checkpoint adaptation) before dying might prevent cells from surviving treatment with rearranged genomes. However, it is unknown whether cells that usually die following checkpoint adaptation need to enter mitosis for cell death to occur and it has been suggested that cells may undergo checkpoint adaptation because they are unable to die in G2 (Lupardus and Cimprich 2004; Syljuåsen et al. 2006). Our results show that HT-29

cells treated with either camptothecin (CPT) or cisplatin are capable of dying when mitosis is inhibited by co-treating cells with CR8. However, chemical inhibitors often target several enzymes. Although we confirmed that mitosis was inhibited when cells were treated with CR8, it is possible that cell death was induced because of a secondary effect of CR8. Thus, the same response might not occur if cells were prevented from entering mitosis using a different Cdk1 inhibitor. To confirm that cells treated with either cisplatin or CPT can die when mitosis is inhibited, cell viability could be measured in cells where siRNA was used to knockdown Cdk1 (Xiao et al. 2009), and in cells co-treated with different Cdk1 inhibitors.

If checkpoint adaptation is to be targeted to increase the efficacy of current cancer treatments by preventing cells from undergoing checkpoint adaptation, then it is necessary to understand if checkpoint adaptation is the same or different following treatment with different genotoxic agents. We therefore compared the response of checkpoint adaptation in HT-29 cells treated with either cisplatin or CPT. We show that HT-29 cells treated with either cisplatin or CPT proceed through the same steps to undergo checkpoint adaptation. Cells treated with either cisplatin or CPT contain damaged DNA, high levels of cyclin B and the majority of cells from both treatments enter mitosis. However, the timing of entry into mitosis with damaged DNA is different in HT-29 cells treated with these different genotoxic agents. Cells treated with CPT enter mitosis 24 h earlier by comparison to cells treated with cisplatin. Both HT-29 and M059K cells treated with CPT also spend longer times in mitosis by comparison to cisplatin treated cells. The cellular response of checkpoint adaptation is therefore not identical in human cancer cells treated with two different genotoxic agents.

In conclusion, checkpoint adaptation is a key step that lies between cell cycle arrest and cell death in cisplatin treated cells. Because checkpoint adaptation occurs in cells treated with ionising radiation (Syljuåsen et al. 2006; Rezacova et al. 2011), CPT, etoposide (Kubara et al. 2012) and cisplatin, it is likely an important step that lies between cell cycle arrest and cell death following treatment with different genotoxic anti-cancer drugs. To improve the efficacy of these drugs it is necessary to understand better the biochemical pathway that induces cells to undergo checkpoint adaptation in treated cancer cells, because some cells can survive checkpoint adaptation and these cells might contain rearranged genomes. Additionally, for the findings in this thesis to translate to the clinic, studies investigating whether checkpoint adaptation occurs in tumour models and *in vivo* need to be undertaken.

In summary we have demonstrated that:

1) Checkpoint adaptation is a major response to treatment with a relatively low but cytotoxic concentration of cisplatin, but cells die by apoptosis when they are treated with a suprapharmacological concentration of cisplatin (chapter 2).

2) A small but biologically significant number of HT-29 cells treated with cisplatin can survive checkpoint adaptation (chapter 3).

3) Cytotoxicity is maintained when entry into mitosis with damaged DNA is inhibited in HT-29 cells treated with either cisplatin or CPT (chapter 3).

4) HT-29 cells enter mitosis with damaged DNA (the final step of checkpoint adaptation) at different times when they are treated with either cisplatin or CPT (chapter 4).

5) Both HT-29 and M059K cells treated with CPT spend longer in mitosis by comparison to cisplatin treated cells. This indicates there is a difference in the timing of checkpoint adaptation when cells are treated with two different genotoxic agents (chapter 4).

REFERENCES

Abe, S., Nagasaka, K., Hirayama, Y., Kozuka-Hata, H., Oyama, M., Aoyagi, Y., Obuse, C. and Hirota, T. (2011) The initiation phase of chromosome condensation requires Cdk1-mediated phosphorylation of the CAP-D3 subunit of condensing II. *Genes and Development* **25**, 863-847

Adler, I.D. and el-Tarras, A. (1989) Clastogenic effects of cis-diamminedichloroplatinum. I. Induction of chromosomal aberrations in somatic and germinal cells of mice. *Mutation Research* **211**, 131-137

Alderden, R.A., Hall, M.D. and Hambley, T.W. (2006) Products of chemistry the discovery and development of cisplatin. *Journal of Chemical Education* **83**, 728-734

Allen, R.T., Hunter, W.J. and Agrawal, D.K. (1997) Morphological and biochemical characterization and analysis of apoptosis. *Journal of Pharmacological and Toxicological Methods* **37**, 215-228

Alnemri, E.S., Livingston, D.J., Nicholson, D.W., Salvesen, G., Thornberry, N.A., Wong, W.W. and Yuan, J. (1996) Human ICE/CED-3 protease nomenclature. *Cell* **87**, 171

Anderson, C.W and Allalunis-Turner, M.J. Human TP53 from the malignant glioma-derived cell lines M059J and M059K has a cancer-associated mutation in exon 8. *Radiation Research* **154**, 473-476

ATCC M059K CRL-2365 Data Sheet 1994 www.atcc.org/products/all/CRL-2365.aspx?slp=1#characteristics (Accessed June 1, 2015)

Baik, M.H., Friesner, R.A. and Lippard, S.J. (2003) Theoretical study of cisplatin binding to purine bases: why does cisplatin prefer guanine over adenine? *Journal of the American Chemical Society* **125**, 14082-14092

Balajee, A.S., Bertucci, A., Taveras, M. and Brenner, D.J. (2014) Multicolour FISH analysis of ionising radiation induced micronucleus formation in human lymphocytes. *Mutagenesis* **29**, 447-455

Bartek, J. and Lukas, J. (2007) DNA damage checkpoints: from initiation to recovery or adaptation. *Current Opinions in Cell Biology* **19**, 238-245

Baskar, R., Lee, K.A., Yeo, R. and Yeoh, K.W. (2012) Cancer and radiation therapy: current advances and future directions. *International Journal of Medical Sciences* **9**, 193-199

Bernier, J., Hall, E.J. and Giaccia, A. (2004) Radiation oncology: a century of achievements. *Nature Reviews Cancer* **4**, 737-747

Bertelsen, B., Nazaryan-Petersen, L., Sun, W., Mehrjouy, M.M., Xie, G., Chen, W., Hjermind, L.E., Taschner, P.E. and Tümer, Z. (2015) A germline chromothripsis event

stably segregating in 11 individuals through three generations. *Genetics in Medicine* doi: 10.1038/gim.2015.112

Bettayeb, K., Oumata, N., Echalier, A., Ferandin, Y., Endicott, J.A., Galons, H. and Meijer, L. (2008) CR8, a potent and selective, roscovitine-derived inhibitor of cyclin-dependent kinases. *Oncogene* **27**, 5797-5807

Bettayeb, K., Baunbaek, D., Delehouze, C., Loaëc, N., Hole, A.J., Baumli, S., Endicott, J.A., Douc-Rasy, S., Bénard, J., Oumata, N., Galons, H. and Meijer, L. (2010) CDK inhibitors roscovitine and CR8 trigger Mcl-1 down-regulation and apoptotic cell death in neuroblastoma cells. *Genes and Cancer* **1**, 369-380

Bishop, R. (2010) Applications of fluorescence in situ hybridization (FISH) in detecting genetic aberrations of medical significance. *Bioscience Horizons* **3**, 85-95

Bhattathiri, V.N., Bharathykkutty, C., Prathapan, R., Chirayathmajiyil, D.A. and Nair, K.M. (1998) Prediction of radiosensitivity of oral cancers by serial cytological assay of nuclear changes. *Radiotherapy Oncology* **49**, 61-65

Bhattathiri, V.N. (2001) Amitotic cell divisions and tumour growth: an alternative model for cell kinetic compartments in solid tumours. *Oral Oncology* **37**, 288-295

Borgne, A., Versteege, I., Mahe, M., Studeny, A., Leonce, S., N-aime, I., Rodriguez, M., Hickman, J.A., Meijer, L. and Golsteyn, R.M. (2006) Analysis of cyclin B1 and Cdk activity during apoptosis induced by camptothecin treatment. *Oncogene* **25**, 7361-7372

Bosl, G.J. and Motzer, R.J. (1997) Testicular germ-cell cancer. *The New England Journal of Medicine* **337**, 242-253

Brandes, A.A., Basso, U., Reni, M., Vastola, F., Tosoni, A., Cavallo, G., Scopece, L., Ferreri, A.J., Panucci, M.G., Monfardini, S. and Ermani, S. (2004) First-line chemotherapy with cisplatin plus fractionated temozolomide in recurrent glioblastoma multiforme: a phase II study of the Gruppod Italiano Cooperativo di Neuro-Oncologia. *Journal of Clinical Oncology* **22**, 1598-1604

Bredesen, D.E. (2008) Toward a mechanistic taxonomy for programmed cell death pathways. In Beyond Apoptosis: Cellular outcomes of Cancer Therapy (Roninson, I.B., Brown, J.M. and Bredesen, D.E. eds.), pp. 73-93, Informa healthcare USA, Inc., New York, USA

Broude, E.V., Loncarek, J.., Wada, I., Cole, K., Hanko, C., Roninson, I.B. and Swift, M. (2008) Mitotic catastrophe in cancer therapy. In Beyond Apoptosis: Cellular outcomes of Cancer Therapy (Roninson, I.B., Brown, J.M. and Bredesen, D.E. eds.), pp. 307-320, Informa healthcare USA, Inc., New York, USA

Brown, J.M. and Attardi, L.D. (2005) The role of apoptosis in cancer development and treatment response. *Nature Reviews Cancer* **5**, 231-37

Brown, J.M. and Wouters, B.G. (1999) Apoptosis, p53, and tumor cell sensitivity to anticancer agents. *Cancer Research* **59**, 1391-1399

Bruyère, C. and Meijer, L. (2013) Targeting cyclin-dependent kinases in anti-neoplastic therapy. *Current Opinion in Cell Biology* **25**, 772-779

Bucher, N. and Britten, C.D. (2008) G2 checkpoint abrogation and checkpoint kinase-1 targeting in the treatment of cancer. *British Journal of Cancer* **98**, 523-528

Bunz, F., Dutriaux, A., Lengauer, C., Waldman, T., Zhou, S., Brown, J.P., Sedivy, J.M., Kinzler, K.W. and Vogelstein, B. (1998) Requirement for p53 and p21 to sustain G2 arrest after DNA damage. *Science* **282**, 1497-1501

Burma, S., Chen, B.P., Murphy, M., Kurimasa, A. and Chen, D.J. (2001) ATM phosphorylates histone H2AX in response to DNA double-strand breaks. *The Journal of Biological Chemistry* **276**, 42462-42467

Burns, E.M., Christopoulou, L., Corish, P. and Tyler-Smith, C. (1999) Quantitative measurement of mammalian chromosome mitotic loss rates using the green fluorescent protein. *Journal of Cell Science* **112**, 2705-2714

Burrell, R.A., McClelland, S.E., Endesfelder, D., Groth, P., Weller, M.C., Shaikh, N., Domingo, E., Kanu, N., Dewhurst, S.M., Gronroos, E., Chew, S.K., Rowan, A.J., Schenk, A., Sheffer, M., Howell, M., Kschischo, M., Behrens, A., Helleday, T., Bartek, J., Tomlinson, I.P. and Swanton, C. (2013) Replication stress links structural and numerical cancer chromosomal instability. *Nature* **494**, 492-496

Cadart, C., Zlotek-Zlotkiewicz, E., Le Berre, M., Piel, M. and Matthews, H.K. (2014) Exploring the function of cell shape and size during mitosis. *Developmental Cell* **29**, 159-169

Cahuzac, N., Studeny, A., Marshall, K., Versteege, I., Wetenhall, K., Pfeiffer, B., Leonce, S., Hickman., J.A, Pierre, A. and Golsteyn, R.M. (2010) An unusual DNA binding compound, S23906, induces mitotic catastrophe in cultured human cells. *Cancer Letters* **289**,178-187

Campisi, J. (2008) Cellular senescence and its effects on carcinogenesis. In Beyond Apoptosis: Cellular outcomes of Cancer Therapy (Roninson, I.B., Brown, J.M. and Bredesen, D.E. eds.), pp. 175-194, Informa healthcare USA, Inc., New York, USA

Carballo, J.A., Pincheira, J. and de la Torre, C. (2006) The G2 checkpoint activated by DNA damage does not prevent genome instability in plant cells. *Biological Research* **39**, 331-340

Castedo, M., Perfettini, J.L., Roumier, T., Andreau, K., Medema, R. and Kroemer, G. (2004a) Cell death by mitotic catastrophe: a molecular definition. *Oncogene* **23**, 2825-2837

Castedo, M., Perfettini, J.L., Roumier, T., Valent, A., Raslova, H., Yakushijin, K., Horne, D., Feunteun, J., Lenoir, G., Medema, R., Vainchenker, W. and Kroemer, G. (2004b) Mitotic catastrophe constitutes a special case of apoptosis whose suppression entails aneuploidy. *Oncogene* **23**, 4362-4370

Chabner, B.A. and Roberts, T.G. (2005) Timeline: chemotherapy and the war on cancer. *Nature Reviews Cancer* **5**, 65-72

Chan, T.A., Hermeking, H., Lengauer, C., Kinzler, K.W. and Vogelstein, B. (1999) 14-3-3 sigma is required to prevent mitotic catastrophe after DNA damage. *Nature* **401**, 616-620

Chang, B.D., Broude, E.V., Dokmanovic, M., Zhu, H., Ruth, A., Xuan, Y., Kandel, E.S., Lausch, E., Christov, K. and Roninson, I.B. (1999) A senescence-like phenotype distinguishes tumor cells that undergo terminal proliferation arrest after exposure to anticancer agents. *Cancer Research* **59**, 3761-3767

Charlier, C., Kintz, P., Dubois, N. and Plomteux, G. (2004) Fatal overdosage with cisplatin. *Journal of Analytical Toxicology* **28**, 138-140

Chen, Z., Xiao, Z., Chen, J., Ng, S., Sowin, T., Sham, H., Rosenberg, S., Fesik, S. and Zhang, H. (2003) Human Chk1 expression is dispensable for somatic cell death and critical for sustaining G2 DNA damage checkpoint. *Molecular Cancer Therapeutics* **2**, 543-548

Chen, T., Stephens, P.A., Middleton, F.A. and Curtin, N.J. (2012) Targeting the S and G2 checkpoint to treat cancer. *Drug Discovery Today* **17**, 194-202

Chen, X., Xie, F., Zhu, X., Lin, F., Pan, S., Gong, L., Qiu, J.G., Zhang, W., Jiang, Q., Mei, X., Xue, Y., Qin, W., Shi, Z. and Yan, X. (2015) Cyclin-dependent kinase inhibitor dinaciclib potently synergizes with cisplatin in preclinical models of ovarian cancer. *Oncotarget* **6**, 14926-14939

Cheung-Ong, K., Giaever, G. and Nislow, C. (2013) DNA-damaging agents in cancer chemotherapy: serendipity and chemical biology. *Chemistry and Biology* **20**, 648-659

Chini, C.C. and Chen, J. (2003) Human claspin is required for replication checkpoint control. *The Journal of Biological Chemistry* **278**, 30057-30062

Choi, Y., Kim, H., Shim, W., Anwar, M.A., Kwon, J., Kwon, H., Kim, H.J., Jeong, H., Kim, H.M., Hwang, D., Kim, H.S. and Choi, S. (2015) Mechanism of cisplatin induced cytotoxicity is correlated to impaired metabolism due to mitochondrial ROS generation. *PLoS One* **10**, e0135083

Chowdhury, D., Keogh, M.C., Ishii, H., Peterson, C.L., Buratowski, S. and Lieberman, J. (2005) Gamma-H2AX dephosphorylation by protein phosphatase 2A facilitates DNA double-strand break repair. *Molecular Cell* **20**, 801-809

Clingen, P.H., Wu, J.Y., Miller, J., Mistry, N., Chin, F., Wynne, P., Prise, K.M. and Hartley, J.A. (2008) Histone H2AX phosphorylation as a molecular pharmacological marker for DNA interstrand crosslink cancer therapy. *Biochemical Pharmacology* **76**, 19-27

Cohen, A., Sato, M., Aldape, K., Mason, C.C., Alfaro-Munoz, K., Heathcock, L., South, S.T., Abegglen, L.M., Schiffman, J.D. and Colman, H. (2015) DNA copy number analysis of grade II-III and grade IV gliomas reveals differences in molecular ontogeny including chromothripsis associated with IDH mutation status. *Acta Neuropathologica Communications* **3**, e34

Coley, H.M., Shotton, C.F., Kokkinos, M.I. and Thomas, H. (2007) The effects of the CDK inhibitor seliciclib alone or in combination with cisplatin in human uterine sarcoma cell lines. *Gynecologic Oncology* **105**, 462-469

Crasta, K., Ganem, N.J., Dagher, R., Lantermann, A.B., Ivanova, E.V., Pan, Y., Nezi, L., Protopopov, A., Chowdhury, D. and Pellman, D. (2012) DNA breaks and chromosome pulverization from errors in mitosis. *Nature* **482**, 53-58

Dabholkar, M., Vionnet, J., Bostick-Bruton, F., Yu, J.J. and Reed, E. (1994) Messenger RNA levels of XPA and ERCC1 in ovarian cancer tissue correlate with response to platinum-based chemotherapy. *Journal of Clinical Investigation* **94**, 703-708

Danial, N.N. and Korsmeyer, S.J. (2004) Cell death: critical control points. *Cell* **116**, 205-209

de Bruin, E.C. and Medema, J.P. (2008) Apoptosis and non-apoptotic deaths in cancer development and treatment response. *Cancer Treatment Reviews* **34**, 737-49

de Cárcer, G., de Castro, I.P. and Malumbres, M. (2007) Targeting cell cycle kinases for cancer therapy. *Current Medicinal Chemistry* **14**, 969-985

de Feraudy, S., Revet, I., Bezrookove, V., Feeney, L. and Cleaver, J.E. (2010) A minority of foci or pan-nuclear apoptotic staining of gammaH2AX in the S phase after UV damage contain DNA double-strand breaks. *Proceedings of the National Academy of Sciences of the United States of America* **107**, 6870-6875

Deibler, R.W. and Kirschner, M.W. (2010) Quantitative reconstitution of mitotic CDK1 activation in somatic cell extracts. *Molecular Cell* **37**, 753-767

Del Monte, U. (2009) Does the cell number 10(9) still really fit one gram of tumour tissue? *Cell Cycle* **8**, 505-506

Delacroix, S., Wagner, J.M., Kobayashi, M., Yamamoto, K. and Karnitz, L.M. (2007) The Rad9-Hus1-Rad1 (9-1-1) clamp activates checkpoint signalling via TOPBP1. *Genes and Development* **21**, 1472-1477

Demarcq, C., Bunch, R.T., Creswell, D. and Eastman, A. (1994) The role of cell cycle progression in cisplatin-induced apoptosis in Chinese hamster ovary cells. *Cell Growth and Differentiation* **5**, 983-993

Deng, C., Zhang, P., Harper, J.W., Elledge, S.J. and Leder, P. (1995) Mice lacking p21 CIP1/WAF1 undergo normal development, but are defective in G1 checkpoint control. *Cell* **82**, 675-684

Dewey, W.C., Ling, C.C. and Meyn, R.E. (1995) Radiation-induced apoptosis: relevance to radiotherapy. *International Journal of Radiation Oncology* **33**, 781-796

Dimri, G.P., Lee, X., Basile, G., Acosta, M., Scott, G., Roskelley, C., Medrano, E.E., Linksens, M., Rubelj, I. and Pereira-Smith, O. (1995) A biomarker that identifies senescent human cells in culture and in aging skin in vivo. *Proceedings of the National Academy of Sciences of the United States of America* **92**, 9363-9367

Domingo-Sananes, M.R., Kapuy, O., Hunt, T. and Novak, B. (2011) Switches and latches: a biochemical tug-of-war between kinases and phosphatases that control mitosis. *Philosophical Transactions of the Royal Society B: Biological Sciences* **366**, 3584-3594

Eapen, V.V., Sugawara, N., Tsabar, M., Wu, W.H. and Haber, J.E. (2012) The Saccharomyces cerevisiae chromatin remodeler Fun30 regulates DNA end resection and checkpoint deactivation. *Molecular and Cellular Biology* **32**, 4727-4740

Eastman, A. (1987) The formation, isolation and characterization of DNA adducts produced by anticancer platinum complexes. *Pharmacology and Therapeutics* **34**, 155-166

Eastman, A. (2006) The mechanism of action of cisplatin: from adducts to apoptosis. In Cisplatin: chemistry and biochemistry of a leading anticancer drug (Lippert, B. ed), pp. 111-134, Verlag Helvetica Chimica Acta., Zürich, Switzerland

Edelweiss, M.I., Trachtenberg, A., Pinheiro, E.X., da-Silva, J., Riegel, M., Lizardo-Daudt, H.M. and Mattevi, M.S. (1995) Clastogenic effect of cisplatin on Wistar rat bone marrow cells. *Brazilian Journal of Medical and Biological Research* **28**, 679-683

Egger, L. (2008) Caspase-independent apoptotic cell death. In Beyond Apoptosis: Cellular outcomes of Cancer Therapy (Roninson, I.B., Brown, J.M. and Bredesen, D.E. eds.), pp. 93-108, Informa healthcare USA, Inc., New York, USA

Elliott, M.J., Stininskiene, L and Lock, R.B. (1998) Expression of Bcl-2 in human epithelial tumor (HeLa) cells enhances clonogenic survival following exposure to 5-

fluoro-2′deoxyuridine or staurosporine, but not following exposure to etoposide or doxorubicin. *Cancer Chemotherapy and Pharmacology* **41**, 457-463

Elliott, M.J., Murphy, K.M., Stibinskiene, L., Ranganathan, V., Sturges, E., Farnsworth, M.L. and Lock, R.B. (1999) Bcl-2 inhibits early apoptotic events and reveals post-mitotic multinucleation without affecting cell cycle arrest in human epithelial tumor cells exposed to etoposide. *Cancer Chemotherapy and Pharmacology* **44**, 1-11

Eom, Y.W., Kim, M.A., Park, S.S., Goo, M.J., Kwon, H.J., Sohn, S., Kim, W.H., Yoon, G. and Choi, K.S. (2005) Two distinct modes of cell death induced by doxorubicin: apoptosis and cell death through mitotic catastrophe accompanied by senescence-like phenotype. *Oncogene* **24**, 4765-4777

Fadok, V.A., Voelker, D.R., Campbell, P.A., Cohen, J.J., Bratton, D.L. and Henson, P.M. (1992) Exposure of phosphatidylserine on the surface of apoptotic lymphocytes triggers specific recognition and removal by macrophages. *Journal of Immunology* **148**, 2207-2216

Falck, J., Mailand, N., Syljuåsen, R.G., Bartek, J. and Lukas, J. (2001) The ATM-Chk2-Cdc25A checkpoint pathway guards against radioresistant DNA synthesis. *Nature* **410**, 842-847

Fan, T.J., Han, L.H., Cong, R.S. and Liang, J. (2005) Caspase family proteases and apoptosis. *Acta Biochimica et Biophysica Sinica* **37**, 719-727

Fenech, M., Kirsch-Volders, M., Natarajan, A.T., Surralles, J., Crott, J.W., Parry, J., Norppa, H., Eastmond, D.A., Tucker, J.D. and Thomas, P. (2011) Molecular mechanisms of micronucleus, nucleoplasmic bridge and nuclear bud formation in mammalian and human cells. *Mutagenesis* **26**, 125-132

Feoktistova, M. and Leverkus, M. (2015) Programmed necrosis and necroptosis signalling. *FEBS Journal* **282**, 19-31

Ferguson, D.O. and Alt, F.W. (2001) DNA double strand break repair and chromosomal translocation: lessons from animal models. *Oncogene* **20**, 5572-5579

Ferguson, A.M., White, L.S., Donovan, P.J. and Piwnica-Worms, H. (2005) Normal cell cycle and checkpoint responses in mice and cells lacking Cdc25B and Cdc25C protein phosphatases. *Molecular and Cellular Biology* **25**, 2853-2860

Fichtinger-Schepman, A.M., van der Veer, J.L., den Hartog, J.H., Lohman, P.H. and Reedijk, J. (1985) Adducts of the antitumor drug cis-diamminedichloroplatinum(II) with DNA: formation, identification and quantification. *Biochemistry* **24**, 707-713

Florea, A. and Büsselberg, D. (2011) Cisplatin as an anti-tumor drug: cellular mechanisms of activity, drug resistance and induced side effects. *Cancers* **3**, 1351-1371

Flynn, R.L. and Zou, L. (2011) ATR: a master conductor of cellular responses to DNA replication stress. *Trends in Biochemical Sciences* **36**, 133-140

Ford, J.H., Schultz, C.J. and Correll, A.T. (1988) Chromosome elimination in micronuclei: a common cause of hypoploidy. *American Journal of Human Genetics* **43**, 733-740

Frankenberg-Schwager, M., Kirchermeier, D., Greif, G., Baer, K., Becker, M. and Frankenberg, D. (2005) Cisplatin-mediated DNA double-strand breaks in replicating but not in quiescent cells of the yeast Saccharomyces cerevisiae. *Toxicology* **212**, 175-184

Forment, J.V., Kaidi, A. and Jackson, S.P. (2012) Chromothripsis and cancer: causes and consequences of chromosome shattering. *Nature Reviews Cancer* **12**, 663-670

Fourest-Lieuvin, A., Peris, L., Gache, V., Garcia-Saez, I., Juillan-Binard, C., Lantez, V. and Job, D. (2006) Microtubule regulation in mitosis: tubulin phosphorylation by the cyclin-dependent kinase Cdk1. *Molecular Biology of the Cell* **17**, 1041-1050

Froelich-Ammon, S.J. and Osheroff, N. (1995) Topoisomerase poisons: harnessing the dark side of enzyme mechanism. *The Journal of Biological Chemistry* **270**, 21429-21432

Fuertes, M.A., Castilla, J., Alonso, C. and Pérez, J.M. (2003) Cisplatin biochemical mechanism of action: from cytotoxicity to induction of cell death through interconnections between apoptotic and necrotic pathways. *Current Medicinal Chemistry* **10**, 257-266

Furuta, T., Takemura, H., Liao, Z.Y., Aune, G.J., Redon, C., Sedelnikova, O.A., Pilch, D.R., Rogakou, E.P., Celeste, A., Chen, H.T., Nussenzweig, A., Aladjem, M.I., Bonner, W.M. and Pommier, Y. (2003) Phosphorylation of histone H2AX and activation of Mre11, Rad50, and Nbs1 in response to replication-dependent DNA double-strand breaks induced by mammalian DNA topoisomerase I cleavage complexes. *The Journal of Biological Chemistry* **278**, 20303-20312

Galgoczy, D.J. and Toczyski, D.P. (2001) Checkpoint adaptation precedes spontaneous and damage-induced genomic instability in yeast. *Molecular and Cellular Biology* **21**, 1710-1718

Galluzzi, L., Vitale, I., Abrams, J.M., Alnemri, E.S., Baehrecke, E.H., Blagosklonny, M.V., Dawson, T.M., Dawson, V.L., El-Deiry, W.S., Fulda, S., Gottlieb, E., Green, D.R., Hengartner, M.O., Kepp, O., Knight, R.A., Kumar, S., Lipton, S.A., Lu, X., Madeo, F., Malorni, W., Mehlen, P., Nuñez, G., Peter, M.E., Piacentini, M., Rubinsztein, D.C., Shi, Y., Simon, H.U., Vandenabeele, P., White, E., Yuan, J., Zhivostovsky, B., Melino, G. and Kroemer, G. (2012) *Cell Death and Differentiation* **19**, 107-120

Gamba, B.F., Richieri-Costa, A., Costa, S., Rosenberg, C. and Ribeiro-Bicudo, L.A. (2015) Chromothripsis with at least 12 breaks at 1p36.33-p35.3 in a boy with multiple congenital abnormalities. *Molecular Genetics and Genomics* doi: 10.1007/s00438-015-1072-0

Gascoigne, K.E. and Taylor, S.S. (2008) Cancer cells display profound intra- and inter-line variation following prolonged exposure to antimitotic drugs. *Cancer Cell* **14**, 111-122

Gately, D.P. and Howell, S.B. (1993) Cellular accumulation of the anticancer agent cisplatin: a review. *British Journal of Cancer* **67**, 1171-1176

Ghospurkar, P.L., Wilson, T.M., Severson, A.L., Klein, S.J., Khaku, S.K., Walther, A.P. and Haring, S.J. (2015) The DNA damage response and checkpoint adaptation in Saccharomyces cerevisiae: distinct roles for the replication protein A2 (Rfa2) N-terminus. *Genetics* **199**, 711-727

Giaccone, G. and Pinedo, H.M. (1996) Drug resistance. *The Oncologist* **1**, 82-87

Giacinti, C. and Giodarno, A. (2006) RB and cell cycle progression. *Oncogene* **25**, 5220-5227

Golstein, P. and Kroemer, G. (2007) Cell death by necrosis: towards a molecular definition. *Trends in Biochemical Sciences* **32**, 37-43

Graves, P.R., Lovly, C.M., Uy, G.L. and Piwnica-Worms, H. (2001) Localization of human Cdc25C is regulated both by nuclear export and 14-3-3 protein binding. *Oncogene* **20**, 1839-1851

Guilleman, G., Ma, E., Mauger, S., Miron, S., Thai, R., Guerois, R., Ochsenbein, F. and Marsolier-Kergoat, M.C. (2007) Mechanisms of checkpoint kinase Rad53 inactivation after a double-strand break in Saccharomyces cerevisiae. *Molecular and Cellular Biology* **27**, 3378-3389

Haese, G.J., Walworth, N., A.M. Carr. and Gould, K.L. (1995) The Wee1 protein kinase regulates T14 phosphorylation of fission yeast Cdc2. *Molecular Biology of the Cell* **6**, 371-385

Hall, E.J. and Giaccia, A.J. (2012) Radiobiology for the radiologist. 7th ed. Lippincott Williams and Wilkins

Hanahan, D. and Weinberg, R.A. (2000) The hallmarks of cancer. *Cell* **100**, 57-70

Hanahan, D. and Weinberg, R.A. (2011) Hallmarks of cancer: the next generation. *Cell* **144**, 646-674

Hartwell, L.H. and Weinert, T.A. (1989) Checkpoints: controls that ensure the order of cell cycle events. *Science* **246**, 629-634

Havelka, A.M., Berndtsson, M., Olofsson, M.H., Shoshan, M.C. and Linder, S. (2007) Mechanisms of action of DNA-damaging anticancer drugs in treatment of carcinomas: is acute apoptosis an "off-target" effect? *Mini Reviews in Medicinal Chemistry* **7**, 1035-1039

Hayashi, M.T. and Karlseder, J. (2013) DNA damage associated with mitosis and cytokinesis failure. *Oncogene* **32**, 4593-4601

Hayflick, L. and Moorhead, P.S. (1961) The serial cultivation of human diploid cell strains. *Experimental Cell Research* **25**, 585-621

Helleday, T., Lo, J., van Gent, D.C. and Engelward, B.P. (2007) DNA-double strand break repair: from mechanistic understanding to cancer treatment. *DNA Repair* **6**, 923-935

Helleday, T., Petermann, E., Lundin, C., Hodgson, B. and Sharma, R.A. (2008) DNA repair pathways as targets for cancer therapy. *Nature Reviews Cancer* **8**, 193-204

Hendzel, M.J., Wei, Y., Mancini, M.A., Hooser, A.V., Ranalli, T., Brinkley, B.R., Bazett-Jones, D.P. and Allis, C.D. (1997) Mitosis-specific phosphorylation of histone H3 initiates primarily within pericentromeric heterochromatin during G2 and spreads in an ordered fashion coincident with mitotic chromosome condensation. *Chromosoma* **106**, 348-360

Heng, Y. and Koh, C. (2010) Actin cytoskeleton dynamics and the cell division cycle. *The International Journal of Biochemistry and Cell Biology* **42**, 1622-1633

Holland, A.J. and Cleveland, D.W. (2009) Boveri revisited: chromosomal instability, aneuploidy and tumorigenesis. *Nature Reviews Molecular Cell Biology* **10**, 478-487

Howell, M., Kschischo, M., Behrens, A., Helleday, T., Bartek, J., Tomlinson, I.P. and Swanton, C. (2013) Replication stress links structural and numerical cancer chromosomal instability. *Nature* **494**, 492-496

Hsiang, Y.H., Hertzberg, R., Hecht, S. and Liu, L.F. (1985) Camptothecin induces protein-linked DNA breaks via mammalian DNA topoisomerase I. *The Journal of Biological Chemistry* **260**, 14873-14878

Hsiang, Y.H., Lihou, M.G. and Liu, L.F. (1989) Arrest of replication forks by drug-stabilized topoisomerase I-DNA cleavable complexes as a mechanism of cell killing by camptothecin. *Cancer Research* **49**, 5077-5082

Hu, F., Wang, Y., Liu, D., Li, Y., Qin, J. and Elledge, S.J. (2001) Regulation of the Bub2/Bfa1 GAP complex by Cdc5 and cell cycle checkpoints. *Cell* **107**, 655-665

Huang, X., Okafuji, M., Traganos, F., Luther, E., Holden, E. and Darzynkiewicz, Z. (2004) Assessment of histone H2AX phosphorylation induced by DNA topoisomerase I and II inhibitors topotecan and mitoxantrone and by the DNA-crosslinking agent cisplatin. *Cytometry Part A* **58**, 99-110

Huang, Y., Jiang, L., Yi, Q., Lv, L., Wang, Z., Zhao, X., Zhong, L., Jiang, H., Rasool, S., Hao, Q., Guo, Z., Cooke, H.J., Fenech, M. and Shi, Q. (2012) Lagging chromosomes entrapped in micronuclei are not "lost" by cells. *Cell Research* **22**, 932-935

Hurley, L.H. (2002) DNA and its associated processes as targets for cancer therapy. *Nature Reviews Cancer* **2**, 188-200

Ianzini, F. and Mackey, M.A. (1997) Spontaneous premature chromosome condensation and mitotic catastrophe following irradiation of HeLa S3 cells. *International Journal of Radiation Biology* **72**, 409-421

Ichijima, Y., Yoshioka, K., Yoshioka, Y., Shinohe, K., Fujimore, H., Unno, J., Takagi, M., Goto, H., Inagaki, M., Mizutani, S. and Teraoka, H. (2010) DNA lesions induced by replication stress trigger mitotic aberration and tetraploidy development. *PLoS One* **5**, e8821

Imataka, G. and Arisaka, O. (2012) Chromosome analysis using spectral karyotyping (SKY). *Cell Biochemistry and Biophysics* **62**, 13-17

Ishida, S., Lee, J., Thiele, D.J. and Herskowitz, I. (2002) Uptake of the anticancer drug cisplatin mediated by the copper transporter Ctr1 in yeast and mammals. *Proceedings of the National Academy of Sciences of the United States of America* **99**, 14298-14302

Jackson, S.P. and Bartek, J. (2009) The DNA-damage response in human biology and disease. *Nature* **461**, 1071-1078

Jain, M.V., Paczulla, A.M., Klonisch, T., Dimgba, F.N., Rao, S.B., Roberg, K., Schweizer, F., Lengerke, C., Davoodpor, P., Palicharla, V.R., Maddika, S. and Los. M. (2013) Interconnections between apoptotic, autophagic and necrotic pathways: implications for cancer therapy development. *Journal of Cellular and Molecular Medicine* **17**, 12-29

Jamieson, E.R. and Lippard, S.J. (1999) Structure, recognition and processing of cisplatin-DNA adducts. *Chemical Reviews* **99**, 2467-2498

Jeggo, P. and Löbrich, M. (2006) Contribution of DNA repair and cell cycle checkpoint arrest to the maintenance of genomic stability. *DNA Repair* **5**, 1192-1198

Jin, J., Ang, X.L., Ye, X., Livingstone, M. and Harper, J.W. (2008) Differential roles for checkpoint kinases in DNA damage-dependent degradation of the Cdc25A protein phosphatase. *The Journal of Biological Chemistry* **283**, 19322-19328

Johnson, N. and Shapiro, G.I. (2010) Cyclin-dependent kinases (Cdks) and the DNA damage response: rationale for cdk inhibitor-chemotherapy combinations as an anticancer strategy for solid tumors. *Expert Opinion on Therapeutic Targets* **14**, 1199-1212

Jonathan, E.C., Bernhard, E.J. and McKenna, W.G. (1999) How does radiation kill cells? *Current Opinion in Chemical Biology* **3**, 77-83

Jordan, M.A., Thrower, D. and Wilson, L. (1991) Mechanism of inhibition of cell proliferation by vinca alkaloids. *Cancer Research* **51**, 2212-2222

Kandoth, C., McLellan, M.D., Vandin, F., Ye, K., Niu, B., Lu, C., Xie, M., Zhang, Q., McMichael, J.F., Wyczalkowski, M.A., Leiserson, M.D., Miller, C.A., Welch, J.S., Walter, M.J, Wendl, M.C., Ley, T.J., Wilson, R.K., Raphael, B.J. and Ding, L. (2013) Mutational landscape and significance across 12 major cancer types. *Nature* **502**, 333-339

Kappas, N.C., Savage, P., Chen, K.C., Walls, A.T. and Sible, J.C. (2000) Dissection of the XChk1 signaling pathway in Xenopus laevis embryos. *Molecular Biology of the Cell* **11**, 3101-3108

Karasawa, T., Sibrian-Vazquez, M.., Strongin, R.M. and Steyger, P.S. (2013) Identification of cisplatin-binding proteins using agarose conjugates of platinum compounds. *PLoS One* **8**, e66220

Karimi-Busheri, F., Rasouli-Nia, A., Allaunis-Turner, J. and Weinfeld, M. (2007) Human polynucleotide kinase participates in repair of DNA double-strand breaks by nonhomologous end joining but not homolgous recombination. *Cancer Research* **67**, 6619-6625

Karlsson, C., Katich, S., Hagting, A., Hoffman, I. and Pines, J. (1999) Cdc25B and Cdc25C differ markedly in their properties as initiators of mitosis. *Journal of Cell Biology* **146**, 573-583

Kastan, M.B. and Bartek, J. (2004) Cell-cycle checkpoints and cancer. *Nature* **432**, 316-323

Kauffman, G.B., Pentimalli, R., Doldi, S. and Hall, M.D. (2010) Michele Peyrone (1813-1883), discoverer of cisplatin. *Platinum Metals Review* **54**, 250-256

Kawai, K., Viars, C., Arden, K., Tarin, D., Urquidi, V. and Goodison, S. (2002) Comprehensive karyotyping of the HT-29 colon adenocarcinoma cell line. *Genes, Chromosomes and Cancer* **34**, 1-18

Kelland, L. (2007) The resurgence of platinum-based cancer chemotherapy. *Nature Reviews Cancer* **7**, 573-584

Kerr, J.F.R., Wyllie, A.H. and Currie, A.H. (1972) Apoptosis: a basic bioloical phenomenon with wide-ranging implications in tissue kinetics. *British Journal of Cancer* **26**, 239-257

Kerr, J.F.R. (2008) A Personal history of the development of the apoptosis concept. In Beyond Apoptosis: Cellular outcomes of Cancer Therapy (Roninson, I.B., Brown, J.M. and Bredesen, D.E. eds.), pp. 1-13, Informa healthcare USA, Inc., New York, USA

Khanna, A. (2015) DNA damage in cancer therapeutics: a boon or a curse? *Cancer Research* **75**, 2133-2138

Khosravi, R., Maya, R., Gottlieb, T., Oren, M., Shiloh, Y. and Shkedy, D. (1999) Rapid ATM dependent phosphorylation of MDM2 precedes p53 accumulation in response to DNA damage. *Proceedings of the National Academy of Sciences of the United States of America* **96**, 14973-14977

Kirsch-Volders, M., Plas, G., Elhajouji, A., Lukamowicz, M., Gonzalez, L., Vander Loock, K. and Decordier, I. (2011) The in vitro MN assay in 2011: origin and fate, biological significance, protocols, high throughput methodologies and toxicolgical relevance. *Archives of Toxicology* **85**, 873-899

Kloosterman, W.P., Guryev, V., van Roosmalen, M., Duran, K.J., de Bruijn, E., Bakker, S.C., Letteboer, T., van Nesselrooij, B., Hochstenbach, R., Poot, M. and Cuppen, E. (2011) Chromothripsis as a mechanism driving complex de novo structural rearrangements in the germline. *Human Molecular Genetics* **20**, 1916-1924

Köberle, B., Masters, J.R., Hartley, J.A. and Wood, R.D. (1999) Defective repair of cisplatin-induced DNA damage caused by reduced XPA protein in testicular germ cell tumours. *Current Biology* **9**, 273-276

Kroemer, G., Galluzzi, L., Vandenabeele, P., Abrams, J., Alnemri, E.S., Baehrecke, E.H., Blagosklonny, M.V., El-Deiry, W.S., Golstein, P., Green, D.R., Hengartner, M., Knight, R.A., Kumar, S., Lipton, S.A., Malomi, W., Nuñez, G., Peter, M.E., Tschopp, J., Yuan, J., Piacentini, M., Zhivotovsky, B. and Melino, G. (2009) Classification of cell death: recommendations of the nomenclature committee on cell death 2009. *Cell Death and Differentiation* **16**, 3-11

Krishnaswamy, G. and Dewey, W.C. (1993) Cisplatin induced cell killing and chromosomal aberratons in CHO cells: treated during G1 or S phase. *Mutation Research/DNA Repair* **293**, 161-172

Krysko, D.V., Vanden Berghe, T., D'Herde, K. and Vandenabeele, P. (2008) Apoptosis and necrosis: detection, discrimination and phagocytosis. *Methods* **44**, 205-221

Kubara, P.M., Kernéis-Golsteyn, S., Studeny, A., Lanser, B.B., Meijer, L. and Golsteyn, R.M. (2012) Human cells enter mitosis with damaged DNA after treatment with pharmacological concentrations of genotoxic agents. *Biochemical Journal* **446**, 373-381

Kumagai, A., Lee, J., Yoo, H.Y. and Dunphy, W.G. (2006) TopBP1 activates the ATR-ATRIP complex. *Cell* **124**, 943-955

Kumari, R., Chaugule, A. and Goyal, P.K. (2005) Karyoanomalic frequency during radiation therapy. *Journal of Cancer Research and Therapeutics* **1**, 187-190

Kuzminov, A. (2001) Single-strand interruptions in replicating chromosomes cause double-strand breaks. *Proceedings of the National Academy of Sciences of the United States of America* **98**, 8241-8246

Kwon, Y., Lee, S.Y., Choi, Y., Greengard, P. and Nairn, A.C. (1997) Cell cycle-dependent phosphorylation of mammalian protein phosphatase 1 by cdc2 kinase. *Proceedings of the National Academy of Sciences of the United States of America* **94**, 2168-2173

Kyprianou, N., King, E.D., Bradbury, D. and Rhee, J.G. (1997) Bcl-2 over-expression delays radiation-induced apoptosis without affecting the clonogenic survival of human prostate cancer cells. *International Journal of Cancer* **70**, 341-348

Larochelle, S., Merrick, K.A., Terret, M.E., Wohlbold, L., Barboza, N.M., Zhang, C., Shokat, K.M., Jallepalli, P.V. and Fisher, R.P. (2007) Requirements for Cdk7 in the assembly of Cdk1/cyclin B and activation of Cdk2 revealed by chemical genetics in human cells. *Molecular Cell* **25**, 839-850

Lee, M.G. and Nurse, P. (1987) Complementation used to clone a human homologue of the fission yeast cell cycle control gene cdc2. *Nature* **327**, 31-35

Lee, J., Kumagai, A. and Dunphy, W.G. (2001) Positive regulation of Wee1 by Chk1 and 14-3-3 proteins. *Molecular Biology of the Cell* **12**, 551-563

Lengauer, C., Kinzler, K.W. and Vogelstein, B. (1998) Genetic instabilities in human cancers. *Nature* **396**, 643-649

Leroy, C., Lee, S.E., Vaze, M.B., Ochsenbein, F., Guerois, R., Haber, J.E. and Marsolier-Kergoat, M.C. (2003) PP2C phosphatases Ptc2 and Ptc3 are required for DNA checkpoint inactivation after a double-strand break. *Molecular Cell* **11**, 827-835

Leung, M.L., Wang, Y., Waters, J. and Navin, N.E. (2015) SNES: single nucleus exome sequencing. *Genome Biology* **16**, 55

Lewis, C.W., Taylor, R.G., Kubara, P.M., Marshall, K., Meijer, L. and Golsteyn, R.M. (2013) A western blot assay to measure cyclin dependent kinase activity in cells or in vitro without the use of radioisotopes. *FEBS Letters* **587**, 3089-3095

Lewis, C.W. (2014) Testing the relationship between checkpoint adaptation and micronuclei in human fibroblastic glioma and normal lung cells. University of Lethbridge, AB, Canada. MSc Thesis.

Leyland-Jones, B., Kelland, L.R., Harrap, K.R. and Hiorns, L.R. (1999) Genomic imbalances associated with acquired resistane to platinum analogues. *The American Journal of Pathology* **155**, 77-84

Li, L.Y., Luo, X. and Wang, X. (2001) Endonuclease G is an apoptotic DNase when released from mitochondria. *Nature* **412**, 95-99

Li, X. and Heyer, W. (2008) Homologous recombination in DNA repair and DNA damage tolerance. *Cell Research* **18**, 99-113

Liang, H., Esposito, A., De, S., Ber, S., Collin, P., Surana, U. and Venkitaraman, A.R. (2014) Homeostatic control of polo-like kinase-1 engenders non-genetic heterogeneity in G2 checkpoint fidelity and timing. *Nature Communications* **5**, 4048

Limoli, C.L., Giedzinski, E., Bonner, W.M. and Cleaver, J.E. (2002) UV-induced replication arrest in the xeroderma pigmentosum variant leads to the DNA double-strand breaks, gamma-H2AX formation and Mre11 relocalization. *Proceedings of the National Academy of Sciences of the United States of America* **99**, 233-238

Liu, Q., Guntuku, S., Cui, X.S., Matsuoka, S., Cortez, D., Tamai,K., Luo, G., Carattini-Rivera, S., DeMayo, F., Bradley, A., Donehower, L.A. and Elledge, S.J. (2000) Chk1 is an essential kinase that is regulated by ATR and required for the G2/M DNA damage checkpoint. *Genes and Development* **14**, 1448-1459

Löbrich, M., Shibata, A., Beucher, A., Fisher, A., Ensminger, M., Goodarzi, A.A., Barton, O. and Jeggo, P.A. (2010) γH2AX foci analysis for monitoring DNA double-strand break repair: strengths, limitations and optimization. *Cell Cycle* **9**, 662-669

Lock, R.B. and Stribinskeine, L. (1996) Dual modes of death induced by etoposide in human epithelial tumor cells allow Bcl-2 to inhibit apoptosis without affecting clonogenic survival. *Cancer Research* **56**, 4006-4012

Lockshin, R.A. and Zakeri, Z. (2008) Historical studies of various forms of cell death. In Beyond Apoptosis: Cellular outcomes of Cancer Therapy (Roninson, I.B., Brown, J.M. and Bredesen, D.E. eds.), pp. 55-72, Informa healthcare USA, Inc., New York, USA

Lopez-Girona, A., Furnari, B., Mondesert, O. and Russell, P. (1999) Nuclear localization of Cdc25 is regulated by DNA damage and a 14-3-3 protein. *Nature* **397**, 172-175

Lopez, M.F., Tollervey, J., Krastins, B., Garces, A., Sarracino, D., Prakash, A., Vogelsang, M., Geesman, G., Valderrama, A., Jordan, I.K. and Lunyak, V.V. (2012) Depletion of nuclear histone H2A variants is associated with chronic DNA damage signaling upon drug-evoked senescence of human somatic cells. *Aging* **4**, 823-842

Lukas, J., Lukas, C. and Bartek, J. (2004) Mammalian cell cycle checkpoints: signaling pathways and their organization in space and time. *DNA Repair* **3**, 997-1007

Lupardus, P.J. and Cimprich, K.A. (2004) Checkpoint adaptation: molecular mechanisms uncovered. *Cell* **117**, 555-556

Magrangeas, F., Avet-Loiseau, H., Munshi, N.C. and Minvielle, S. (2011) Chromothripsis identifies a rare and aggressive entity among newly diagnosed multiple myeloma patients. *Blood* **118**, 675-678

Mailand, N., Falck, J., Lukas, C., Syljuåsen, R.G., Welcker, M., Bartek, J. and Lukas, J. (2000) Rapid destruction of human Cdc25A in response to DNA damage. *Science* **288**, 1425-1429

Mah, L.J., El-Osta, A. and Karagiannis, T.C. (2010) γH2AX: a sensitive molecular marker of DNA damage and repair. *Leukemia* **24**, 679-686

Majno, G., La Gattuta, M. and Thompson, T.E. (1960) Cellular death and necrosis: chemical, physical and morphologic changes in rat liver. *Virchows Archiv: The European Journal of Pathology* **333**, 421-465

Malumbres, M. and Barbacid, M. (2005) Mammalian cyclin-dependent kinases. *Trends in Biochemical Sciences* **30**, 630-641

Malumbres, M. (2014) Cyclin-dependent kinases. *Genome Biology* **15**, 122

Mani, R. and Chinnaiyan, A.M. (2010) Triggers for genomic rearrangements: insights into genomic, cellular and environmental influences. *Nature Reviews Genetics* **11**, 819-829

Manning, A.L., Benes, C. and Dyson, N.J. (2013) Whole chromosome instability resulting from the synergistic effects of pRB and p53 inactivation. *Oncogene* **33**, 2487-2494

Margalit, A., Vlcek, S., Gruenbaum, Y. and Foisner, R. (2005) Breaking and making of the nuclear envelope. *Journal of Cellular Biochemistry* **95**, 454-464

Marti, T.M., Hefner, E., Feeney, L., Natale, V. and Cleaver, J.E. (2006) H2AX phosphorylation within the G1 phase after UV irradiation depends on nucleotide excision repair and not DNA double-strand breaks. *Proceedings of the National Academy of Sciences of the United States of America* **27**, 9891-9896

Matsuoka, S., Ballif, B.A., Smogorzewska, A., McDonald, E.R., Hurov, K.E., Luo, J., Bakalarski, C.E., Zhao, Z., Solimini, N., Lerenthal, Y., Shiloh, Y., Gygi, S.P. and Elledge, S.J. (2007) ATM and ATR substrate analysis reveals extensive protein networks responsive to DNA damage. *Science* **316**, 1160-1166

Maya, R., Balass, M., Kim, S.T., Shkedy, D., Leal, J.M., Shifman, O., Moas, M., Buschmann, T., Ronai, Z., Shiloh, Y., Kastan, M.B., Katzir, E. and Oren, M. (2001) ATM-dependent phosphorylation of Mdm2 on serine 395: role in p53 activation by DNA damage. *Genes and Development* **15**, 1067-1077

Mayer, F., Stoop, H., Scheffer, G.L., Scheper, R., Oosterhuis, J.W., Looijenga, L.H. and Bokemeyer, C. (2003) Molecular determinants of treatment response in human germ cell tumors. *Clinical Cancer Research* **9**, 767-773

McKeague, A.L., Wilson, D.J. and Nelson, J. (2003) Staurosporine-induced apoptosis and hydrogen peroxide-induced necrosis in two human breast cell lines. *British Journal of Cancer* **88**, 125-131

Meijer, M., Karimi-Busheri, F., Huang, T.Y., Weinfeld, M. and Young, D. (2002) Pnk1, a DNA kinase/phosphatase required for normal response to DNA damage by gamma-

radiation or camptothecin in Schizosaccharomyces pombe. *The Journal of Biological Chemistry* **277**, 4050-4055

Mendoza, J., Martinez, J., Hernández, C., Pérez-Montiel, D., Castro, C., Fabián-Morales, E., Santibáñez, M., González-Barrios, D., Diaz-Chávez, J., Andonegui, M.A., Reynoso, N., Oñate, L.F., Jiménez, M.A., Núñez, M., Dyer, R. and Herrera, L.A. Association between ERCC1 and XPA expression and polymorphisms and the response to cisplatin in testicular germ cell tumours. *British Journal of Cancer* **109**, 68-75

Meyer, B., Voss, K.O., Tobias, F., Jakob, B.,Durante, M. and Taucher-Scholz, G. (2013) Clustered DNA damage induces pan-nuclear H2AX phosphorylation mediated by ATM and DNA-PK. *Nuclear Acids Research* **41**, 6109-6118

Mikhailov, A., Cole, R.W. and Rieder, C.L. (2002) DNA damage during mitosis in human cells delays the metaphase/anaphase transition via the spindle-assembly checkpoint. *Current Biology* **12**, 1797-1806

Millar, J.B. and Russell, P. (1992) The Cdc25 M-phase inducer: an unconventional protein phosphatase. *Cell* **68**, 407-410

Morgan. D.O. (2007) The Cell Cycle: Principles of Control 1st ed. New Science Press Ltd., London, UK

Musacchio, A. and Salmon, E.D. (2007) The spindle-assembly checkpoint in space and time. *Nature Reviews Molecular Cell Biology* **8**, 379-393

Nakada, S., Katsuki, Y., Imoto, I., Yokoyama, T., Nagasawa, M., Inazawa, J. and Mizutani, S. (2006) Early G2/M checkpoint failure as a molecular mechanism underlying etoposide-induced chromosomal aberrations. *Journal of Clinical Investigation* **116**, 80-89

Nazarov, I.B., Smirnova, A.N., Krutilina, R.I., Svetlova, M.P., Solovjeva, L.V., Nikiforov, A.A., Oei, S.L., Zalenskaya, I.A., Yau, P.M., Bradbury, E.M. and Tomilin, N.V. (2003) Dephosphorylation of histone gamma-H2AX during repair of DNA double-strand breaks in mammalian cells and its inhibition by calyculin A. *Radiation Research* **160**, 309-317

Negrini, S., Gorgoulis, V.G. and Halazonetis, T.D. (2010) Genomic instability- an evolving hallmark of cancer. *Nature Reviews Molecular Cell Biology* **11**, 220-228

Nessling, M., Kern, M.A., Schadendorf, D. and Lichter, P. (1999) Association of genomic imbalances with resistance to therapeutic drugs in human melanoma cell lines. *Cytogenetics and Cell Genetics* **87**, 286-290

Ngan, C.Y., Yamamoto, H., Takagi, A., Fujie, Y., Takemasa, I., Ikeda, M., Takahashi-Yanaga, F., Sasaguri, T., Sekimoto, M., Matsuura, N. and Monden, M. (2008) Oxaliplatin induces mitotic catastrophe and apoptosis in esophageal cancer cells. *Cancer Science* **99**, 129-39

Nicklas, R.B. (1997) How cells get the right chromosomes. *Science* **275**, 632-637

Nitta, M., Kobayashi, O., Honda, S., Hirota, T., Kuninaka, S., Marumoto, T., Ushio, Y. and Saya, H. (2004) Spindle checkpoint function is required for mitotic catastrophe induced by DNA-damaging agents. *Oncogene* **23**, 6548-6558

Nitiss, J. and Wang, J.C. (1988) DNA topoisomerase-targeting antitumor drugs can be studied in yeast. *Proceedings of the National Academy of Sciences of the United States of America* **85**, 7501-7505

Noel, E.E., Perry, J., Chaplin, T., Mao, X., Cazier, J.B., Joel, S.P., Oliver, R.T., Young, B.D. and Lu, Y.J. (2008) Identification of genomic changes associated with cisplatin resistance in testicular germ cell tumor cell lines. *Genes, Chromosomes and Cancer* **47**, 604-613

Oldfield, E.H., Dedrick, R.L., Yeager, R.L., Clark, W.C., DeVroom, H.L., Chatterji, D.C. and Doppman, J.L. (1985) Reduced systemic drug exposure by combining intra-arterial checmotherapy with hemoperfusion of regional venous drainage. *Journal of Neurosurgery* **63**, 726-732

Olive, P.L. and Banàth, J.P. (2009) Kinetics of H2AX phosphorylation after exposure to cisplatin. *Cytometry Part B-Clinical Cytometry* **76**, 79-90

Oliver, T.G., Mercer, K.L., Sayles, L.C., Burke, J.R., Mendus, D., Lovejoy, K.S., Cheng, M.H., Subramanian, A., Mu, D., Powers, S., Crowley, D., Bronson, R.T., Whittaker, C.A., Bhutkar, A., Lippard, S.J., Golub, T., Thomale, J., Jacks, T. and Sweet-Cordero, E.A. (2010) Chronic cisplatin treatment promotes enhanced damage repair and tumor progression in a mouse model of lung cancer. *Genes and Development* **24**, 837-852

On, K.F., Chen, Y., Ma, H.T., Chow, J.P. and Poon, R.Y. (2011) Determinants of mitotic catastrophe on abrogation of the G2 DNA damage checkpoint by UCN-01. *Molecular Cancer Therapeutics* **10**, 784-794

Orthwein, A., Fradet-Turcotte, A., Noordermeer, S.M., Canny, M.D., Brun, C.M., Strecker, J., Escribano-Diaz, C. and Durocher, D. (2014) Mitosis inhibits DNA double-strand break repair to guard against telomere fusions. *Science* **344**, 189-193

Österberg, L., Levan, K., Partheen, K., Staaf, J., Sundfelt, K. and Horvath, G. (2009) High-resolution genomic profiling of carboplatin resistance in early-stage epithelial ovarian carcinoma. *Cytogenetic and Genome Research* **125**, 8-18

Pan, Y., Ren, K.H., He, H.W. and Shao, R.G. (2009) Knockdown of Chk1 sensitizes human colon carcinoma HCT116 cells in a p53-dependent manner to lidamycin through abrogation of a G2/M checkpoint and induction of apoptosis. *Cancer Biology and Therapy* **8**, 37-41

Papamichos-Chronakis, M., Krebs, J.E. and Peterson, C.L. (2006) Interplay between Ino80 and Swr1 chromatin remodeling enymes regulates cell cycle checkpoint adaptation in response to DNA damage. *Genes and Development* **20**, 2437-2449

Pellicioli, A., Lee, S.E., Lucca, C., Foiani, M. and Haber, J.E. (2001) Regulation of Saccharomyces Rad53 checkpoint kinase during adaptation from DNA damage-induced G2/M arrest. *Molecular Cell* **7**, 293-300

Pikor, L., Thu, K., Vucic, E. and Lam, W. (2013) The detection and implication of genome instability in cancer. *Cancer and Metastasis Reviews* **32**, 341-352

Pines, J. and Hunter, T. (1989) Isolation of a human cyclin cDNA: evidence for cyclin mRNA and protein regulation in the cell cycle and for interaction with $p34^{cdc2}$. *Cell* **58**, 833-846

Piskareva, O., Harvey, H., Nolan, J., Conlon, R., Alcock, L., Buckley, P., Dowling, P., O'Sullivan, F., Bray, I. and Stallings, R.L. (2015) The development of cisplatin resistance in neuroblastoma is accompanied by epithelial to mesenchymal transition in vitro. *Cancer Letters* **364**, 142-155

Pommier, Y. (2006) Topoisomerase I inhibitors: camptothecins and beyond. *Nature Reviews Cancer* **6**, 789-802

Pommier, Y., Barcelo, J., Rao, V.A., Sordet, O., Jobson, A.G., Thibaut, L., Miao, Z., Seiler, J., Zhang, H., Marchand, C., Agama, K. and Redon, C. (2006) Repair of topoisomerase-I mediated DNA damage. *Progress in Nucleic Acid Research and Molecular Biology* **81**, 179-229

Przybytkowski, E., Lenkiewicz, E., Barrett, M.T., Klein, K., Nabavi, S., Greenwood, C.M. and Basik, M. (2014) Chromosome-breakage genomic instability and chromothripsis in breast cancer. *BMC Genomics* **15**, 579

Qiao, L., Koutsos, M., Tsai, L.L., Kozoni, V., Guzman, J., Shiff, S.J. and Rigas, B. (1996) Staurosporine inhibits the proliferation, alters the cell cycle distribution and induces apoptosis in HT-29 human colon adenocarcinoma cells. *Cancer Letters* **107**, 83-89

Rahman, T. (2013) Analysis of colon cancer cells that survive checkpoint adaptation after treatment with a genotoxic agent. University of Lethbridge, AB, Canada. MSc Thesis.

Rao, P.H., Houldsworth, J., Palanisamy, N., Murty, V.V., Reuter, V.E., Motzer, R.J., Bosl, G.J. and Chaganti, R.S. (1998) Chromosomal amplification is associated with cisplatin resistance of human male germ cell tumors. *Cancer Research* **58**, 4260-4263

Rausch, R., Jones, D.T.W., Zapatka, M., Stütz, A.M., Zichner, T., Weischenfelt, J., Jäger, N., Remke, M., Shih, D., Northcott, P.A., Pfaff, E., Tica, J., Wang, Q., Massimi, L., Witt, H., Bender, S., Pleier, S., Cin, H., Hawkins, C., Beck, C., von Deimling A., Hans, V., Brors, B., Eils, R., Scheurlen, W., Blake, J., Benes, V., Kulozik, A.E., Witt, O., Martin, D., Zhang, C., Porat, R., Merino, D.M., Wasserman, J., Jabado, N., Fontebasso, A.,

Bullinger, L., Rücker, F.G., Döhner, K., Döhner, H., Koster, J., Molenaar, J.J., Versteeg, R., Kool, M., Tabori, U., Malkin, D., Korshunov, A., Taylor, M.D., Lichter, P., Pfister, S.M and Korbel, J.O. (2012) Genome sequencing of pediatric medulloblastoma links catastrophic DNA rearrangements with TP53 mutations. *Cell* **148**, 59-71

Raymond, E., Campone, M., Stupp, R., Menten, J., Chollet, P., Lesimple, T., Fety-Deporte, R., Lacombe, D., Paoletti, X. and Fumoleau, P. (2002) Multicentre phase II and pharmacokinetic study of RFS2000 (9-nitro-camptothecin) administered orally 5 days a week in patients with glioblastoma multiforme. *European Journal of Cancer* **38**, 1348-1350

Rello-Varona, S., Kepp, O., Vitale, I., Michaud, M., Senovilla, L., Jemaá, M., Joza, N., Galluzzi, L., Castedo, M. and Kroemer, G. (2010) An automated fluorescence videomicroscopy assay for the detection of mitotic catastrophe. *Cell Death and Disease* **1**, e25

Revet, I., Feeney, L., Bruguera, S., Wilson, W., Dong, T.K., Oh, D.H., Dankort, D. and Cleaver J.E. (2011) Functional relevance of the histone gamma H2AX in the response to DNA damaging agents. *Proceedings of the National Academy of Sciences of the United States of America* **108**, 8663-8667

Rezáčová, M., Rudolfova, G., Tichy, A., Bacikova, D.M., Havelek, R., Vavrova, J., Odrazka, K., Lukasova, E. and Kozubek, S. (2011) Accumulation of DNA damage and cell death after fractionated irradiation. *Radiation Research* **175**, 708-718

Rhind, N. and Russell, P. (2000) Chk1 and Cds1: linchpins of the DNA damage and replication checkpoint pathways. *Journal of Cell Science* **113**, 3889-3896

Ricci, S.M. and Zong, W. (2006) Chemotherapeutic approaches for targeting cell death pathways. *The Oncologist* **11**, 342-357

Rieder, C.L. and Maiato, H. (2004) Stuck in division or passing through: what happens when cells cannot satisfy the spindle assembly checkpoint. *Developmental Cell* **7**, 637-651

Rodrigues, N.R., Rowan, A., Smith, M.E.F., Kerr, I.B., Bodmer, W.F., Gannon, J.V. and Lane, D.P. (1990) p53 mutations in colorectal cancer. *Proceedings of the National Academy of Sciences of the United States of America* **87**, 7555-7559

Rogakou, E.P., Pilch, D.R., Orr, A.H., Ivanova, V.S. and Bonner, W.M. (1998) DNA double-stranded breaks induce histone H2AX phosphorylation on serine 139. *The Journal of Biological Chemistry* **273**, 5858-5868

Roninson, I.B., Broude, E.V. and Chang, B.D. (2001) If not apoptosis, then what? Treatment-induced senescence and mitotic catastrophe in tumour cells. *Drug Resistance Updates* **4**, 303-313

Rosenberg, B., Vancamp, L. and Krigas, T. (1965) Inhibition of cell division in Eschericia coli by electrolysis products from a platinum electrode. *Nature* **205**, 698-699

Rosenberg, B., Vancamp, L., Trosko, J.E. and Mansour, V.H. (1969) Platinum compounds: a new class of potent antitumour agents. *Nature* **222**, 385-386

Rosenberg, B. and Vancamp, L. (1970) The successful regression of large solid sarcoma 180 tumors by platinum compounds. *Cancer Research* **30**, 1799-1802

Rowinsky, E.K. (1997) The development and clinical utility of the taxane class of antimicrotubule chemotherapy agents. *Annual Review of Medicine* **48**, 353-374

Ruth, A.C. and Roninson, I.B. (2000) Effects of the multidrug transporter P-glycoprotein on cellular responses to ionizing radiation. *Cancer Research* **60**, 2576-2578

Saikumar, P., Dong, Z., Mikhailov, V., Denton, M., Weinberg, J.M. and Venkatachalam, M.A. (1999) Apoptosis: definition, mechanisms and relevance to disease. *American Journal of Medicine* **107**, 489-506

Sallam, H., El-Serafi, I., Meijer, L. and Hassan, M. (2013) Pharmacokinetics and biodistribution of the cyclin-dependent kinase inhibitor CR8 in mice. *BioMed Central Pharmacology and Toxicology* **14**, doi: 10.1186/2050-6511-14-50

Sanchez, Y., Bachant, J., Wang, H., Hu, F., Liu, D., Tetzlaff, M. and Elledge, S.J. (1999) Control of the DNA damage checkpoint by Chk1 and Rad53 protein kinases through distinct mechanisms. *Science* **286**, 1166-1171

Sandell, L.L. and Zakian, V.A. (1993) Loss of a yeast telomere: arrest, recovery, and chromosome loss. *Cell* **75**, 729-739

Schwartz, G.K. and Shah, M.A. (2005) Targeting the cell cycle: a new approach to cancer therapy. *Journal of Clinical Oncology* **23**, 9408-9421

Shaltiel, I.A., Krenning, L., Bruinsma, W. and Medema, R.H. (2015) The same, only different- DNA damage checkpoints and their reversal throughout the cell cycle. *Journal of Cell Science* **128**, 1-14

Sharma, A., Singh, K. and Almasan, A. (2012) Histone H2AX phosphorylation: a marker for DNA damage. *Methods in Molecular Biology* **920**, 613-626

Shen, Z. (2011) Genomic instability and cancer: an introduction. *Journal of Molecular Cell Biology* **3**, 1-3

Shen, D.W., Pouliot, L.M., Hall, M.D. and Gottesman, M.M. (2012) Cisplatin resistance: a cellular self-defense mechanism resulting from multiple epigenetic and genetic changes. *Pharmacological Reviews* **64**, 706-721

Shrivastav, M., De Haro, L.P. and Nickoloff, J.A. (2008) Regulation of DNA double-strand break repair pathway choice. *Cell Research* **18**,134-147

Siemeister, G., Lücking, U., Wengner, A.M., Lienau, P., Steinke, W., Schatz, C., Mumberg, D. and Ziegelbauer, K. (2012) BAY 1000394, a novel cyclin-dependent kinase inhibitor, with potent antitumor activity in mono- and in combination treatment upon oral application. *Molecular Cancer Therapeutics* **11**, 2265-2273

Smith, J., Tho, L.M., Xu, N. and Gillespie, D.A. (2010) The ATM-Chk2 and ATR-Chk1 pathways in DNA damage signaling and cancer. *Advances in Cancer Research* **108**, 73-112

Sorenson, C.M. and Eastman, A. (1988a) Mechanism of cis-diamminedichloroplatinum(II)-induced cytotoxicity: role of G2 arrest and DNA double-strand breaks. *Cancer Research* **48**, 4484-4488

Sorenson, C.M. and Eastman, A. (1988b) Influence of cis-diamminedichloroplatinum(II) on DNA synthesis and cell cycle progression in excision repair proficient and deficient Chinese hamster ovary cells. *Cancer Research* **48**, 6703-6707

Sørenson, C.S., Syljuåsen, R.G., Falck, J., Schroeder, T., Rönnstrand, L., Khanna, K.K., Zhou, B.B., Bartek, J. and Lukas, J. (2003) Chk1 regulates the S-phase checkpoint by coupling the physiological turnover and ionizing radiation-induced accelerated proteolysis of Cdc25A. *Cancer Cell* **3**, 247-258

Stephens, P.J., Greenman., C.D, Fu, B., Yang, F., Bignell, G.R., Mudie, L.J., Pleasance, E.D., Lau, K.W., Beare, D., Stebbings, L.A., McLaren, S., Lin, M.L., McBride, D.J., Varela, I., Nik-Zainal, S., Leroy, C., Jia, M., Menzies, A., Butler, A.P., Teague, J.W., Quail, M.A., Burton, J., Swerdlow, H., Carter, N.P., Morsberger, L.A., Iacobuzio-Donahue, C., Follows, G.A., Green, A.R., Flanagan, A.M., Stratton, M.R., Futreal, P.A., Campbell, P.J. (2011) Massive genomic rearrangement acquired in a single catastrophic event during cancer development. *Cell* **144**, 27-40

Stewart, B.W. and Wild, C.P. (2014) World Cancer Report. WHO Press

Stiff, T., O'Driscoll, M., Rief, N., Iwabuchi, K., Löbrich, M. and Jeggo, P.A. (2004) ATM and DNA-PK function redundantly to phosphorylate H2AX after exposure to ionizing radiation. *Cancer Research* **64**, 2390-2396

Stratton, M.R., Campbell, P.J. and Futreal, P.A. (2009) The cancer genome. *Nature* **458**, 719-724

Stratton, M.R. (2011) Exploring the genomes of cancer cells: progress and promise. *Science* **331**, 1553-1558

Sudakin, V., Ganoth, D., Dahan, A., Heller, H., Hershko, J., Luca, F.C., Ruderman, J.V. and Hershko, A. (1995) The cyclosome, a large complex containing cyclin-selective

ubiquitin ligase activity, targets cyclins for destruction at the end of mitosis. *Molecular Biology of the Cell* **6**, 185-197

Susin, S.A., Lorenzo, H.K., Zamzami, N., Marzo, I., Snow, B.E., Brothers, G.M., Mangion, J., Jacotot, E., Constantini, P., Loeffler, M., Larochette, N., Goodlett, D.R., Aebersold, R., Siderovski, D.P., Penninger, J.M. and Kroemer, G. (1999) Molecular characterization of mitochondrial apoptosis-inducing factor. *Nature* **397**, 441-446

Swift, L.H. and Golsteyn, R.M. (2014) Genotoxic anti-cancer agents and their relationship to DNA damage, mitosis and checkpoint adaptation in proliferating cancer cells. *International Journal of Molecular Sciences* **15**, 3403-3431

Syljuåsen, R.G., Jensen, S., Bartek, J. and Lukas, J. (2006) Adaptation to the ionizing radiation-induced G2 checkpoint occurs in human cells and depends on checkpoint kinase 1 and polo-like kinase 1 kinases. *Cancer Research* **21**, 10253-10257

Syljuåsen, R.G. (2007) Checkpoint adaptation in human cells. *Oncogene* **26**, 5833-5839

Tannock, I.F. and Lee, C. (2001) Evidence against apoptosis as a major mechanism for reproductive cell death following treatment of cell lines with anti-cancer drugs. *British Journal of Cancer* **84**, 100-105

Tao, R., Xue, H., Zhang, J., Liu, J., Deng, H. and Chen, Y.G. (2013) Deacetylase Rpd3 facilitates checkpoint adaptation by preventing Rad53 overactivation. *Molecular and Cellular Biology* **33**, 4214-4224

Terasima, T. and Tolmach, L.J. (1963) Growth and nucleic acid synthesis in synchronously dividing populations of HeLa cells. *Experimental Cell Research* **30**, 344-362

Thompson, S.L. and Compton, D.A. (2011) Chromosomes and cancer cells. *Chromosome Research* **19**, 433-444

Toczyski, D.P., Galgoczy, D.J. and Hartwell, L.H. (1997) CDC5 and CKII control adaptation to the yeast DNA damage checkpoint. *Cell* **90**, 1097-1106

Tounetki, O., Pron, G., Belehradek, J. and Mir L.M. (1993) Bleomycin, an apoptosis-mimetic drug that induces two types of cell death depending on the number of molecules internalized. *Cancer Research* **53**, 5462-5469

Ubersax, J.A., Woodbury, E.L., Quang, P.N., Paraz, M., Blethrow, J.D., Shah, K., Shokat, K.M. and Morgan, D.O. (2003) Targets of the cyclin-dependent kinase Cdk1. *Nature* **425**, 859-864

Vakifahmetoglu, H., Olsson, M., Tamm, C., Heidari, N., Orrenius, S. and Zhivotovsky, B. (2008) DNA damage induces two distinct modes of cell death in ovarian carcinomas. *Cell Death and Differentiation* **15**, 555-566

van Engeland, M., Nieland, L.J., Ramaekers, F.C., Schutte, B. and Reutelingsperger, C.P. (1998) Annexin-V affinity assay: a review on an apoptosis detection system based on phosphatidylserine exposure. *Cytometry* **31**, 1-9

van Waardenburg, R.C., de Jong, L.A., van Delft, F., van Eijndhoven, M.A., Bohlander, M., Bjornsti, M.A., Brouwer, J. and Schellens, J.H. (2004) Homologous recombination is a highly conserved determinant of the synergistic cytotoxicity between cisplatin and DNA topoisomerase I poisons. *Molecular Cancer Therapeutics* **3**, 393-402

Vasquez, R.J., Howell, B., Yvon, A.M., Wadsworth, P. and Cassimeris, L. (1997) Nanomolar concentrations of nocodazole alter microtubule dynamic instability in vivo and in vitro. *Molecular Biology of the Cell* **8**, 973-985

Vermeulen, K., van Bockstaele, D.R. and Berneman, Z.N. (2003) The cell cycle: a review of regulation, deregulation and therapeutic targets in cancer. *Cell Proliferation* **36**, 131-149

Vermorken, J.B., van der Vijgh, W.J., Klein, I., Hart, A.A., Gall, H.E. and Pinedo, H.M. (1984) Pharmacokinetics of free and total platinum species after short-term infusion of cisplatin. *Cancer Treatment Reports* **68**, 505-513

Vidanes, G.M., Sweeney, F.D., Galicia, S., Cheung, S., Doyle, J.P., Durocher, D., Toczyski, D.P. (2010) CDC5 inhibits the hyperphosphorylation of the checkpoint kinase Rad53, leading to checkpoint adaptation. *PLoS One* **8**, e1000286

Villani, G., Tanguy Le Gac, N. and Hoffmann, J. (2006) Replication of platinated DNA and its mutagenic consequences. In Cisplatin: chemistry and biochemistry of a leading anticancer drug (Lippert, B. ed), pp. 135-157, Verlag Helvetica Chimica Acta., Zürich, Switzerland

Vitale, I., Galluzzi, L., Castedo, M. and Kroemer, G. (2011) Mitotic catastrophe: a mechanism for avoiding genomic instability. *Nature Reviews Molecular and Cellular Biology* **12**, 385-392

Walker, M., Black, E.J., Oehler, V., Gillespie, D.A. and Scott, M.T. (2009) Chk1 C-terminal regulatory phosphorylation mediates checkpoint activation by de-repression of Chk1 catalytic activity. *Oncogene* **28**, 2314-2323

Wang, X.Q., Zhu, Y.Q., Liu, K.S., Cai, Q., Lu, P. and Poon, R.T. (2008) Aberrant polo-like kinase 1 Cdc25A pathway in metastatic hepatocellular carcinoma. *Clinical Cancer Research* **14**, 6813-6820

Ward, I.M. and Chen, J. (2001) Histone H2AX is phosphorylated in an ATR-dependent manner in response to replicational stress. *The Journal of Biological Chemistry* **276**, 47759-47762

Wasenius, V.M., Jekunen, A., Monni, O., Joensuu, H., Aebi, S., Howell, S.B. and Knuutila, S. (1997) Comparative genomic hybridisation analysis of chromosomal changes occurring during development of acquired resistance to cisplatin in human ovarian carcinoma cells. *Genes, Chromosomes and Cancer* **18**, 286-291

Weinert, T.A., Kiser, G.L. and Hartwell, L.H. (1994) Mitotic checkpoint genes in budding yeast and the dependence of mitosis on DNA replication and repair. *Genes and Development* **8**, 652-665

Weiss, M.M., Hermsen, M.A., Meijer, G.A., van Grieken, N.C., Baak, J.P., Kuipers, E.J. and van Diest, P.J. (1999) Comparative genomic hybridisation. *Molecular Pathology* **52**, 243-251

Weiss, R.S., Matsuoka, S., Elledge, S.J. and Leder, P. (2002) Hus1 acts upstream of Chk1 in a mammalian DNA damage response pathway. *Current Biology* **12**, 73-77

Werner, A. (1913) Nobel Lectures Chemistry 1901-1921. Elsevier publishing company, Amsterdam, Holland.

Westphal, D., Dewson, G., Czabotar, P.E. and Kluck, R.M. (2011) Molecular biology of Bax and Bak activation and action. *Biochimica et Biophysica Alta* **1813**, 521-531

Wheate, N.J., Walker, S., Craig, G.E. and Oun, R. (2010) The status of platinum anticancer drugs in the clinic and in clinical trials. *Dalton Transactions* **39**, 8113-8127

Widel, M., Jedrus, S., Owczarek, S., Konopacka, M., Lubecka, B. and Kolosza, Z. (1999) The increment of micronucleus frequency in cervical carcinoma during irradiation in vivo and its prognostic value for tumour radiocurability. *British Journal of Cancer* **80**, 1599-1607

Wilson, C., Yang, J., Strefford, J.C., Summersgill, B., Young, B.D., Shipley, J., Oliver, T. and Lu, Y. (2005) Overexpression of genes on 16q associated with cisplatin resistance of testicular germ cell tumor cell lines. *Genes, Chromosomes and Cancer* **43**, 211-216

Wiltshaw, W. (1979) Cisplatin in the treatment of cancer. *Platinum Metals Review* **23**, 90-98

Wirth, M., Joachim, J. and Tooze, S.A. (2013) Autophagosome formation- the role of ULK1 and Beclin1-PI3KC3 complexes in setting the stage. *Seminars in Cancer Biology* **23**, 301-309

Wisnovsky, S.P., Wilson, J.J., Radford, R.J., Pereira, M.P., Chan, M.R., Laposa, R.R., Lippard, S.J. and Kelley, S.O. (2013) Targeting mitochondrial DNA with a platinum-based anticancer agent *Chemistry and Biology* **20**, 1323-1328

Woo, R.A. and Poon, R.Y. (2003) Cyclin-dependent kinases and S phase control in mammalian cells. *Cell Cycle* **2**, 316-324

Woods, D. and Turchi, J.J. (2013) Chemotherapy induced DNA damage response. *Cancer Biology and Therapy* **14**, 379-389

Wouters, B.G., Denko, N.C., Giaccia, A.J. and Brown, J.M. (1999) A p53 and apoptotic independent role for p21/waf1 in tumour response to radiation therapy. *Oncogene* **18**, 6540-6545

Woźniak, K. and Blasiak, J. (2002) Recognition and repair of DNA-cisplatin adducts. *Acta Biochimica Polonica* **49**, 583-596

Yamada, M. and Puck, T.T. (1961) Action of radiation on mammalian cells, IV. Reversible mitotic lag in the S3 HeLa cell produced by low doses of X-rays. *Proceedings of the National Academy of Sciences of the United States of America* **47**, 1181-1191

Yang, Z., Schumaker, L.M., Egorin, M.J., Zuhowski, E.G., Guo, Z. and Cullen, K.J. (2006) Cisplatin preferentially binds mitochondrial DNA and voltage-dependent anion channel protein in the mitochondrial membrane of head and neck squamous cell carcinoma: possible role in apoptosis. *Clinical Cancer Research* **12**, 5817-5825

Yin, D.X. and Schimke, R.T. (1995) Bcl-2 expression delays drug-induced apoptosis but does not increase clonogenic survival after drug treatment in HeLa cells. *Cancer Research* **55**, 4922-4928

Yoo, H.Y., Kumagai, A., Shevchenko, A. and Dunphy, W.G. (2004) Adaptation of a DNA replication checkpoint response depends upon inactivation of claspin by the polo-like kinase. *Cell* **117**, 575-588

Yoshikawa, R., Kusunoki, M., Yanagi, H., Noda, M., Furuyama, J.I., Yamamura, T. and Hashimoto-Tamaoki, T. (2001) Dual antitumour effects of 5-fluorouracil on the cell cycle in colorectal carcinoma cells: a novel target mechanism concept for pharmacokinetic modulating chemotherapy. *Cancer Research* **61**, 1029-1037

Zamble, D.B. and Lippard, S.J. (1995) Cisplatin and DNA repair in cancer chemotherapy. *Trends in Biochemical Sciences* **20**, 435-439

Zhang, X.D., Gillespie, S.K. and Hersey, P. (2004) Staurosporine induces apoptosis of melanoma by both caspase-dependent and -independent apoptotic pathways. *Molecular Cancer Therapeutics* **3**, 187-197

Zhang, W., Peng, G., Lin, S. and Zhang, P. (2011) DNA damage response is suppressed by the high cyclin-dependent kinase 1 activity in mitotic mammalian cells. *The Journal of Biological Chemistry* **286**, 35899-35905

Zhang, C.Z., Spektor, A., Cornils, H., Francis, J.M., Jackson, E.K., Liu, S., Meyerson, M. and Pellman, D. (2015) Chromothripsis from DNA damage in micronuclei. *Nature* **522**, 179-184

Zhao, H. and Piwnica-Worms, H. (2001) ATR-mediated checkpoint pathways regulate phosphorylation and activation of human Chk1. *Molecular and Cellular Biology* **21**, 4129-4139

Zhivotovsky, B. and Kroemer, G. (2004) Apoptosis and genomic instability. *Nature Reviews Molecular and Cell Biology* **5**, 752-762

Zhou, B.B. and Elledge, S.J. (2000) The DNA damage response: putting checkpoints in perspective. *Nature* **408**, 433-439

Zhou, D., Cong, Y., Qi, Y., He, S., Xiong, H., Wu, Y., Xie, Z., Chen, X., Jing, X. and Huang, Y. (2014) Overcoming tumor resistance to cisplatin through micelle-mediated combination chemotherapy. *Biomaterials Science* doi: 10.1039/c4bm00305e

Zolzer, F., Alberti, W., Pelzer, T., Lamberti, G., Hulskamp, F.H. and Streffer, C. (1995) Changes in S-phase fraction and micronucleus frequency as prognostic factors in radiotherapy of cervical carcinoma. *Radiotherapy Oncology* **36**, 128-132

Zou, L. and Elledge, S.J. (2003a) Replication protein A mediated recruitment and activation of Rad17 complexes. *Proceedings of the National Academy of Sciences of the United States of America* **100**, 13827-13832

Zou, L. and Elledge, S.J. (2003b) Sensing DNA damage through ATRIP recognition of RPA-ssDNA complexes. *Science* **300**, 1542-1548